



**NTNU – Trondheim**  
Norwegian University of  
Science and Technology

# Imaging Reservoir Geology of the Troll West Field in the North Sea by 3D Seismic Interpretation

**Muhammad Amjad**

Petroleum Geosciences

Submission date: July 2014

Supervisor: Ståle Emil Johansen, IPT

Norwegian University of Science and Technology  
Department of Petroleum Engineering and Applied Geophysics





**NTNU**

Norwegian University of  
Science and Technology

# **Imaging Reservoir Geology of the Troll West Field in the North Sea by 3D Seismic Interpretation**

**Muhammad Amjad**

**Petroleum Geoscience**

**Submission Date: 07/07/2014**

**Supervisor: Ståle Emil Johansen**

**Norwegian University of Science and Technology**

**Department of Petroleum Engineering and Applied Geophysics**

## **ACKNOWLEDGMENTS**

In the name of **ALLAHA**, the one who gave me the courage to complete this thesis work.

I would like to offer my gratitude to my supervisor **Ståle Emil Johansen** who has open mind to discuss various interpretation issues, keen eye and patient to support me throughout the work. This thesis would not have been possible without his unconditional guidance.

**The Department of Petroleum Engineering and Applied Geophysics** provided the facilities that I needed to complete my thesis.

Last but not least, thank to my family, friends and classmates for moral and technical support, especially to Hammad Majeed, Tanveer Ahmad and Dicky Harishidayat.

## **ABSTRACT**

The Troll Field is called “super giant gas field”. This is the second largest gas field of offshore Europe with its 1670 billion m<sup>3</sup> of gas and 615 million m<sup>3</sup> of oil initially in place. The Troll Field was discovered in 1979 and located about 80 km offshore Norway on the northwestern edge of the Horda Platform and eastern edge of the Viking graben in the water depth of 300 – 355 meter. The total area of the field is about 710 km<sup>2</sup> and extends over four Norwegian Blocks (31/2, 31/3, 31/5 and 31/6).

The reservoir successions contain the Sognefjord, Fensfjord, Heather and Krossfjord Formations of the Jurassic Viking Group. Deposition occurred as a cyclic sequence of shallow marine sand stone with alternations of transgressive and regressive shoreface facies.

The main goal of this study is detailed integrated seismic and well data study of reservoir units to determine the reservoir distribution and depositional environments.

The main reservoir unit is the Sognefjord Formation and contains about 90% of the field hydrocarbon reserves. This Formation is seismically characterized by low angle clinofolds and the seismic data shows westward Progradation. The Flat Spot is the prominent characteristic of the seismic data. The Sognefjord, Fensfjord, and Krossfjord formations interpreted as tide, wave and fluvial dominated environment.

## Table of Contents

1	INTRODUCTION.....	1
1.1	Previous Work.....	3
1.2	Objectives.....	4
2	GEOLOGICAL SETTINGS.....	5
2.1	Regional tectonics.....	5
2.1.1	Permo-Triassic rift:.....	5
2.1.2	Mid Jurassic-Early Cretaceous rift:.....	5
2.1.3	Cretaceous post rift:.....	6
2.2	Regional Stratigraphy.....	11
2.2.1	Devonian.....	11
2.2.2	Triassic.....	12
2.2.3	Jurassic.....	12
2.2.3.1	Dunlin Group.....	12
2.2.3.2	Brent Group.....	12
2.2.3.3	Viking Group.....	12
2.2.4	Cretaceous.....	13
2.2.5	Cenozoic.....	13
2.3	Viking group depositional environments:.....	16
2.3.1	Fensfjord Formation.....	16
2.3.2	Heather B and Sognefjord Formations.....	16
2.3.3	Heather C Unit.....	16
2.4	Tectonic-Stratigraphical evolution of the Horda Platform.....	18
2.4.1	Mid Jurassic (Bathonian-latest Callovian).....	18
2.4.2	Late Jurassic (Oxfjordian-Kimmeridgian).....	18
2.4.3	Early-Middle Volgian.....	18
2.5	Structural outline of the Troll Field.....	20
2.6	Key Parameters in the evolution of Hydrocarbon traps at Troll.....	21
2.7	Basin infill.....	23
3	DATASET AND METHODOLOGY.....	25

3.1	Dataset .....	25
3.2	Well data .....	25
3.2.1	Well 31/2-1 .....	26
3.2.2	Well 31/5-5 .....	27
3.2.3	Well 31/2-3 .....	27
3.2.4	Well 31/3-1 .....	27
3.3	Seismic data .....	27
3.4	Methodology.....	29
3.4.1	Software.....	29
3.4.2	Data Import.....	29
3.4.3	Seismic to well tie .....	30
3.4.4	Seismic interpretation.....	30
3.4.5	Map generation.....	30
4	SEISMIC INTERPRETATIONS .....	32
4.1	Seismic Well Tie .....	32
4.2	Regional Interpretation.....	37
4.2.1	Structural Description .....	38
4.3	Troll west Interpretation.....	42
4.3.1	Base of Quarternary.....	42
4.3.2	Top of Draupen Formation .....	46
4.3.3	Top of Sognefjord Formation .....	48
4.3.4	Top of Heather B Formation .....	49
4.3.5	Top of Fensfjord Formation .....	55
4.3.6	Top of Krossfjord Formation .....	56
4.3.7	Top of the Brent Gp .....	56
4.3.8	Top of the Dunlin Gp.....	59
4.4	Fault Interpretation.....	60
4.4.1	Fault Family 1 .....	62
4.4.2	Fault Family 2 .....	62
4.5	Reservoir Description.....	67
4.5.1	Sognefjord Formation .....	68

4.5.1.1	Reflection Pattern .....	70
4.5.1.2	Time Structure Mapping (Z values).....	72
4.5.1.3	Amplitude Mapping .....	75
4.5.1.4	Facies Description .....	77
4.5.1.5	Wireline-log Signature .....	77
4.5.1.6	Interpretation.....	80
4.5.2	Fensfjord Formation.....	82
4.5.2.1	Facies Association 1 .....	90
4.5.2.2	Wireline-log Signature .....	91
4.5.2.3	Interpretation.....	91
4.5.2.4	Facies Association 2 .....	92
4.5.2.5	Wireline-log Signature .....	92
4.5.2.6	Interpretation.....	92
4.5.3	Krossfjord Formation .....	95
4.5.3.1	Delta-front Facies Association .....	100
4.5.3.2	Wireline-log Signature .....	102
4.5.3.3	Interpretation.....	102
5	DISCUSSIONS .....	105
5.1	Fault Trend.....	105
5.2	Geological cross section.....	106
5.3	Depositional model for the Sognefjord Formation.....	108
5.4	Depositional model for the Krossfjord and Fensfjord Formations .....	113
5.4.1	East to west change in depositional environments in the Troll Field .....	114
5.4.1.1	Depositional model 1 .....	114
5.4.1.2	Depositional model 2 .....	114
5.4.2	Vertical Increase in abundance of tide dominated deposits .....	114
5.4.3	Absence of coastal plain deposits .....	115
6	CONCLUSIONS .....	120
7	FURTHER RESEARCH .....	121
	REFERENCES .....	122
	APPENDIX.....	125



## List of Figures

Figure 1.1 Location map of the Troll Field (Dreyer et al., 2005). .....	2
Figure 1.2: Outline of the Troll Field, Red colour is showing gas province while green colour is for oil province (Dreyer et al., 2005). .....	3
Figure 2.1(a) Map of the north Viking Graben is highlighting the Horda Platform, and the Troll Field (b) Palaeoenvironmental map of the northern North Sea during Callovian. (c) Geoseismic Profile showing major fault blocks across the Viking Graben (Holgate et al., 2013). .....	7
Figure 2.2 Patterns of Triassic rift phase (Zanella and Coward, 2003). .....	8
Figure 2.3 Patterns of Jurassic rift phase (Zanella and Coward, 2003). .....	9
Figure 2.4 Map of the structural evolution of the northern North Sea from Triassic to Cretaceous (Zanella and Coward, 2003). .....	10
Figure 2.5 Example of gravity slides on the western margin of the Viking Graben (Gabrielsen 1991). .....	11
Figure 2.6: Generalized chronostratigraphic chart of the Northern North Sea (www.nhm2.uio.no). .....	14
Figure 2.7 Stratigraphic column of the Troll Field (Bolle L.1992). .....	15
Figure 2.8: Correlation between eustatic curve and Troll deposits (Haq et al., 1987). .....	17
Figure 2.9 SW-NE Tectonostratigraphic cross- section with curves of global sea level changes (Johnsen Jan R. 1995). .....	19
Figure 2.10 Map of the Troll Field is showing proximities to source (Left) and top of the Troll reservoir (Right) (Bolle L.1992). .....	20
Figure 2.11 Structural cross section and distribution of hydrocarbons through Troll Field (Johnsen et. al., 1995). .....	21
Figure 2.12 Source and possible migration paths for the Troll Field (Johnsen et al., 1995). .....	22
Figure 2.13 Rift Basin infill models: (A) Non marine rift-Basin infill models: (B) Mixed non marine and shallow marine:(C) Deep marine rift-Basin infill models (Ravnas et al.2000). .....	24
Figure 3.1 The Troll Field outline with well locations. .....	26
Figure 3.2: Two Types of data polarity, American and European (Brown 2005). .....	28
Figure 3.3: Sea bottom is interpreted as a peak (Red) .....	28
Figure 3.4: Peaks showing interpreted sea bottom. .....	29
Figure 3.5 Flow chart shows the procedure of seismic interpretation. ....	31
Figure 4.1: Main steps of Seismic well tie process. ....	33
Figure 4.2: The process of Sonic Calibration for the well 31/2-3 with main well tops. ....	34
Figure 4.3: The process of synthetic generation for the well 31/2-3 with main well tops. ....	35
Figure 4.4 Seismic cross-section showing integrated seismic well tie results for well 31/2-1 and 31/2-3 with key well tops . For location of section see Fig. 4.5 .....	37
Figure 4.5: Location of seismic section in Fig. 4.4 .....	37
Figure 4.6 Interpreted 2D regional seismic line MN9103-308. ....	39
Figure 4.7 Interpreted 2D regional seismic line MN9103-308A. ....	40
Figure 4.8 Regional profile model made from interpretation of 2D seismic lines. ....	41
Figure 4.9: Time structure map of interpreted base of Quarternary .....	42

Figure 4.10: Seismic inline 862 shows major truncating angular unconformity. ....	43
Figure 4.11: Seismic section through well 31/2-1 and 31/2-3 showing interpreted Horizons. See Fig.4.12 for location.....	44
Figure 4.12: Location of interpreted Horizon section in Fig. 4.11 .....	45
Figure 4.13: Seismic Section showing interpreted top of Draupen FM. See Fig.4.14 for location. ....	46
Figure 4.14: Location of interpreted horizons in reservoir section. ....	47
Figure 4.15: Time structure map of interpreted Draupen Formation. ....	48
Figure 4.16: Seismic Section showing interpreted top of Heather B Formation. For location see Fig. 4.14 .....	49
Figure 4.17: Seismic section showing dimming of reflection pattern towards east. See Fig.4.18 for location .....	50
Figure 4.18 : Location of seismic section in Fig. 4.17.....	51
Figure 4.19: Seismic section showing off lapping of strata in Heather B Formation. See Fig. 4.20 for location of this section.....	52
Figure 4.20: Location of seismic section in Fig. 4.19.....	53
Figure 4.21: Surface map of Heather B Formation. ....	54
Figure 4.22: RMS attribute map of Heather B Formation.....	55
Figure 4.23: Seismic Section showing interpreted top of Brent GP. See Fig. 4.14 for location.....	56
Figure 4.24: Seismic section shows dim reflection pattern of top of Brent GP in western part of the Troll Field. See Fig. 4.25 for location.....	57
Figure 4.25: Location of seismic section in Fig. 4.24.....	58
Figure 4.26: Time structure map of interpreted top of Brent GP.....	59
Figure 4.27: Time structure map of interpreted top of Dunlin GP .....	60
Figure 4.28 Sognefjord surface map along with trends of interpreted fault families and listric faults.....	61
Figure 4.29: Random line shows the interpreted fault family 1. See Fig. 4.30 for location .....	62
Figure 4.30: Location of interpreted fault family 1 section in Fig. 4.29.....	63
Figure 4.31: Zoomed out Random line shows fault family 2. See Fig. 4.33 for location. ....	64
Figure 4.32: Seismic section showing Synthetic, antithetic faults and roll over-drag. ....	65
Figure 4.33: Location of seismic sections in Fig. 4.31-32.....	65
Figure 4.34 The pattern of major faults of fault family 1 in 3D window. See Fig.4.28 for location.....	66
Figure 4.35: Model of interpreted faults showing anthetic and synthetic Faults and reverse drag along major synthetic fault.....	67
Figure 4.36: Seismic Section showing interpreted Sognefjord Formation. See Fig.4.14 for location. ....	69
Figure 4.37: Seismic section shows dim reflection pattern of the Sognefjord Formation in eastern part of the in-lines. See Fig. 4.39 for location.....	70
Figure 4.38: Seismic section shows the merging of the Sognefjord reflection with the Draupen Formation reflection in the eastern part. See Fig. 4.39 for location. ....	71
Figure 4.39:Location of seismic section in Figs.4.37-38.....	72
Figure 4.40 Time structure map of the Sognefjord Formation in 3D window.....	73
Figure 4.41: Seismic section shows the erosion of the Sognefjord Formation by truncation of strata. See Fig. 4.42 for location. ....	74
Figure 4.42: Location of seismic section in Fig. 4.41.....	75

Figure 4.43: Amplitude attribute map (RMS) of the Sognefjord Formation.....	76
Figure 4.44: Wireline log through well 31/2-1 shows the major depositional cycles of Sognefjord Formation.....	78
Figure 4.45: Ideal shelf-upper shoreface coarsening upward cycle 31/2-1 (modified from (Stewart et al., 1995). ....	79
Figure 4.46: Cross-line 762 shows southward offlap of the Sognefjord Formation. See Fig. 4.47 for location. ....	81
Figure 4.47: Location of seismic section in Fig. 4.46.....	82
Figure 4.48: Seismic section shows the interpreted Fensfjord Formation. See Fig. 4.14 for location. ....	83
Figure 4.49: Seismic section shows dim reflection pattern of the Fensfjord Formation in western part of the inlines. See Fig. 4.25 for location.....	84
Figure 4.50: Seismic section shows the positive e polarity of the Fensfjord Formation along flat spot in well 31/2-3.....	85
Figure 4.51: Location of seismic section in Fig. 4.50.....	86
Figure 4.52: Seismic section shows the negative polarity of the Fensfjord Formation along flat spot in well 31/2-1.....	87
Figure 4.53: Location of seismic section in Fig. 4.52.....	88
Figure 4.54: Time Structure map of Fensfjord Formation in 3D window .....	89
Figure 4.55: RMS map of Fensfjord Formation.....	90
Figure 4.56 Wireline log shows main facies distribution in Fensfjord Formation.....	93
Figure 4.57: Lithological column of major facies of the Fensfjord Formation.....	94
Figure 4.58: Seismic section showing the interpreted Krossfjord Formation. See Fig. 4.14 for location...	96
Figure 4.59: Seismic section shows dim reflection pattern of the Krossfjord Formation in western part of the in-lines. See Fig. 4.25 for location.....	97
Figure 4.60: Time structure map of the Krossfjord Formation in 3D window.....	98
Figure 4.61: Amplitude map (RMS) of the Krossfjord Formation.....	99
Figure 4.62 Wireline log through the Krossfjord Formation.....	101
Figure 4.63 Wireline log shows characteristics at carbonaceous debris and calcite cemented intervals. ....	103
Figure 4.64: Lithological column of the Krossfjord Formation. ....	104
Figure 5.1: Showing the development of half graben from series of normal faults dipping in similar direction ( <a href="http://www.geosci.usyd.edu.au">www.geosci.usyd.edu.au</a> ) .....	105
Figure 5.2: Rollover dragging of the strata along normal fault ( <a href="http://www.homepage.ufp.pt">www.homepage.ufp.pt</a> ).....	106
Figure 5.3: Geological cross section of the Troll Field made from interpreted horizon.....	107
Figure 5.4: 3D seismic section from Troll West Field showing down lapping of seismic reflectors towards west (Stewart et al., 1995).....	109
Figure 5.5: The NE-SW Correlation between well 31/3-1 and 31/2-1 shows thinning of the Sognefjord Formation towards west. For location of wells see Fig. 3.1 .....	110
Figure 5.6: Generalized depositional model of Upper and lower Sognefjord FM showing tide influenced delta, spit barrier and lower shoreface (modified from Dreyer et al., 2005). ....	111
Figure 5.7: Block diagram for depositional model of the Sognefjord Formation showing coastal plain channels, tidal back basin and tide influenced embayment (modified from Dreyer et al., 2005). ....	112

Figure 5.8: The model shows gentle Troll fault block tilted eastwards. Less accommodation space and erosion took place over Troll West resulted in high energy conditions due to the elevation of the area above wave base for a longer period (modified from Stewart et al., 1995). ..... 113

Figure 5.9: Forced regression cause more erosion as compared to normal regression (www.aapgbull.geoscienceworld.org). ..... 115

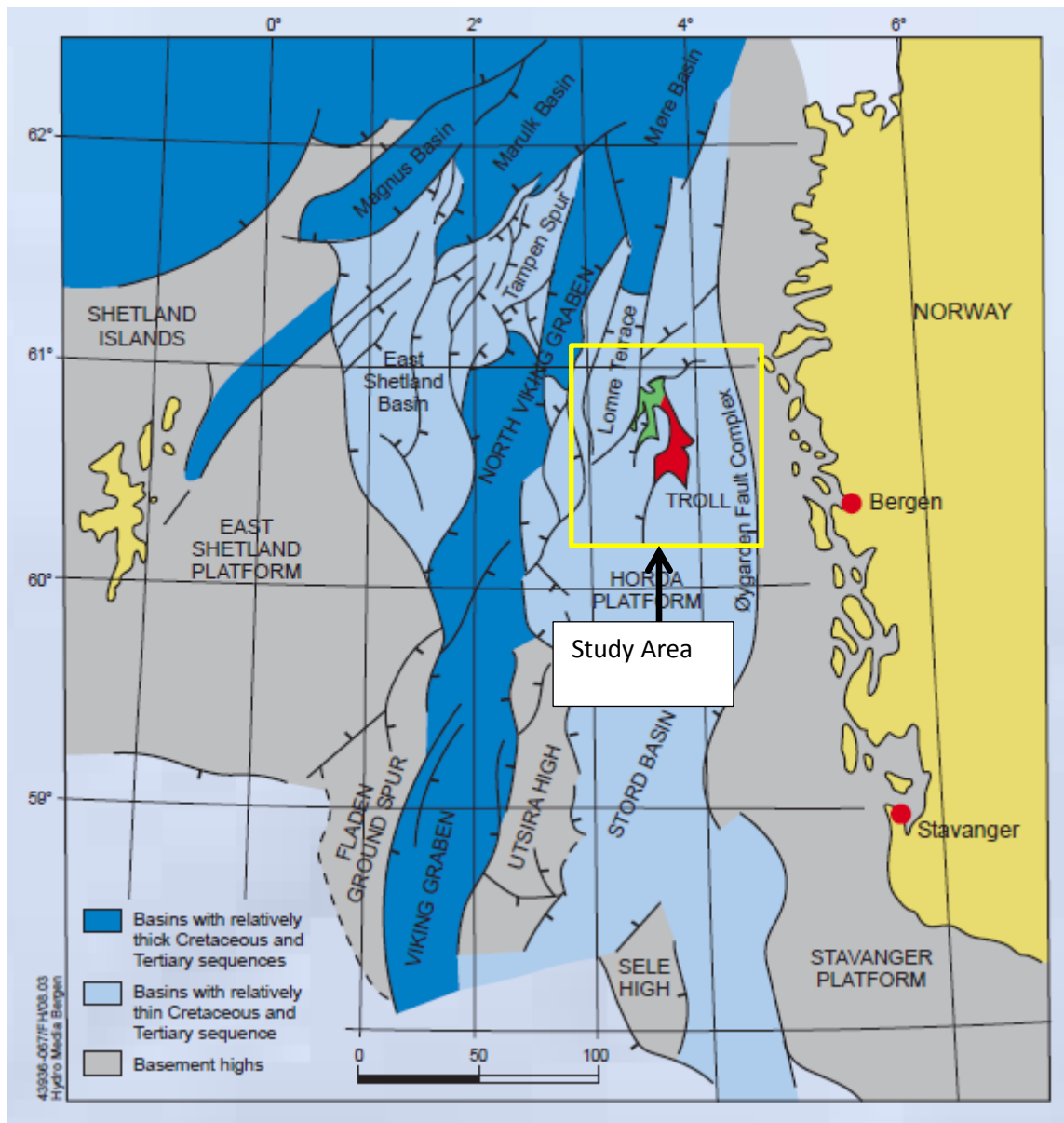
Figure 5.10: Block diagram showing depositional models. Two models are shown: (a) spatial variation in depositional environments with a wave-dominated spit system ; and (b) temporal variation in depositional environments with tide dominated, wave influenced embayment and development of shoreface on inner-middle shelf (t=1), Evolving into wave-dominated shoreface due to progradation to the outer shelf (t=2), (c) combination of spatial and temporal variation. (Modified from Holgate et al., 2013). ..... 119

Figure 7.1: The Broadseis data is showing more detail and dynamic range than the conventional data (www.cggveritas.com) ..... 121

## **1 INTRODUCTION**

The study area is located offshore Norway on the western margin of Horda Platform, east of Oseberg Field. The field stretches over four Norwegian exploration blocks ( 31/2, 31/3, 31/5, and 31/6) and it is about 45 km long and 30 km wide i.e. encompasses an area of 710 km<sup>2</sup> (Bolle L.1992).

Troll Field is called “super giant gas field”. This is second largest gas field of offshore Europe with its 1670 billion m<sup>3</sup> of gas and 615 million m<sup>3</sup> of oil initially in place.



**Figure 1.1** Location map of the Troll Field with types of basins (Dreyer et al., 2005).

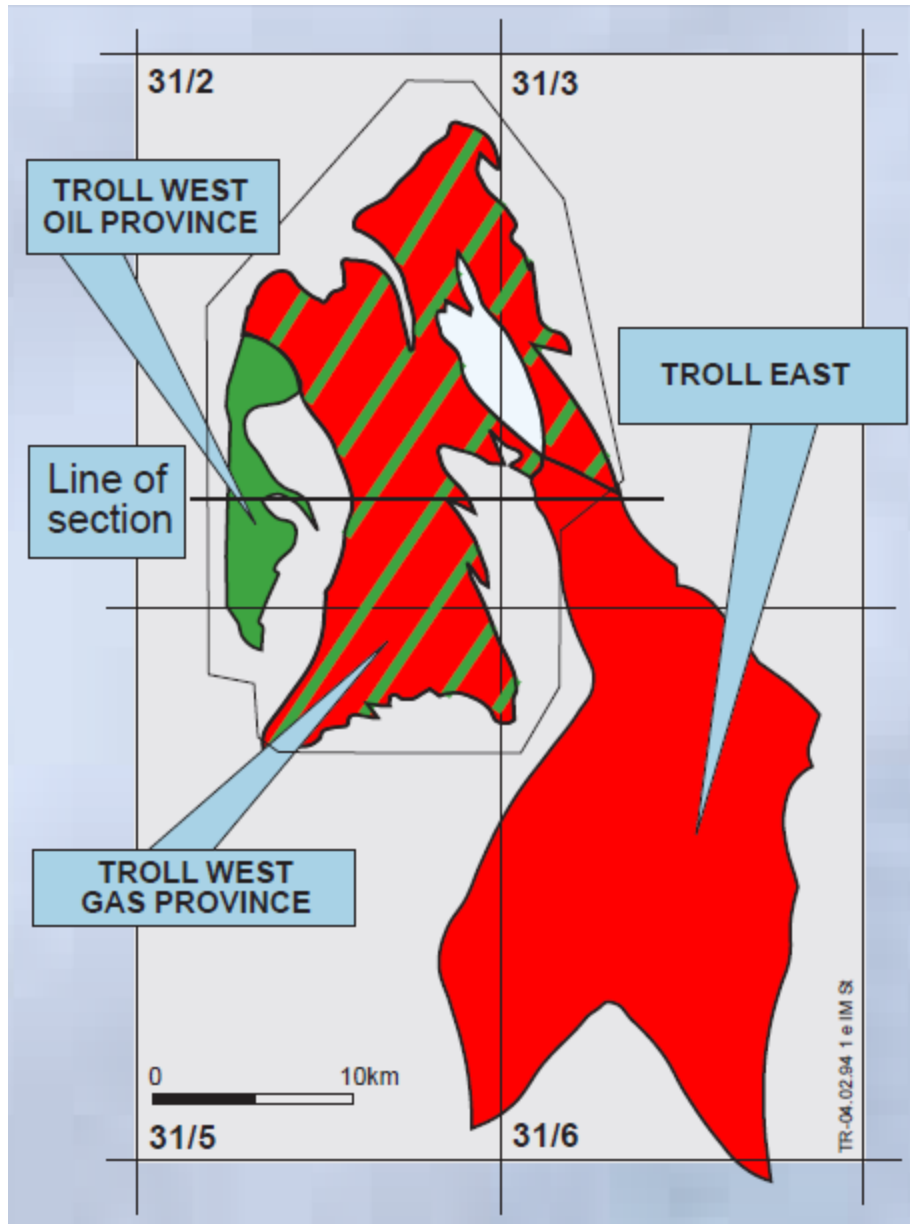


**Figure 1.2:** Outline of the Troll Field, red colour is showing gas province while green colour is for oil province (Dreyer et al., 2005).

### 1.1 Previous Work

A large data has been published from the Troll Field and surrounding areas of Horda Platform. The availability of core data (4 km) from the Upper Jurassic makes the interesting and valuable study area (Stewart et al., 1995).

The most comprehensive publications on the Troll Field are by Badley M.E.(1984), Hellem et al. (1986), Osborne and Evans (1987), Gabrielsen (1990), Bolle (1992), Gabrielsen R.H. and Dore A. G. (1995), Stewart et al. (1995), Sneider J.S. et al. (1995), Ravanias and Bondevik (1997),

Christiansson et al. (2000), Coward et al. (2003), Dreyer (2005), Whitaker et al. (2005), and Holgate N. E. et al.(2013).

## **1.2 Objectives**

The main objectives of this study are:

- Interpretation of 3D seismic data and mapping of main reservoir units of the Troll Field i.e. Sognefjord Formation, Fensfjord Formation, and Krossfjord Formation.
- Detailed integrated seismic and well data study of main reservoir units to determine the reservoir distribution and depositional environments.



## **2 GEOLOGICAL SETTINGS**

### **2.1 Regional tectonics**

The several multiphase tectonic events resulted in structural changes of the Northern North Sea. There are two important rift phases which occurred in Permian-early Triassic and in mid Jurassic –early Cretaceous time. The thermal cooling phase followed each rifting phase, characterized by regional subsidence (Christiansson et al., 2000).

The main structural elements (Fig.2.1a) of the eastern part of the Northern North Sea comprise the Horda Platform to the east, Viking Graben to the west and intervening Lomre Terrace. The large rotated fault blocks with sedimentary basins in asymmetric half-grabens, characterize this area (Christiansson et al., 2000).

#### **2.1.1 Permo-Triassic rift:**

The axis of this rift is centered beneath the Horda platform (Fig.2.2). Within the marginal areas of the Viking Graben, the effects of this rifting can be observed easily. The north-south structures, e.g. north-south striking rotated fault blocks are special characteristics of permo-Triassic rift. The Oygarden Fault Zone in the east and East Shetland Platform in the west bound the structures within northern North Sea rift basin. Christiansson et al., (2000) gave the evidence which shows that these areas were tectonically active during Permo-Triassic rift stage. This is based on the Devonian and older sediments from few wells in East Shetland. In Pre-Triassic half grabens, no wells reached the sediments but there are certain reasons to believe the presence of Devonian sediments there as well (Christiansson et al., 2000).

#### **2.1.2 Mid Jurassic-Early Cretaceous rift:**

The rift axis lies beneath the present Viking Graben(Fig.2.3). The extension direction was east-west initially. Later, the direction changed into northwest-southeast . This change in direction resulted in the prominent northeast-southwest trending North Viking Graben. It is not clear when this shift occurred but mid-late Jurassic or early Cretaceous age is generally believed. The late Jurassic block faulting and extensional structuring ended in early to mid Cretaceous. During the Cretaceous and Paleogene times , a period of rapid subsidence occurred. Only minor fault movements occurred along some of the master faults (Christiansson et al., 2000).

Due to the thermal cooling and reactivation of faults along the margin of basin, the initial stages of the Jurassic rifting impacted more significantly on the architecture of the graben. As a result, the Viking Graben became wider and development of a mature topography with platforms, sub-platforms and interior grabens along its axis occurred. This later activity is believed to be a gravity driven (Fig.2.5) where faulting was related to escarpments of the master faults (Christiansson et al., 2000).

### **2.1.3 Cretaceous post rift:**

The regional subsidence in the basin was caused by a phase of regional cooling after the late Jurassic rift phase. This regional subsidence led to deep water conditions at the basin center. The normal faults were still active in the early cretaceous in the North Sea. The clastic sediments were deposited in the form of onlap features terminated at erosional surfaces e.g. the Base Cretaceous Unconformity (Coward et al., 2003). The eustatic sea level rised due to the deposition of deep- water sediments in the graben depressions. In the southern and central North Sea, thick Upper Cretaceous chalk formed while in the northern North Sea, terrigenous sediments deposited. The source of clastic sediments was uplifted areas in north and west of northern North Sea. Presently, the post rift deposit is present as a relatively flat-lying sequence over he faulted synrift strata.

In a nutshell, from the late Paleozoic to the late Mesozoic, the normal faulting systems were repeatedly reactivated as shown in Fig.2.3 (Christiansson et al., 2000).

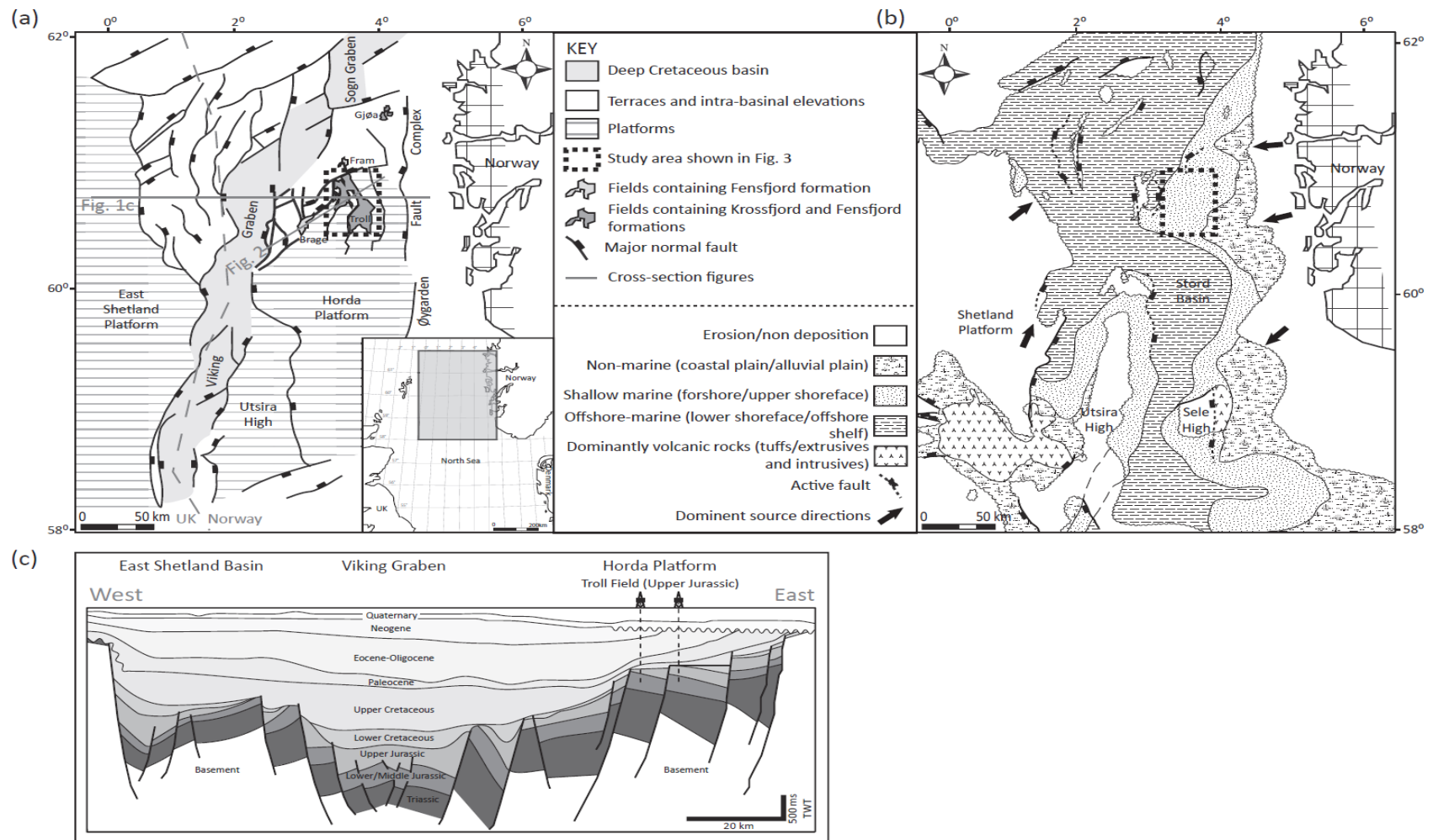


**Figure 2.1**(a) Map of the north Viking Graben is highlighting the Horda Platform, and the Troll Field (b) Palaeoenvironmental map of the northern North Sea during Callovian. (c) Geoseismic Profile showing major fault blocks across the Viking Graben (Holgate et al., 2013).

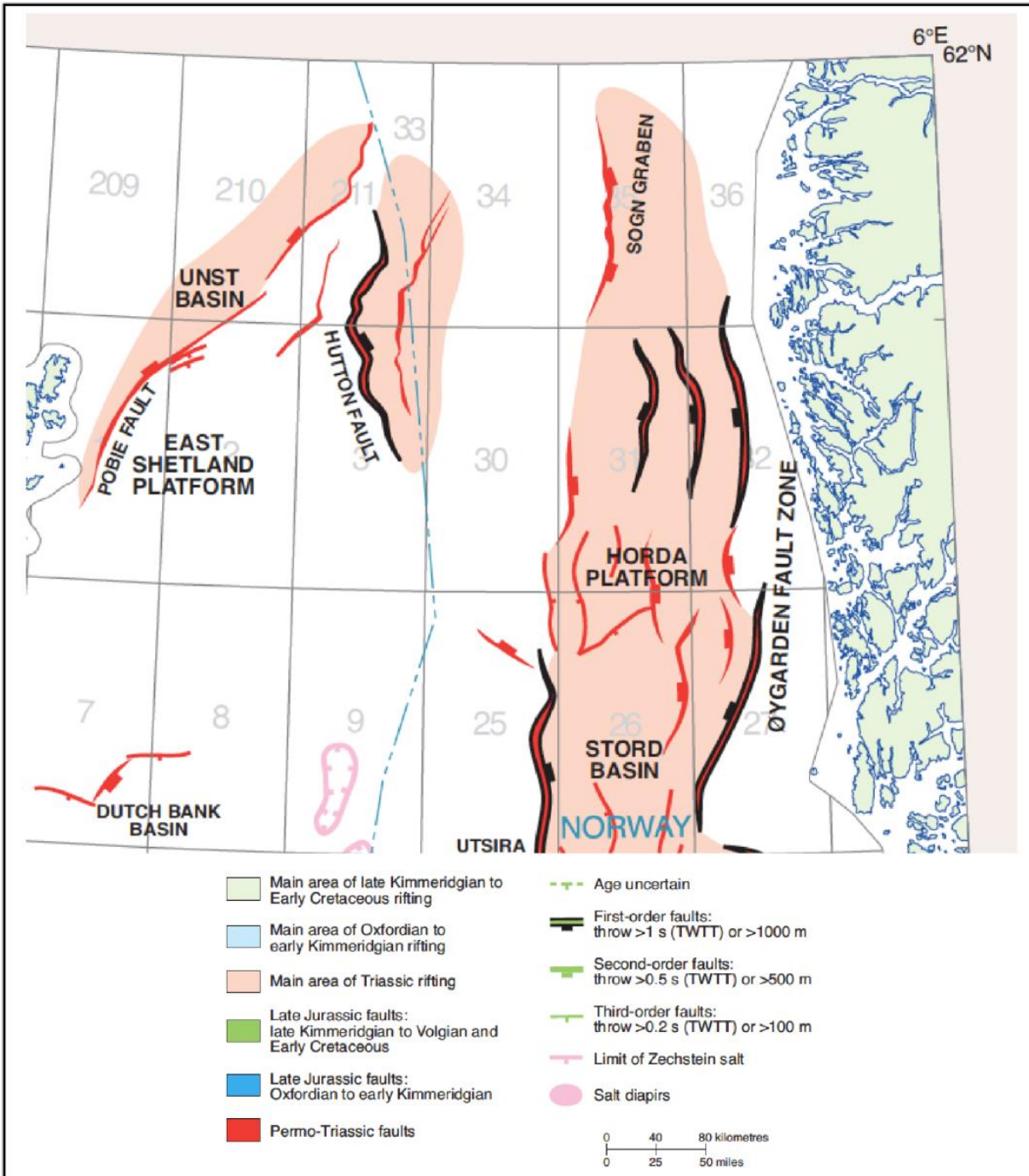


Figure 2.2 Patterns of Triassic rift phase (Zanella and Coward, 2003).

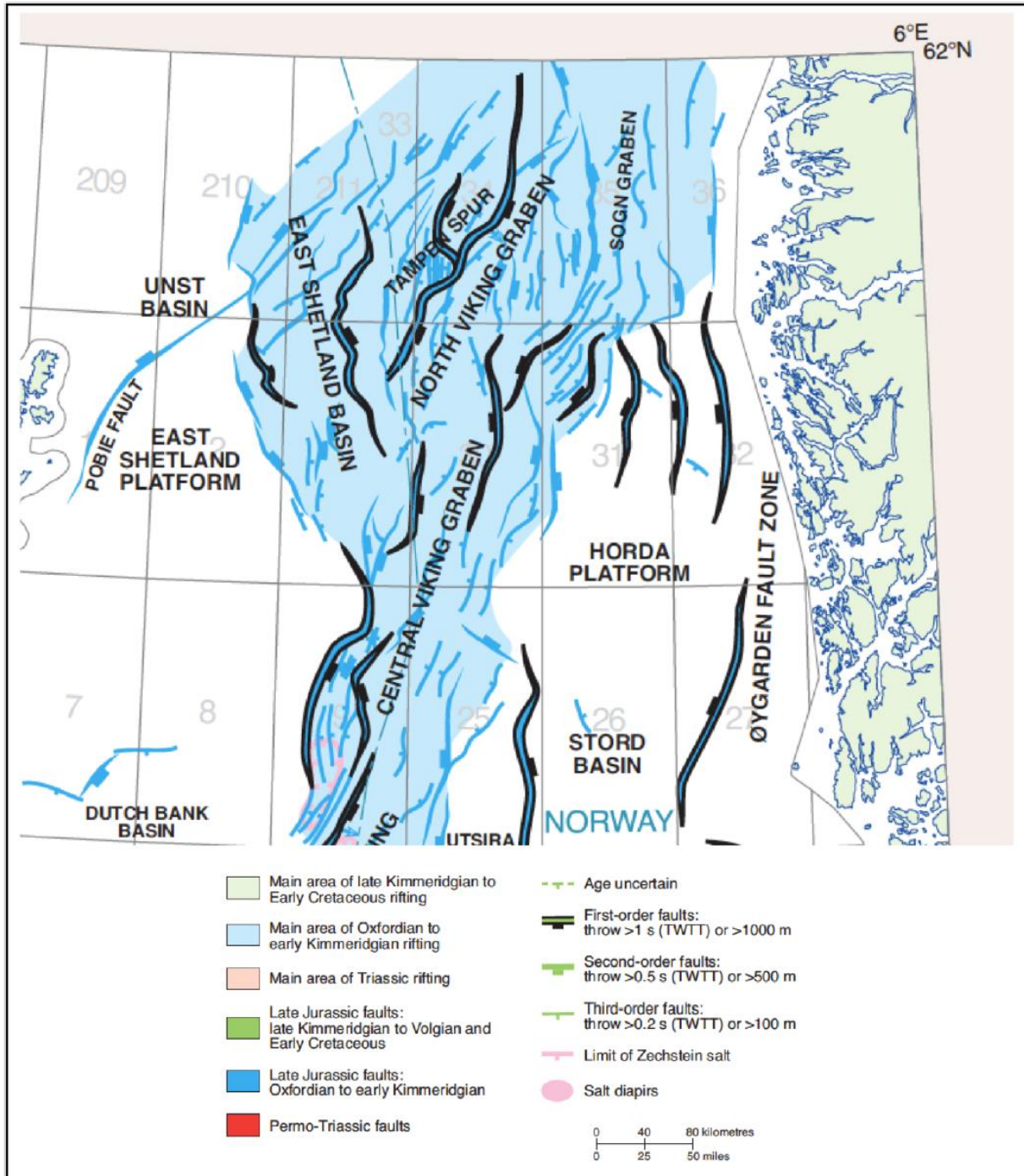
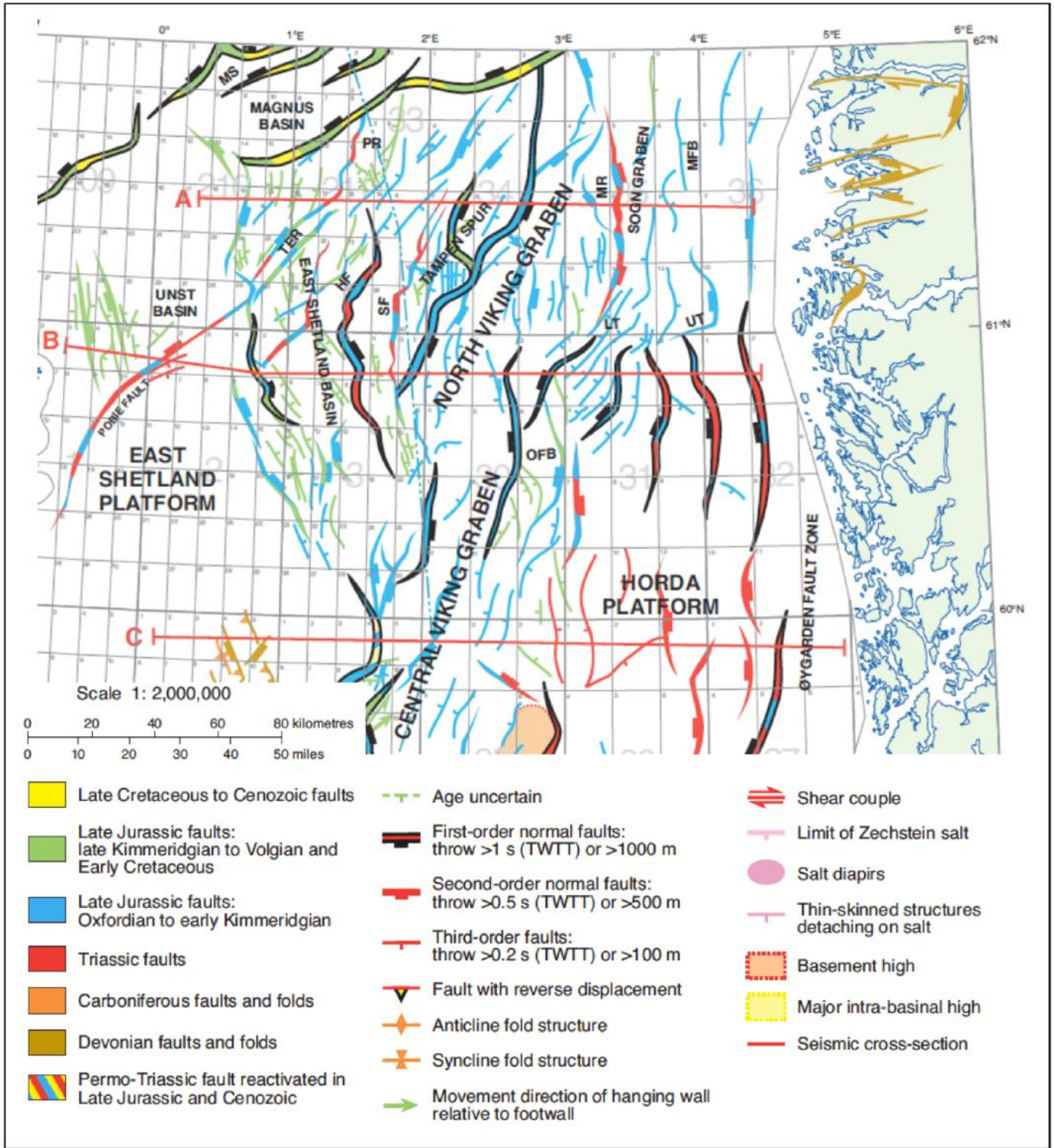
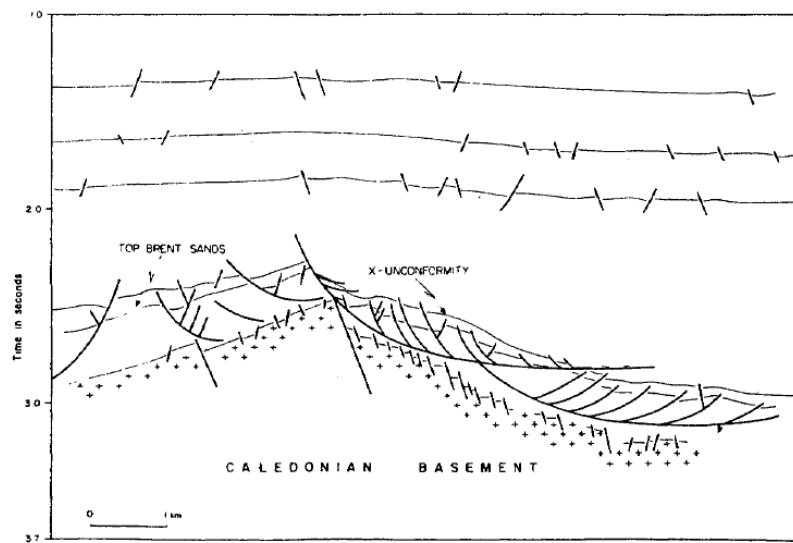
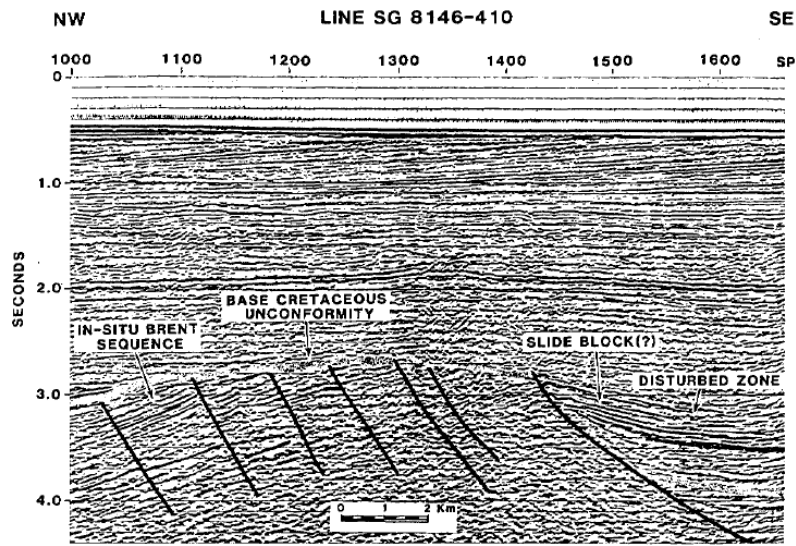


Figure 2.3 Patterns of Jurassic rift phase (Zanella and Coward, 2003).



**Figure 2.4** Map of the structural evolution of the northern North Sea from Triassic to Cretaceous (Zanella and Coward, 2003).



**Figure 2.5** Example of gravity slides on the western margin of the Viking Graben (Gabrielsen 1991).

## 2.2 Regional Stratigraphy

A generalised stratigraphic column for north viking group is shown in Fig.2.6

### 2.2.1 Devonian

In the north Northern Sea Devonian sediments are present in only few well. However, there are certain reasons to believe the presence of these sediment regionally in deeper parts of viking Graben, Horda Platform and East Shetland Basin ( Faleide et al., 2010).

## **2.2.2 Triassic**

Triassic rocks contain about 5% of the petroleum reserves and the strata are non-fossiliferous continental red beds ( Goldmith et al., 2003). The informal name of the group is Triassic Group which consist of the Cormorant Formation. The Teist, Lomvi and Lunde Formations of the Hegre Group replaced the Cormorant Formation ( Vollset and Dore, 1984).

Rifting in this period caused a pattern which reflects repeated outbuilding of sediment wedges from Norwegian and East Shetland hinterland. The continental Triassic megasequence were deposited as a result of differential subsidence. The Oygarden fault zone was active during most of this period (Steel and Ryseth, 1990).

The Triassic strata were deposited in alluvial fan, fluvial and lacustrine environments. The sediments are mainly sandstones and mudstones (Goldmith et al., 2003).

## **2.2.3 Jurassic**

### **2.2.3.1 Dunlin Group**

Dunlin Group consists of Drake, Cook, Amundsen, Johansen and Burton Formations. The Johansen Formation consists of northwestward prograding deltaic sandstones, the Cook Formation also consists of basinward wedging sandstone bodies. The Amundsen and Drake Formations consist of claystones and sandstones ( Marjanac, 1995).

This group is deposited during westward progradation and an erosional unconformity can be seen above the Johansen Formation. The beginning of regressive cycle and transition from the non-marine Triassic to marine shales of the Lower Jurassic is marked by the top of Statfjord Formation ( Sneider et al., 1995).

### **2.2.3.2 Brent Group**

The Brent Group ( Middle Jurassic ) deposited during a regressive period and consists of deltaic lithofacies. The deltaic systems prograded from south and was controlled by a domal uplift area at tripple junction between the Central, Witch Ground and Viking Graben ( Eynon, 1981). During the deposition of the lower part of the Brent Group tectonic activity was limited. However, during the deposition of upper part of the Brent Group the tectonic activity changed from slow subsidence to faster subsidence. The base of the succession represents a maximum flooding interval (Stewart et.al, 1995).

### **2.2.3.3 Viking Group**

The reservoir rocks of the Troll Field belong to the Viking Group. There are three major sandstone tongues (Fig.2.8) of Middle-Late Jurassic age i.e., Krossfjord, Fensfjord and Sognefjord formations of the Viking Group. The thickness of each of these formations is 100-300 m near the rift margin which pinch-out westwards into Heather Formation deposits.



Deposition took place as a cyclic sequence of transgressive sands and silt and progradational shoreface facies (Stewart et.al, 1995).

#### **2.2.4 Cretaceous**

The deposition of Cretaceous sediments occurred unconformably on late Jurassic sediments of the North Sea. This major unconformity is called Base Cretaceous Unconformity (BCU). The lower Cretaceous sediments consist of shallow marine mudstones, shales, and some sands. These sediments are placed in the Cromer Kroll Group (Vollset and Dore, 1984). In the late Cretaceous, the sea level was at its maximum and as a result the clastic sediments ceased. The sedimentation was dominated by Planktonic carbonate algae during late Cretaceous. The upper Cretaceous sediments consist of mudstones and minor interbedded limestones of the Shetland Group (Surlyk et al., 2003).

#### **2.2.5 Cenozoic**

The sediment architecture in the Cenozoic was affected by vertical movements. These movements are caused by tectonic activity related to the opening of the NE Atlantic Ocean (Faleide et al., 2010).

The uplifted Shetland Platform was a source of sediments for major depositional basins during the Late Paleocene to Early Eocene. Prograding wedges developed in the rapidly subsiding basin. The volcanism related to the opening of the Atlantic Ocean caused regional deposition of volcanic sediments. Progradation from the Scotland/Shetland area was mainly from the Shetland Platform in Eocene times with main developing depocentres in the Viking Graben (Faleide et al., 2010).

The swallowing of the North Sea was caused by a combination of uplift and progradation in the Eocene-Miocene times. The progradation of the Utsira Formation towards the coast in the northern North Sea shows the Late Miocene- Early Pliocene uplift and erosion of mainland Norway. The Pliocene-Pleistocene sediments are poorly sorted, glacial and partly marine reworked sediments (Faleide et al., 2010).

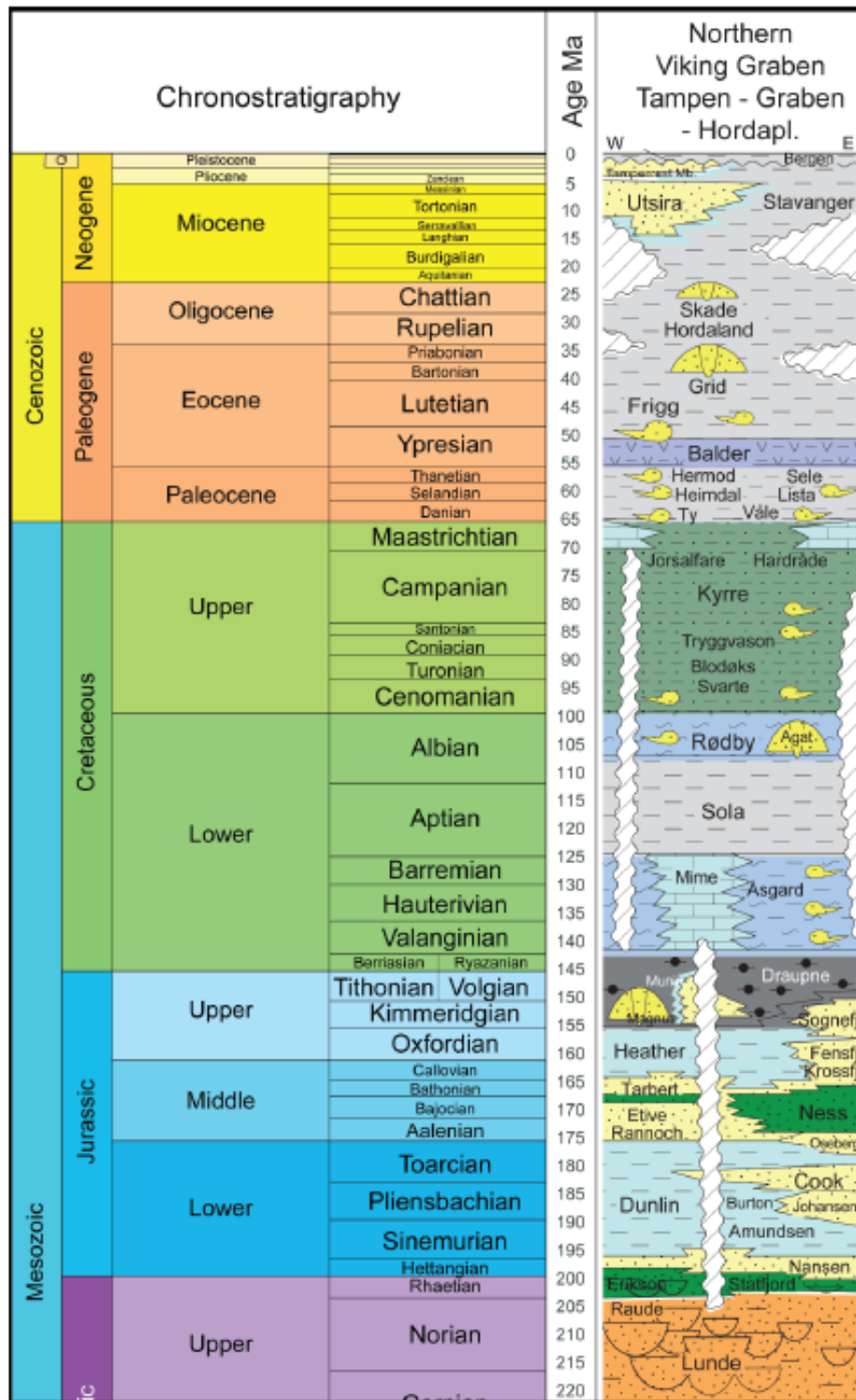


Figure 2.6: Generalized chronostratigraphic chart of the Northern North Sea (www.nhm2.uio.no).

CHRONOSTRATIGRAPHY		LITHOSTRATIGRAPHY	
PERIOD	STAGE	GROUP	FORMATION
EARLY TERTIARY	EOCENE	ROGALAND	BALDER
	PALEOCENE		SELE
			LISTA
			MAUREEN
LATE CRETACEOUS		SHETLAND	
EARLY CRETACEOUS		CROMER KNOLL	
LATE JURASSIC	RYAZANIAN		DRAUPNE
	VOLGIAN		U. HEATHER
	KIMMERIDGIAN		SOGNE
	OXFORDIAN		MID. FJORD
MIDDLE JURASSIC	CALLOVIAN	VIKING	HEATHER
			FENSFJORD
	BATHONIAN		KROSS-LOWER FJORD
			HEATHER
	BAJOCIAN	BRENT	TARBERT
	AALENIAN		NESS
			ETIVE
EARLY JURASSIC	TOARCIAN	DUNLIN	DRAKE
	PLIENSBAKIAN		COOK
	SINEMURIAN		U. AMUNDSEN
			JOHANSEN
	HETTANGIAN		L. AMUNDSEN
			STATFJORD
TRIASSIC	RHAETIAN	HEGRE	

Figure 2.7 Stratigraphic column of the Troll Field (Bolle L.1992).

## **2.3 Viking group depositional environments:**

### **2.3.1 Fensfjord Formation**

The Fensfjord Formation consists of shallow marine sequence. The maximum gross thickness of sequence is about 300 m and porosities range from 25 to 30%. Only a minor portion of the hydrocarbon is accommodated in this formation, but the bulk of aquifer is underlying this formation (Stewart et.al, 1995).

### **2.3.2 Heather B and Sognefjord Formations**

The Heather B and Sognefjord Formations consist of six depositional cycles, each characterized by a rapid rise in sea level. Every cycle starts with low energy fine micaceous sand at base and ends with clean sand at top. There are excellent reservoir properties in clean sands with porosities up to 35%. The lower energy sands exhibit porosities of about 26 to 32%. The maximum thickness of this pack is about 220 m and contains the bulk of hydrocarbons as well as an important segment of the aquifer (Stewart et.al, 1995).

### **2.3.3 Heather C Unit**

Unit C of the Heather Formation is a poor reservoir as compare to the Sognefjord Formation. It is low energy siltstone facies that is well cemented. Porosities are below 20% and permeabilities are on the order of 10 md. This unit forms a rapid westward pinching-out wedge with a maximum thickness of 44 m (Bolle L.1992).

The link between “regional” eustatic curve and Troll reservoir stratification has been revealed by recent research (Fig. 2.8). All stratigraphic boundaries can be linked to maximum flooding surface and sequence boundaries in the North Sea (Bolle L.1992).

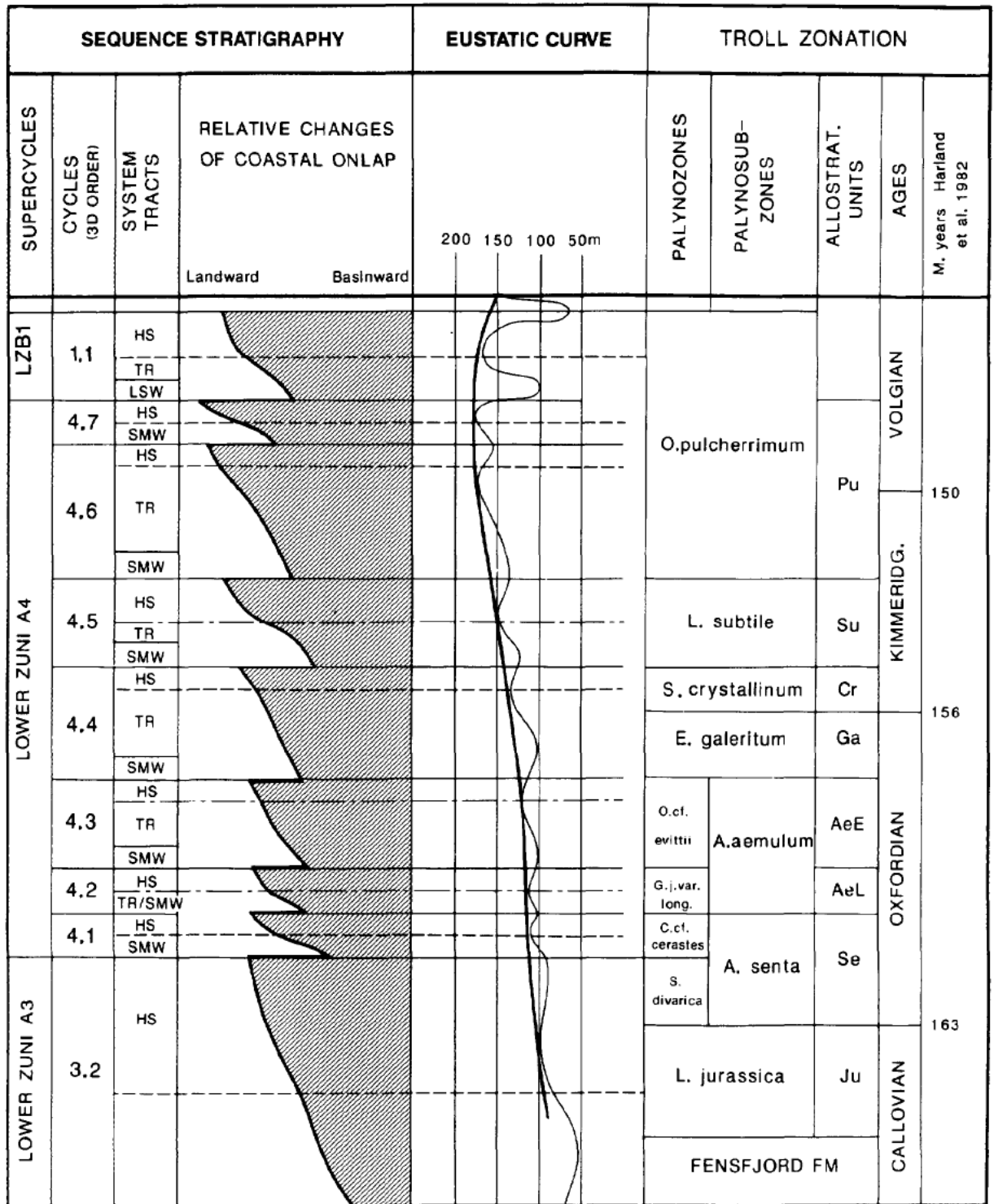


Figure 2.8: Correlation between eustatic curve and Troll deposits (Haq et al., 1987).

## **2.4 Tectonic-Stratigraphical evolution of the Horda Platform**

A generalized SW-NE tectonostratigraphic cross section is shown in Fig.2.9. The tectonostratigraphical evolution of the North Sea rift system resulted in three structural Provinces: (1) Horda Platform to the east; (2) a number of half grabens that consist of the Brage, Oseberg, Troll and Fram fields; (3) North Viking Graben to the west (Holgate, Jackson et al. 2013).

### **2.4.1 Mid Jurassic (Bathonian-latest Callovian)**

Initially the development of faulted terraces between the Viking Graben and the Horda Platform occurred. The Krossfjord and Fensfjord formations were deposited in this period. In the Troll Field, the Krossfjord and Fensfjord Formations are characterized by progradation of sand rich delta and regressive fine grained sandstones respectively. During the Late Callovian, the regression was at its peak and Fensfjord Delta covered the whole Horda Platform.

### **2.4.2 Late Jurassic (Oxfjordian-Kimmeridgian) .**

The Sognefjord Formation was deposited during this period and rifting was at its climax, creating the major structural division between the Viking Graben and the Horda Platform. Uplifting and tilting of the fault blocks occurred as a result of increased extension. On the footwall crests, erosion allowed older sediments of Sognefjord Formation to be reworked and deposited.

### **2.4.3 Early-Middle Volgian.**

The final stage of the rifting led to the development of extensive faulting in the west of the Viking Graben and minor reactivation of the faults on the Horda Platform. As a result the uplifting and eastwards tilting of normal fault blocks occurred. Consequently, many fault blocks collapsed which led to truncation of Lower-Middle Jurassic strata beneath Upper Jurassic strata in different locations of the Horda Platform. Marine flooding terminated deposition of Sognefjord Formation which resulted in deposition of deep marine Draupne Formation

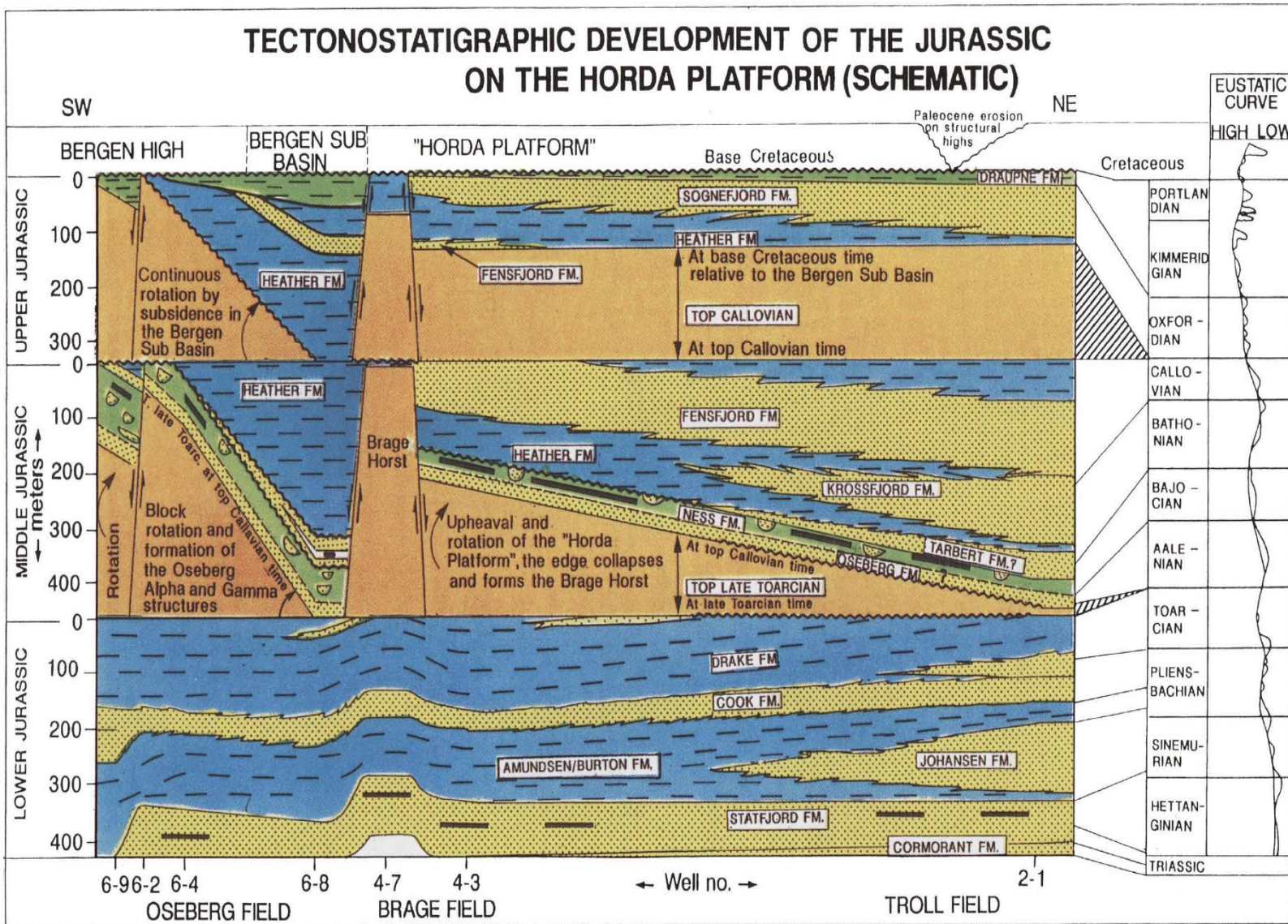
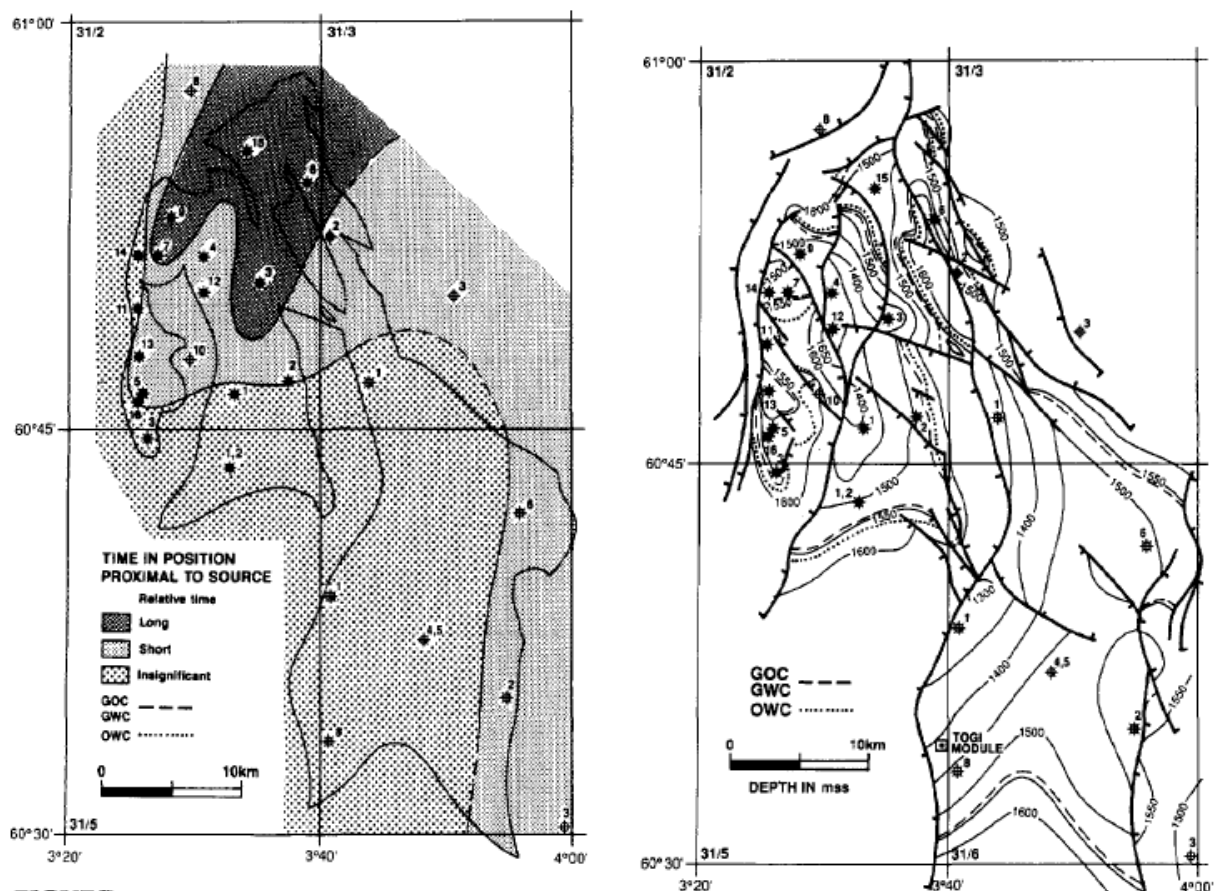


Figure 2.9 SW-NE Tectonostratigraphic cross-section with curves of global sea level changes (Johnsen Jan R. 1995).

## 2.5 Structural outline of the Troll Field

To the west; the troll field is bounded by the N-S trending Bergen high, to the north; it is bounded by a complex transform fault zone. To the south and the east the field is bounded by Stord graben and Oygarden fault zone respectively. The Troll field can be subdivided into three major fault blocks (Johnsen et al., 1995).

- a north- south fault block , it is consist of the Troll East gas province(TEP)
- a north west-south east fault block which makes the Troll west gas province (TWGP)
- a north west-south east fault block that is consist of the Troll west oil province (TWOP).



**Figure 2.10** Map of the Troll Field is showing proximities to source (Left) and top of the Troll reservoir (Right) (Bolle L.1992).



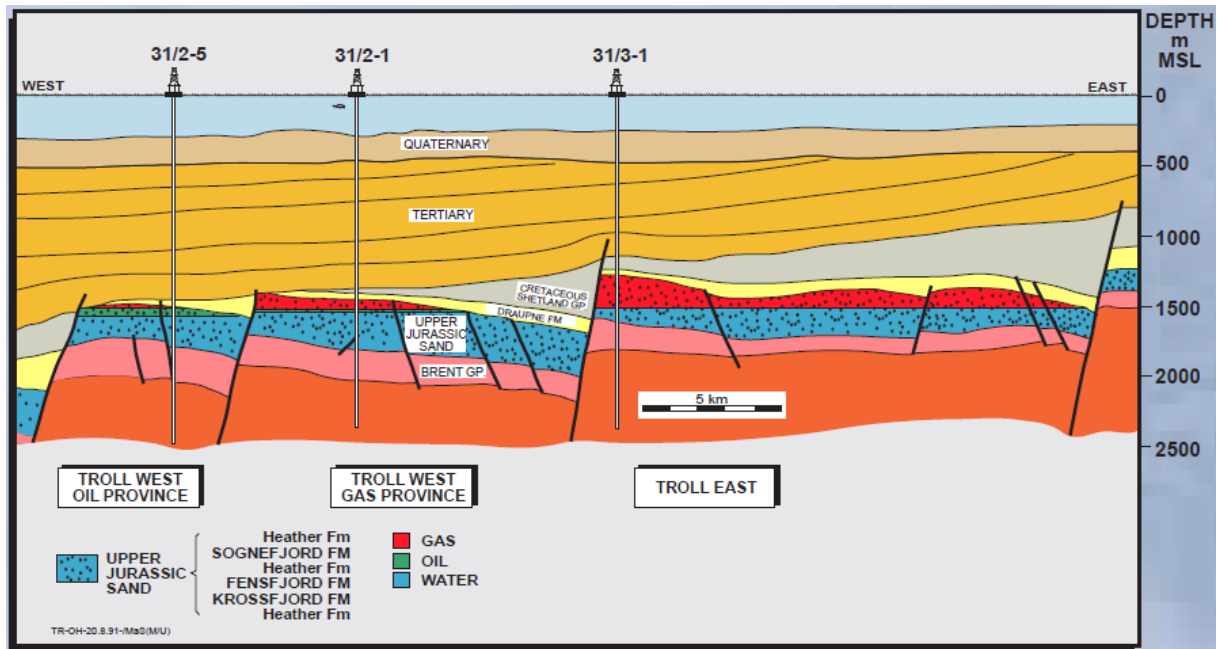


**Figure 2.11** Structural cross section and distribution of hydrocarbons through Troll Field (Johnsen et. al., 1995).

## 2.6 Key Parameters in the evolution of Hydrocarbon traps at Troll

In general, there are three key parameters which are required by the hydrocarbon traps: 1) a reservoir structure, 2) the source rock, 3) a seal. All three are present at Troll:

- The Troll field consists of horst and graben structure. These structures play important role in trapping of hydrocarbons.
- The source rock is the Draupne Formation. A considerable amount of lateral migration of oil, up to 40 km, has been documented. According to Thomas et al. (1985), the Troll “Kitchen” was located to the WNW of the field and migration of oil occurred as early as Upper Cretaceous.
- The Upper Jurassic clay stones to Cretaceous marls to Tertiary clay stones form the seal from east to west within each block sequence.

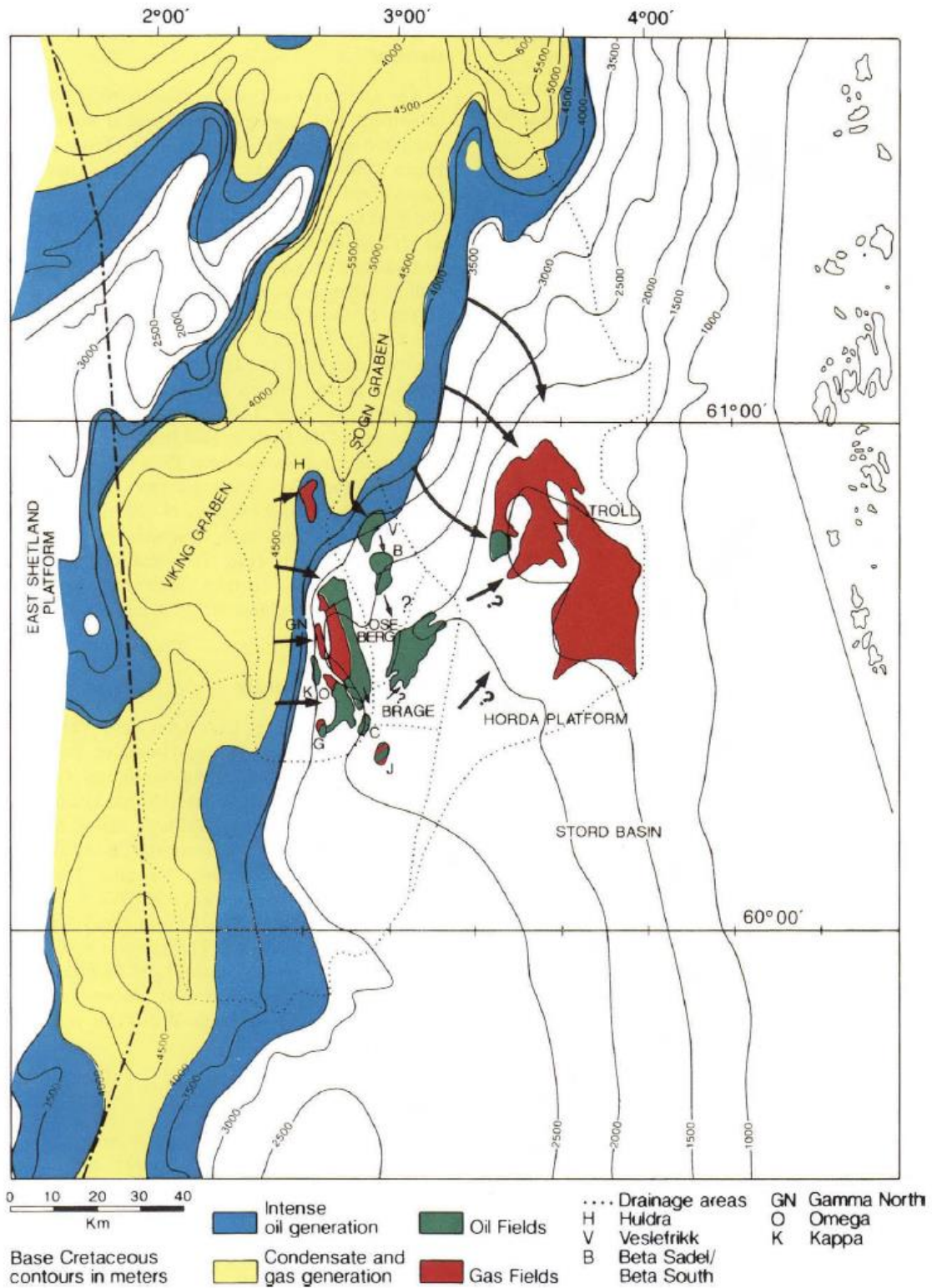


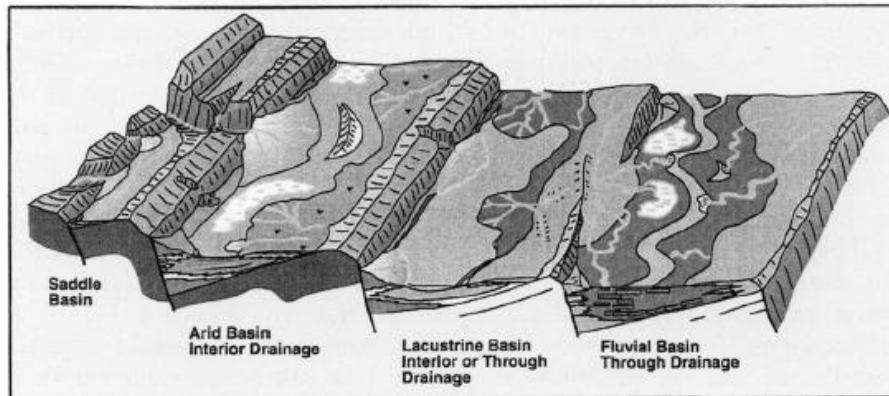
**Figure 2.12** Source and possible migration paths for the Troll Field (Johnsen et al., 1995).

## **2.7 Basin infill**

The syn-rift infill of the North Sea varies from non-marine during the late Permian- early Triassic rift episode to dominantly marine (Fig.2.13) during the middle-late Jurassic rift episode. The nature of the synrift infill is different between the distinct rift phases. The paleo-morphology of the basement and the syn-sedimentary fault activity caused a strong impact on the thickness variations. The Troll field reservoir has been heavily influenced by a series of erosional events that occurred at the end of the Late Jurassic. Main source of sediments was from hinterland, forming wedge like depositional structure in grabens (Ravnas R. et al.,2000).

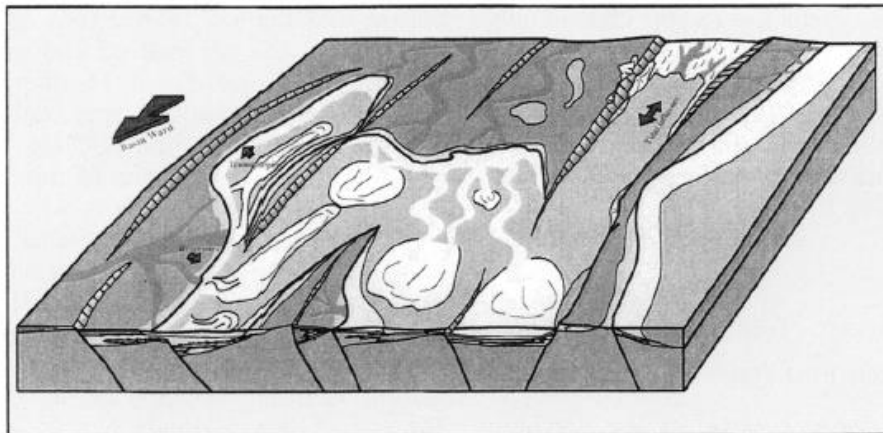
A)

**NON - MARINE RIFT - BASIN INFILL MODELS**



B)

**MIXED NON/MARINE AND SHALLOW-MARINE RIFT-BASIN INFILL MODELS**



C)

**DEEP - MARINE RIFT - BASIN INFILL MODELS**

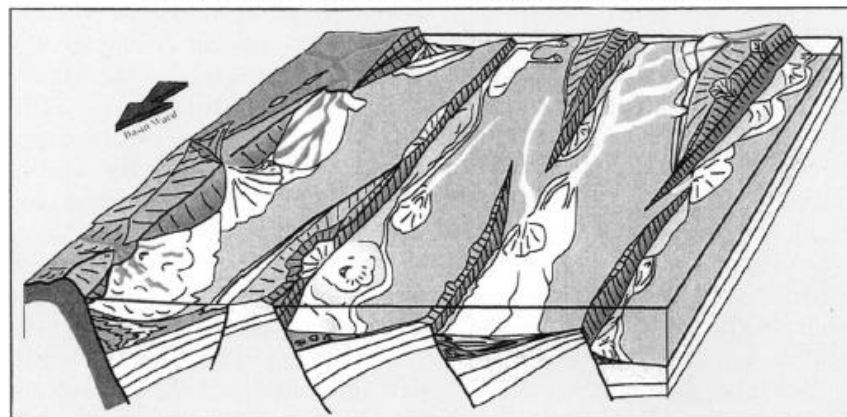


**Figure 2.13** Rift Basin infill models: (A) Non marine rift-Basin infill models: (B) Mixed non marine and shallow marine:(C) Deep marine rift-Basin infill models (Ravnas et al.2000).

### 3 DATASET AND METHODOLOGY

#### 3.1 Dataset

The dataset was provided by the Department of Petroleum Engineering and Applied Geophysics, Faculty of Engineering Science and Technology, NTNU. It consists of 3D seismic data and well data. The results of this thesis comprise the academic study that integrates seismic data and wireline logs to explain reservoir characteristics of Viking Group in the Troll West Field and its implications on hydrocarbon exploration.

#### 3.2 Well data

Well data comprise of four exploration wells (31/2-1, 31/5-5, 31/2-3, 31/3-1) that were used for detailed reservoir study. All wells contain required wireline logs and checkshots that were carefully reviewed and adjusted.

Lithostratigraphic Units	Top Depth (m)			
	Well 31/2-1	Well 31/5-5	Well 31/2-3	Well 31/3-1
Draupen FM	1414	–	–	1320
Sognefjord FM	1440	1572	1384	1352
Heather B FM	1532	1660	1508	1497
Fensfjord FM	1595	1725	1561	1516
Krossfjord FM	1742	1855	1677	1668
Heather FM	1880	–	1755	1779
Brent GP	1881	–	1812	1796
Dunlin GP	1985	–	1902	1844

Table 3.1 Stratigraphic units within reservoir encountered in different wells along with their depth.

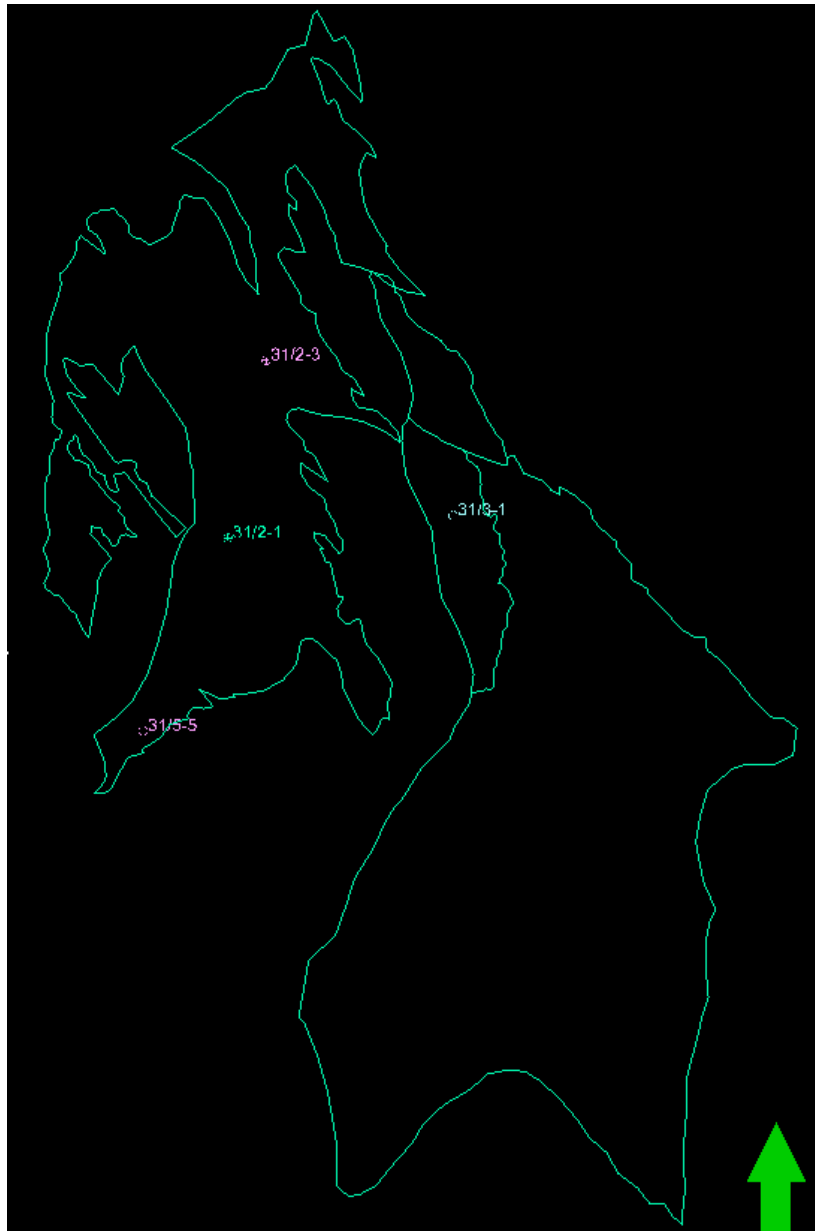


**Figure 3.1** The Troll Field outline with well locations.

### 3.2.1 Well 31/2-1

This well is the Troll West oil and gas discovery well. The well was drilled to establish the basic stratigraphy in this area, and to evaluate the prospectivity of the Jurassic sequence. The structure is formed by a tilted Jurassic fault block on the Sogn Spur High between the North Viking Graben and the Horda Platform. The migration path from Viking Graben kitchen area is provided by fault blocks. The presence of “Flatspot” was the most dominant characteristics of the structure. The cretaceous and Paleocene Claystones are sealing rocks. The well is type well for the Sognefjord, Fensfjord and Krossfjord Formations ([www.npd.no](http://www.npd.no)).

### **3.2.2 Well 31/5-5**

This well was drilled as a part of appraisal programme. The main objectives of the well were to provide geological, geophysical and petrophysical data for evaluation of oil producers in Troll West Gas Province (TWGP9); and to provide data on the Fensfjord and Krossfjord Formations to improve aquifer modelling. The well was further planned for late re-entry for vertical recompletion for Sognefjord Formation reservoir monitoring ([www.npd.no](http://www.npd.no)).

### **3.2.3 Well 31/2-3**

This well was drilled about 8 km NNE of the Troll Discovery well 31/2-1. The objective of the well was to appraise the Troll Discovery. It should evaluate reservoir parameters along maximum gross hydrocarbon column; prove maximum hydrocarbon reserves in major northern fault block; confirm the significance of the seismic flatspot; and evaluate the earlier Kimmerian fault movements on reservoir characteristics. ([www.npd.no](http://www.npd.no))

### **3.2.4 Well 31/3-1**

The wildcat well was drilled in the Troll East area. The well established the existence of a Troll East gas Field. The objective of this well was to test possible hydrocarbon accumulations in Jurassic age sandstones. The secondary objective was to test hydrocarbon accumulation in Late Triassic Formations ([www.npd.no](http://www.npd.no)).

## **3.3 Seismic data**

Seismic data include two regional lines (MN9103-308 and MN9103-308A) 3D seismic survey named NH 9101-NH8901. 3D seismic cube is used for detail interpretation of reservoir section. The total numbers of inlines and cross lines in seismic cube are 1659 and 2749 while Inlines and cross lines interval is 18.75 and 12.50 respectively. The polarity of 3D seismic data is normal (American standard) as shown in Fig. 3.2 and 3.3 by increasing acoustic impedance with depth. These Figs. show that peak (Red) is taken as sea bottom. The quality of data considered as good.

## Data Polarity

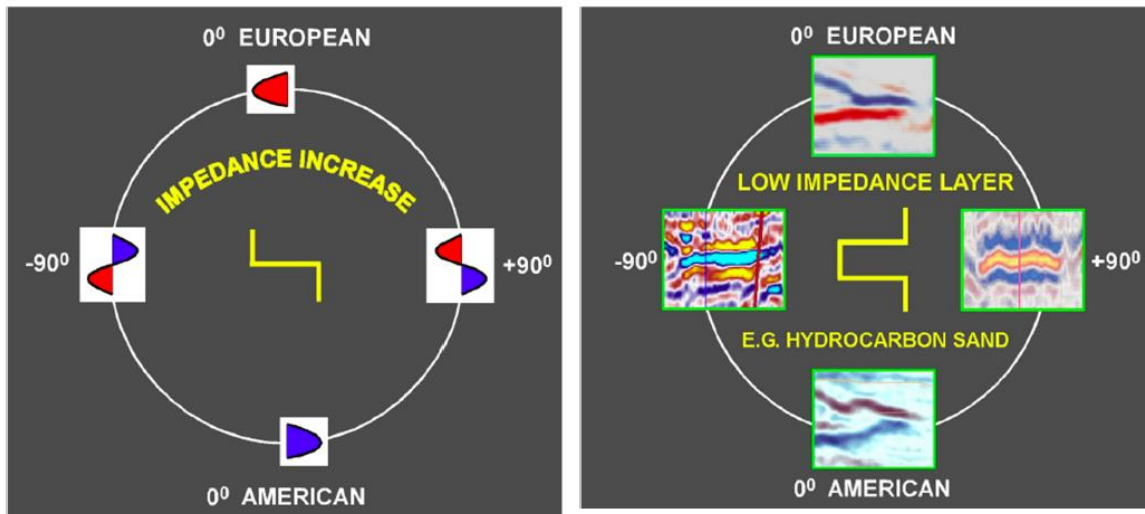


**Figure 3.2:** Two Types of data polarity, American and European (Brown 2005).

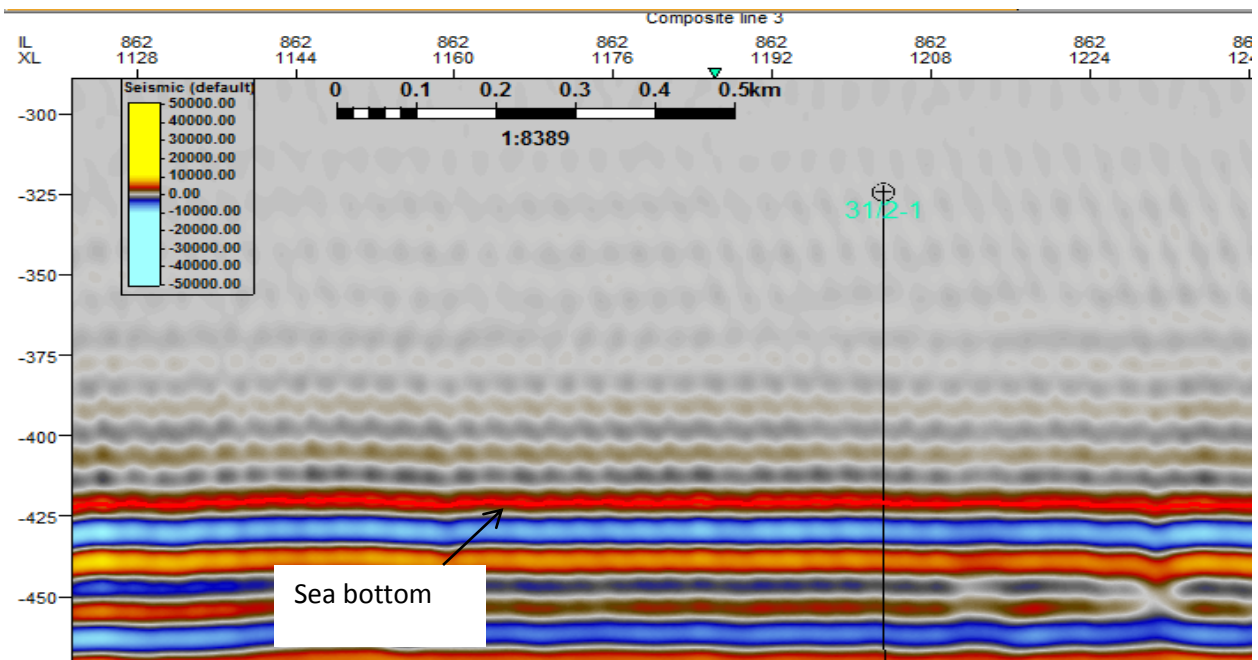


**Figure 3.3:** Sea bottom is interpreted as a peak (Red)



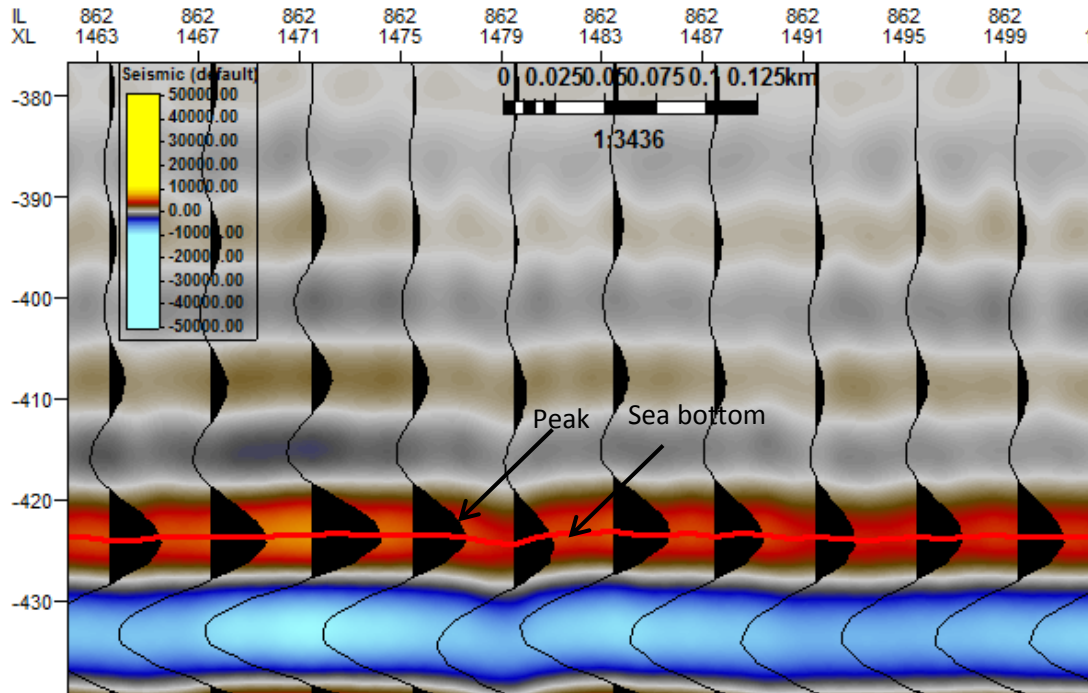


**Figure 3.4:** Peaks showing interpreted sea bottom.

## 3.4 Methodology

### 3.4.1 Software

Petrel (version 2013), Tech log, and Illustrator have been used for this thesis. Petrel is window based software and is assets of Schlumberger. Petrel can perform various operations, including interpretation of seismic data, well correlation, reservoir modelling, volume calculations etc. Following are the features that are used during the work.

### 3.4.2 Data Import

This process involves the loading of data into the software. That includes well data and 2D/3D seismic data which is loaded in SEG-Y format. The first step for the import of well data is to insert a new well. Then to give coordinates for the particular well along with the Kelly bushing value. Well tops folder is generated to enter the well tops. Similarly checkshot data is imported into the data base.

The new seismic main folder is generated by using insert option for loading of 3D seismic data. Then a subfolder is generated named as seismic survey. Finally all kind of seismic data is stored into the software as a SEG-Y format.

### **3.4.3 Seismic to well tie**

Before starting the seismic interpretation process, it is necessary to do seismic to well tie. This step is very important because the interpretation of certain horizons is based on this step. The sonic and density logs were used to create a synthetic seismogram. The synthetic seismograms for the above wells were created and the seismic reflectors were time shifted. The well top depths are obtained from Norwegian Petroleum Directory and these well tops assigned to the wells penetrating the interval of interest.

### **3.4.4 Seismic interpretation**

Three kinds of windows are used to perform seismic interpretation. These are 3D, 2D and interpretation window. Horizons can be interpreted by four different ways. These are the followings:

- Manual interpretation
- Guided auto tracking
- Seeded 2D auto tracking
- Seeded 3D auto tracking

Most of the selected horizons were interpreted by Guide auto tacking.

### **3.4.5 Map generation**

After interpretation of seismic data various maps can be generated e.g. time structure map, time thickness map etc. The resulted maps can be viewed in 3D, 2D and Map window in order to understand the results of interpretation in terms of stratigraphy and tectonics. For generation of maps the process of Make/edit surface is used after complete interpretation of certain horizons. Finally the result of these certain horizons is viewed in desired window. The following flow chart explains the procedure for seismic interpretation.

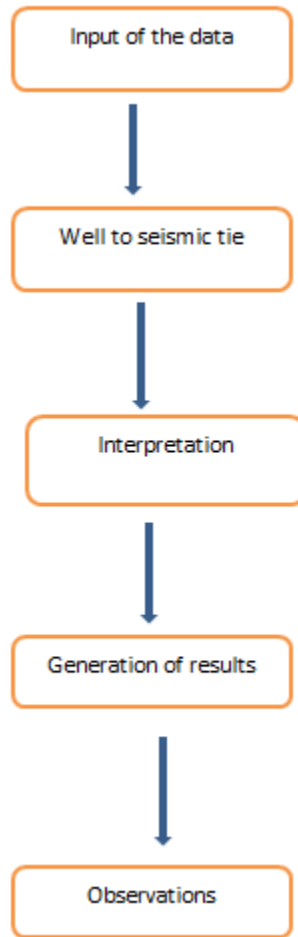


**Figure 3.5** Flow chart shows the procedure of seismic interpretation.

## 4 SEISMIC INTERPRETATIONS

Seismic interpretation was performed in order to understand the reservoir distribution, depositional environments and depositional elements along the Troll West field. Firstly, seismic well tie process was performed to ensure the correlation between well and seismic data. It was followed by the horizon interpretation which was challenging in some parts due to partial erosion and poor data quality. Structural interpretation was focused on major faults.

### 4.1 Seismic Well Tie

Seismic well tie is the critical process to bridge the well data with seismic data by making synthetic seismogram. The seismic well tie process is performed for the wells 31/5-5, 31/2-1 and 31/2-3. The synthetic seismograms were created from logs and seismic data was used to extract the wavelet. Extraction of wavelets based on statistical methods to get a reliable level of confidence.

Sonic logs were corrected for caving and invasion. Time depth relationship was initially corrected by using checkshot data. The correlation between the synthetic and seismic data was improved by making further corrections to the time-depth relationship. The Fig. 4.2 shows the process of Sonic Calibration for the well 31/2-3. seismic well tie process for well 31/2-3. The relationship of time and depth at reservoir zones is good for further interpretation. The Fig. 4.3 the process of synthetic generation for the well 31/2-3 with main well tops. The Fig. 4.4 shows integrated seismic well tie results for well 31/2-1 and 31/2-3 with key well tops . The following figure 4.1 shows three main steps of seismic to well tie:

1. Sonic calibration
2. Synthetic generation
3. Integrated seismic well tie

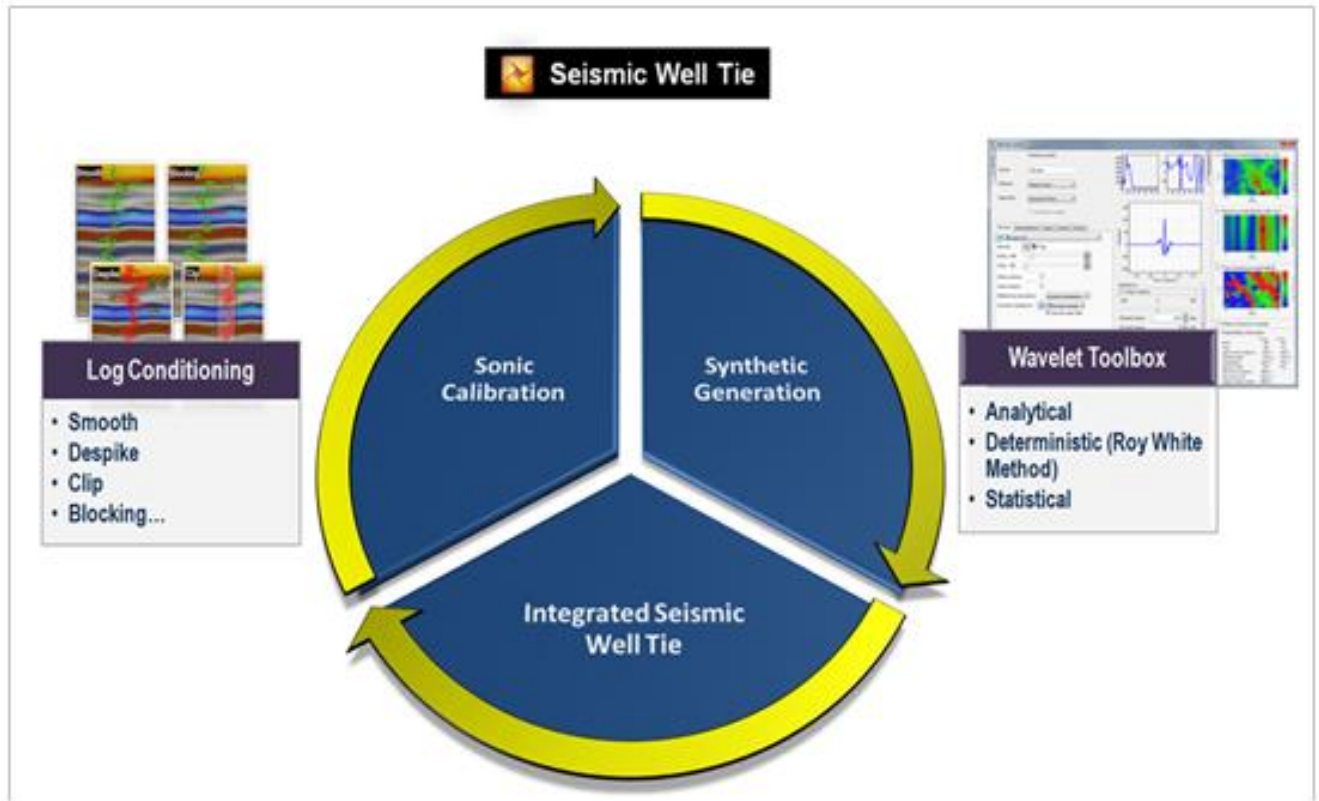


**Figure 4.1:** Main steps of Seismic well tie process

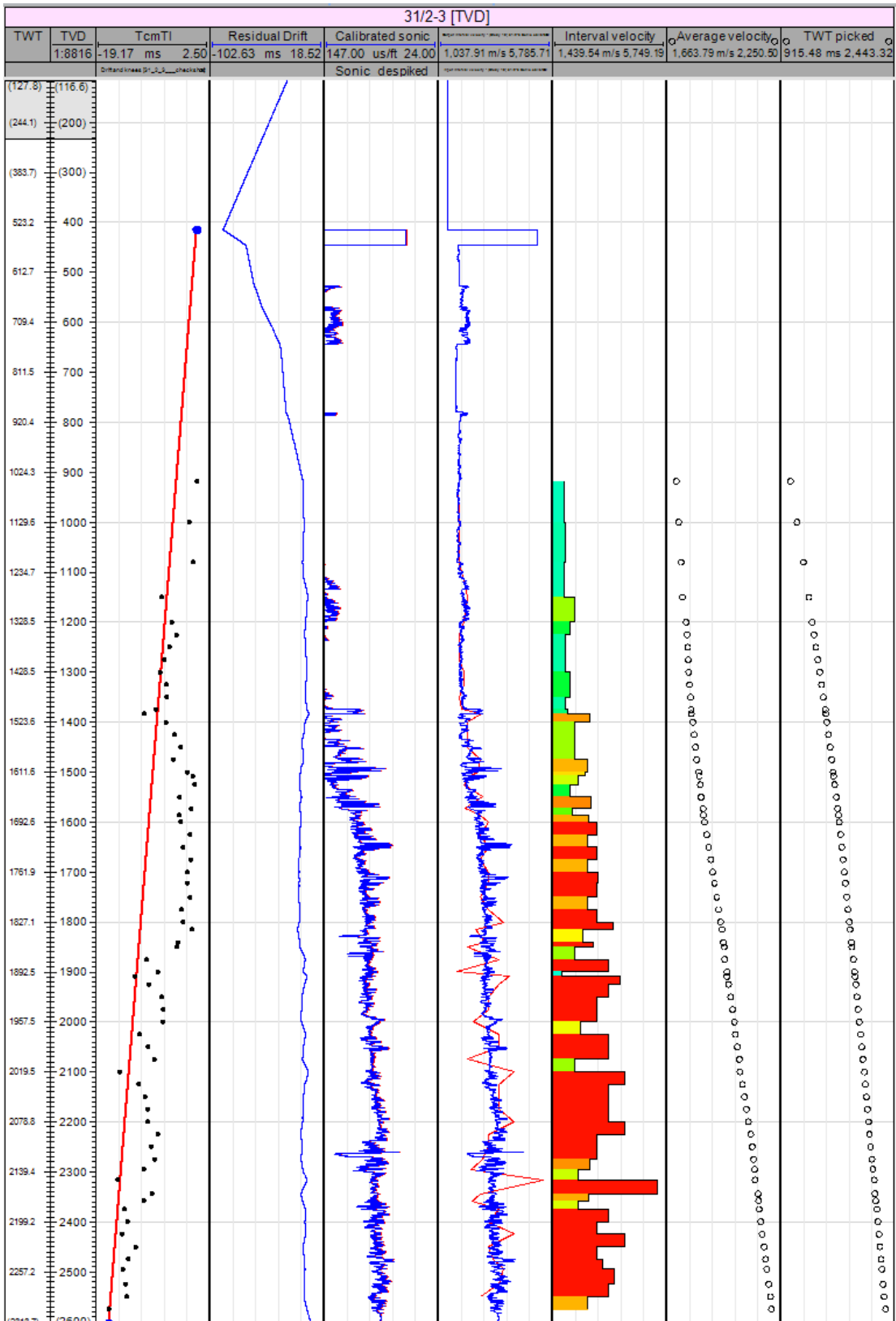


Figure 4.2: The process of Sonic Calibration for the well 31/2-3 with main well tops.

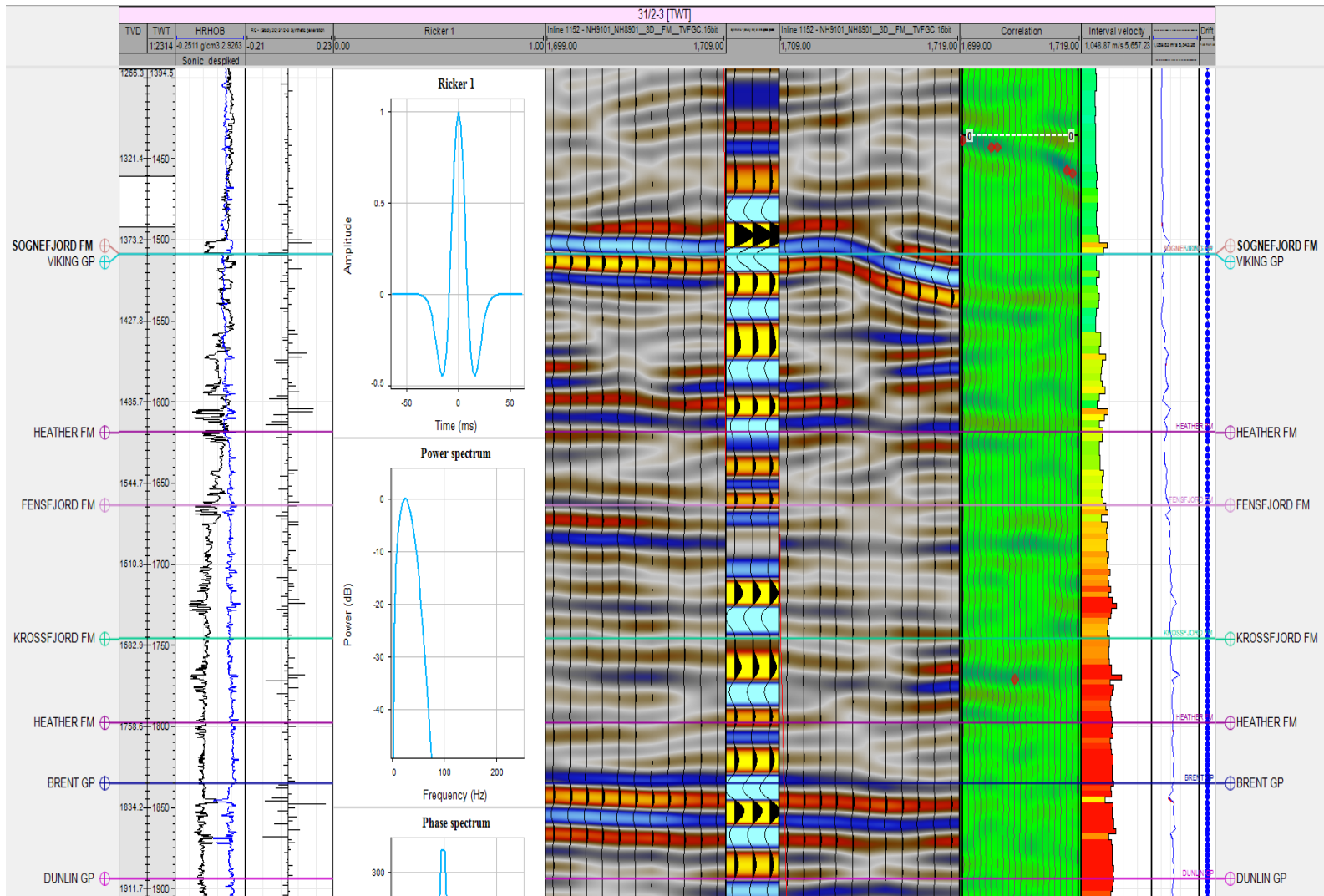
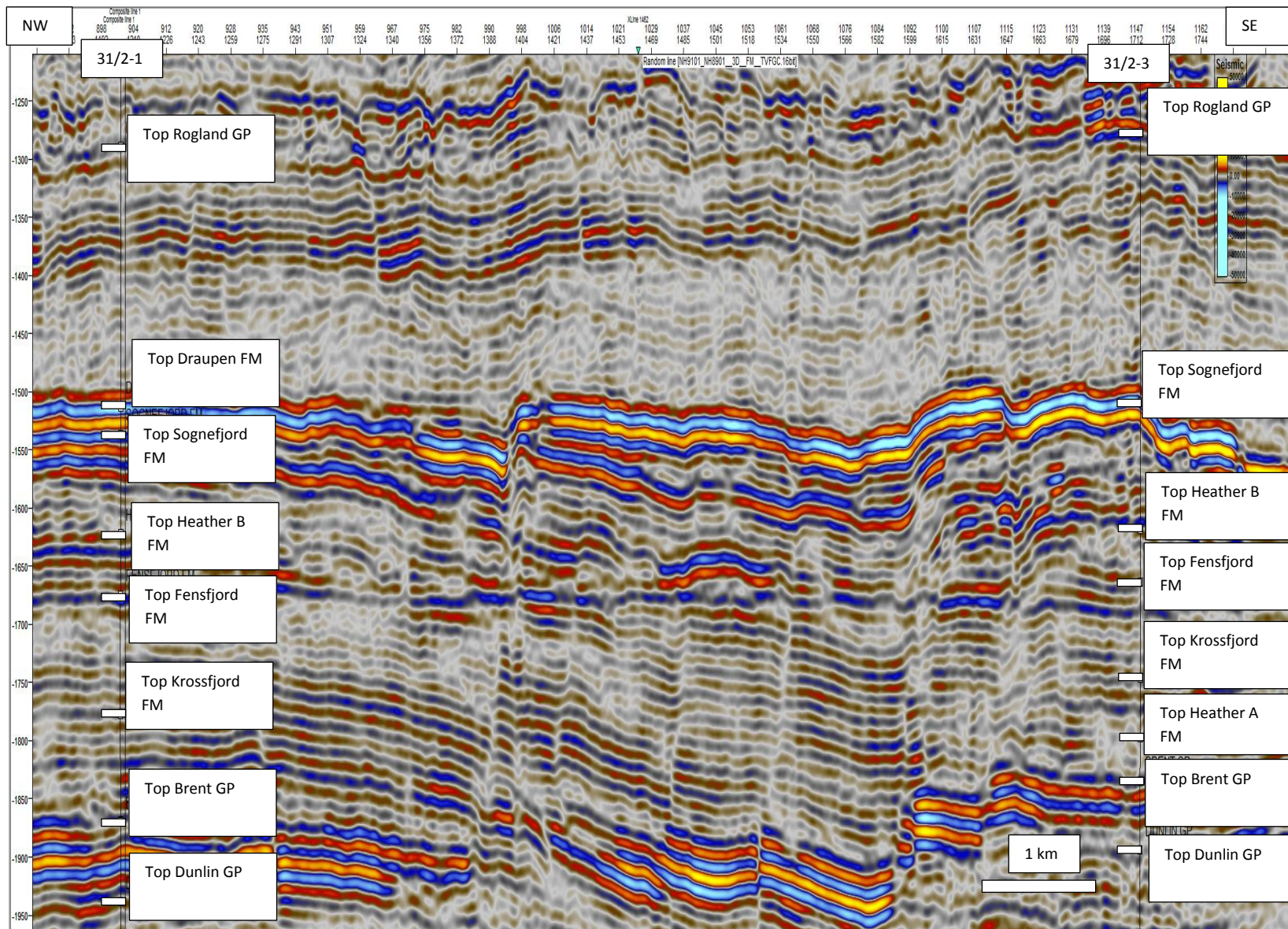
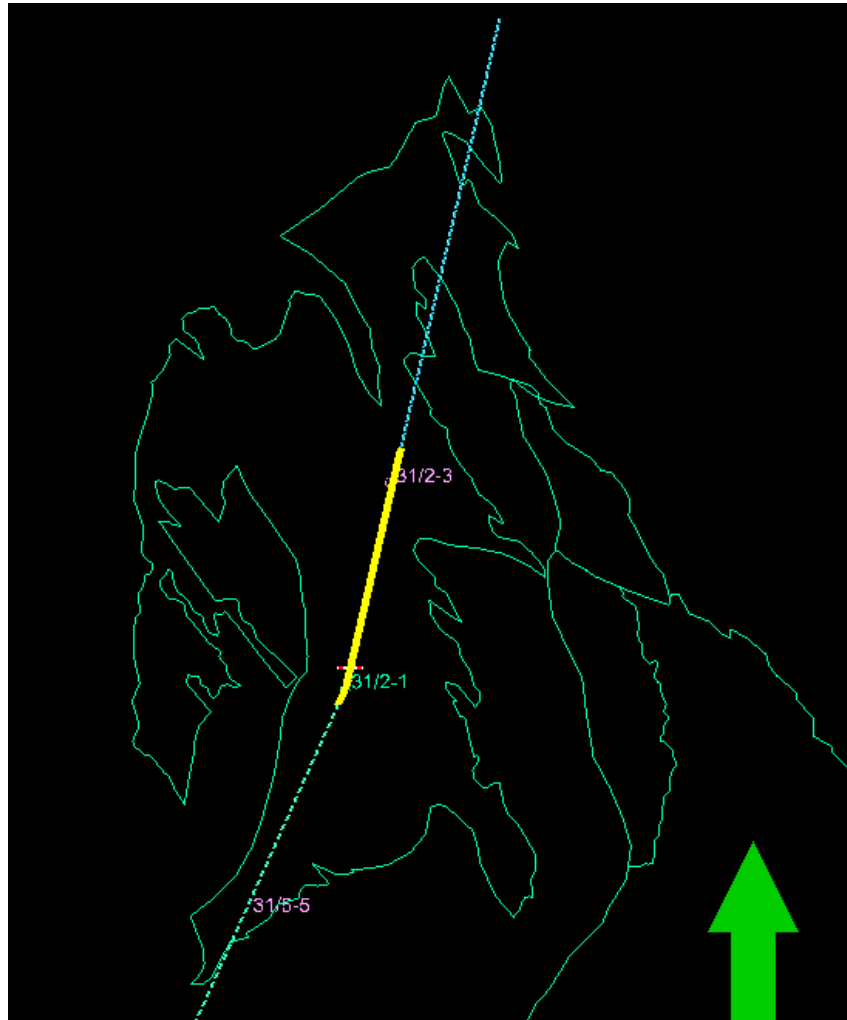


Figure 4.3: The process of synthetic generation for the well 31/2-3 with main well tops.





**Figure 4.4** Seismic cross-section showing integrated seismic well tie results for well 31/2-1 and 31/2-3 with key well tops . For location of section see Fig. 4.5



**Figure 4.5:** Location of seismic section in Fig. 4.4

## 4.2 Regional Interpretation

The evolution of the northern North Sea is considered to be simple and consistent from section to section. The present thesis study shows significant inhomogeneities in this simple picture.

Several regional and semi regional unconformities are identified. The most prominent is transition between basement and the Triassic. In addition, some steeply dipping sequences within the Lower Triassic are identified. These sequences become flatten progressively into Middle and Upper Triassic strata which are broadly conformable with overlying lower Jurassic strata. Rotated fault blocks are also interpreted which may have caused local unconformities (Gabrielsen 1990).

#### 4.2.1 Structural Description

To the extreme east a faulted shallow basement is identified. The faults are characteristically normal syn and antithetic faults. Locally half graben like basins with minor sediment filled (Gabrielsen, 1990).

The Oygarden Fault Zone (Fig. 4.8) is an extensional fault separating the shallow basement area from the Horda Platform. The sequences above the unconformity ( between basement and the Triassic) in the hanging walls of the Oygarden Fault Zone dip regionally towards the west, i.e. towards the basin. On the other hand, the sequences below the Unconformity dip in the opposite direction. i.e. towards the Oygarden Fault Zone. These differences may be indicative of reactivation of the faults of this zone (Gabrielsen 1990).

The Mesozoic and Palaeozoic mega units can be followed towards west across the faulted Horda Platform where an abrupt change in the dip of the sequences occurs at one of the major faults (Fault A). Crossing this fault, the dip in the lower Jurassic sequence is changing from westerly to easterly. On the contrary, the upper Jurassic and the Cretaceous sequences still dip towards the west, down-lapping the previous sequence (Gabrielsen, 1990).

The Horda Platform area is bounded to the west by the Eastern Graben Margin Fault system(EGMF). This fault system is seen as a series of normal faults which makes a “Book Shelf Model”. The eastern faults in this system border easterly- tilted fault blocks, whereas the western faults border the westerly tilted fault blocks. The number of antithetic faults also increases here (Gabrielsen, 1990).

The eastern margin of the Viking Graben (Fig. 4.8) is the point where the tilt of the fault blocks changes from easterly to westerly. The western margin of the depression coincides with a sub platform. This sub platform is bounded by a series of westerly rotated fault blocks defining the Western Graben Margin Fault system ( WGMFS), (Gabrielsen, 1990).

The Tampen Spur is characterized by several large, rotated fault blocks with internal listric fault systems. The rotated fault blocks, which consist of the giant oil fields of the Viking Graben province like Gullfaks, are delineated by large faults with deep roots (Gabrielsen 1990).

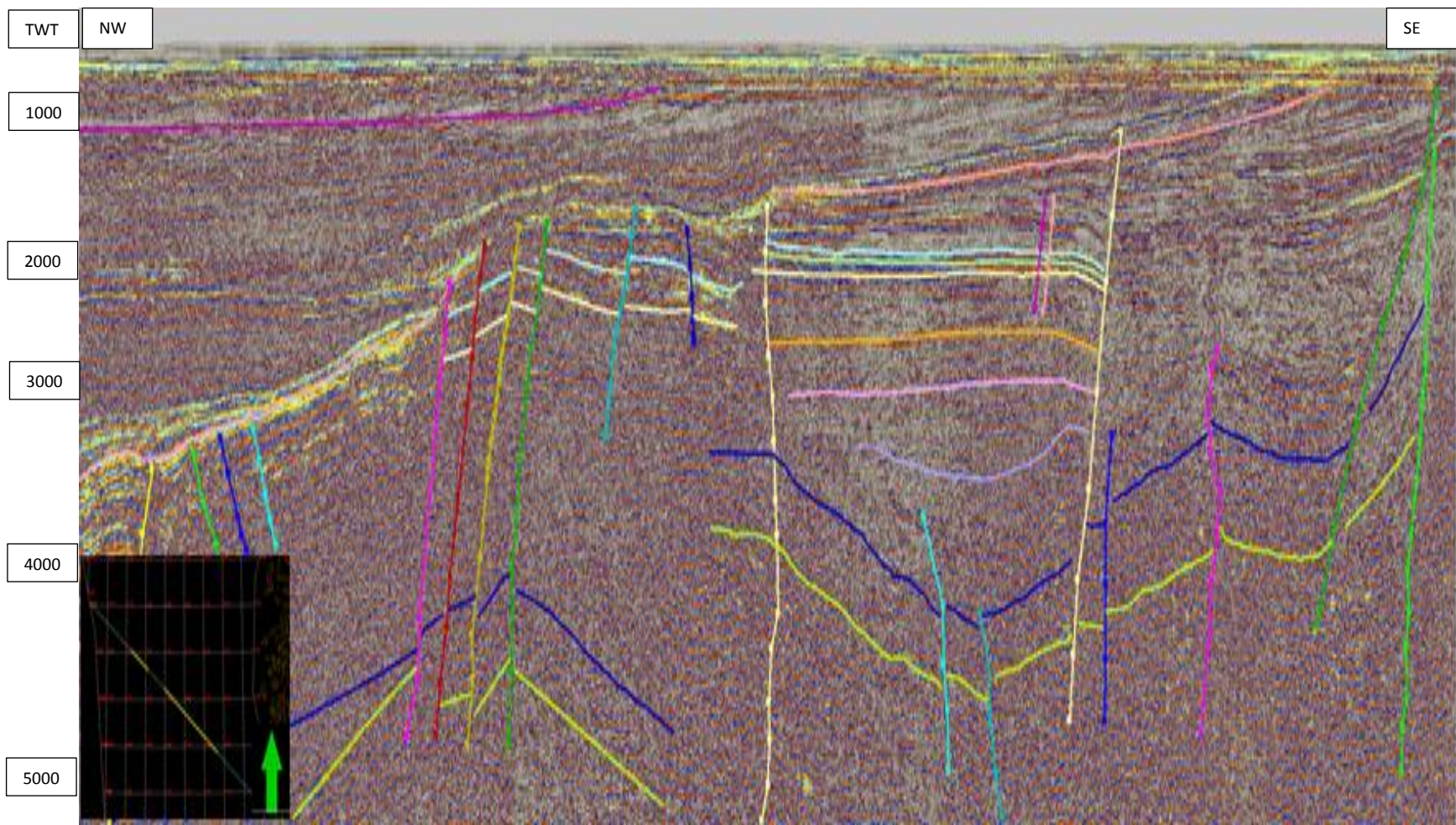


Figure 4.6 Interpreted 2D regional seismic line MN9103-308.

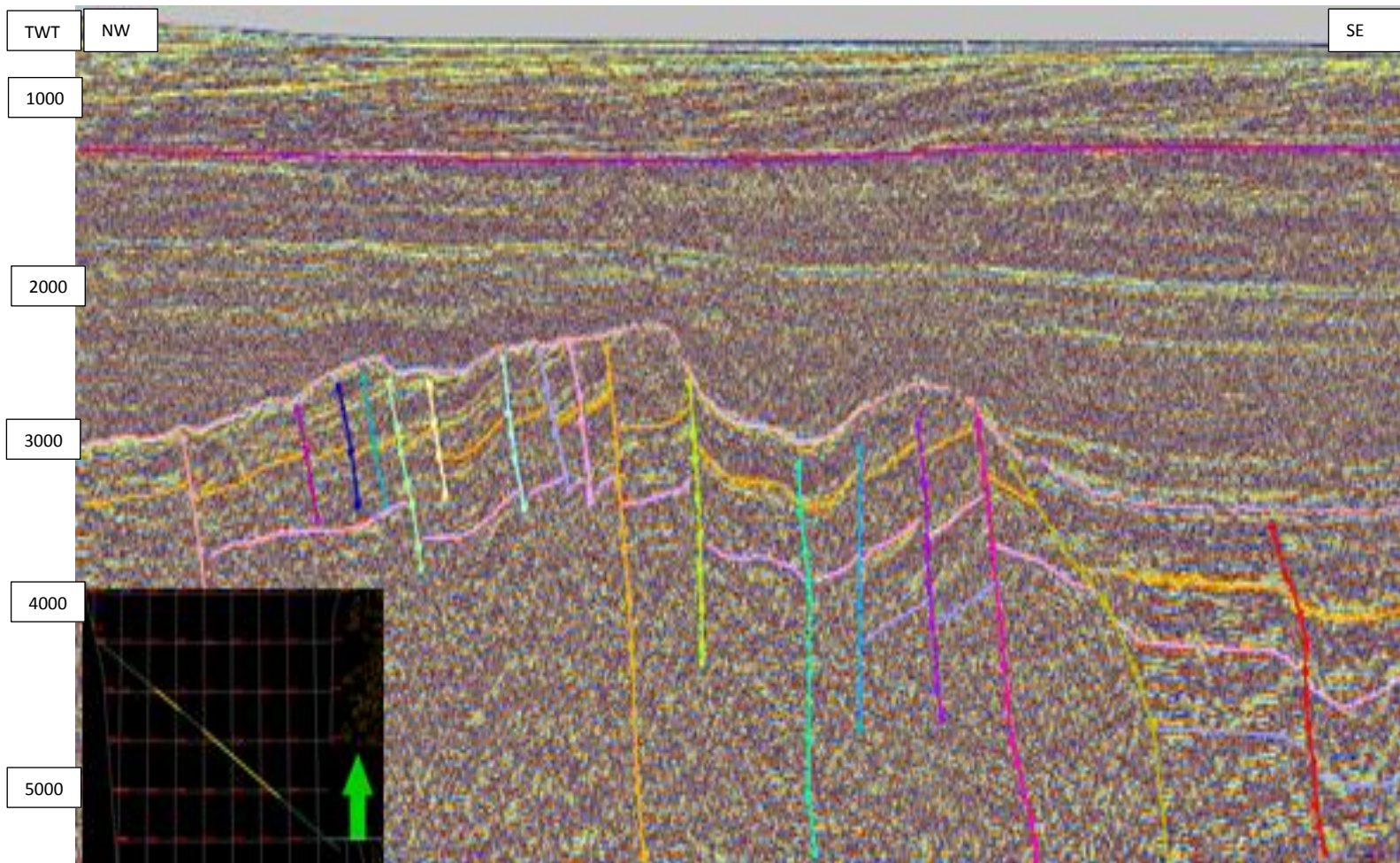
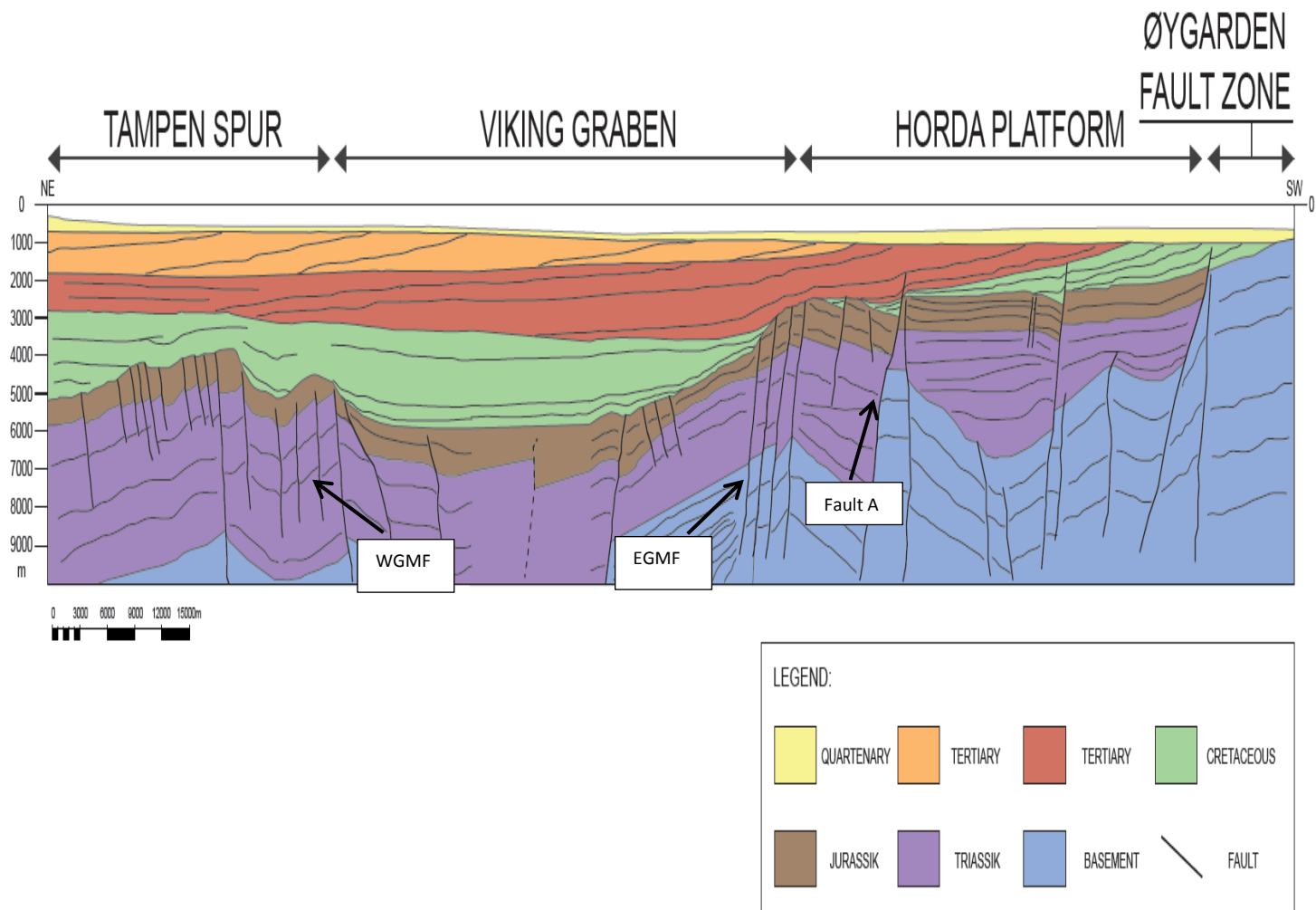


Figure 4.7 Interpreted 2D regional seismic line MN9103-308A.



**Figure 4.8** Regional profile model made from interpretation of 2D seismic lines.

### 4.3 Troll west Interpretation

#### 4.3.1 Base of Quarternary

This marker is highly continuous and defines a major truncating angular unconformity as can be seen by truncation of strata in Fig. 4.10 The time structure map of interpreted horizon is shown in Fig..

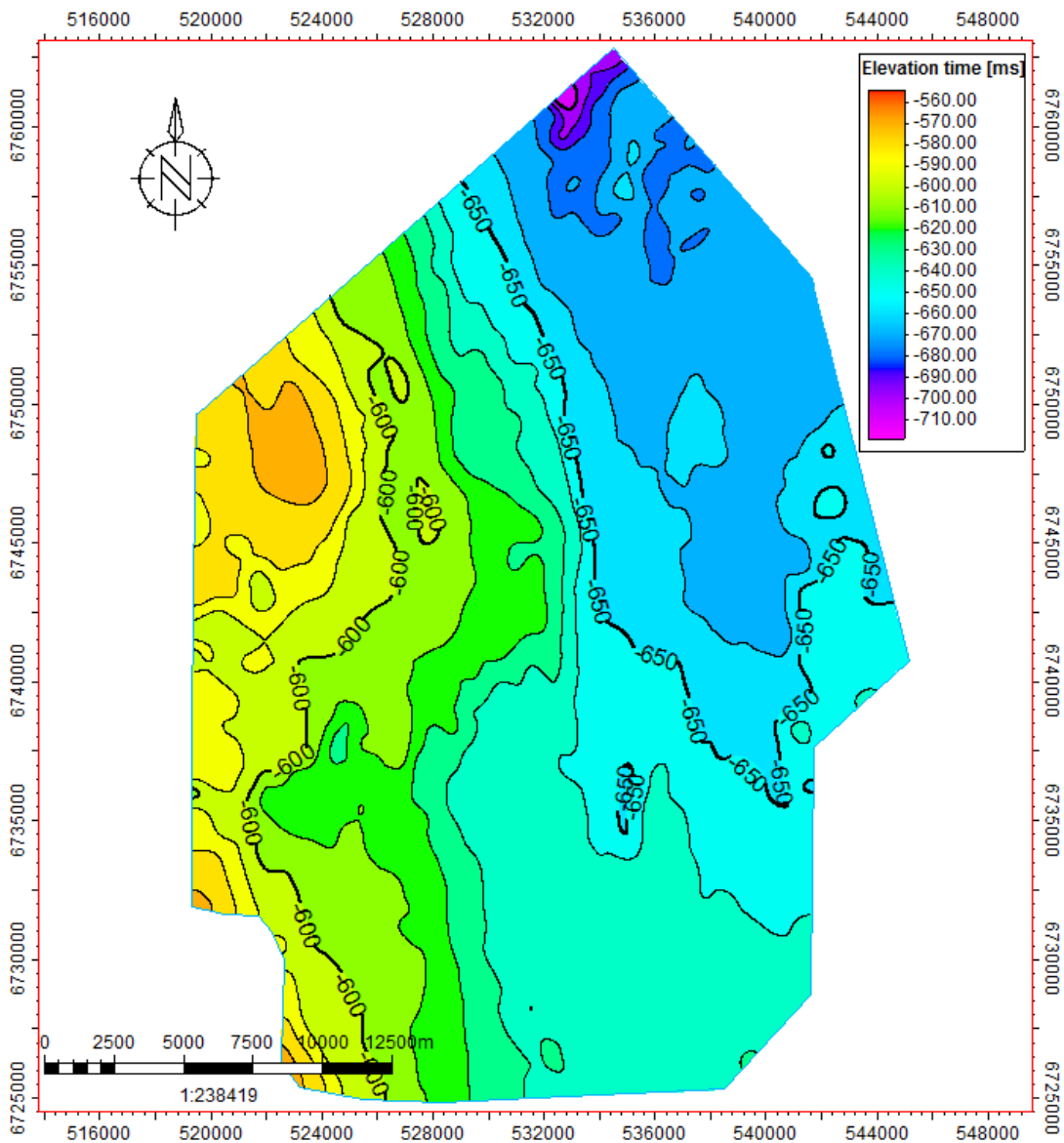
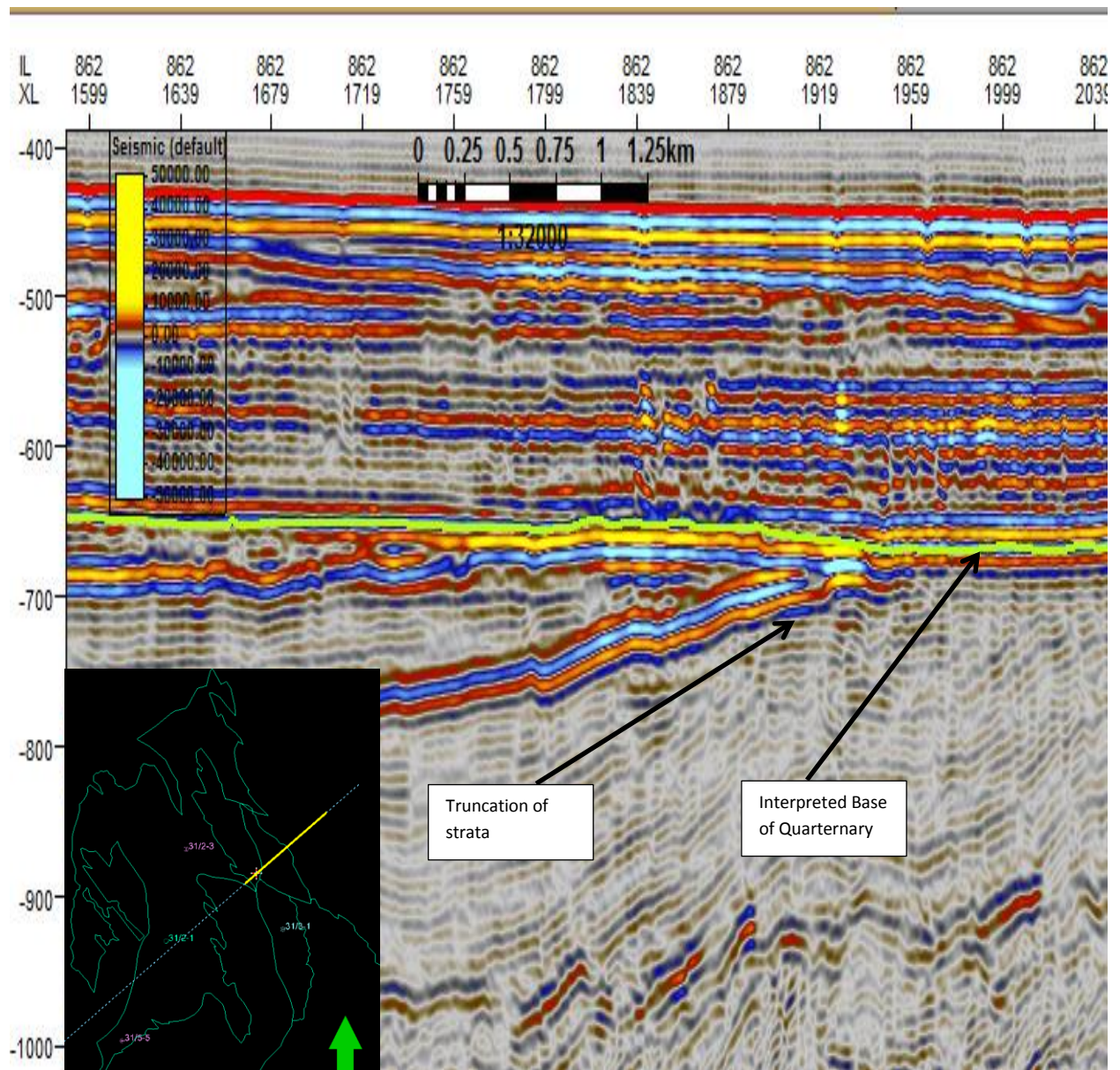
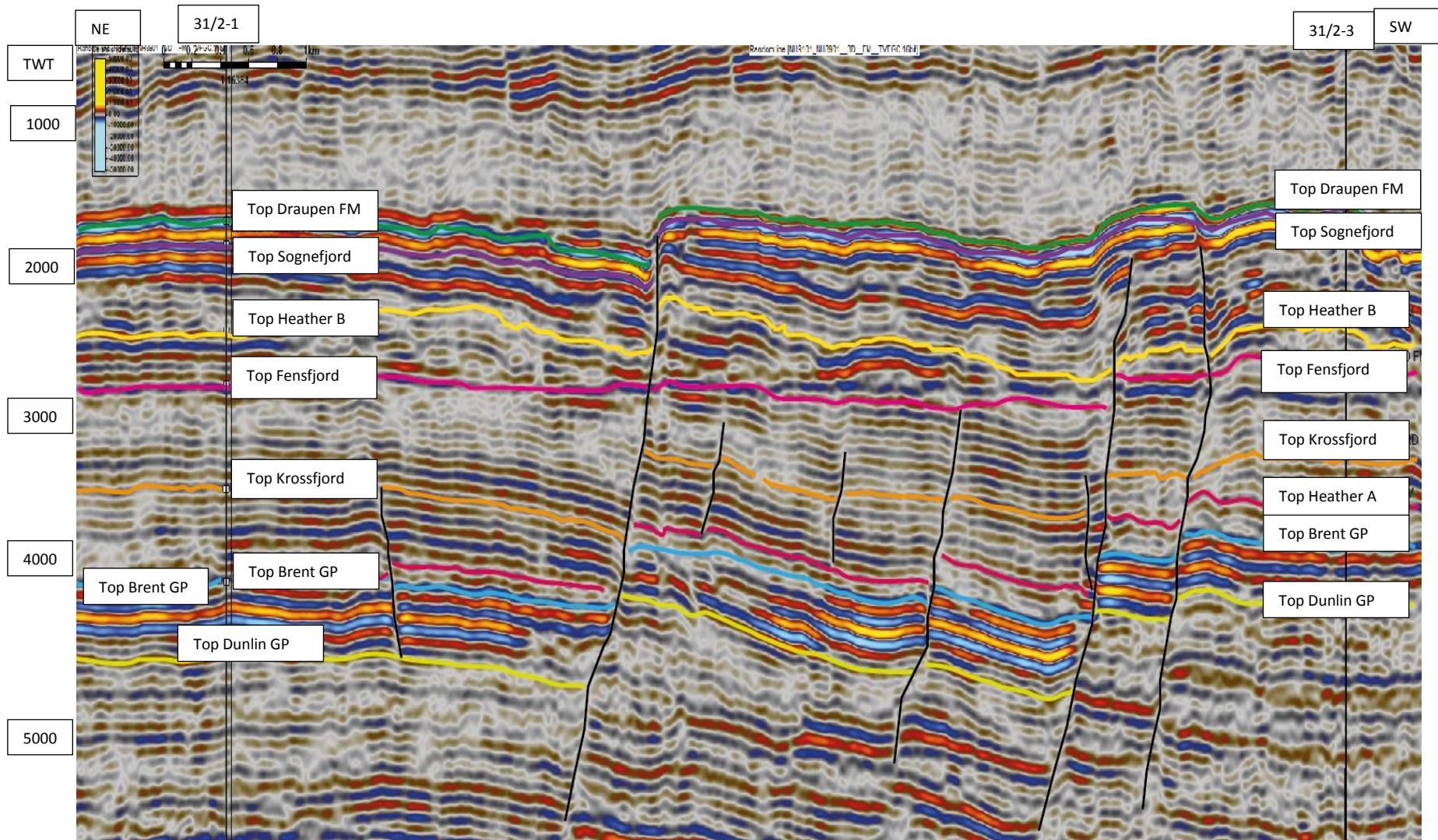


Figure 4.9: Time structure map of interpreted base of Quarternary



**Figure 4.10:** Seismic inline 862 shows major truncating angular unconformity.



**Figure 4.11:** Seismic section through well 31/2-1 and 31/2-3 showing interpreted Horizons. See Fig.4.12 for location.



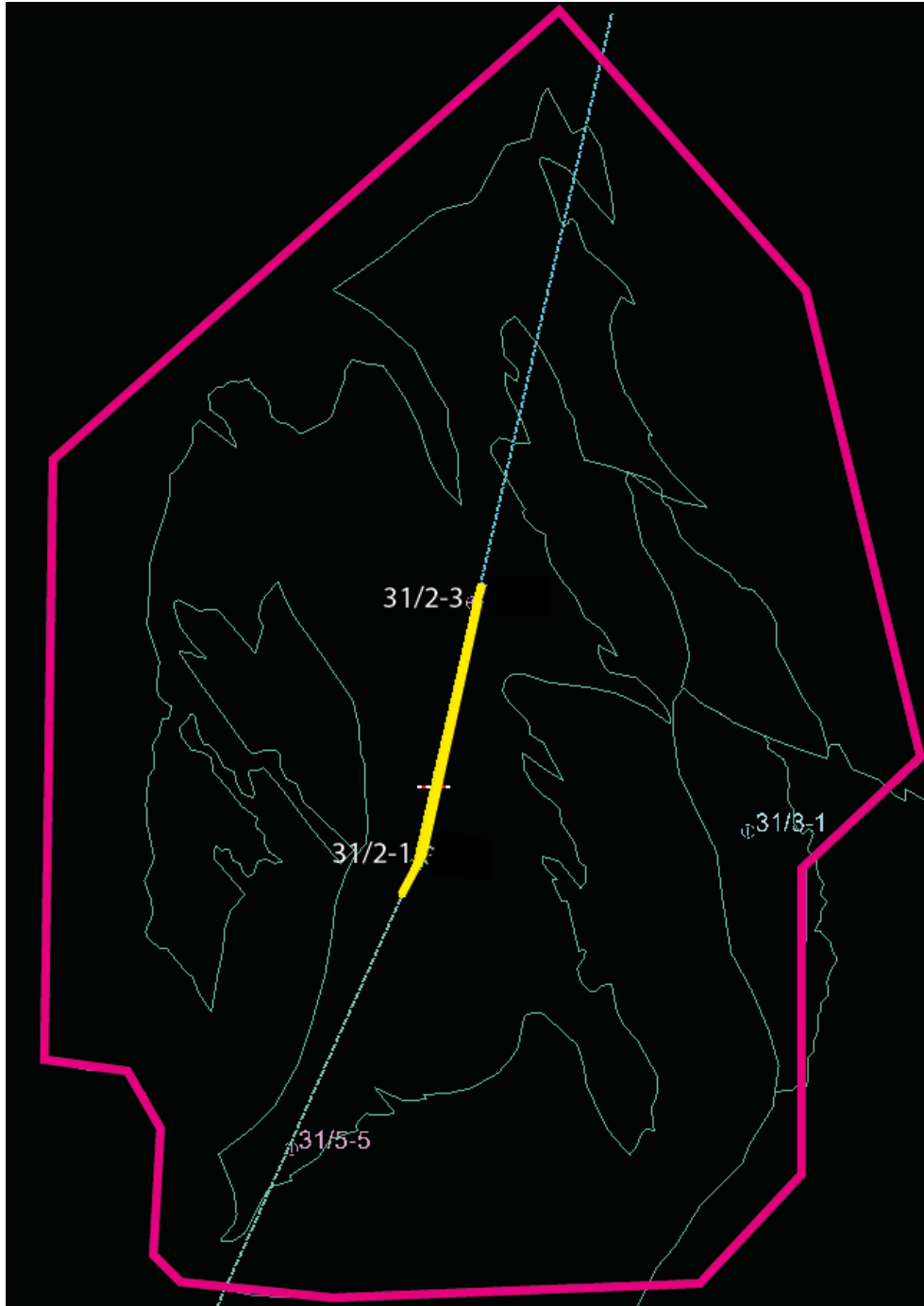


**Figure 4.12:** Location of interpreted Horizon section in Fig. 4.11

### 4.3.2 Top of Draupen Formation

Top Draupen Formation is present in well 31/2-1. It ties in a trough and interpreted confidently. This surface represented as a clear parallel reflector that partially to completely eroded on the flanks. The time structure map is shown in Fig. 4.15

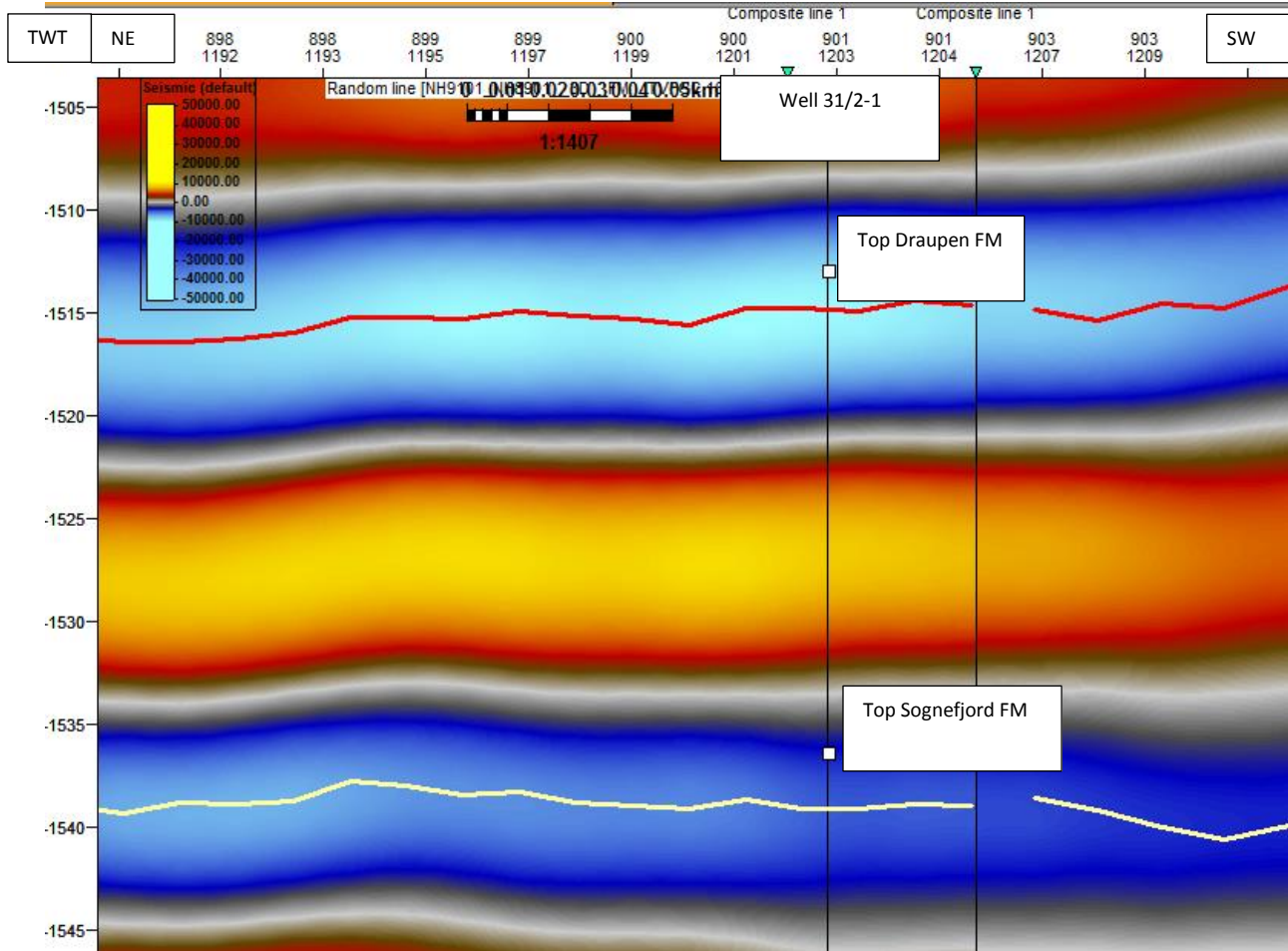


**Figure 4.13:** Seismic Section showing interpreted top of Draupen FM. See Fig.4.14 for location.

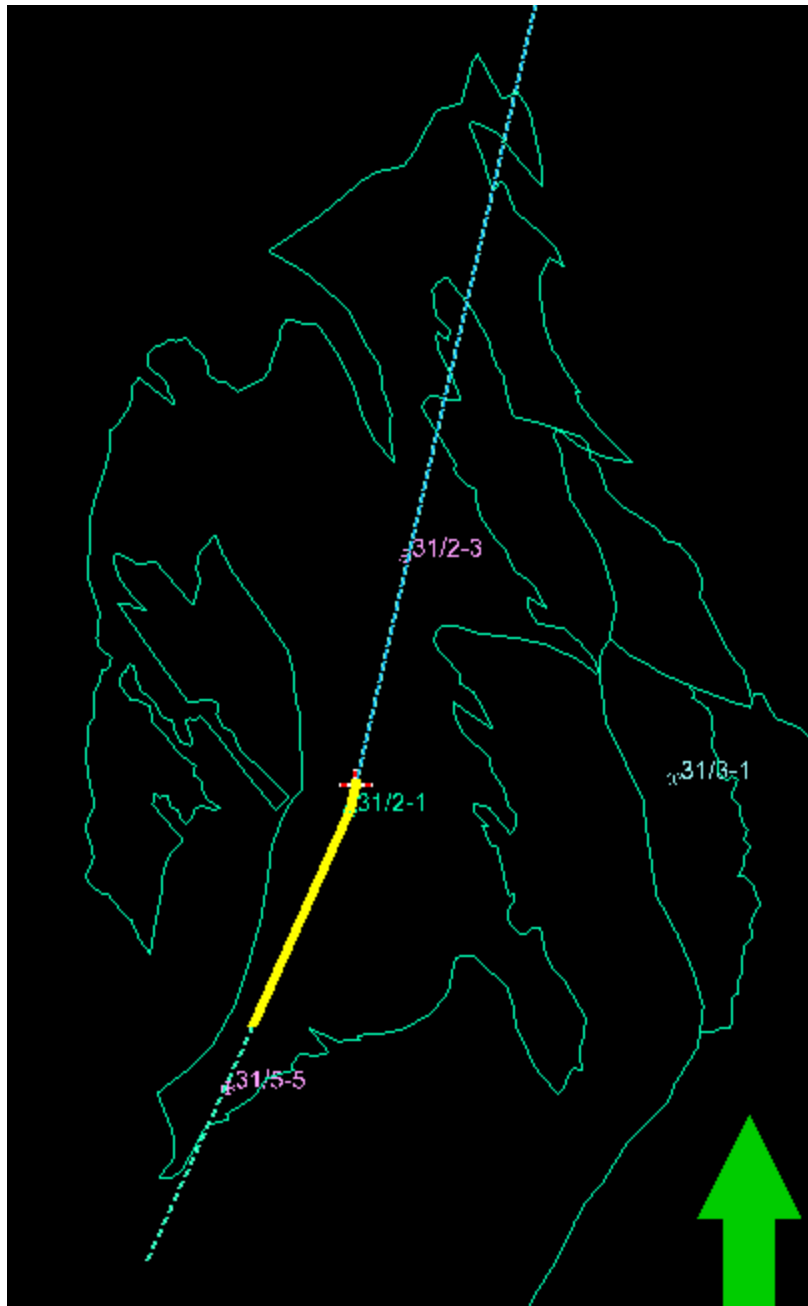


**Figure 4.14:** Location of interpreted horizons in reservoir section.

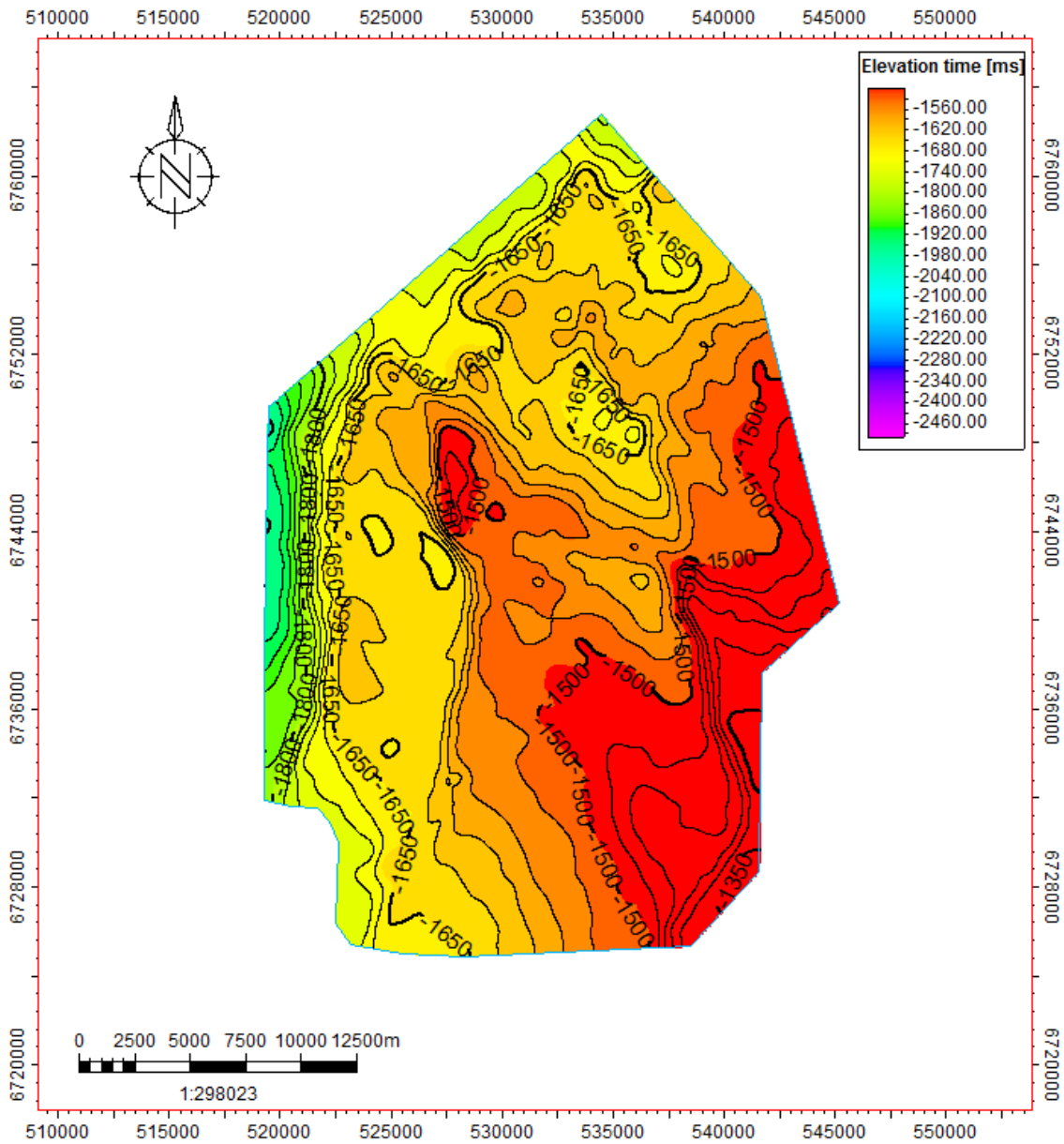


**Figure 4.15:** Time structure map of interpreted Draupen Formation.

### 4.3.3 Top of Sognefjord Formation

Top Sognefjord is present in all studied wells. As a Top Sognefjord, horizon near top Draupen Formation (erosional surface) was picked. It corresponds to a trough at the well locations (Fig. 4.4) and picked confidently. The time structure map is shown in (Fig. 4.40). It has also been eroded, especially around local highs and in western end of the field (Fig. 4.41) There is seismic evidence of Progradation (Fig. 4.46) towards the west across the Horda Platform. As a result,

the top of the Sognefjord is strongly diachronous: clean sands pinch-out and interfinger with micaceous silts towards the west

#### 4.3.4 Top of Heather B Formation

It ties in a peak in well 31/2-1 and 31/2-3 (Fig. 4.4) The interpretation of this marker was challenging as it was faulted and represented by low amplitude reflector in particular areas. Its reflection pattern dims out towards eastern part of inlines as shown in Fig. 4.17 The seismic data shows westwards progradation as shown by off lapping of seismic reflectors in Fig. 4.19 The time structure and RMS maps are shown in Figs. 4.21-4.22 respectively In time structure map the high time values indicate main structural lows where as low time values indicate main structural highs. In RMS attribute map the negative amplitude shows the area with more hydrocarbon contents.

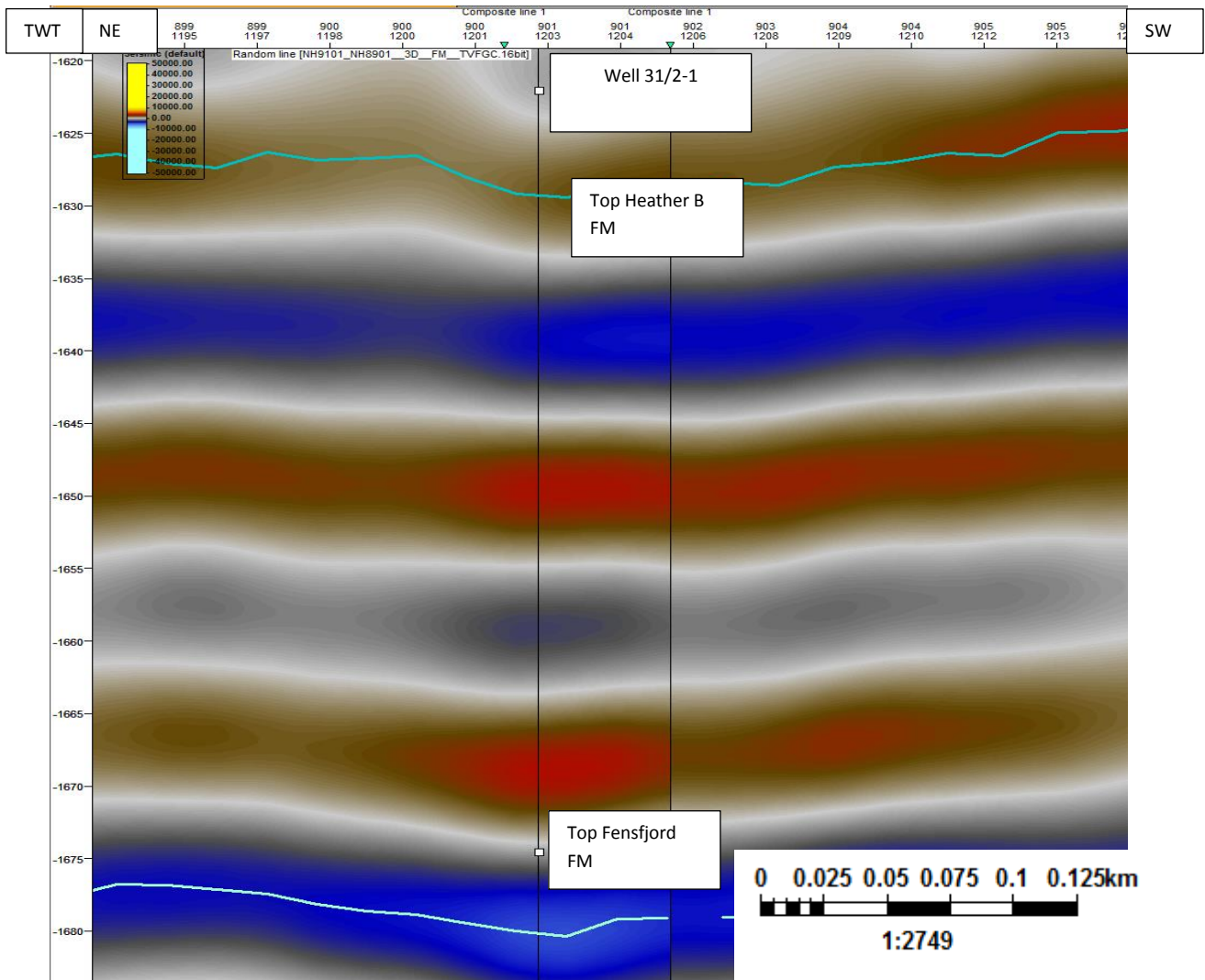


**Figure 4.16:** Seismic Section showing interpreted top of Heather B Formation. For location see Fig. 4.14

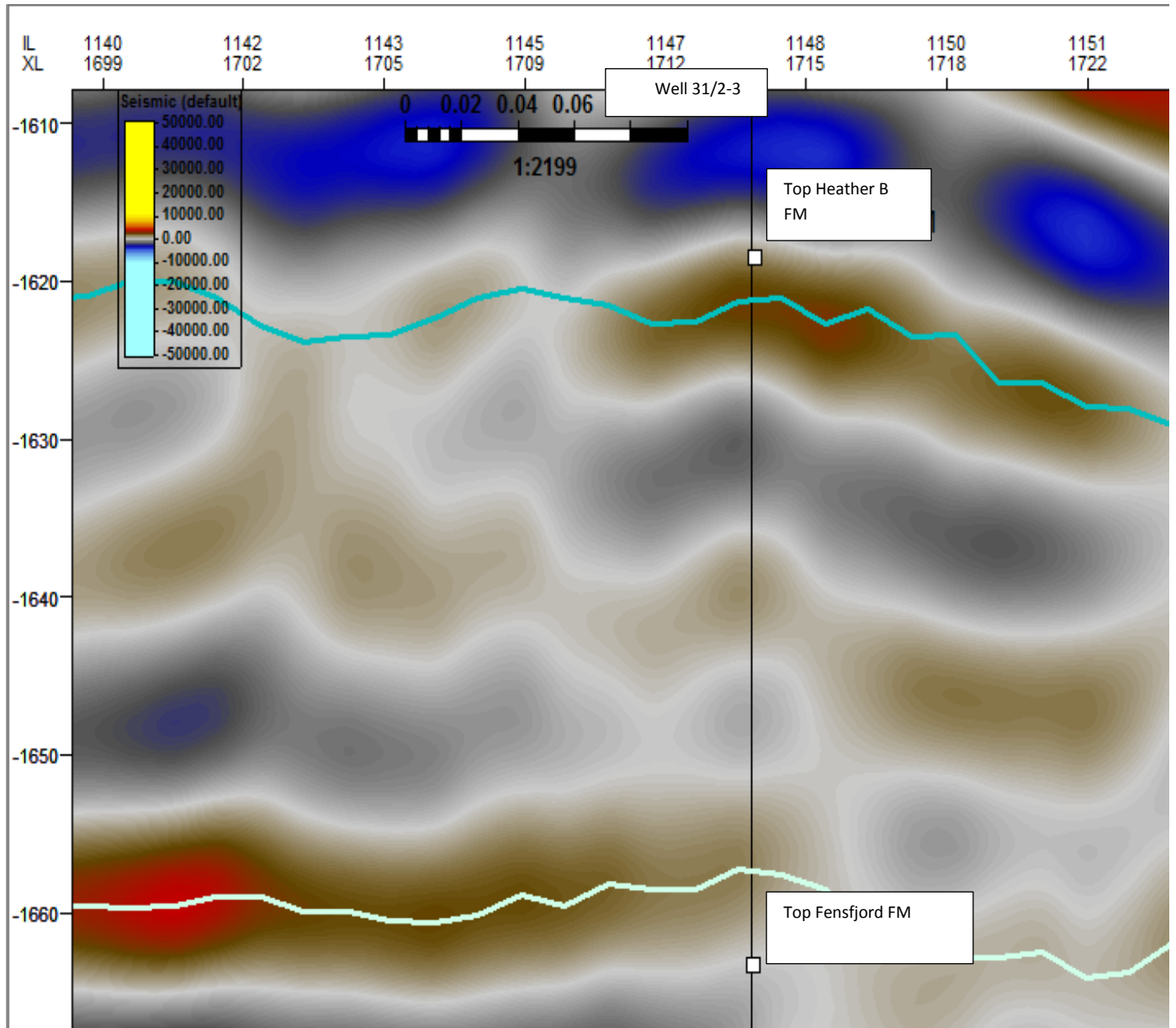


**Figure 4.17:** Seismic section showing dimming of reflection pattern towards east. See Fig.4.18 for location

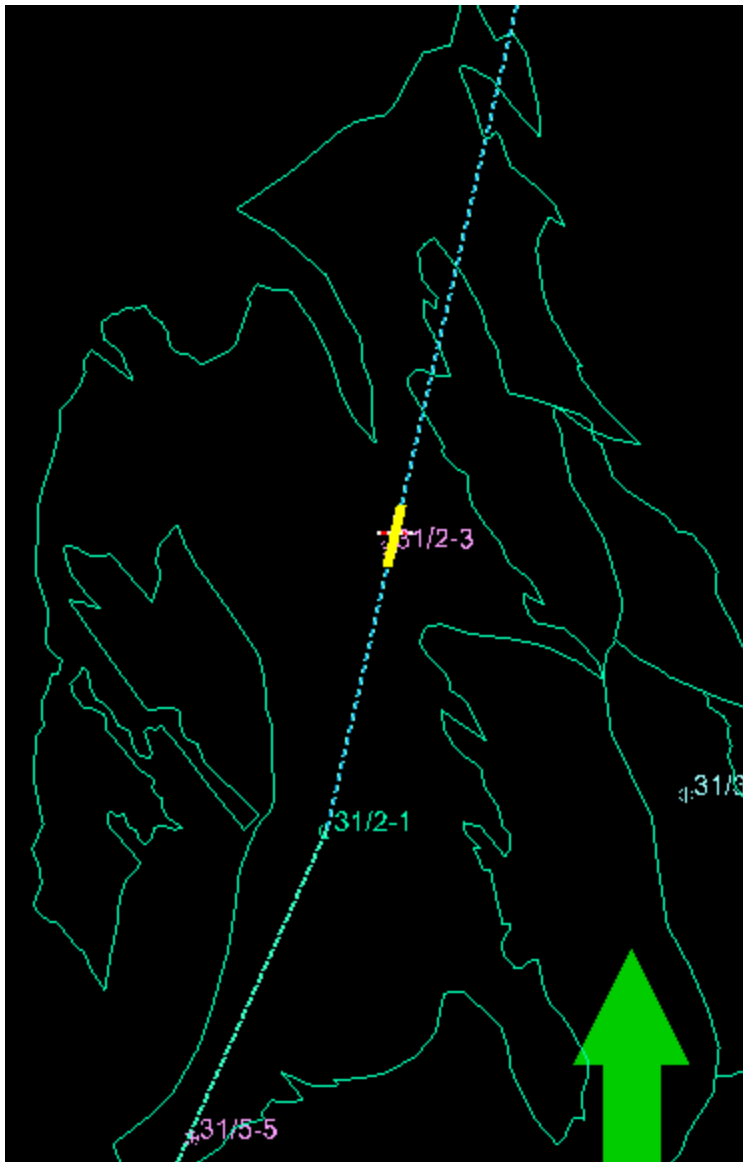


**Figure 4.18** : Location of seismic section in Fig. 4.17.

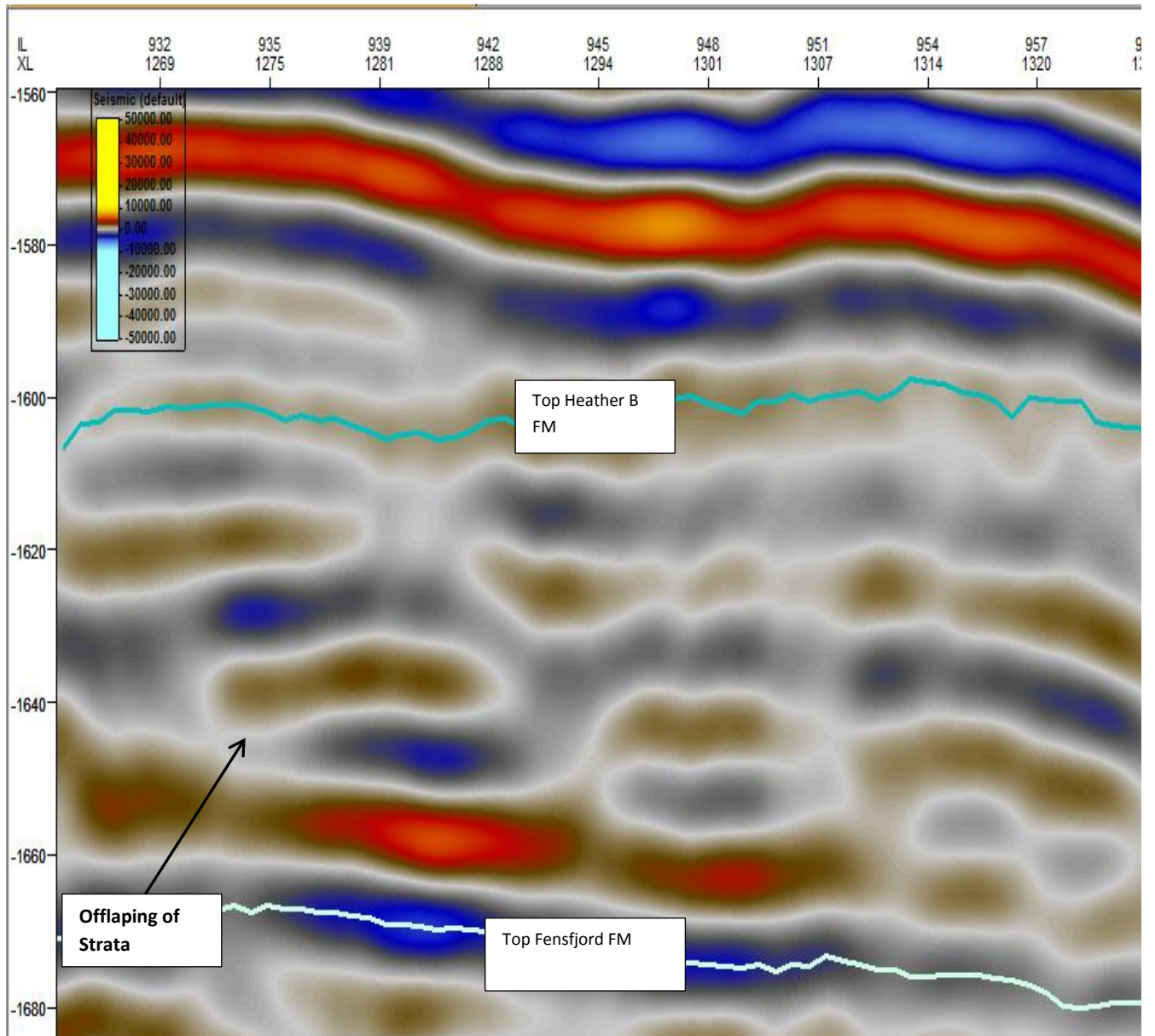


**Figure 4.19:** Seismic section showing off lapping of strata in Heather B Formation. See Fig. 4.20 for location of this section.



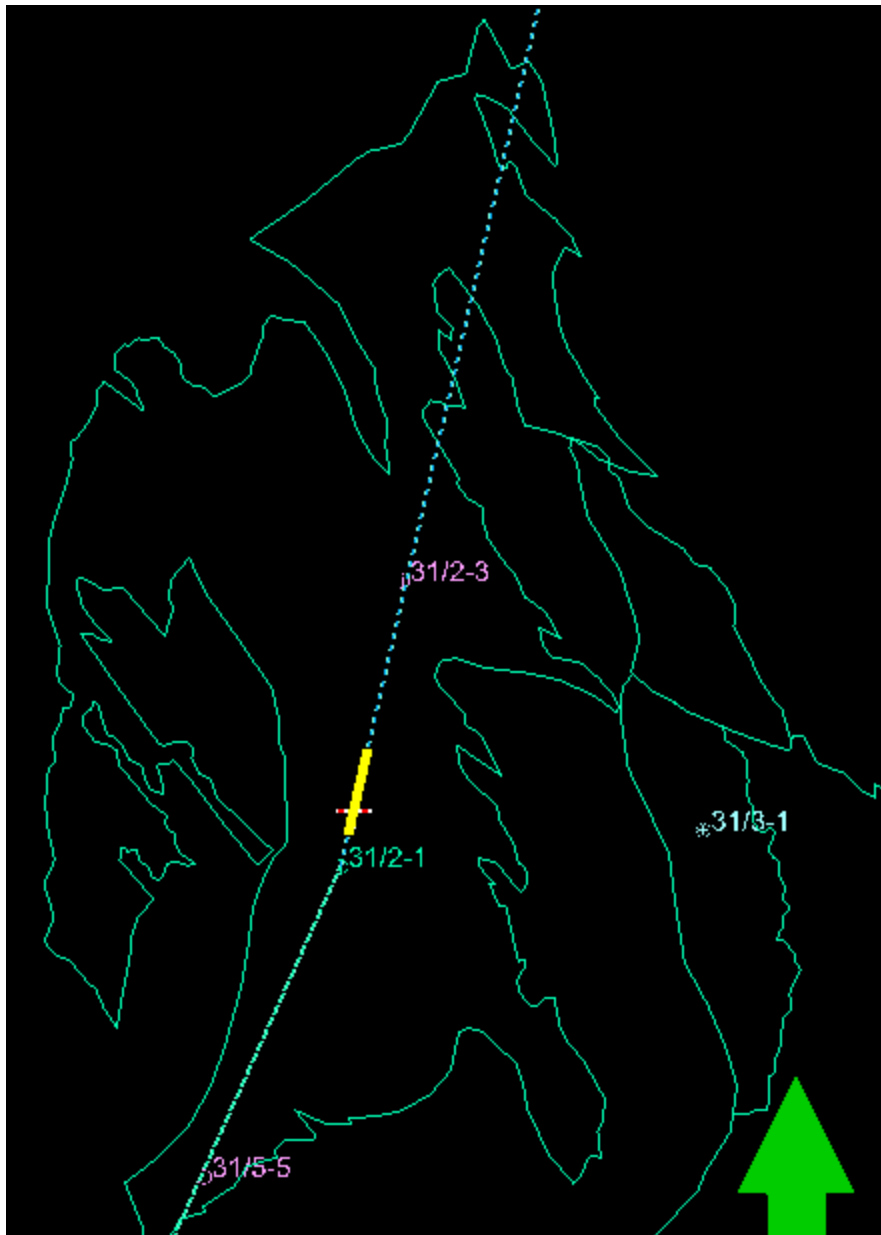
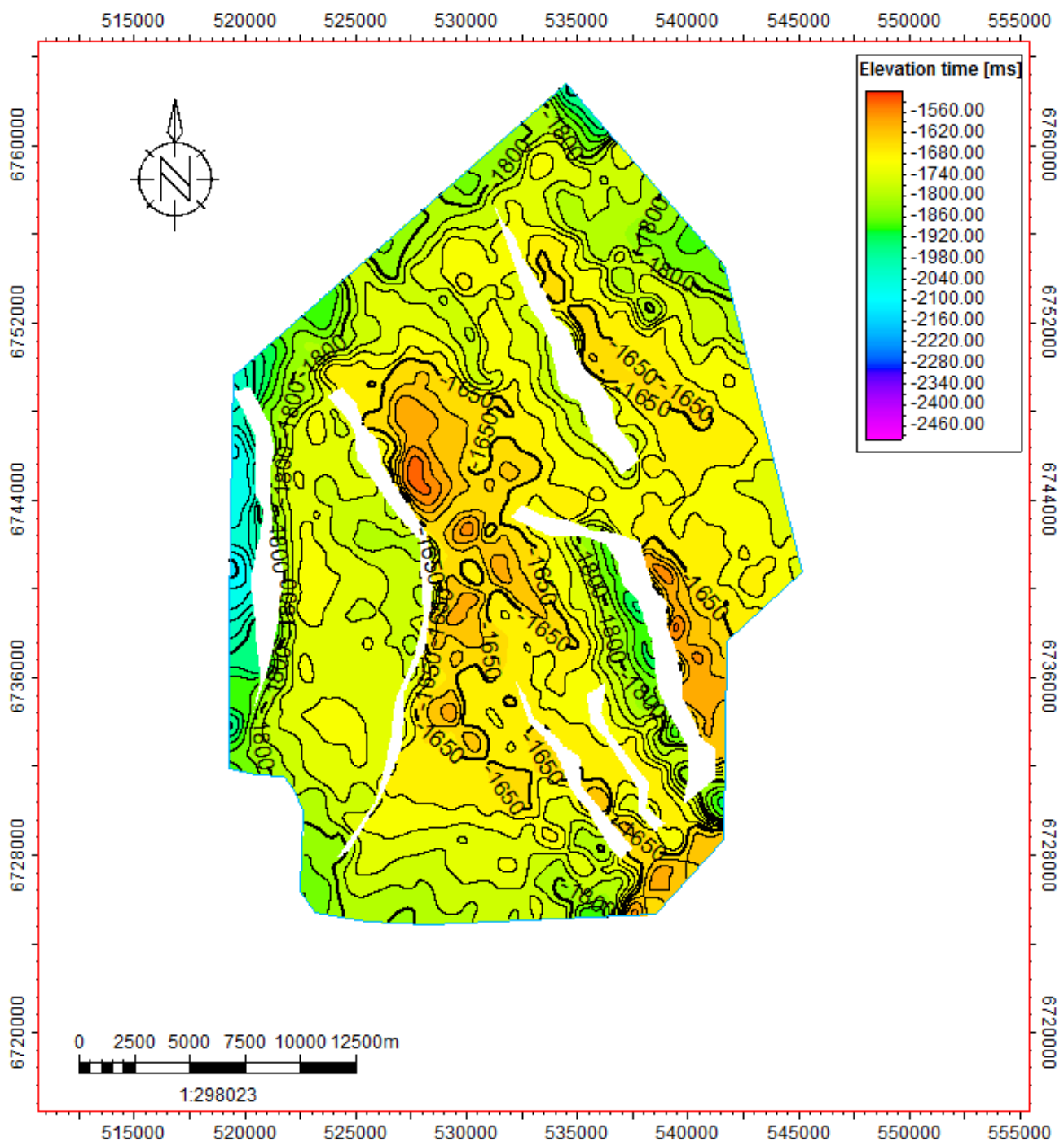
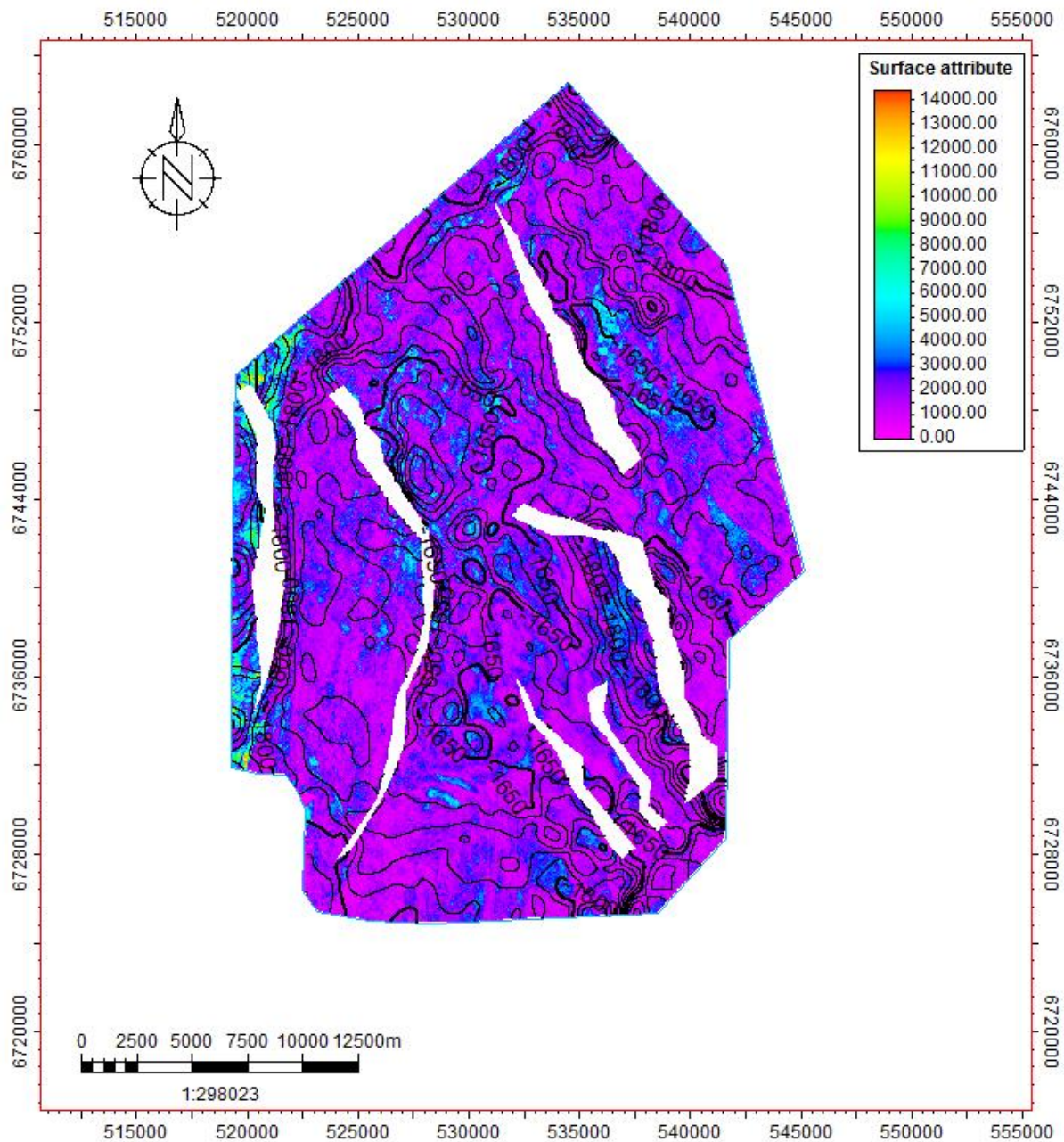


Figure 4.20: Location of seismic section in Fig. 4.19.



**Figure 4.21:** Surface map of Heather B Formation.



**Figure 4.22:** RMS attribute map of Heather B Formation.

#### 4.3.5 Top of Fensfjord Formation

The top of the Fensfjord appears as a fairly continuous event but with varying brightness (Fig. 4.48-4.49). It can sometimes be seen to dim-out (Fig. 4.49) and was identified from well control points. It changes its polarity. In well 31/2-1 (Fig.4.4), it ties in trough while in other two wells it ties in peaks. It shows positive (peak) amplitude above the flat spot and negative (through) when below the flat spot (Fig.4.51-52). The time structure map is shown in Fig. 4.54.

### 4.3.6 Top of Krossfjord Formation

Top Krossfjord ties in peaks in all studied wells. The Interpretation of this horizon was also challenging because of discontinuous and low amplitude reflector (Fig. 4.58) that disperse in graben areas. The time structure map is shown in Fig. 4.60.

### 4.3.7 Top of the Brent Gp

It ties to a trough in 31/2-1 and 31/2-3 wells (4.4). It is bright and one of the best defined reflectors (Fig.4.23). Its reflection dims out towards western ends of inlines (Fig. 4.24). The time structure map is shown in Fig. 4.26.

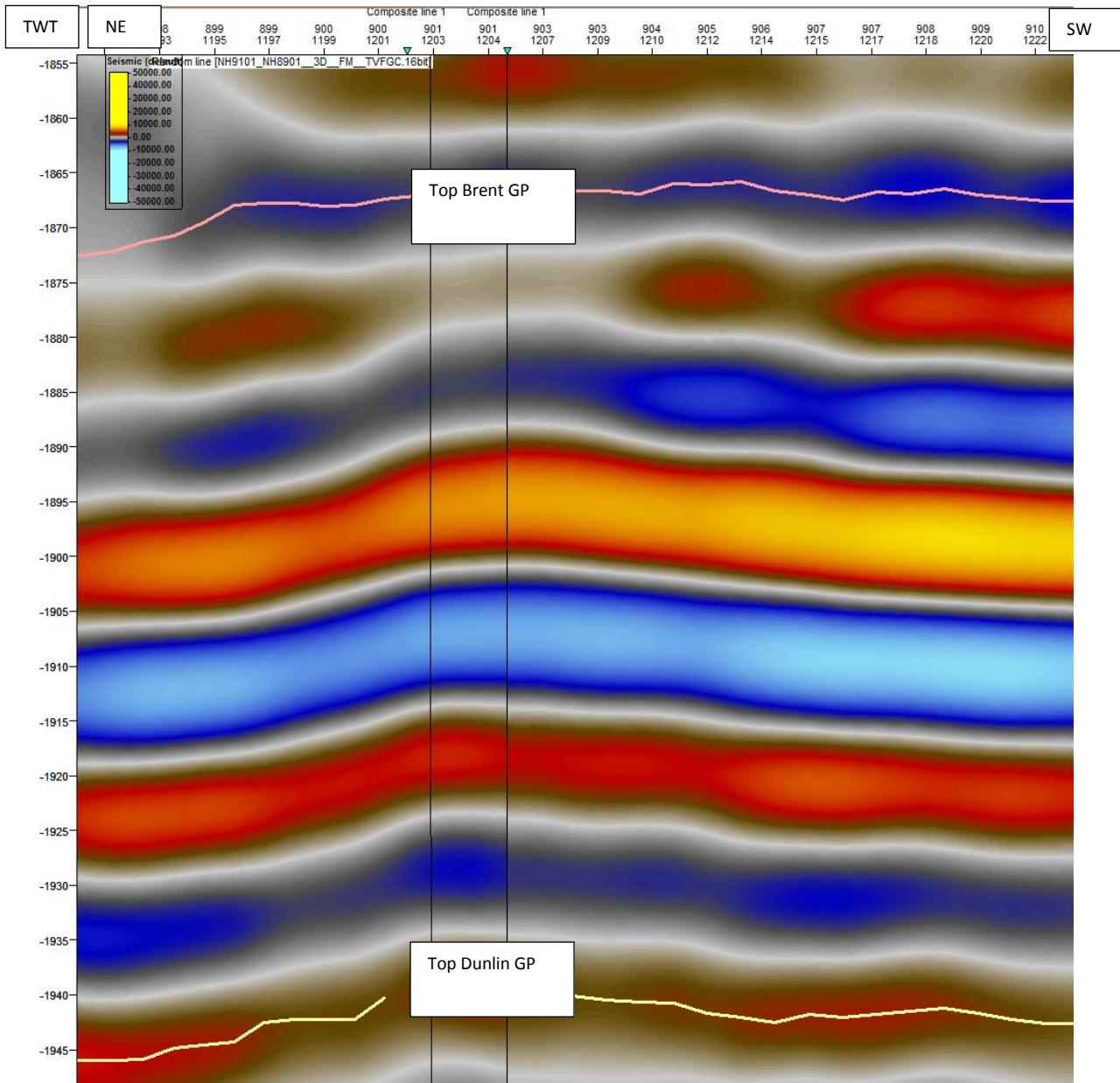


**Figure 4.23:** Seismic Section showing interpreted top of Brent GP. See Fig. 4.14 for location.

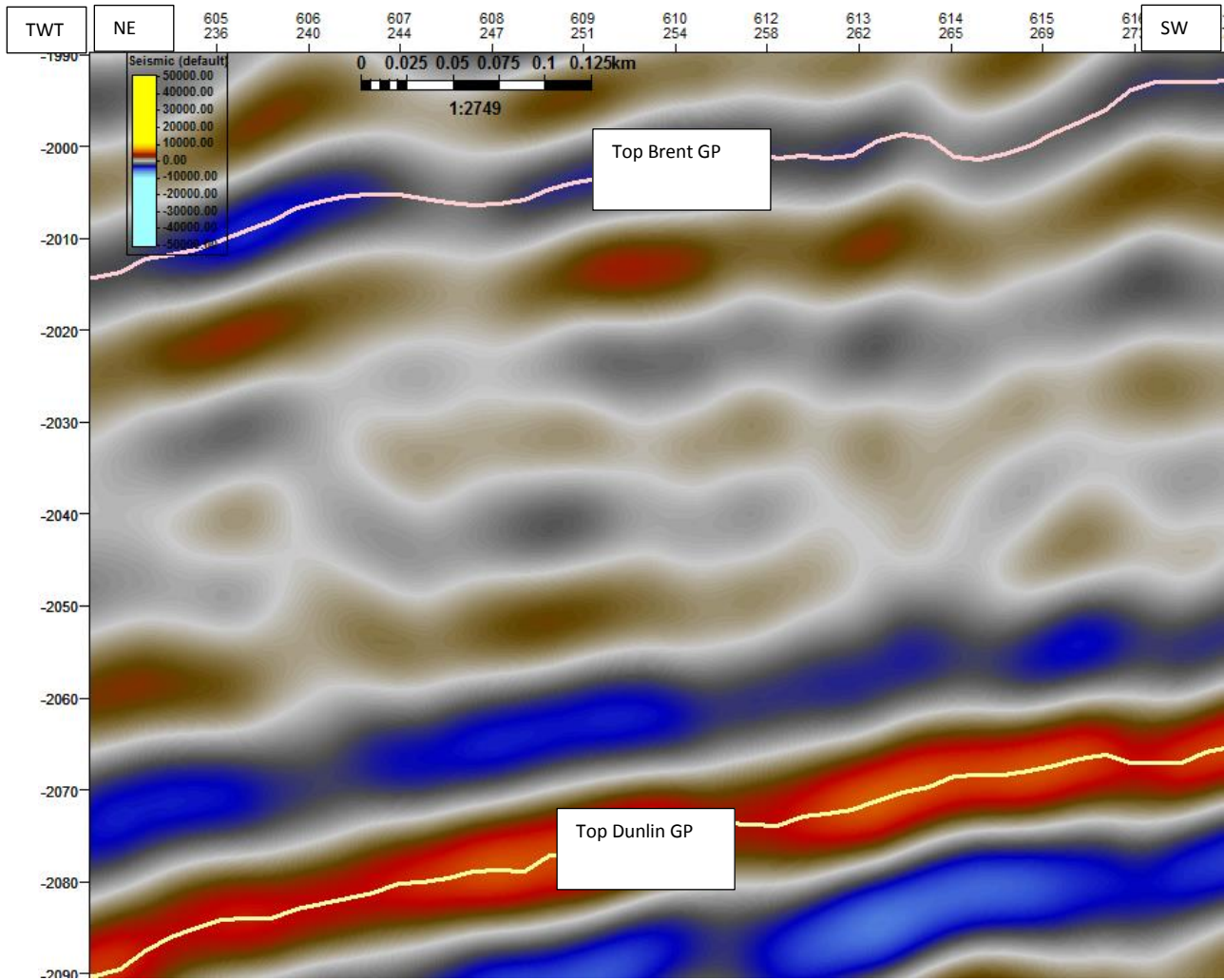


**Figure 4.24:** Seismic section shows dim reflection pattern of top of Brent GP in western part of the Troll Field. See Fig. 4.25 for location.

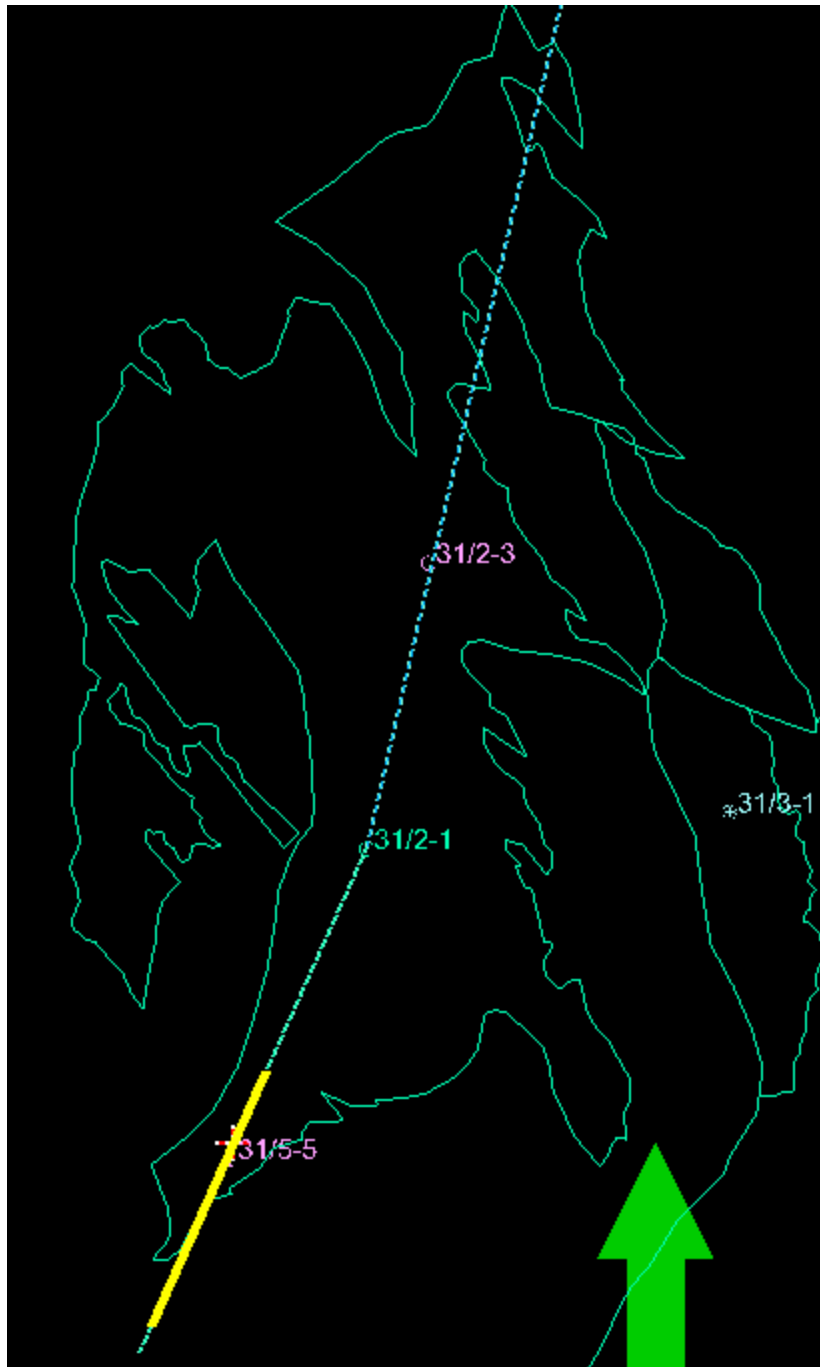
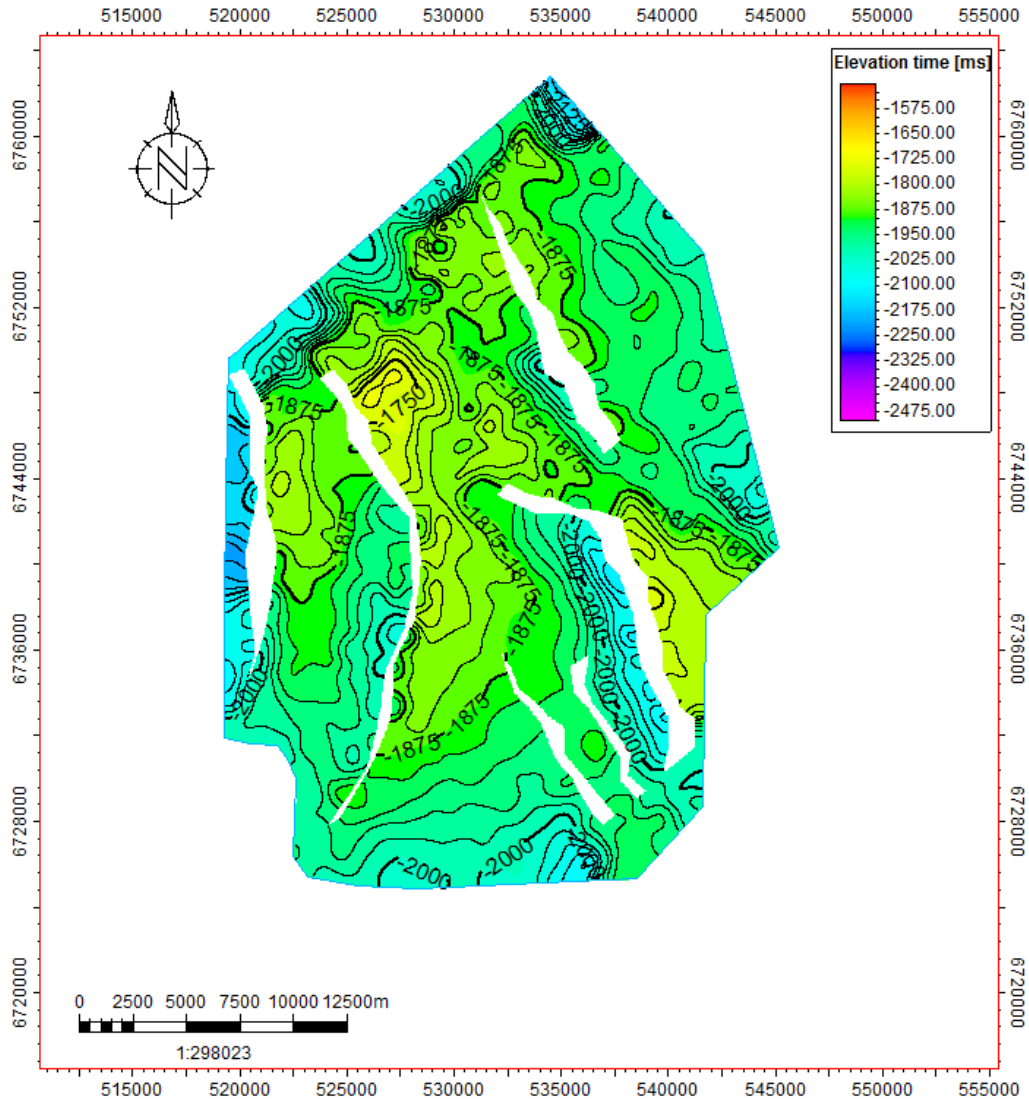


Figure 4.25: Location of seismic section in Fig. 4.24.



**Figure 4.26:** Time structure map of interpreted top of Brent GP.

#### 4.3.8 Top of the Dunlin Gp

It is continuous reflector with low amplitude. It ties to a peak in wells Fig. 4.4 The interpretation of this Horizon was an easy task. Time structure map is shown in Fig. 4.27.

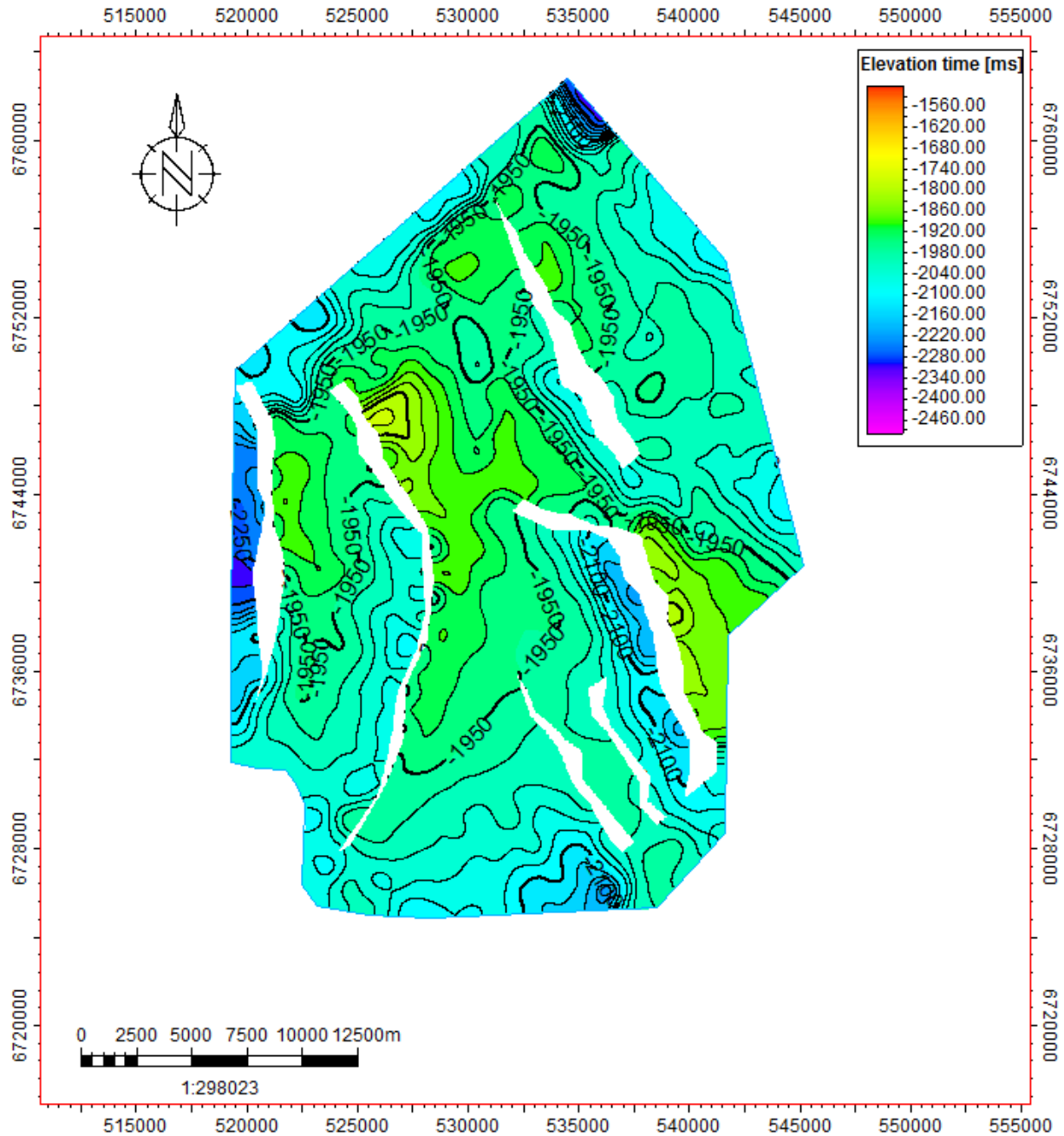


**Figure 4.27:** Time structure map of interpreted top of Dunlin GP

#### 4.4 Fault Interpretation

The few key faults were interpreted in the study area in order to show the impact of faults activity on depositional settings. Two types of normal fault families dominate the Troll Field. Faults are grouped into fault families according to similar structural settings.



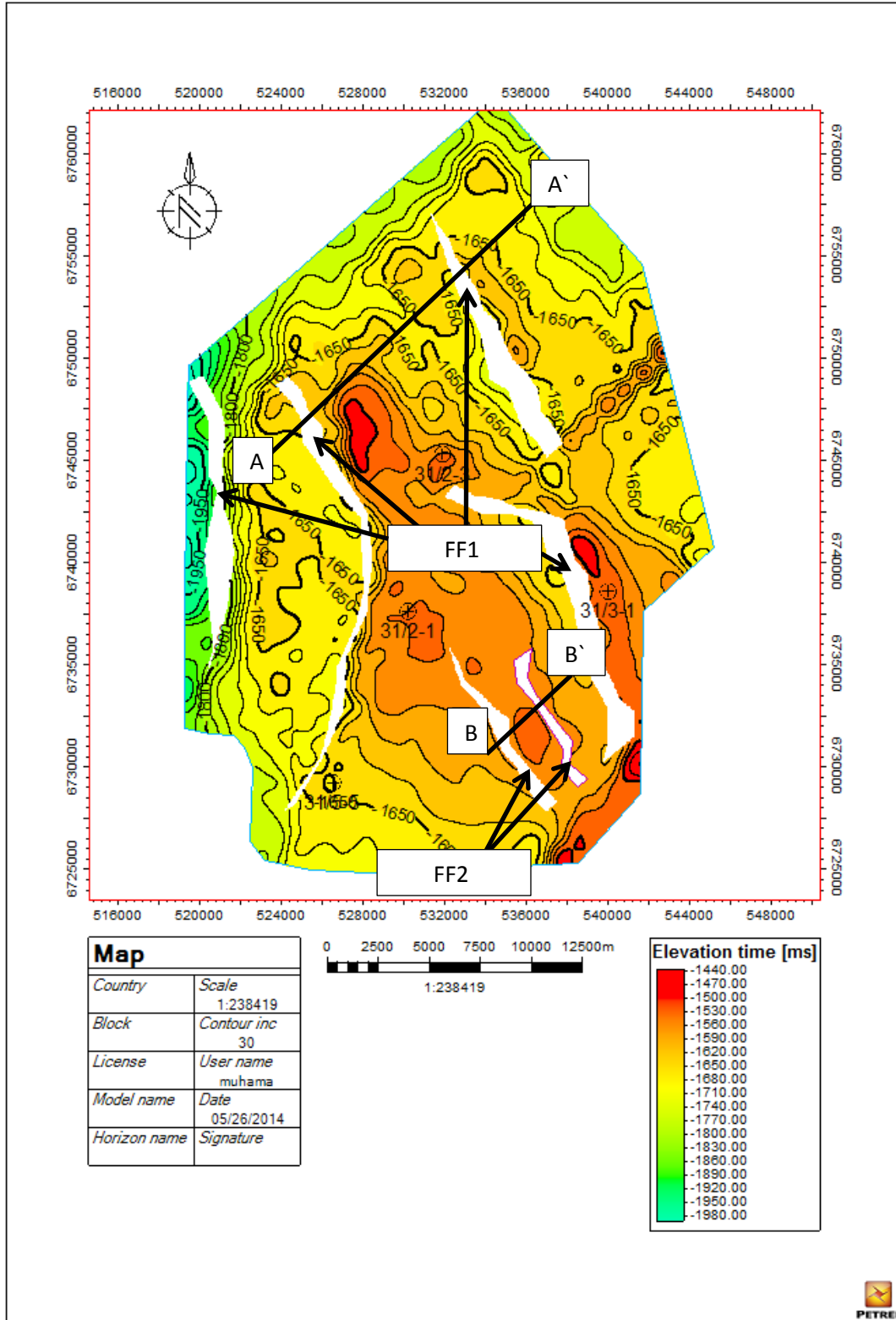


**Figure 4.28** Sognefjord surface map along with trends of interpreted fault families and listric faults.

#### 4.4.1 Fault Family 1

This family is defined by normal faults with main trend in NW to SE direction with NE - SW extension and mainly dips towards SW forming horst structure (Fig. 4.28 and 4.29). Generally they are 40-60 degree high angle faults. The displacement varies from 200 m to about 600 m in the northern and central part of the field. The pattern of major faults of fault family 1 in 3D window is shown in Fig. 4.34.

In the southern part, the trend of few faults changes from NW-SE to NE-SW direction with main extension in E-W direction. This change is mainly due to rotation.

#### 4.4.2 Fault Family 2

This family is also defined by normal faults with main trend in NS direction. The faults dip in NE direction and have E-W extension (Fig. 4.28 and 4.31). This family mainly exposed in eastern and northern part of the field and form graben structure.

These planar normal faults are often concentrated in complex fault scarps developed in front of major tilted blocks. Planar normal faulting had occurred during all phases of basin development, particularly with syn-fault sedimentation. Planar normal faults have played very important role in the development of major tilted fault blocks during post rift stage (Badly, 1984).

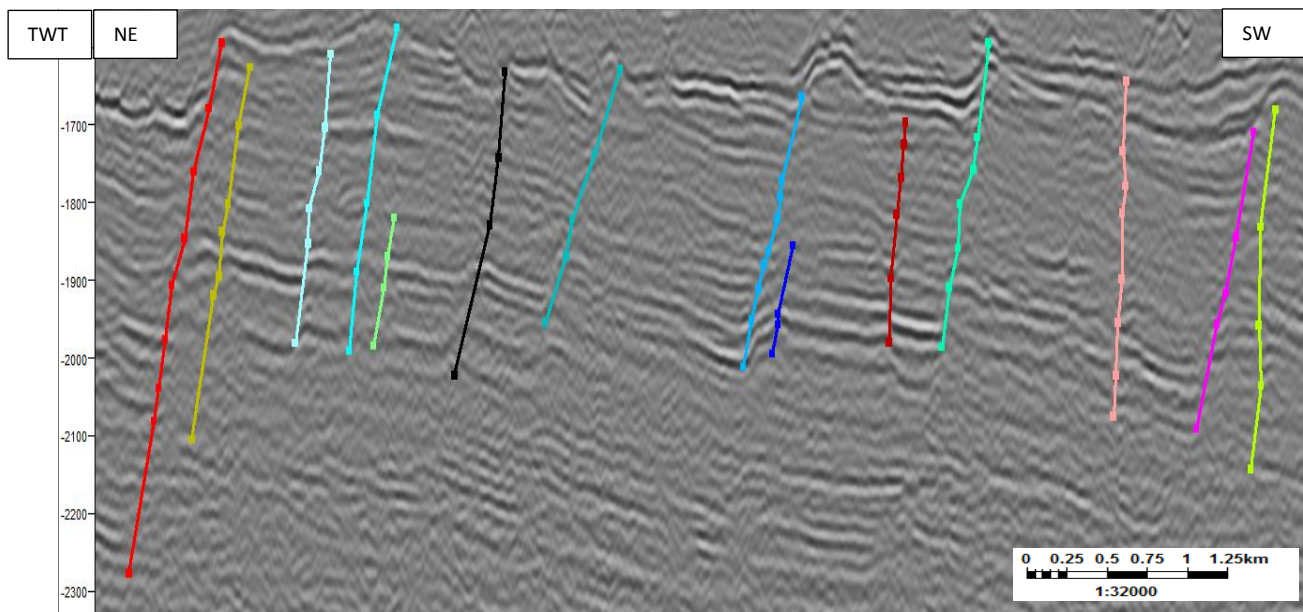


**Figure 4.29:** Random line shows the interpreted fault family 1. See Fig. 4.30 for location

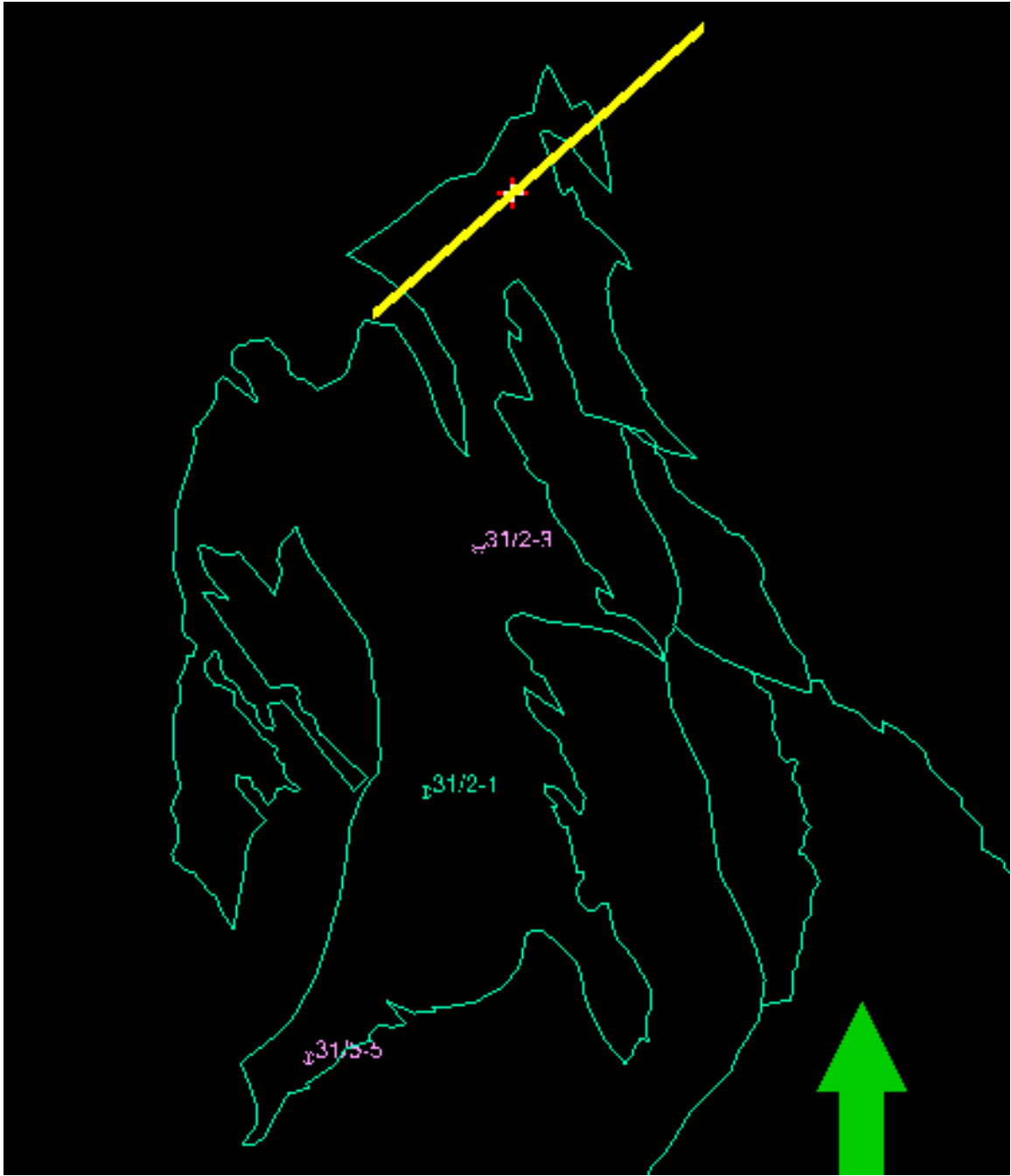
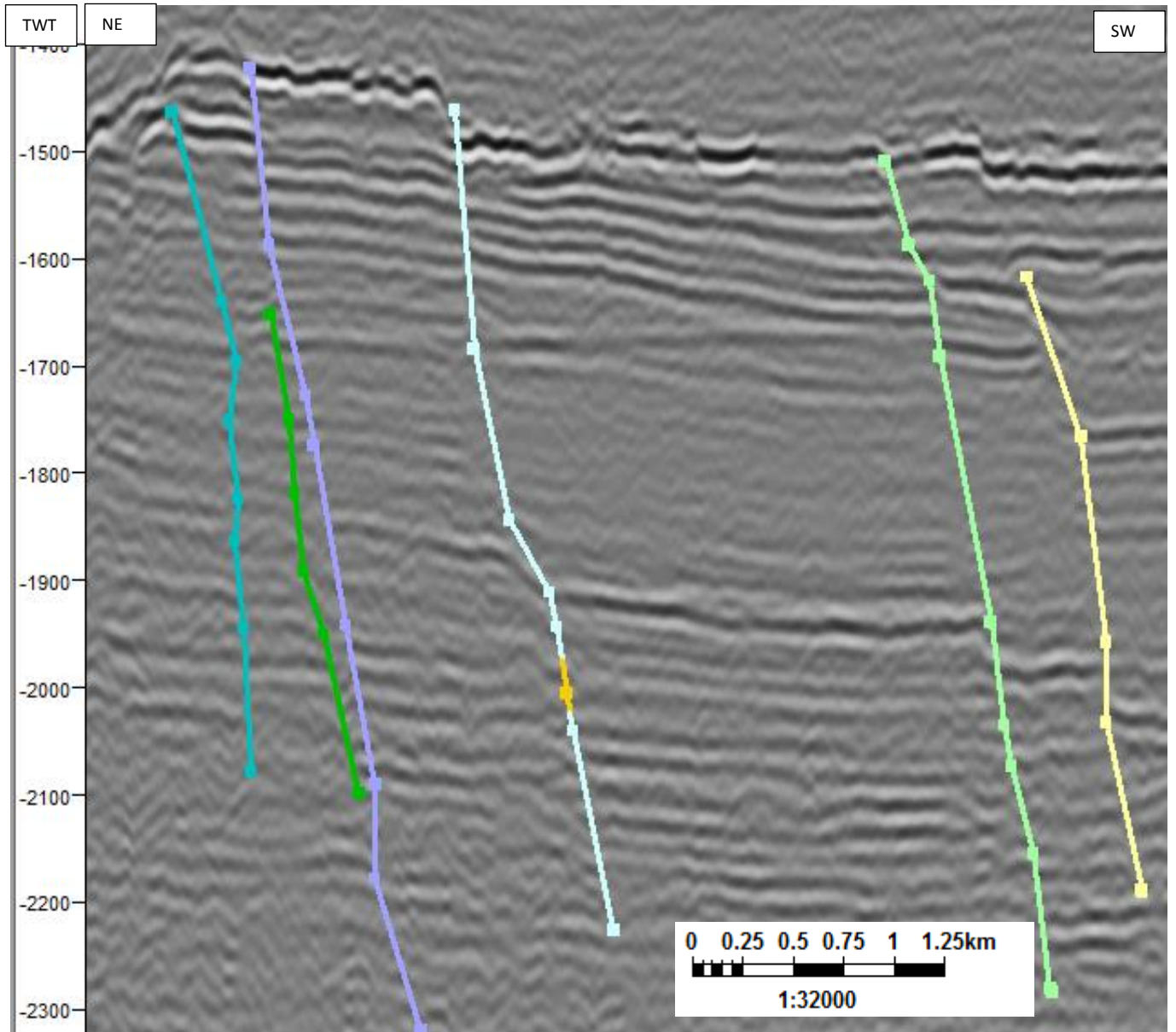
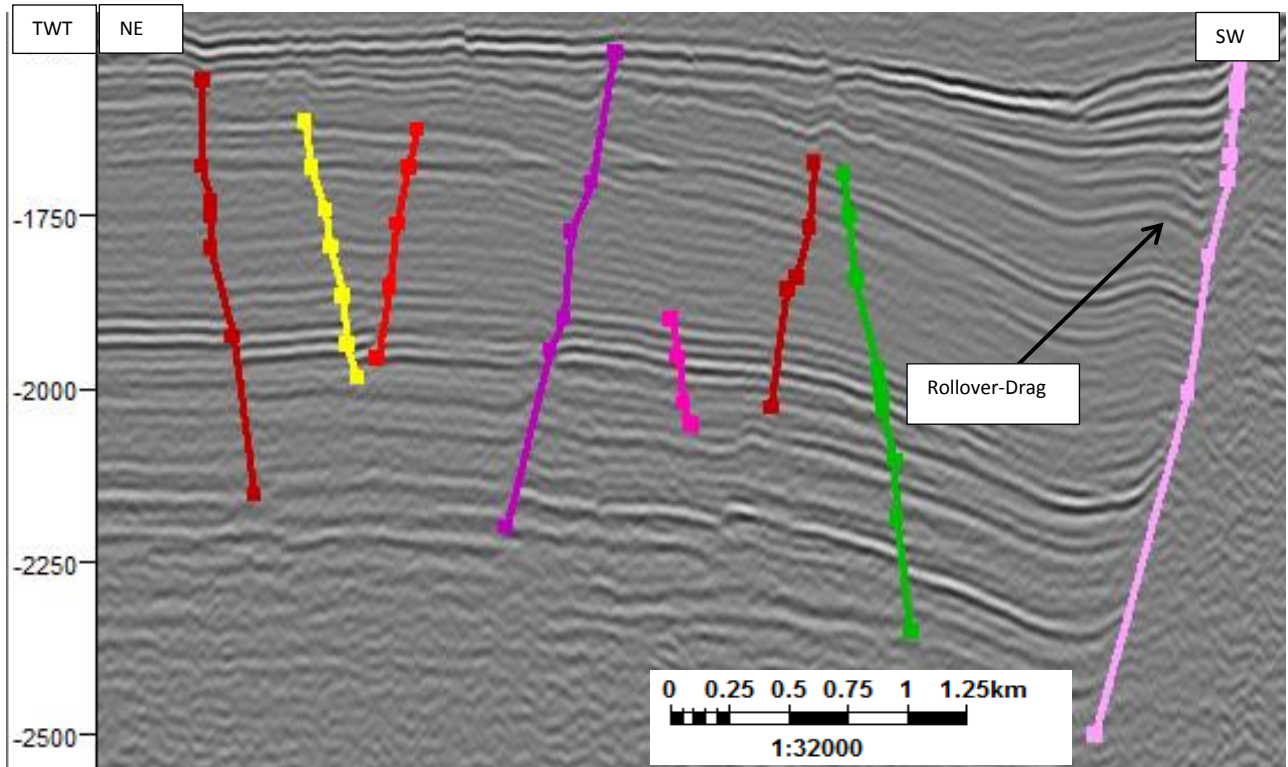


Figure 4.30: Location of interpreted fault family 1 section in Fig. 4.29.



**Figure 4.31:** Zoomed out Random line shows fault family 2. See Fig. 4.33 for location.



**Figure 4.32:** Seismic section showing Synthetic, antithetic faults and roll over-drag.

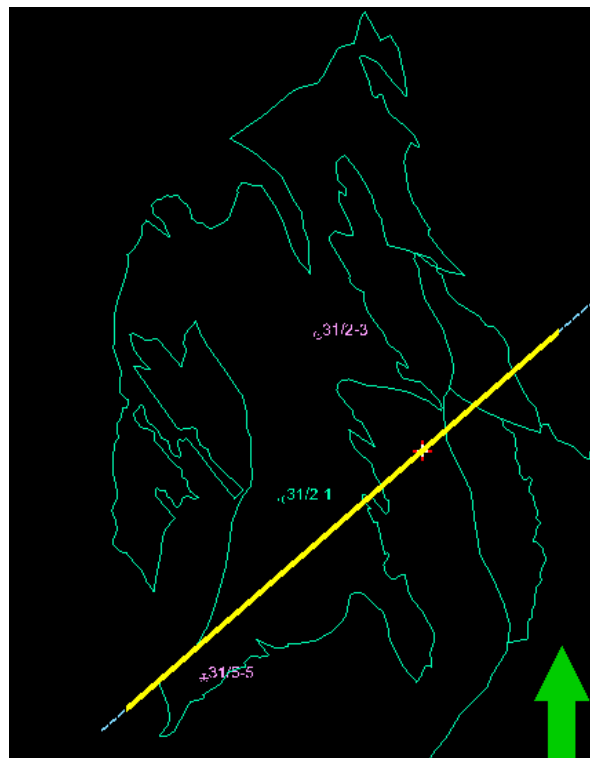


**Figure 4.33:** Location of seismic sections in Fig. 4.31-32.

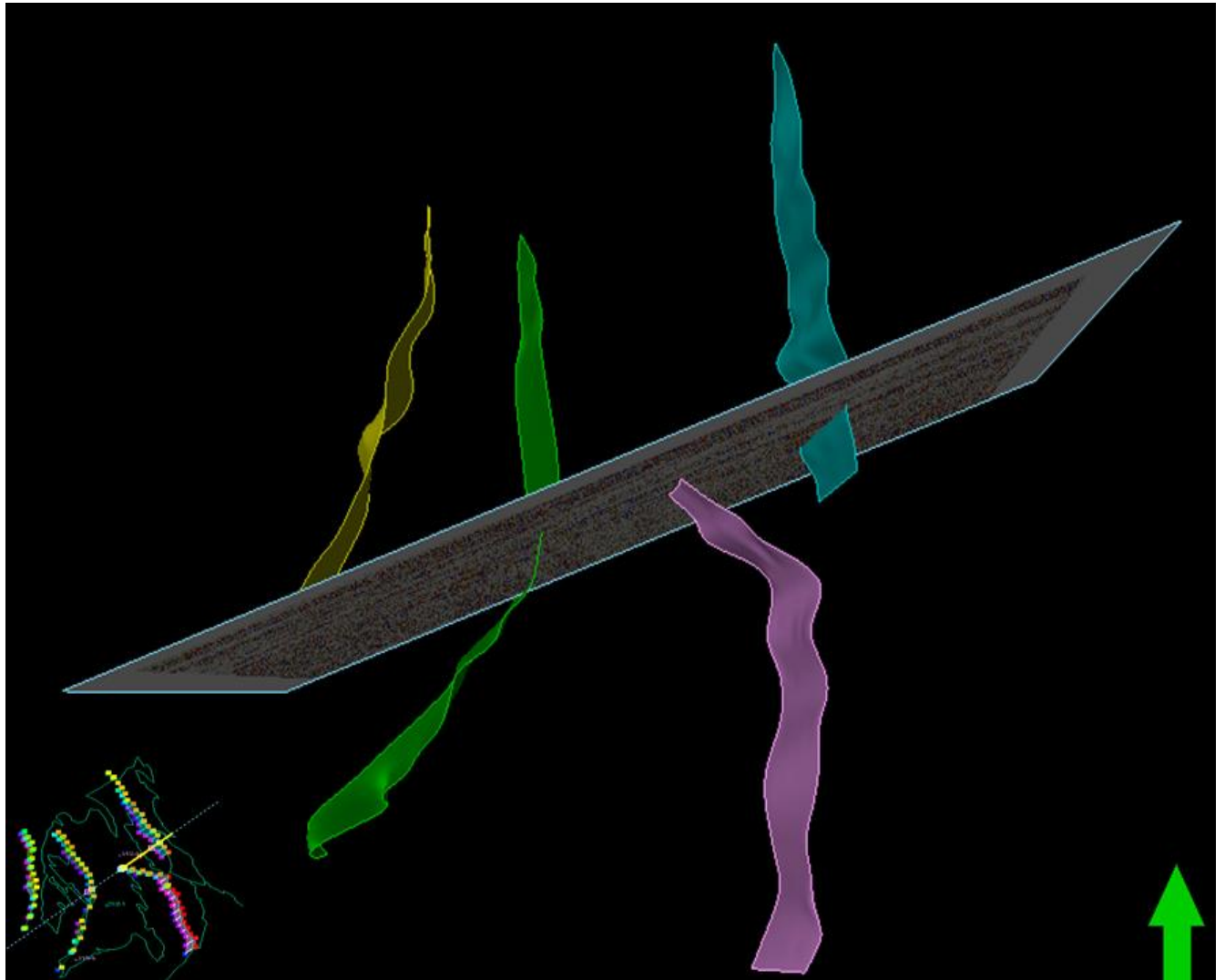


**Figure 4.34** The pattern of major faults of fault family 1 in 3D window. See Fig.4.28 for location.

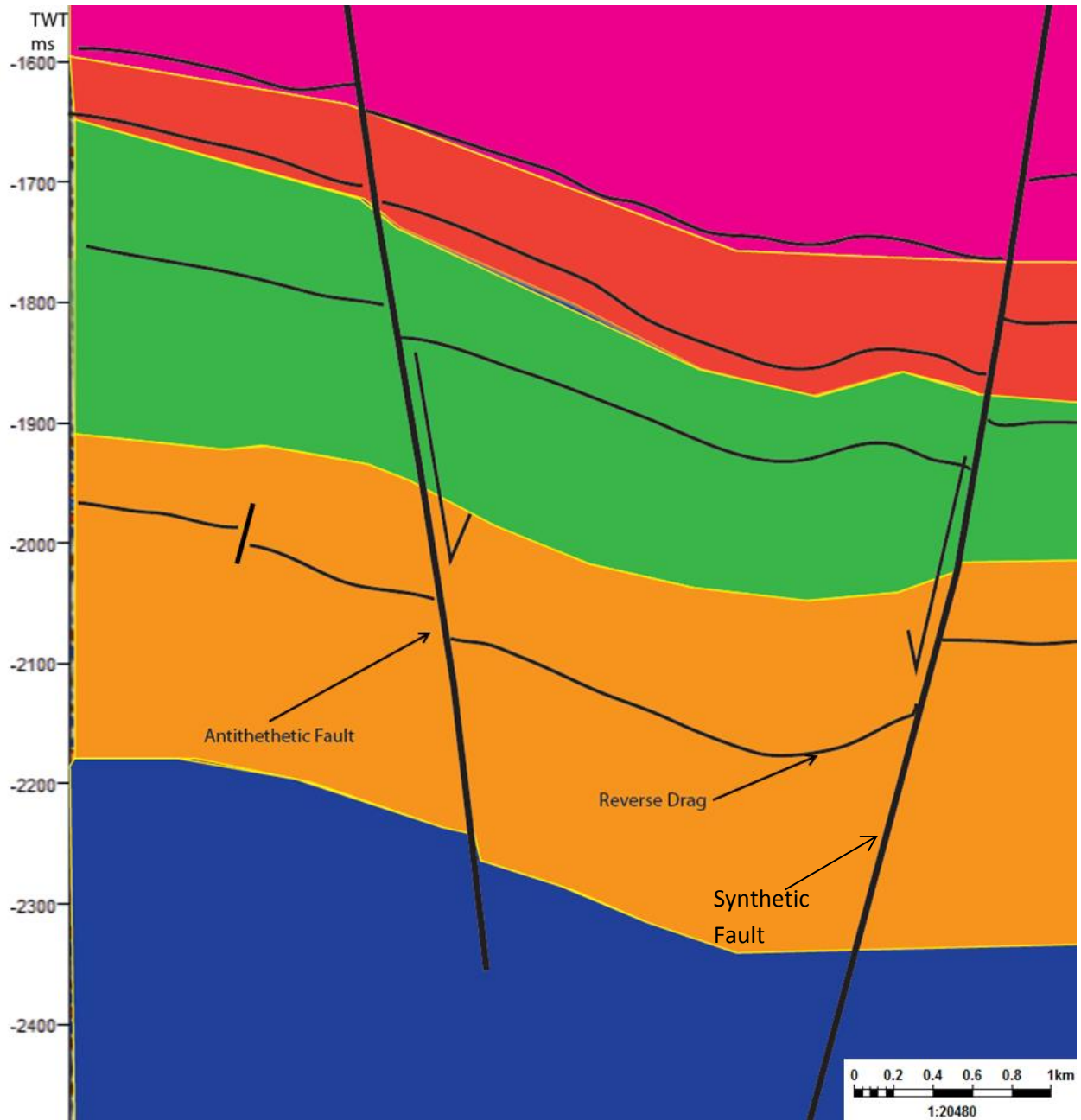


**Figure 4.35:** Model of interpreted faults showing antithetic and synthetic Faults and reverse drag along major synthetic fault.

#### 4.5 Reservoir Description

The oil and gas in the troll structure are present in medium-to-coarse grained, highly consolidated and fine micaceous sandstones and siltstones of the Middle-to-Upper Jurassic

Viking Group. In the Troll area, the Viking group consists of a stacked shallow marine sand sequence (Fig.2.7) of Krossfjord, Fensfjord, Sognefjord and Heather Formations Bolle L.1992).

Deposition occurred on a coast-attached shelf as a cyclic sequence. This cyclic sequence is characterized by alternations of transgressive sands and silts and progradational shoreface facies. The sequence architecture is controlled by minor fluctuations in regional sea level that are framed in the major Callovian-early Volgian regional transgression (Bolle L.1992).

#### **4.5.1 Sognefjord Formation**

Major part of the reservoir in the Troll Field is present in Sognefjord Formation which marks with maximum thickness of 170m in this area. (Dreyer T. et al., 2005).



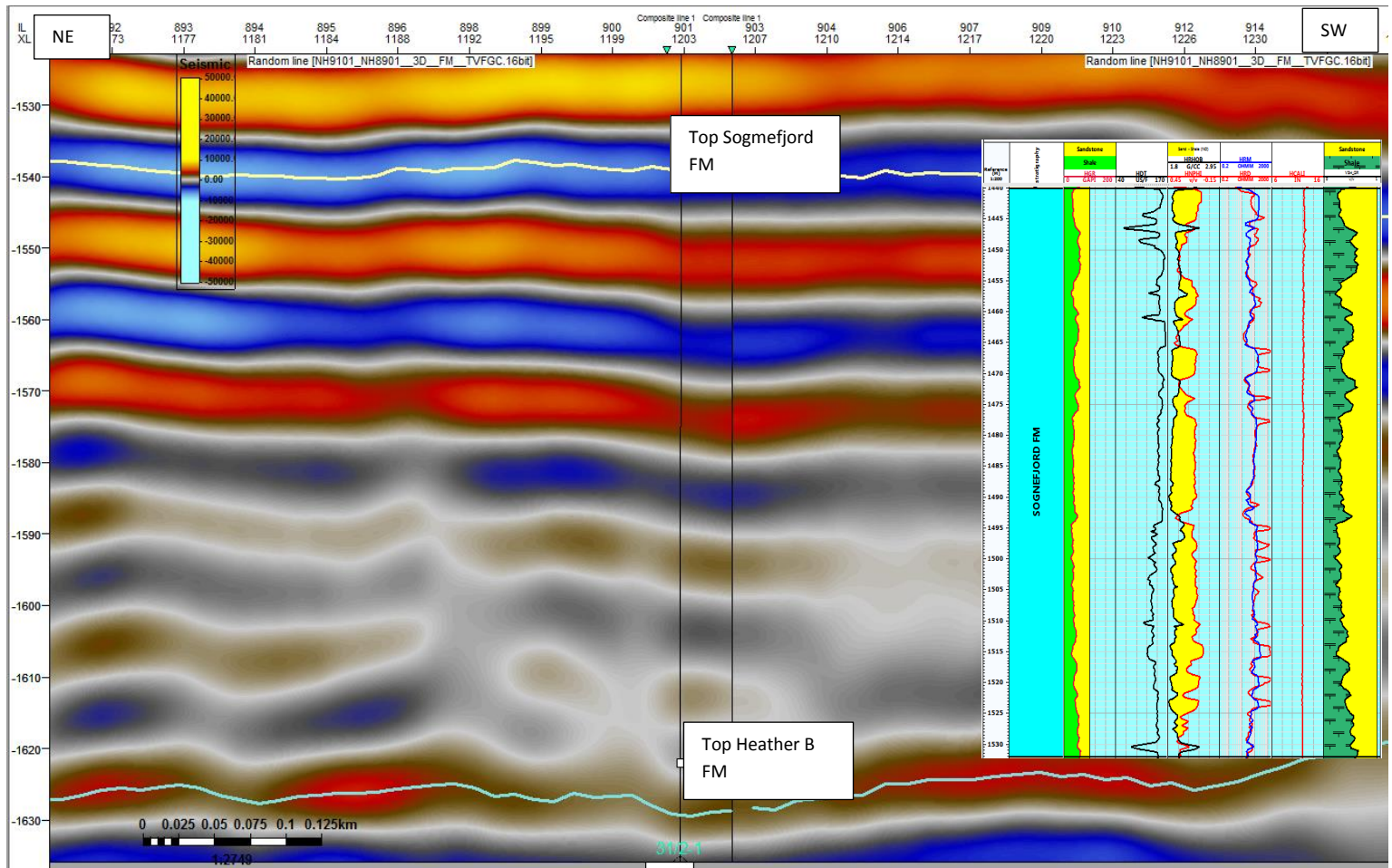
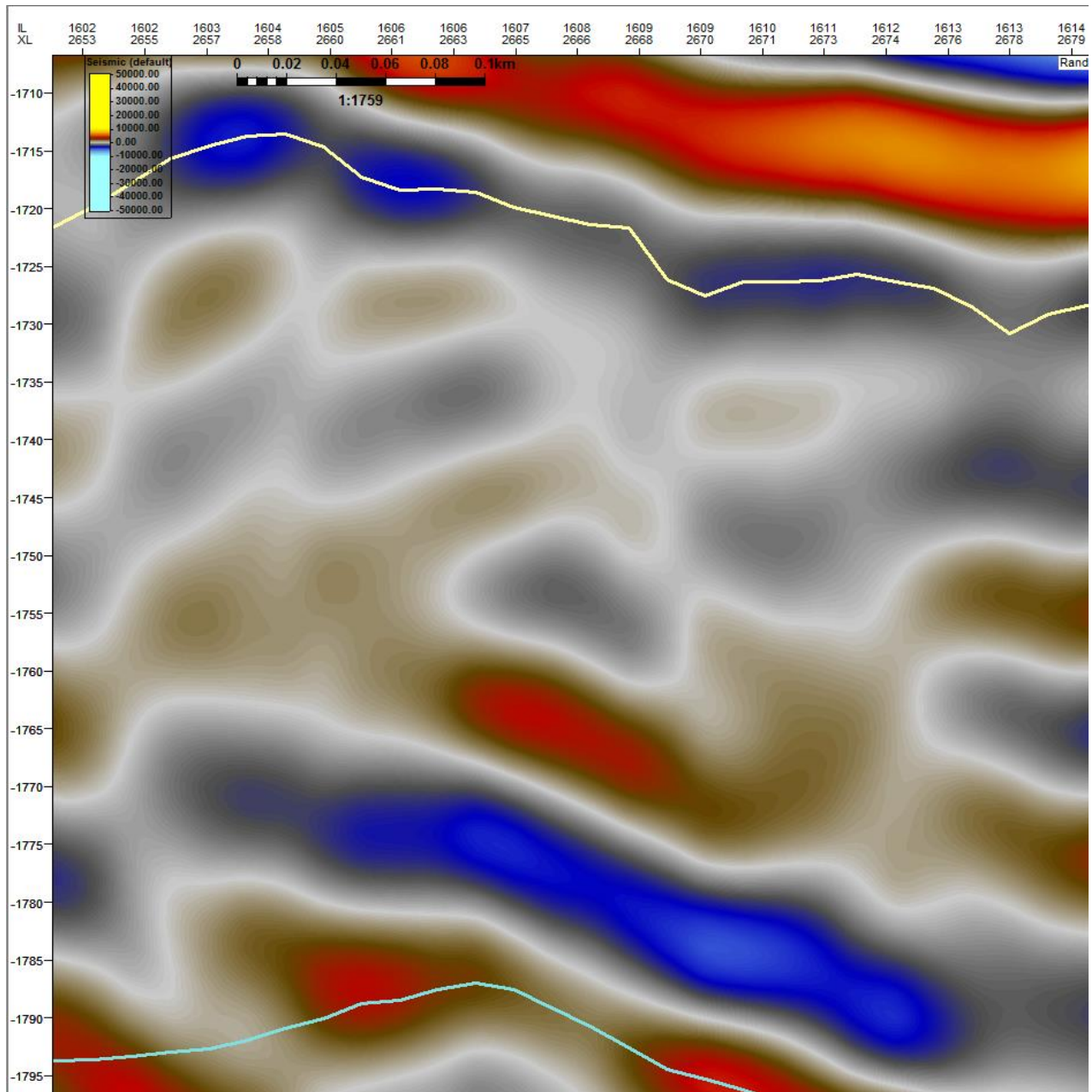


Figure 4.36: Seismic Section showing interpreted Sognefjord Formation. See Fig.4.14 for location.

#### 4.5.1.1 Reflection Pattern

Reflection pattern of the Sognefjord Formation is discontinuous along the Faults. This horizon is very clear in the inner part of in lines but gradually faints out towards the eastern part (Fig. 4.37). At the edges of the fault blocks, the reflection merges with Draupen Formation reflection (Fig. 4.38).



**Figure 4.37:** Seismic section shows dim reflection pattern of the Sognefjord Formation in eastern part of the in-lines. See Fig. 4.39 for location.

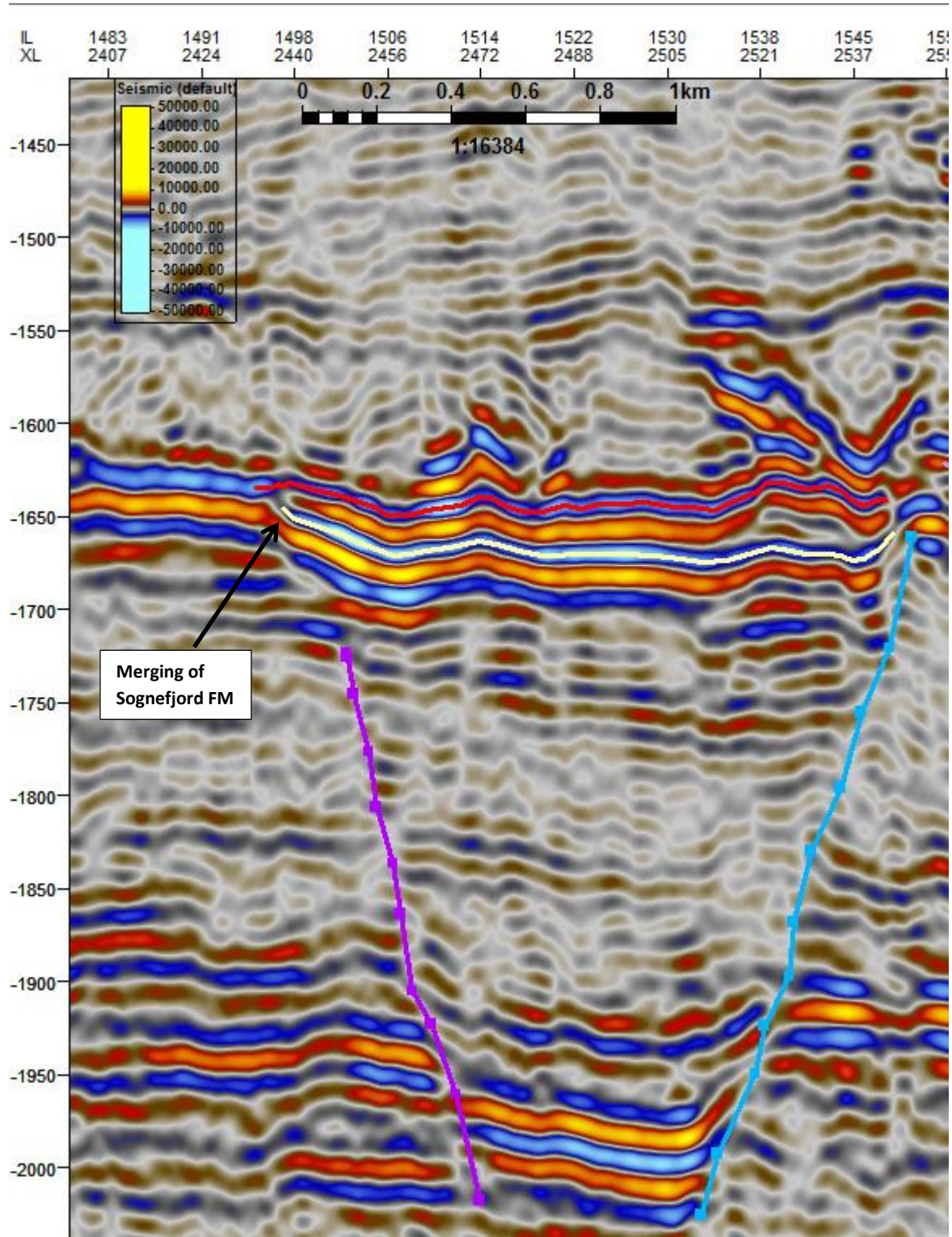


**Figure 4.38:** Seismic section shows the merging of the Sognefjord reflection with the Draupen Formation reflection in the eastern part. See Fig. 4.39 for location.

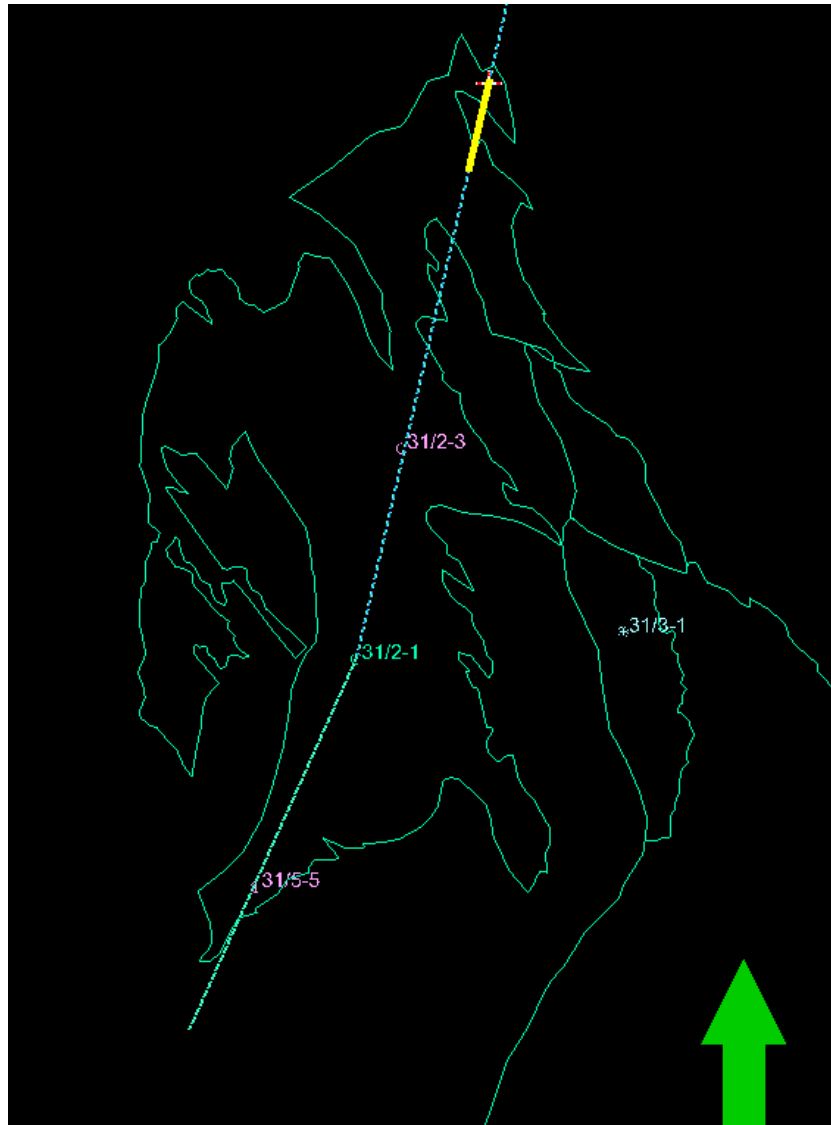


**Figure 4.39:**Location of seismic section in Figs.4.37-38.

#### 4.5.1.2 Time Structure Mapping (Z values)

Interpreted surface map of the Sognefjord Formation is shown in Fig.4.40. The High time values (light green colours) indicate main structural lows where as low time values (Red colours) indicate main structural highs. Structural highest position lies in the eastern side of the area with 3 way dip closure. The closure with 3 way dip is also found in the middle of the area. Structurally lowest position is shown on western side. The structurally high positions show erosion of the Sognefjord Formation as can be seen by truncation of strata in Fig. 4.41.

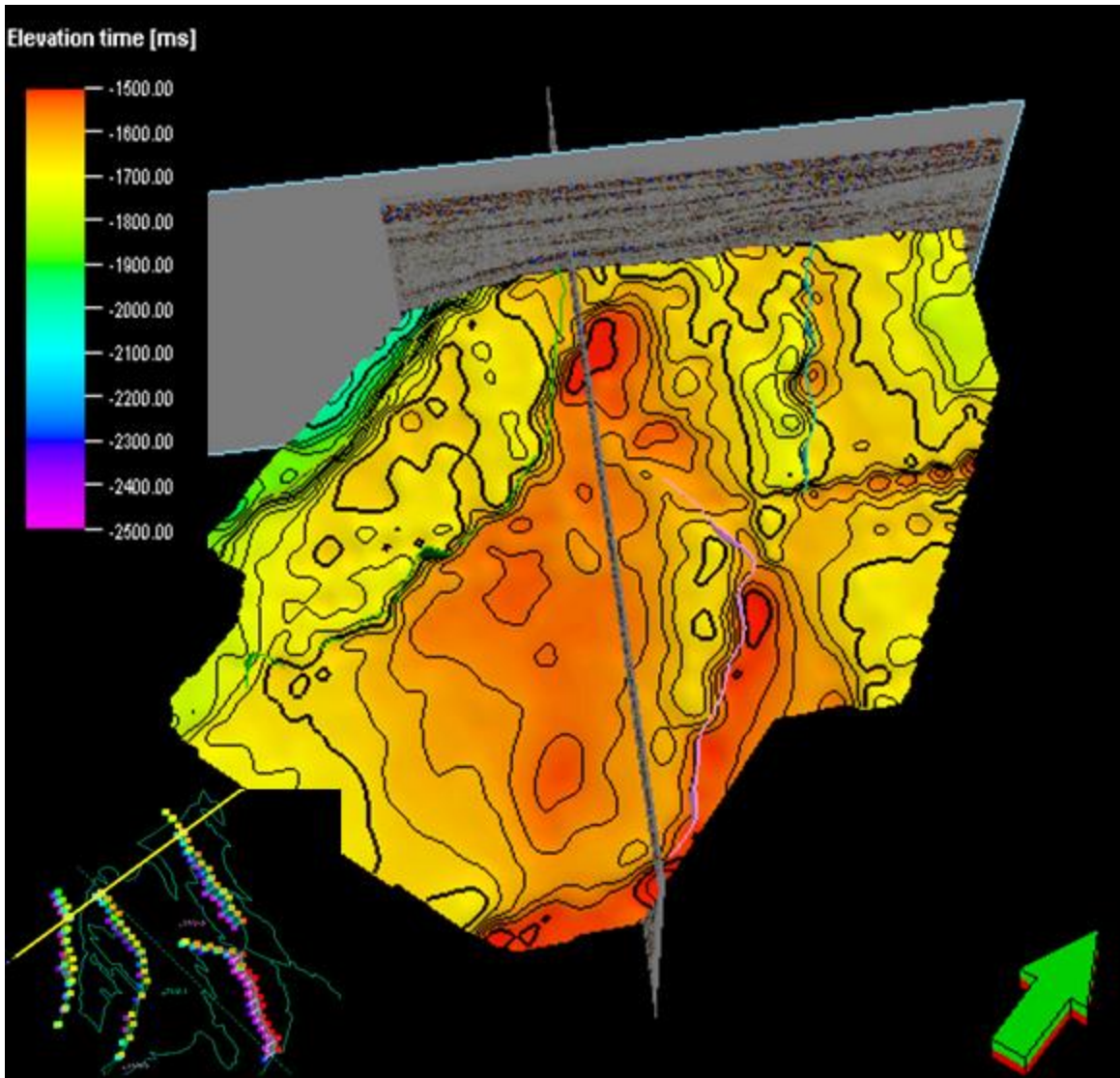


**Figure 4.40** Time structure map of the Sognefjord Formation in 3D window.

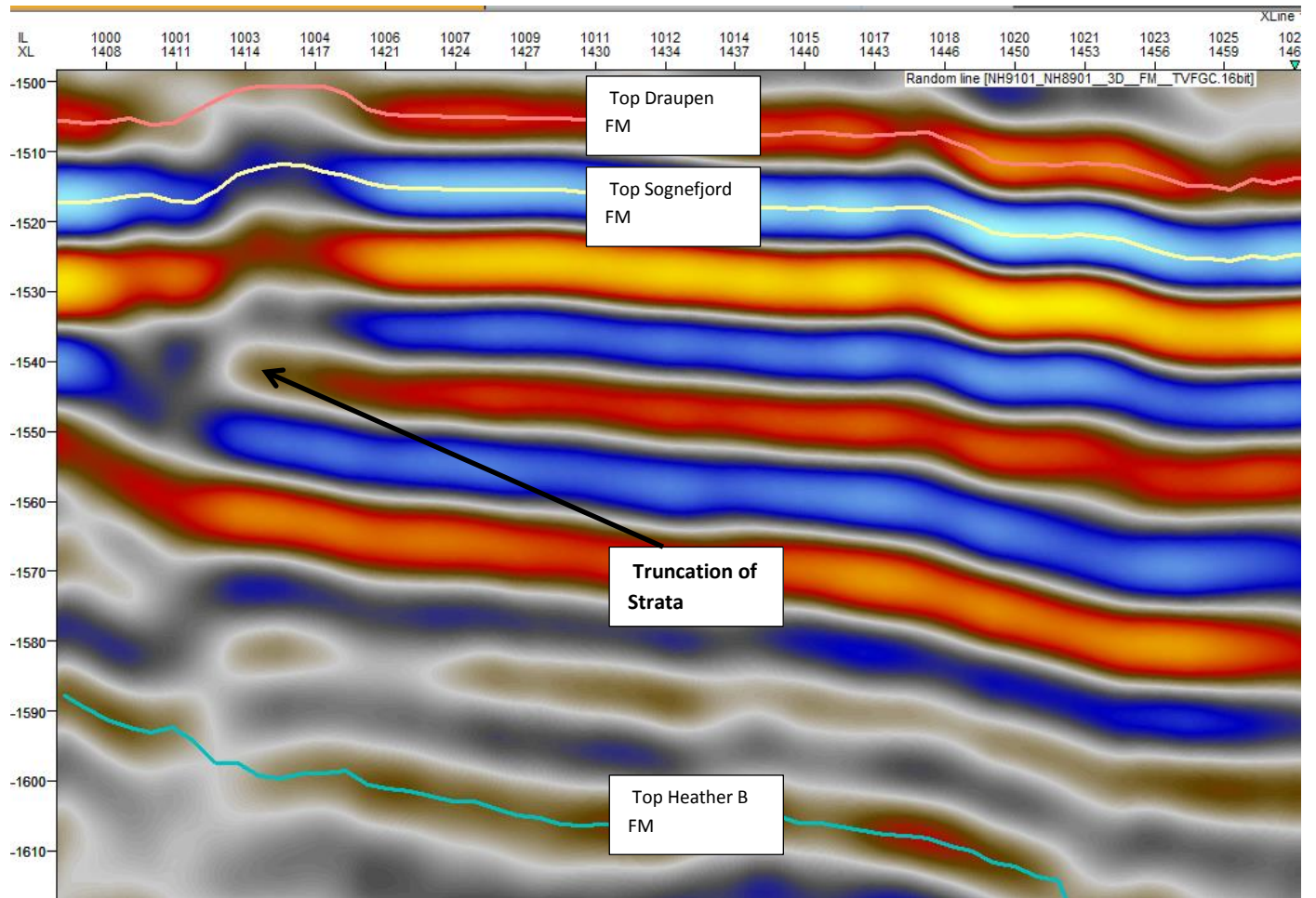


**Figure 4.41:** Seismic section shows the erosion of the Sognefjord Formation by truncation of strata. See Fig. 4.42 for location.

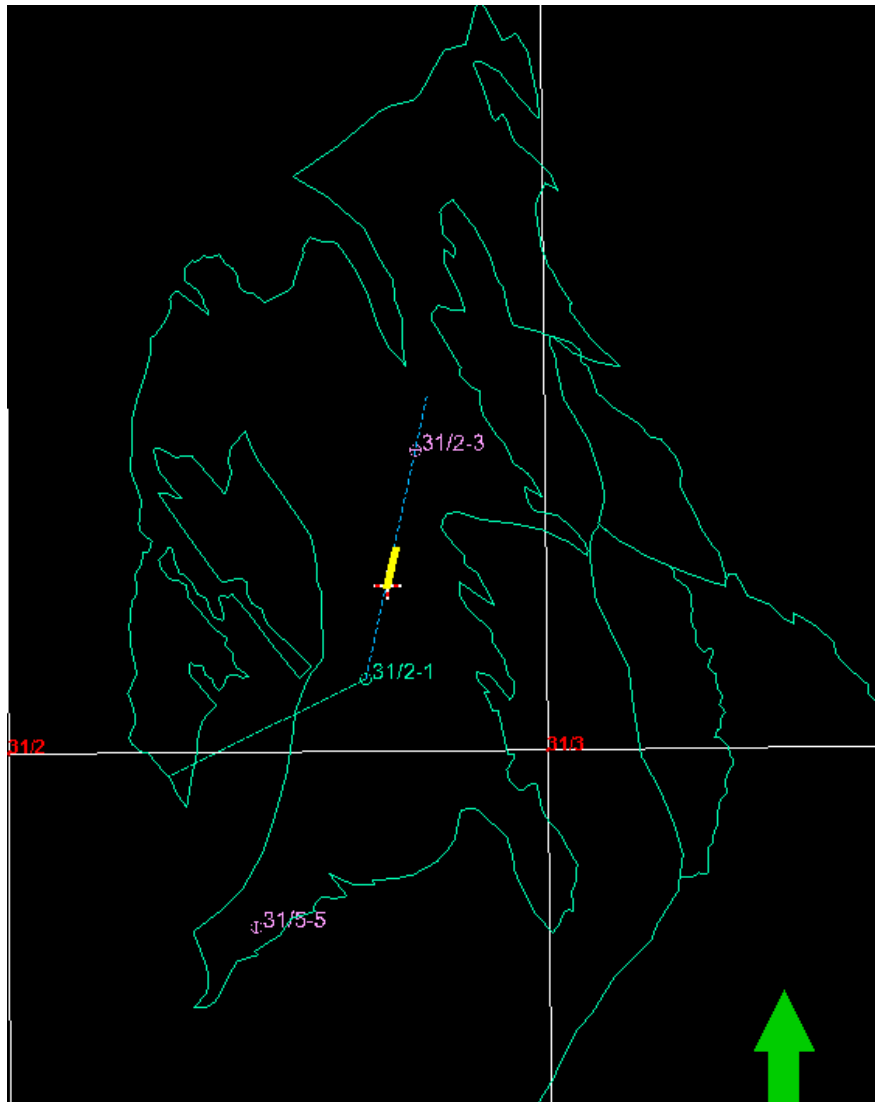


**Figure 4.42:** Location of seismic section in Fig. 4.41.

### 4.5.1.3 Amplitude Mapping

This is very important attribute for the Sognefjord Formation. The negative amplitude shows the area with more hydrocarbon contents. Thus blue area shows the area of Flat-spot.

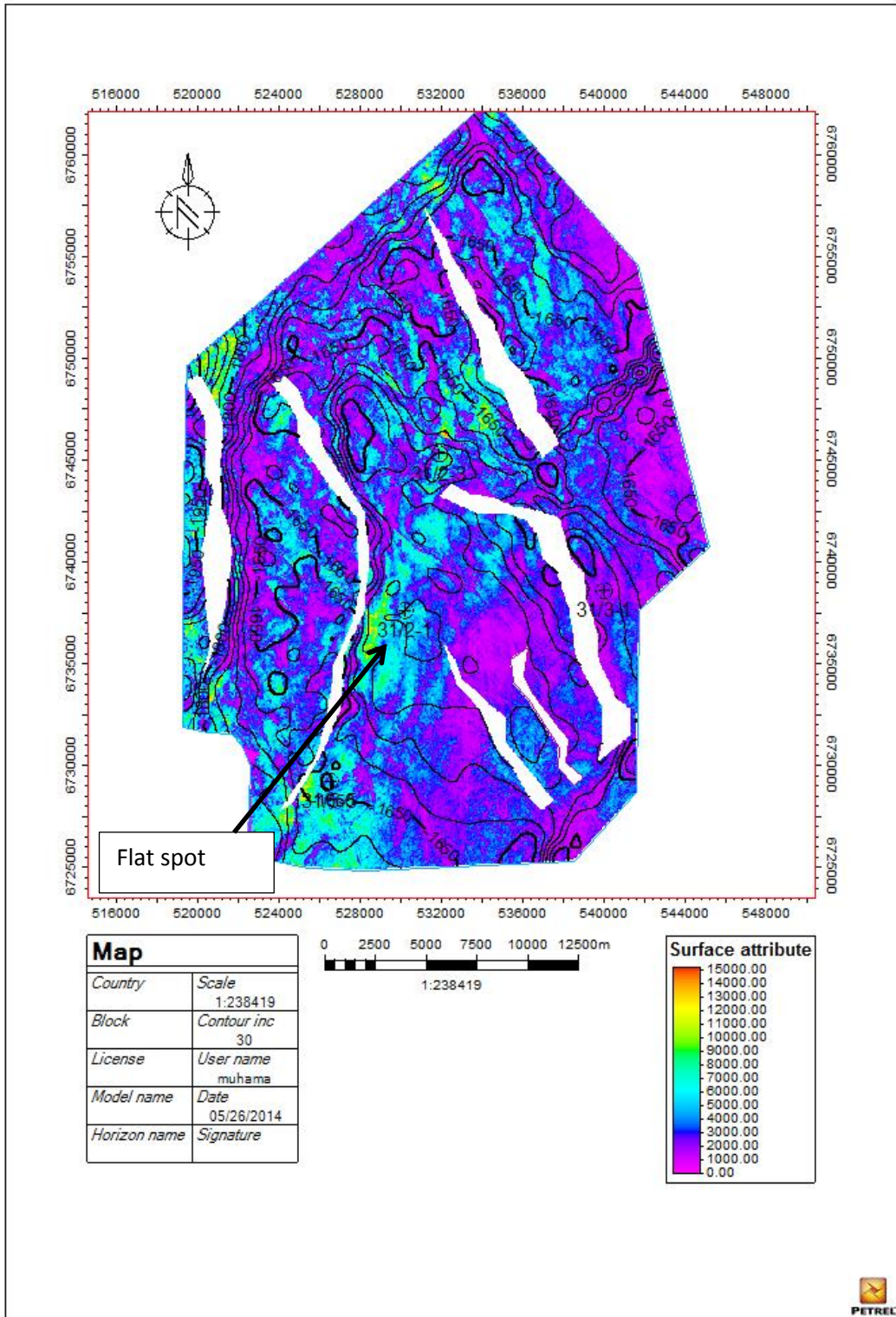


Figure 4.43: Amplitude attribute map (RMS) of the Sognefjord Formation.



#### **4.5.1.4 Facies Description**

The Sognefjord Formation consists of six depositional cycles (Fig.4.44). Every cycle shows a rapid rise in sea level. All cycles begin with a distal, low energy, fine mica rich sand at the base and end with clean sand at the top as shown in Fig. 4.45. This clean sand at the top of every cycle shows shoreface progradation. Subsequent transgressive phases deposits frequently cover the storm deposits from proximal settings (Bolle L.1992).

The cycles range in thickness from 10 m to about 20 m. The character of these cycles varies in space and time. In the Troll west Field, the high energy facies are dominant and cycles are characterized by “base absent” (Fig.4.45). The “base absent” mean that these cycles are lack of fine grained bioturbated part of the ideal sequence (Stewart et al., 1995).

The Sognefjord Formation exhibit excellent porosities, upto 35%, in the clean sands. The permeability is in the darcy range. The low energy micaceous sands show porosities ranging from 26% to 32% and very low permeability (Bolle L.1992).

#### **4.5.1.5 Wireline-log Signature**

The low gamma and density values in the upper part of each cycle show the lack of clay and mica contents and high porosities values as compared to lower part. The high values of gamma ray log and low values of sonic log in the upper part of the formation (e.g.1462-1438 m, Fig.4.44) show high acoustic impedance contrast between stratal layers as shown in Fig. 4.36. It is clear from density and neutron cross over that this formation contains a bulk of hydrocarbons.

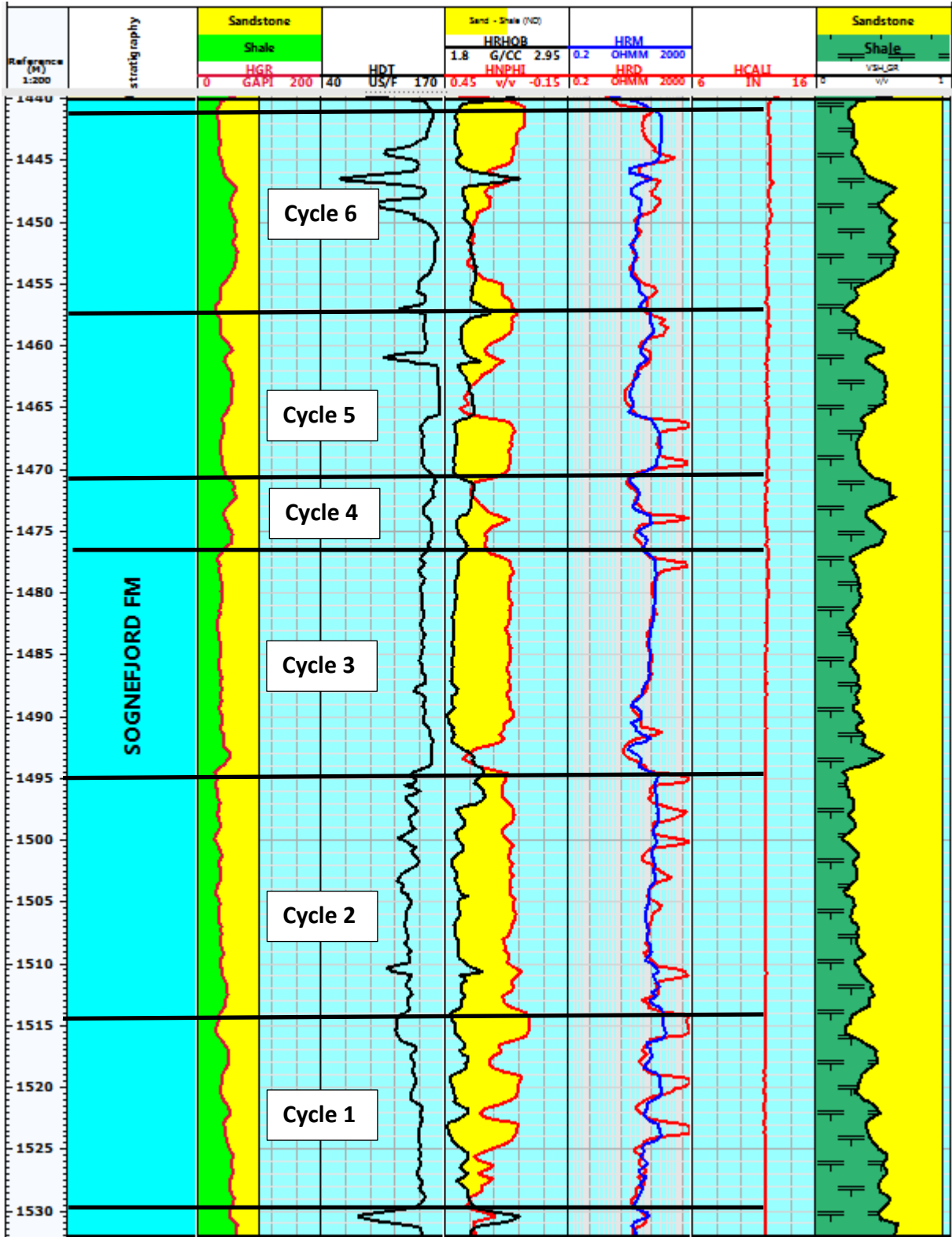


**Figure 4.44:** Wireline log through well 31/2-1 shows the major depositional cycles of Sognefjord Formation

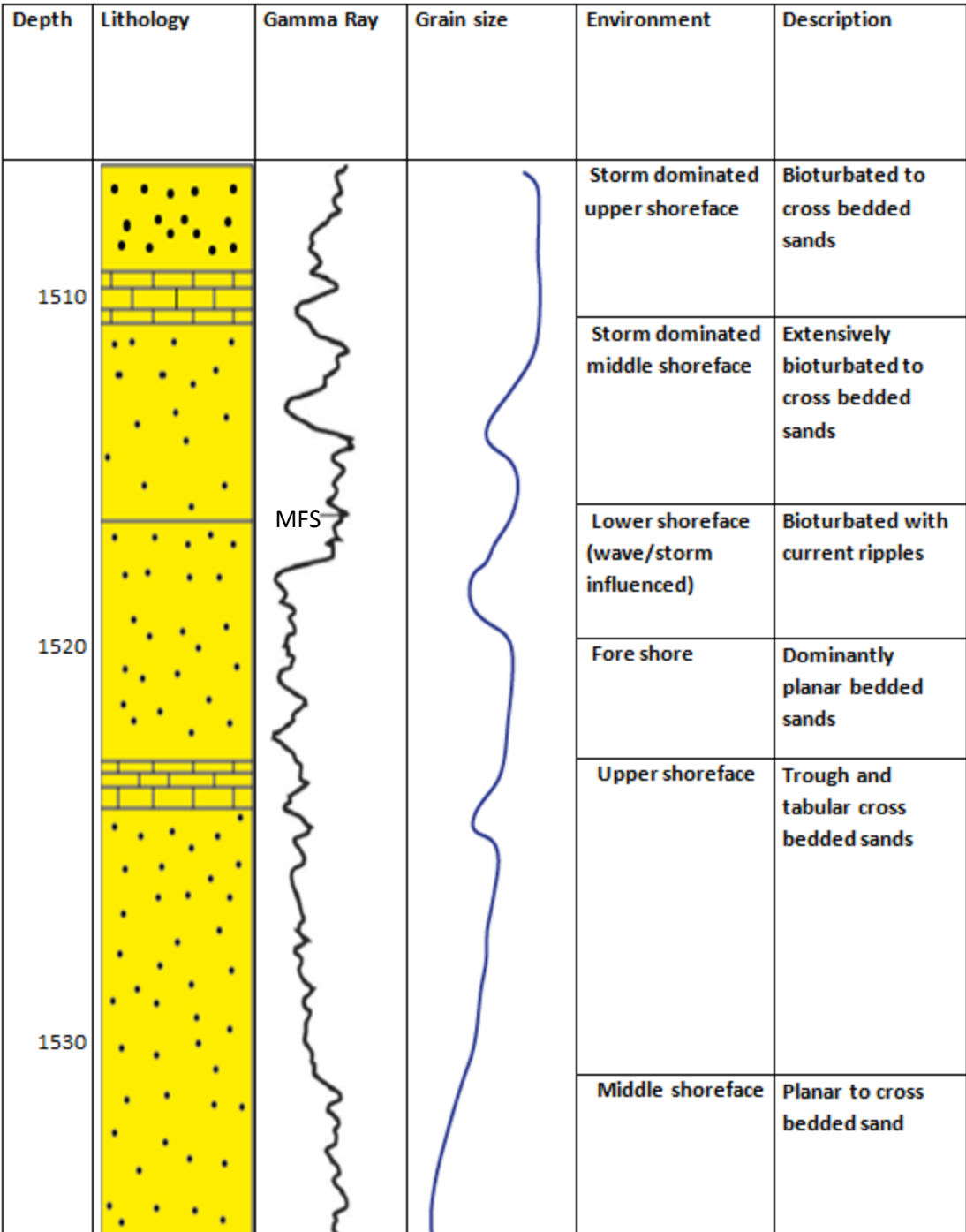


**Figure 4.45:** Ideal shelf-upper shoreface coarsening upward cycle 31/2-1 (modified from (Stewart et al., 1995).

#### **4.5.1.6 Interpretation**

The Sognefjord Formation on the Troll West deposited in shallow marine settings. This Formation is seismically characterized by low angle clinoforms.

Lower Sognefjord Fm: Spit-shoreface system (wave dominated).

Upper Sognefjord Fm: Tide dominated delta (Dreyer T. et al., 2005).

The Sognefjord Formation shows a shoreface transgression, followed by progradation across the shelf. The evidence from well and seismic data shows that during the deposition of Sognefjord Formation, the sediment dispersal followed a complex pattern (Fig. 5.7) and westward progradation occurred (Fig. 4.46) (Stewart et al., 1995).

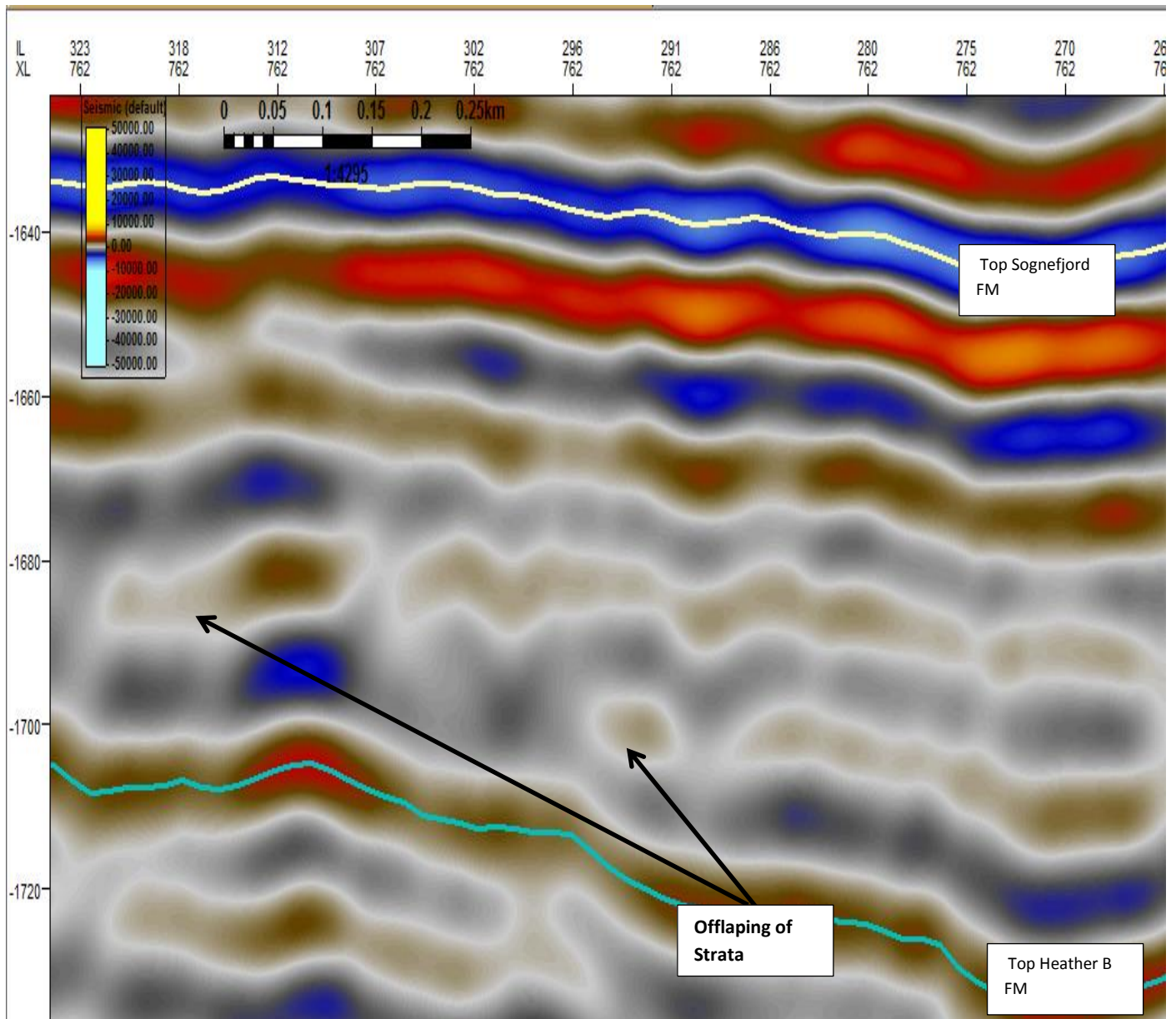


**Figure 4.46:** Cross-line 762 shows southward offlap of the Sognefjord Formation. See Fig. 4.47 for location.

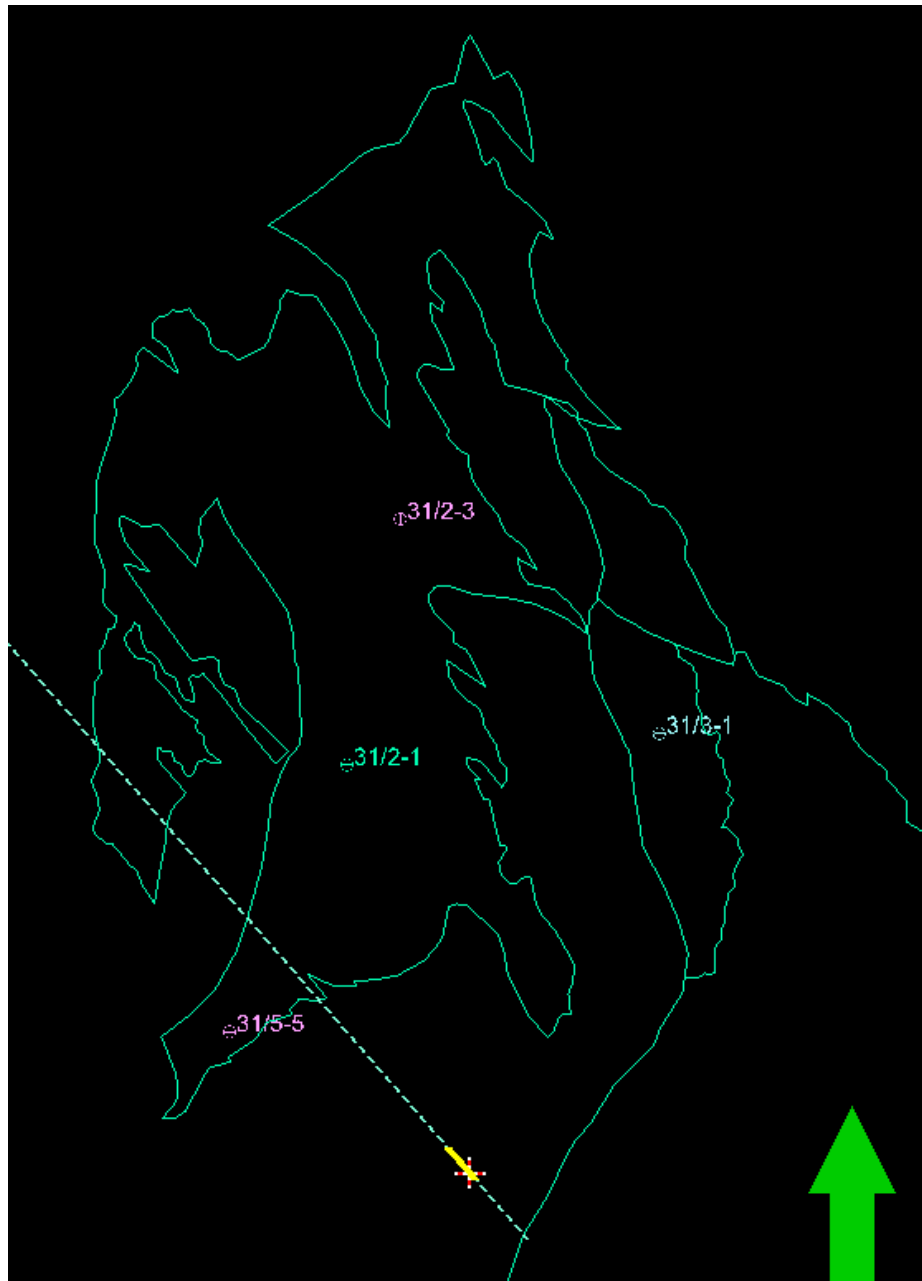


**Figure 4.47:** Location of seismic section in Fig. 4.46.

#### 4.5.2 Fensfjord Formation

Reflection pattern of the Fensfjord Formation is continuous in the middle part of inlines (Fig. 4.48) but dims out in the western part (Fig. 4.49). This horizon changes its polarity above and along the flatspot. The horizon shows the negative amplitude/trough (Blue) along the flat spot (Fig. 4.52) while positive amplitude/peak (Red) above the flat-spot (Fig. 4.50).

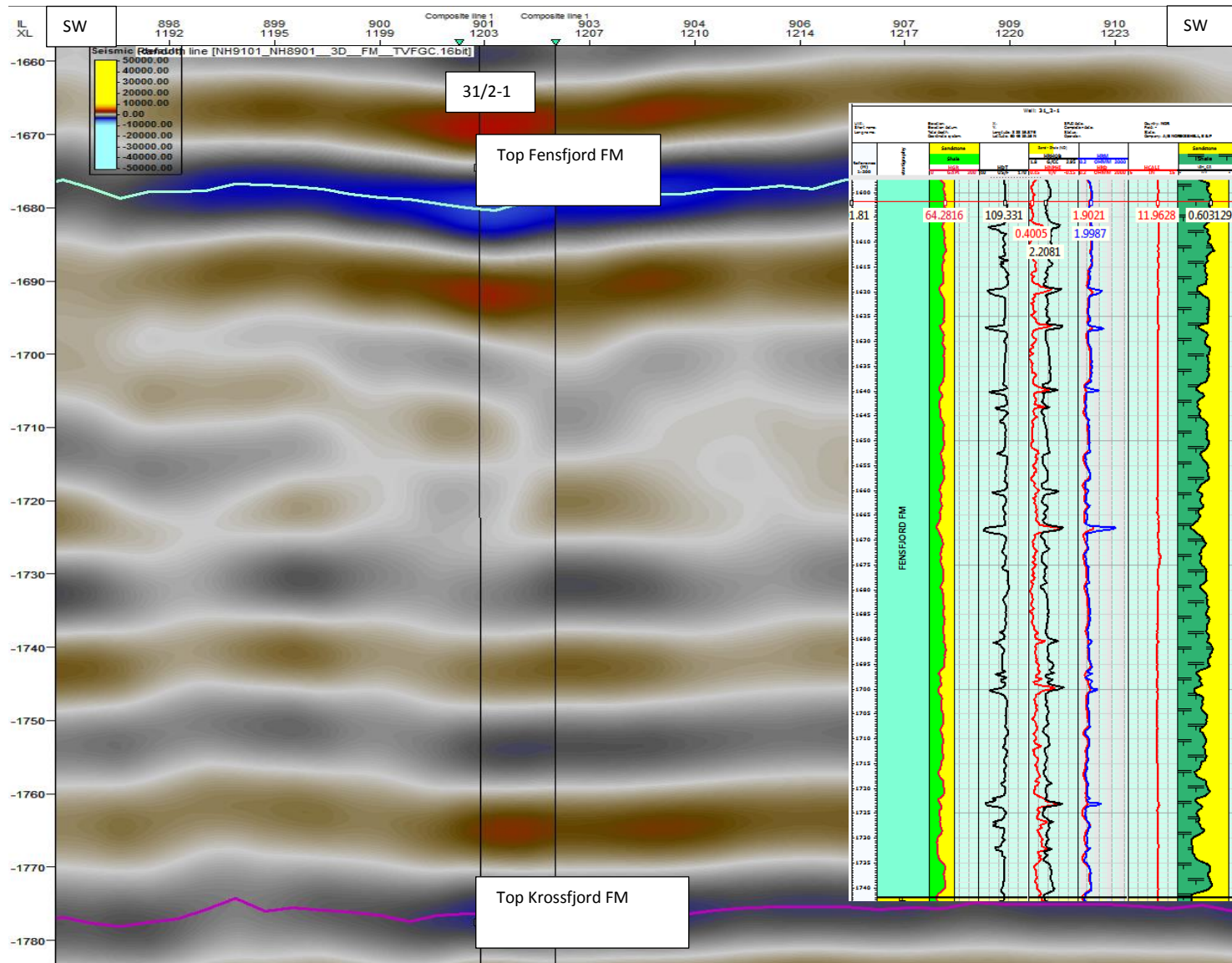
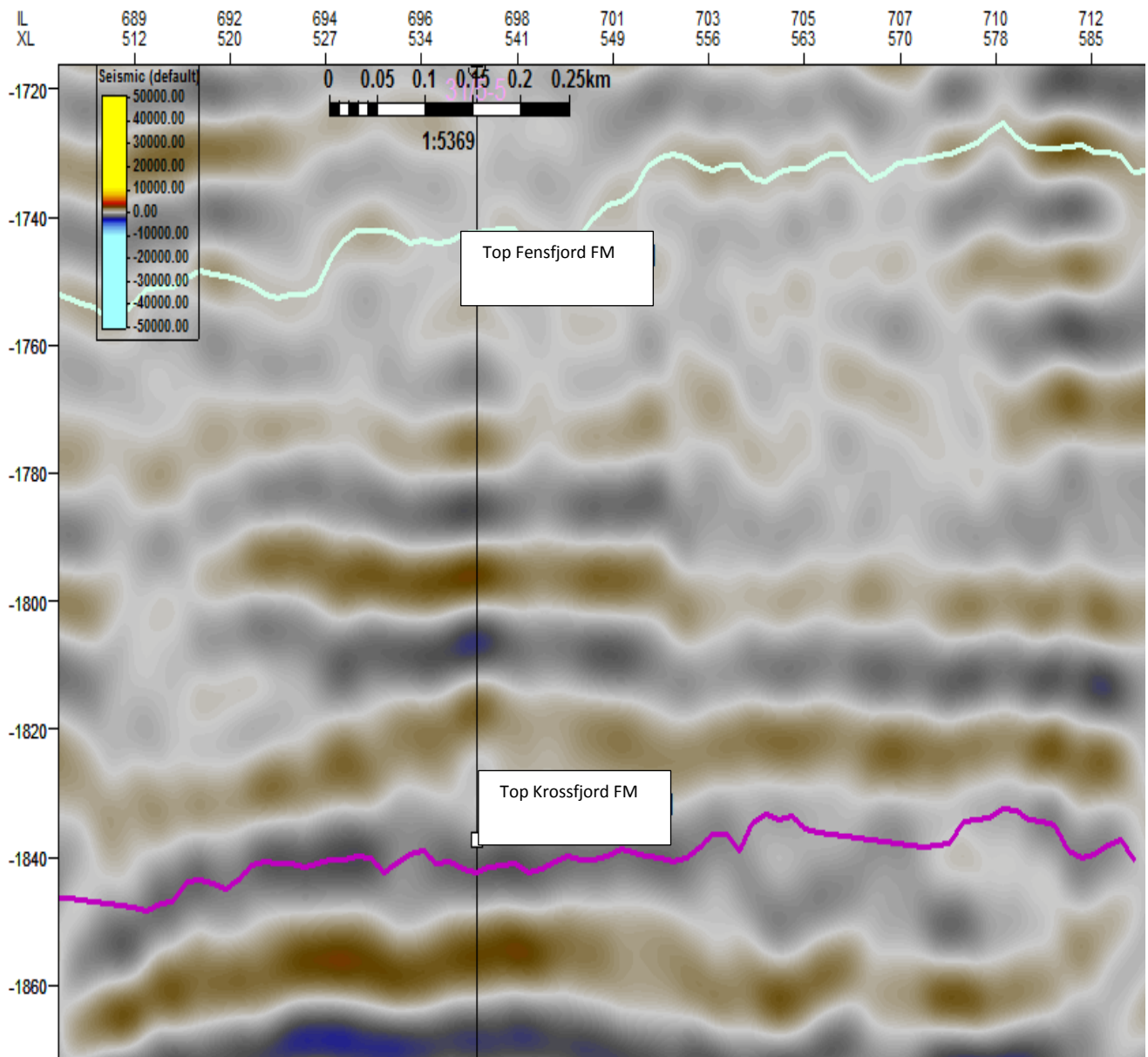
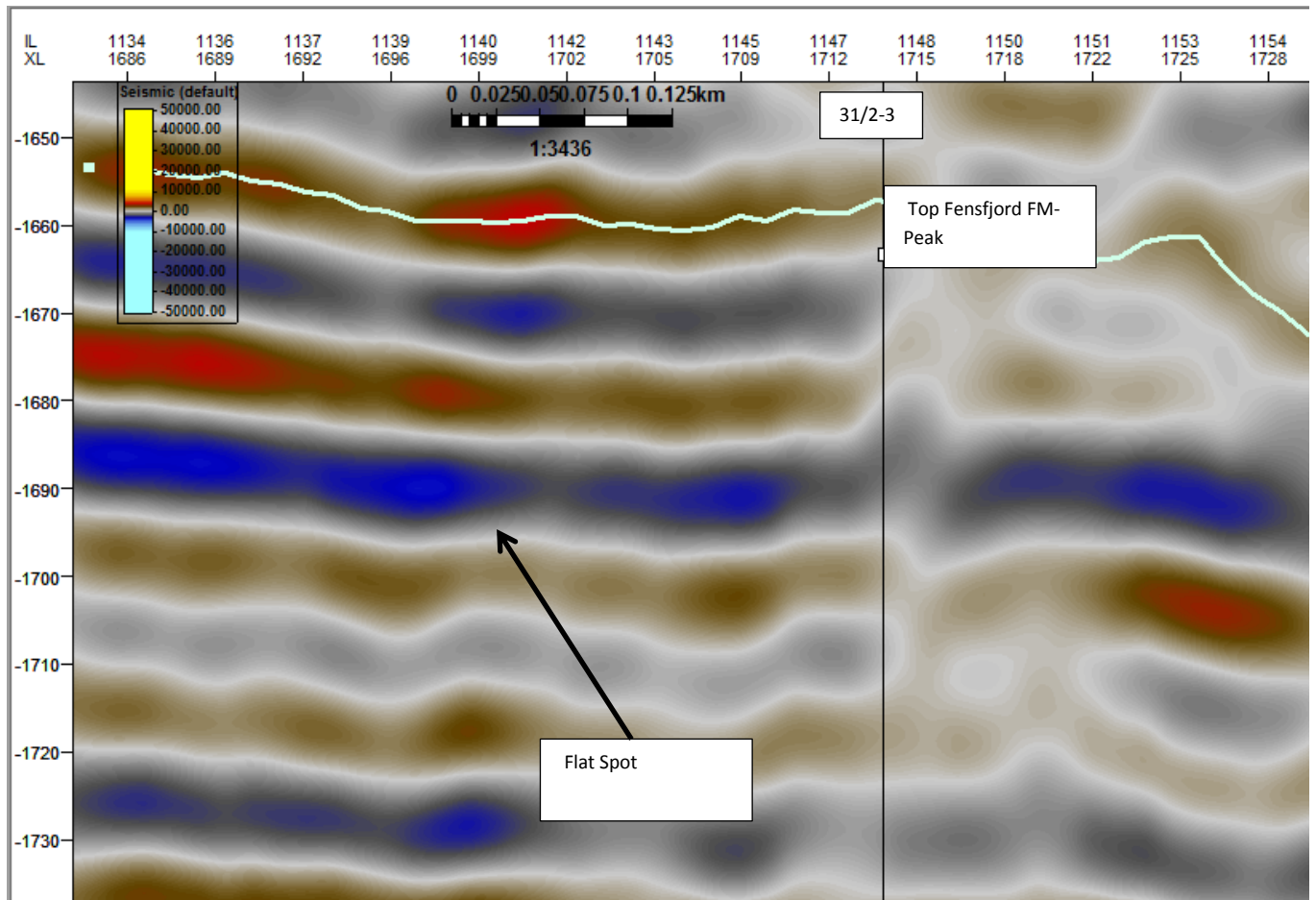


Figure 4.48: Seismic section shows the interpreted Fensfjord Formation. See Fig. 4.14 for location.



**Figure 4.49:** Seismic section shows dim reflection pattern of the Fensfjord Formation in western part of the inlines. See Fig. 4.25 for location.





**Figure 4.50:** Seismic section shows the positive e polarity of the Fensfjord Formation along flat spot in well 31/2-3.

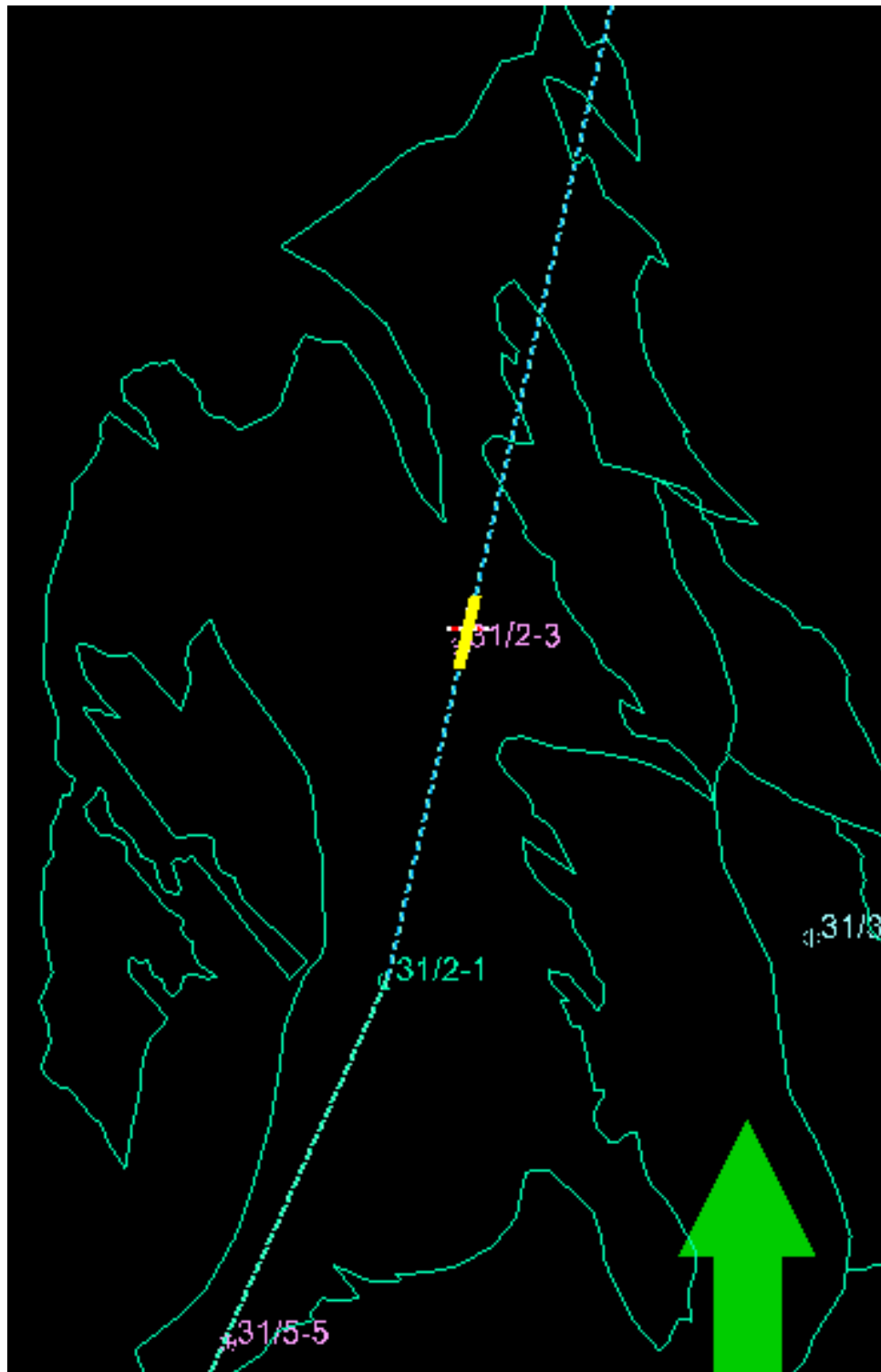
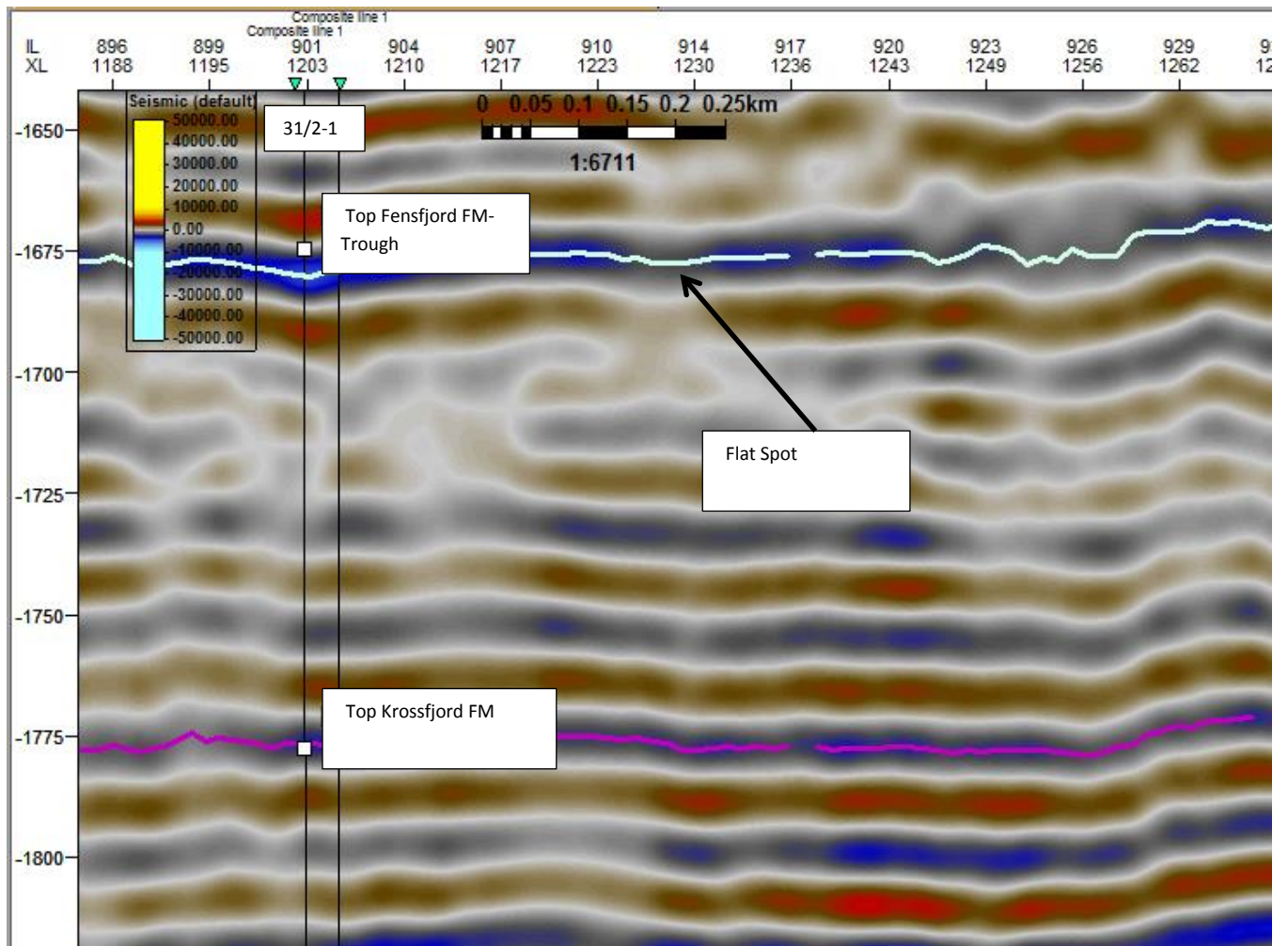
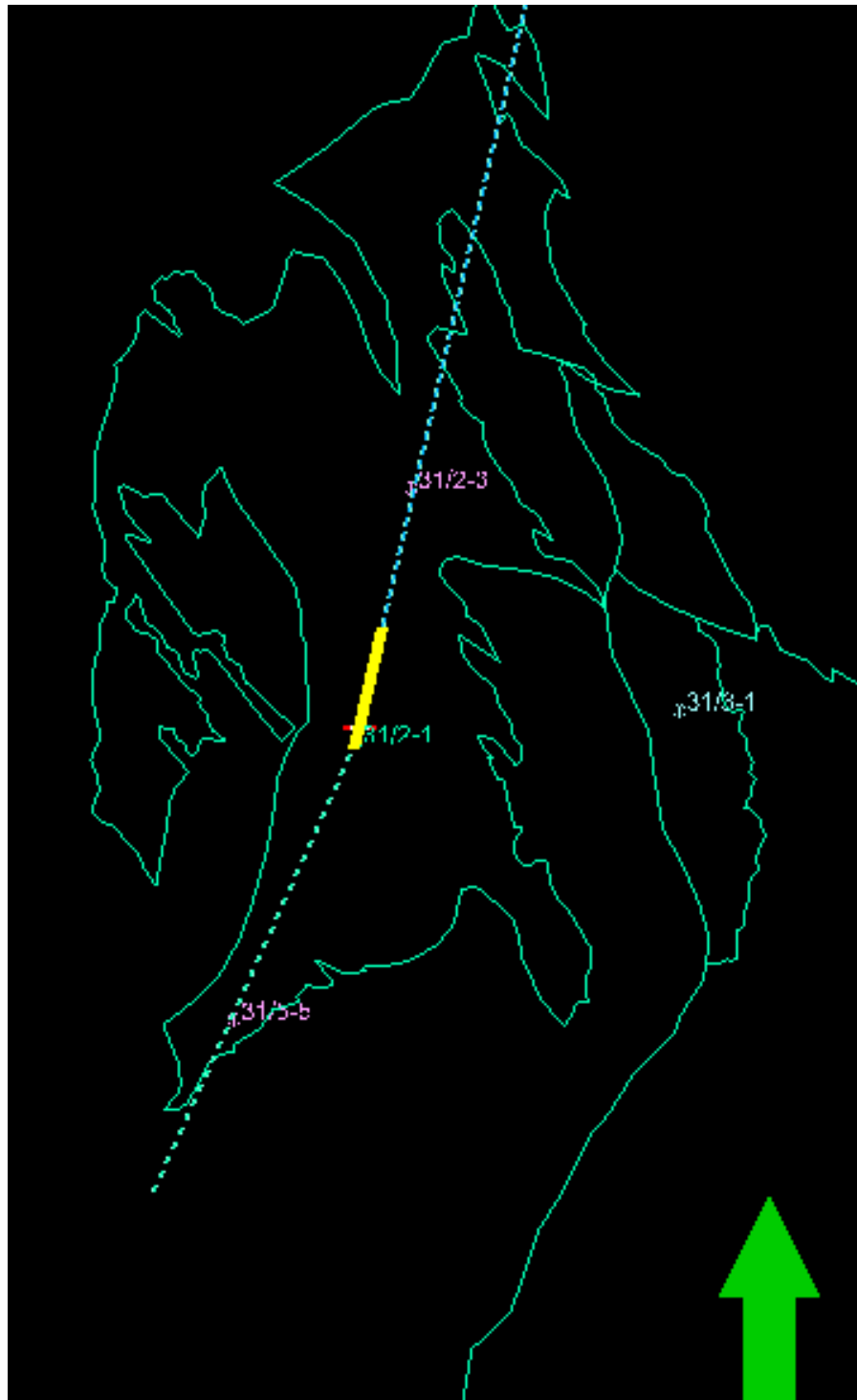


Figure 4.51: Location of seismic section in Fig. 4.50.



**Figure 4.52:** Seismic section shows the negative polarity of the Fensfjord Formation along flat spot in well 31/2-1.



**Figure 4.53:** Location of seismic section in Fig. 4.52.

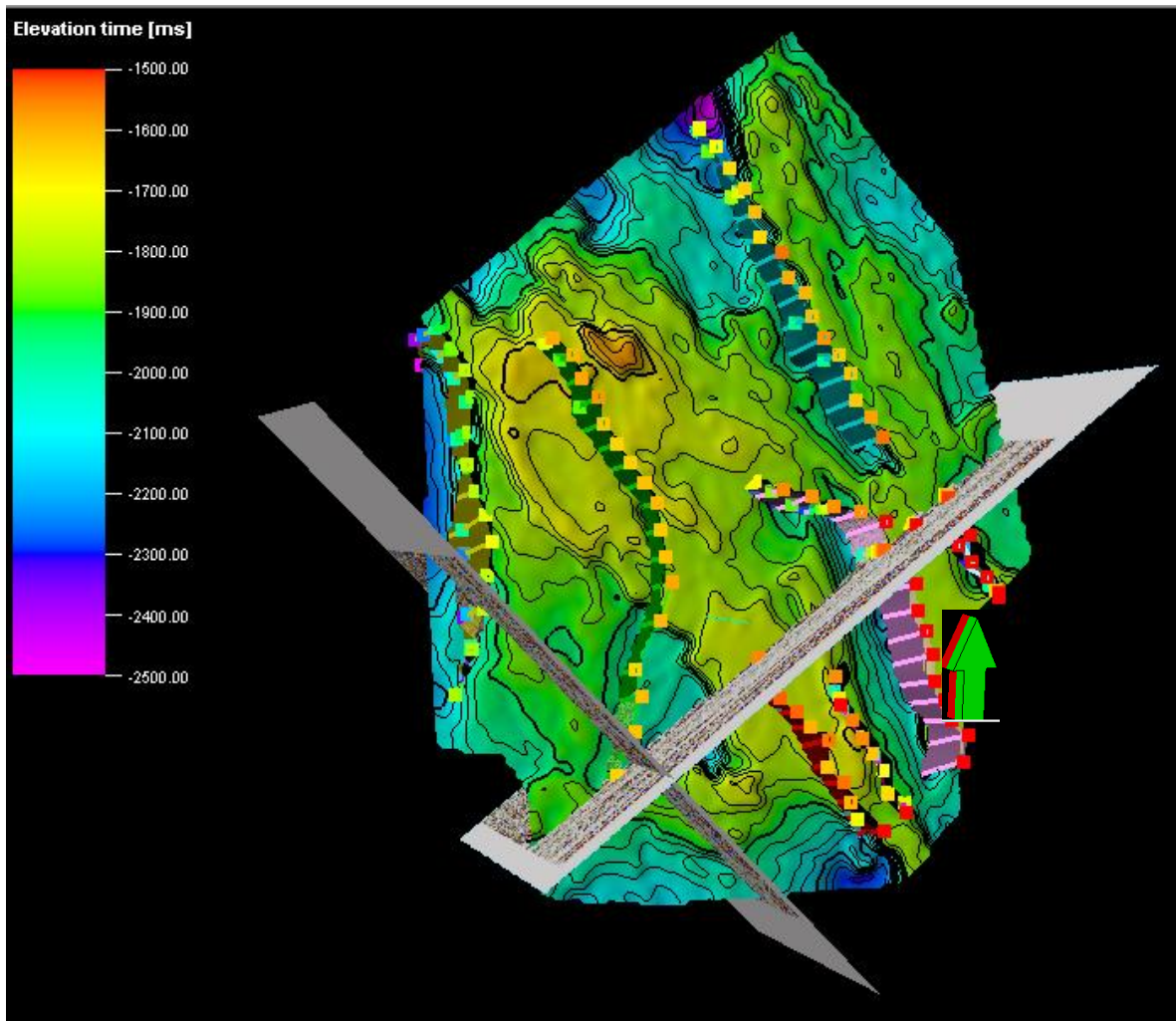


**Figure 4.54:** Time Structure map of Fensfjord Formation in 3D window

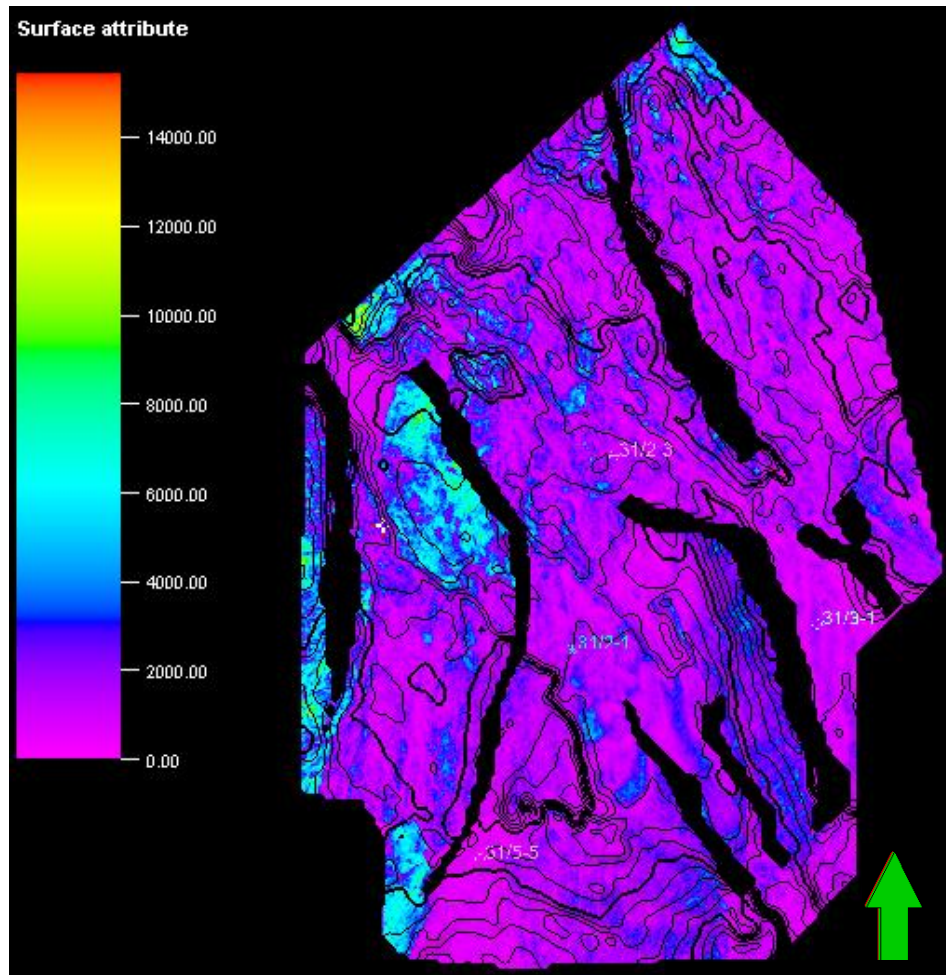


**Figure 4.55:** RMS map of Fensfjord Formation.

#### 4.5.2.1 Facies Association 1

In Fensfjord and Krossfjord Formations different facies are present which are identified with help of logs and core data. Brief description is given below

Facies	Description
<b>A</b>	Very fine grained, moderately sorted, mica contents are common
<b>B</b>	Fine to medium grained, moderately sorted, mica contents are

	common
<b>C</b>	Coarse grains, coarsening upwards, calcite cement present
<b>D</b>	Medium to coarse grained, well sorted, mica contents are rare
<b>E</b>	Medium to coarse grained, moderately well sorted,

**Table 4.1** Summary of facies in Fensfjord and Krossfjord Formations (Holgate et al., 2013).

Facies association 1 consists of 20m thick successions of Facies B and C. These successions are coarsening upwards. Very-fine to medium grained sandstone that have rare lamination (Facies B) passes upwards into fine to medium grained sandstone that consist of rhythmically interbedded intervals (Facies C). The structureless beds of granular to fine-grained sandstone (Facies I) occur within Facies B and C (Holgate, Jackson et al. 2013).

#### 4.5.2.2 Wireline-log Signature

The upwards decrease in gamma-ray and density-log values, and upward increase in neutron and sonic log values (e.g. from 1618 to 1612 in Fig.4.56) reflects the transition from Facies B to C. The overall high gamma-ray values show high mica contents in Facies A and B (Holgate, Jackson et al. 2013).

#### 4.5.2.3 Interpretation

This Facies Association is deposited under fair weather suspension settling and more energetic hydrodynamic conditions.

Facies B consists of interbedded sandstone and siltstone which indicate fluctuating energy conditions ( Bourgeois 1980; Dott and Bourgeois 1982; Duke 1985). Siltstone is deposited under fair-weather suspension settling while sandstone reflects deposition in suspension currents generated by storms. The high bioturbation index of siltstones suggests that they have gone through prolonged fair-weather conditions that caused biogenic reworking of sediments. These are typical characteristics of “Transition Zone”. This transition zone lies above storm wave base and below fair -weather wave base which is referred to as the “distal lower shore face”. (Holgate, Jackson et al. 2013)

The Facies C is deposited under combined flow formed by unidirectional current generated by a storm which carried out sand from the coast due to high amplitude waves. Then the sand was dispersed by waves through oscillatory motion. Deposited it as hummocks ( Bourgeois 1980; Dott and Bourgeois 1982; Duke 1985) .The Hummocky Cross- Stratification (HCS) is typical characteristics of such flows.(Holgate, Jackson et al. 2013)

The presence of HCS in Facies C shows a more proximal lower shoreface location as compared to Facies B. Thin beds of Facies I were deposited by gravity-driven or storm related flows (Holgate, Jackson et al. 2013).

#### **4.5.2.4 Facies Association 2**

This Facies Association is about 25m thick and consists of Facies D and E. Facies D is coarse grained, well sorted, and laminated to tabular cross-bedded sandstone. This facies is interbedded with or coarsens upwards into Facies E. Facies E is medium to coarse grained structureless sandstone. Facies Association 2 always overlies FA2 in upward coarsening succession (Holgate et al., 2013).

#### **4.5.2.5 Wireline-log Signature**

Low gamma-ray values show the lack of clay and mica contents. This Facies Association has more porosity as compared to FA2 as shown by low density values. Log signatures of FA3 are variable and this variability is due to patchy calcite cementation (Holgate et al., 2013).

#### **4.5.2.6 Interpretation**

Facies D consists of Planar lamination and trough cross bedding (Fig.4.57). The well sorted character of this facies shows extensive reworking in a high energy environment above fair-weather wave base i.e. upper shore face. Alternation of trough cross bedding and planar lamination may be interpreted by the migration of longshore bars and troughs (Nielsen and Johannessen 2001). The bars were dominated by unidirectional currents, which removed the fine-grained material. However, the parallel lamination formed by passage of weaker currents (Holgate et al., 2013).

Facies E is common in upper part of FA3. This facies deposited under constant wave action as indicated by very well- sorted character of sandstone. This wave action removed the fine-grained material (Hart and Plint 1995). The structureless appearance and lack of parallel lamination shows deposition in a foreshore environment (Holgate et al., 2013).





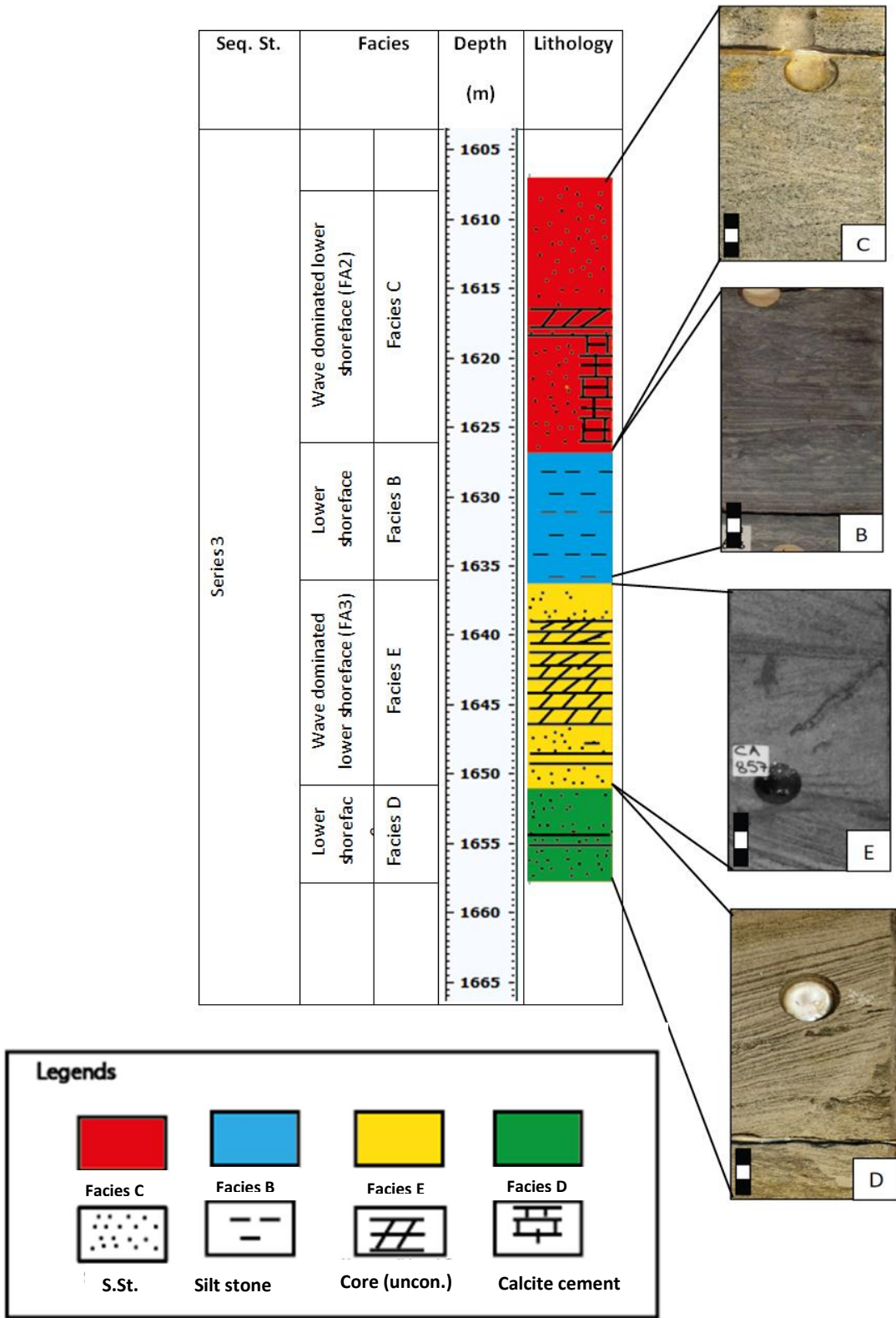


**Figure 4.57:** Lithological column of major facies of the Fensfjord Formation.

### **4.5.3 Krossfjord Formation**

Reflection pattern of the Krossfjord Formation is continuous in the most part of the formation. This horizon is also very clear in the western part but gradually fades out towards the eastern part,(Fig.4.59).

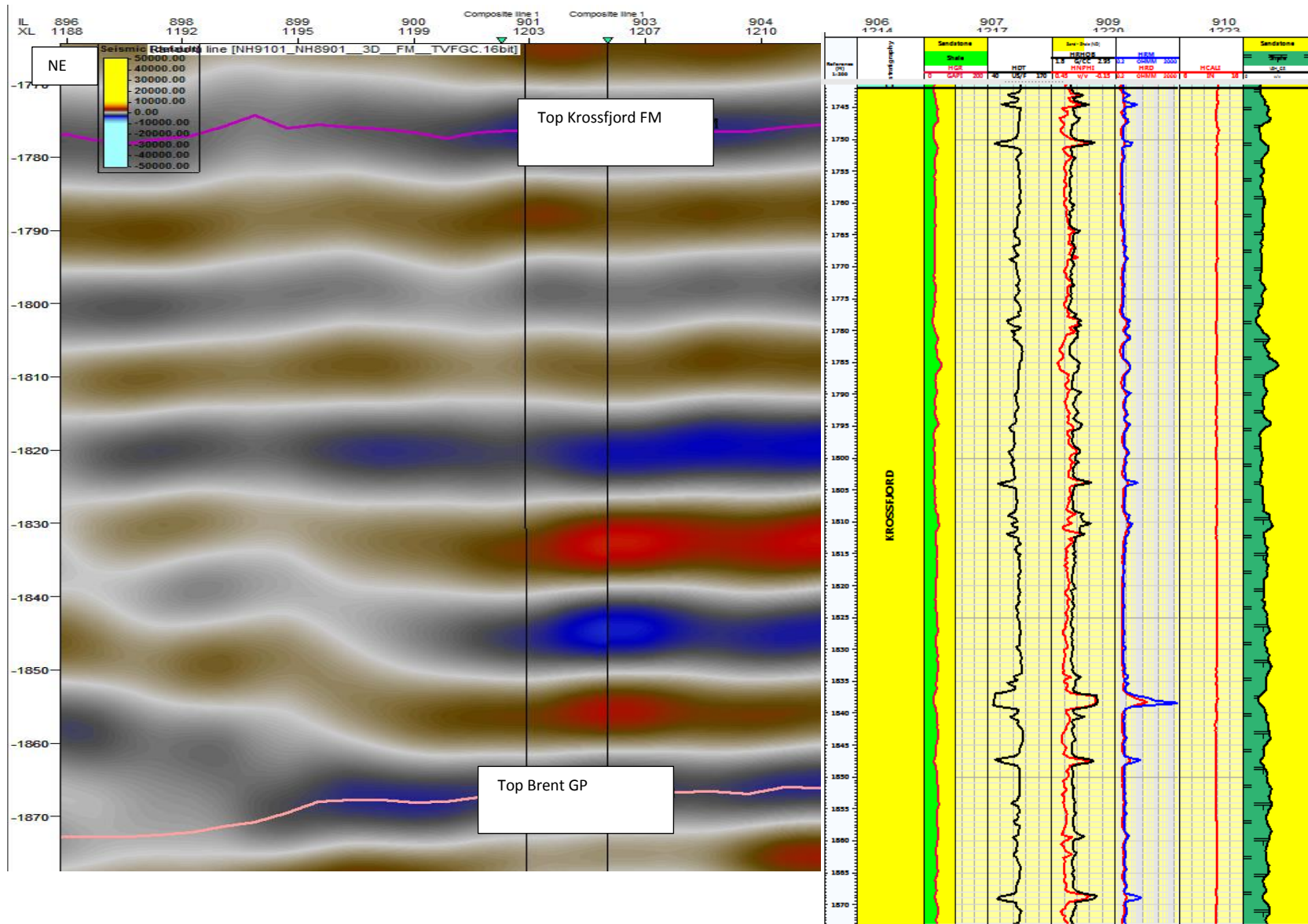


**Figure 4.58:** Seismic section showing the interpreted Krossfjord Formation. See Fig. 4.14 for location.

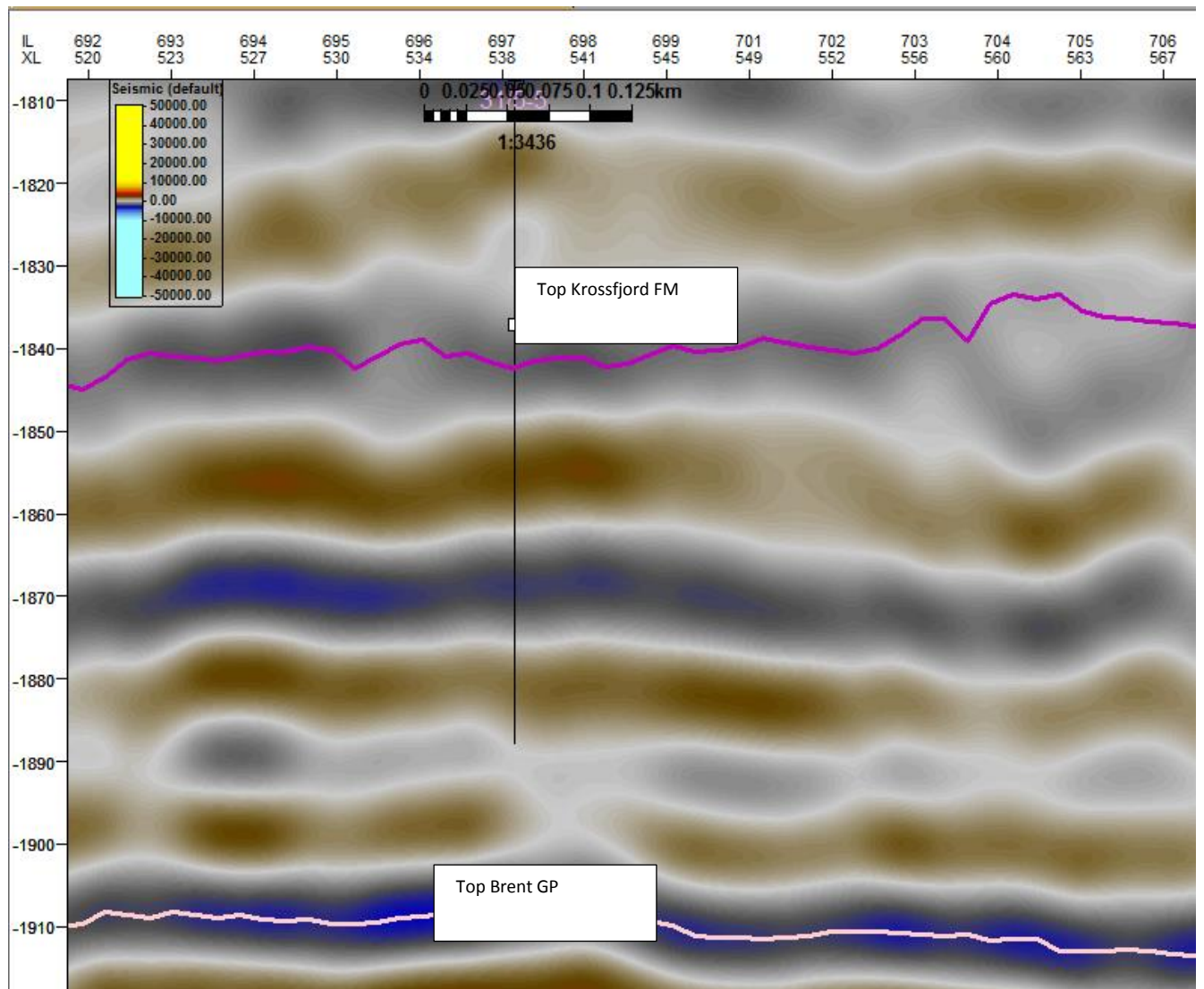


**Figure 4.59:** Seismic section shows dim reflection pattern of the Krossfjord Formation in western part of the in-lines. See Fig. 4.25 for location.

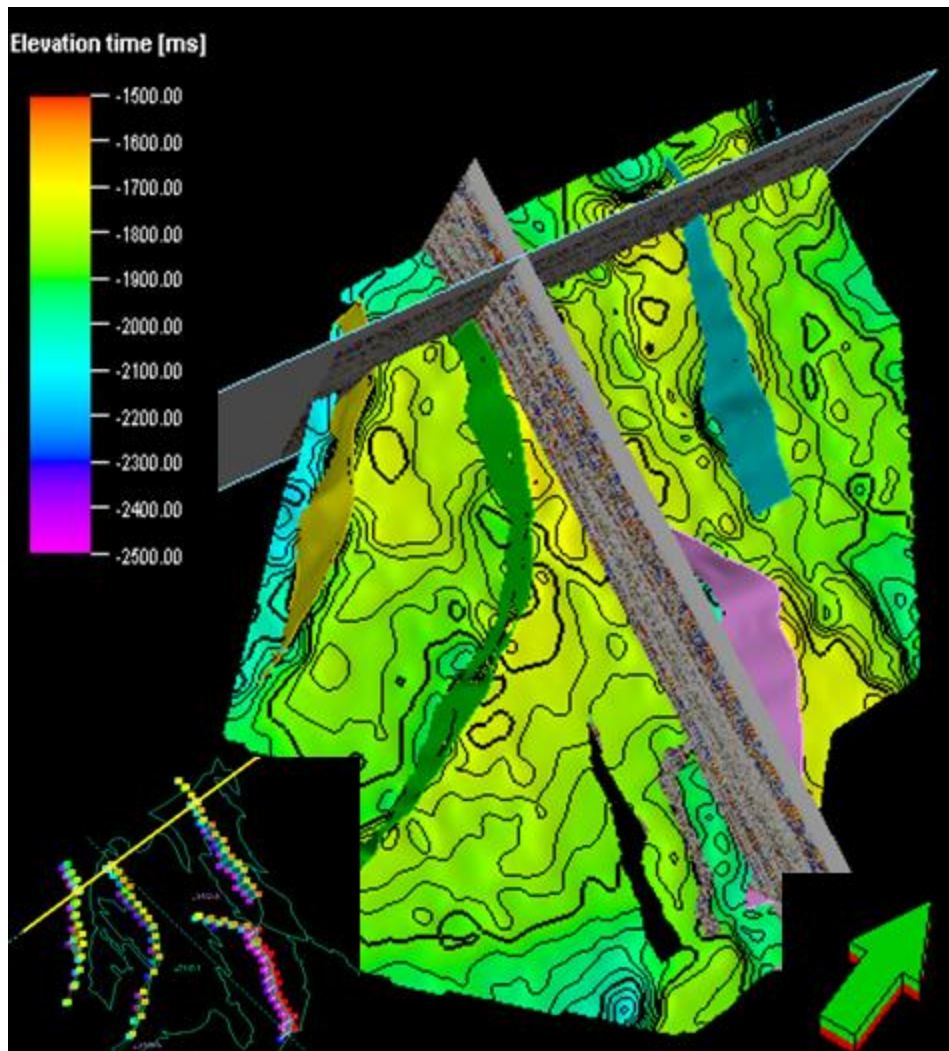


**Figure 4.60:** Time structure map of the Krossfjord Formation in 3D window.

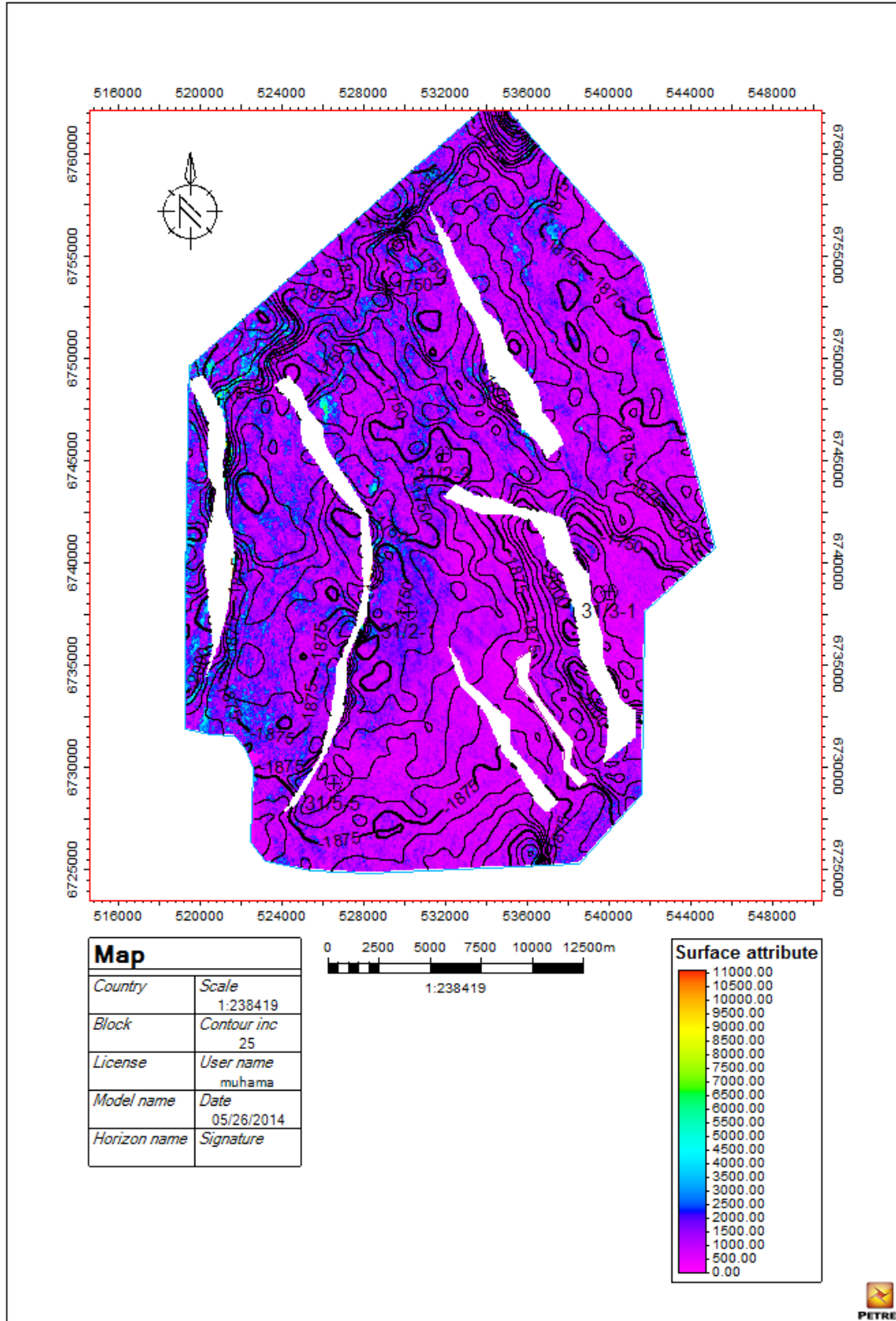


Figure 4.61: Amplitude map (RMS) of the Krossfjord Formation.

#### **4.5.3.1 Delta-front Facies Association**

Krossfjord Formation mainly consists of delta front facies association. This facies association is characterized by fining-upwards, medium to coarse-grained sandstone (Facies I) and small intervals of Facies B. These amalgamated units (Fig. 4.62), which can be identified by almost constant values of gamma ray log, are structureless, although rare lamination is present. Rare and Small intervals of this facies are calcite cemented. The tops of fining upwards units consist of thin intervals of Facies B (Holgate et al., 2013).



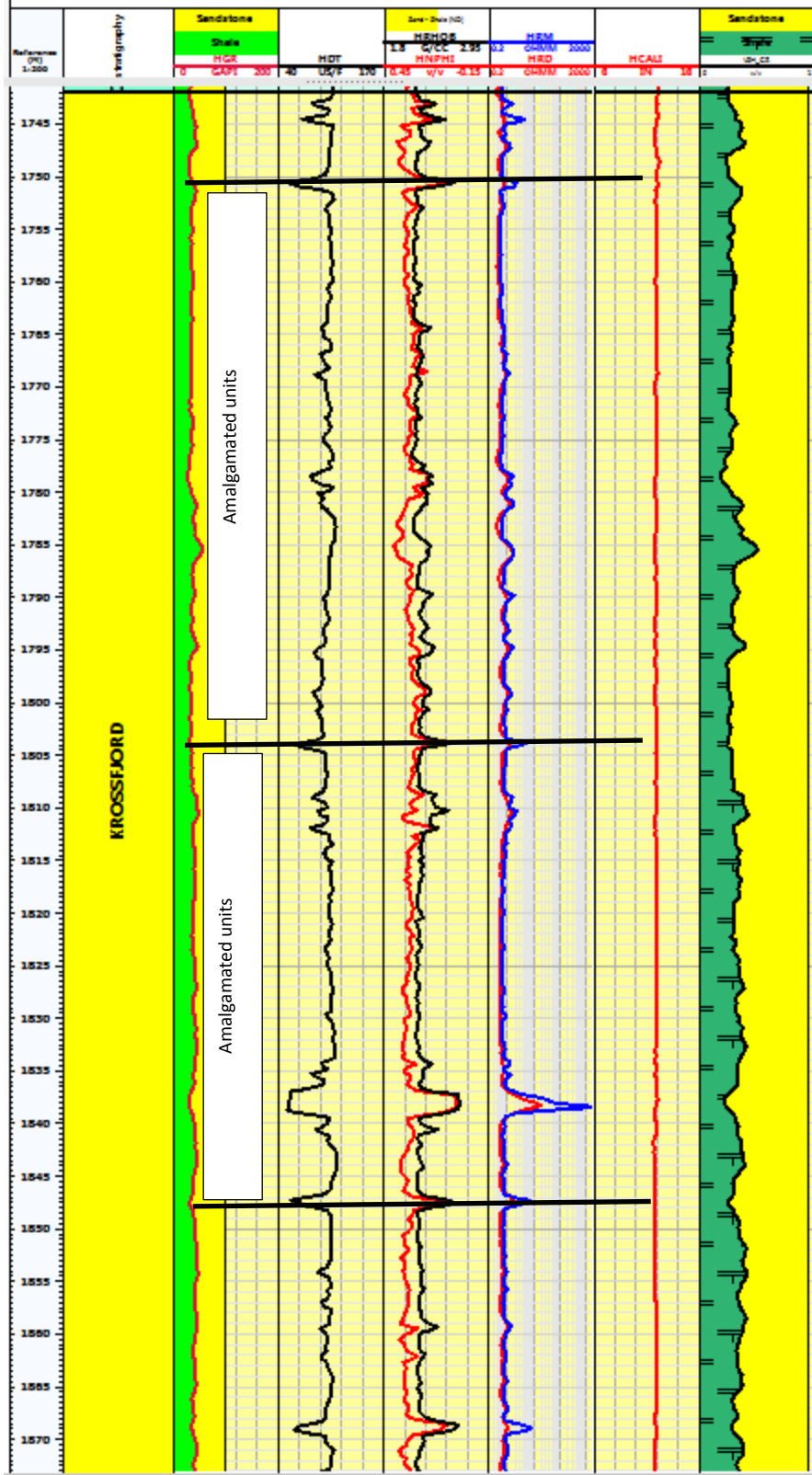


Figure 4.62 Wireline log through the Krossfjord Formation.

#### **4.5.3.2 Wireline-log Signature**

This facies association is characterized by high values of neutron porosity and low values of density and gamma-ray values. These values are almost uniform. Calcite cemented intervals are characterized by decrease in neutron and sonic log values, and an increase in density values (e.g. at 1752 in Fig.4.63). High concentrations of carbonaceous debris have caused local increment in gamma-ray values (e.g. at 1795 m in Fig.4.63) (Holgate et al., 2013).

#### **4.5.3.3 Interpretation**

Fining upwards beds of structureless and parallel-laminated sandstone were deposited by high energy, high concentration submarine gravity flows. These flows were characterized by a high rate of deposition. The amalgamated nature shows repeated gravity flows (e.g. from 1755-1775 m in Fig.4.62) (Holgate *et al.*, 2013).

There are two main mechanisms which may produce gravity flows that deposited thick-bedded sandstone of this facies association. First, the entrance of dense and sediment laden water from rivers into the basin could generate sustained flows (Mulder et al., 2003). Second, repeated, retrogressive failure of sand rich, shallow marine mouth bars could produce turbidity currents (Olariu et al., 2010).

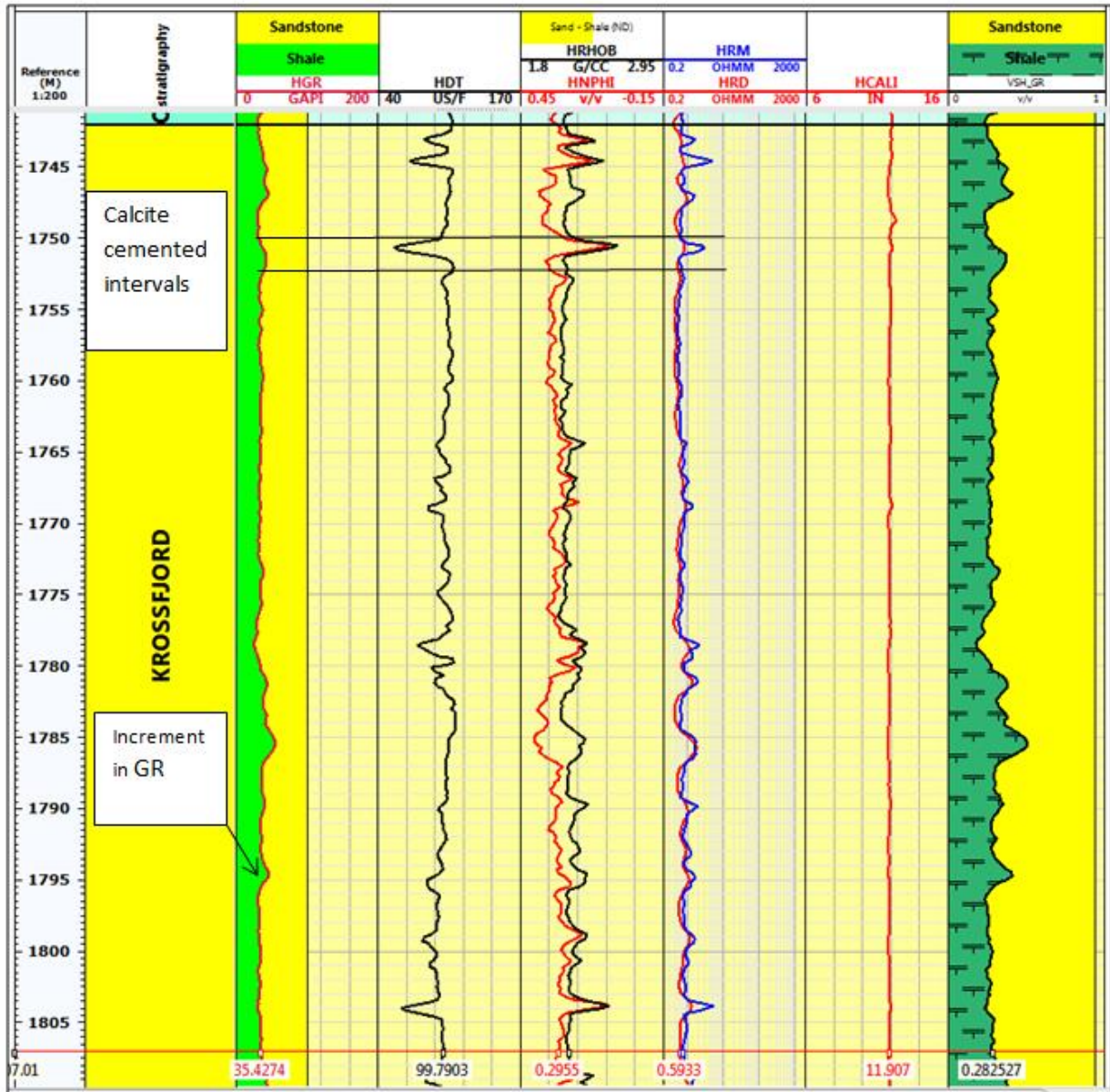


**Figure 4.63** Wireline log shows characteristics at carbonaceous debris and calcite cemented intervals.

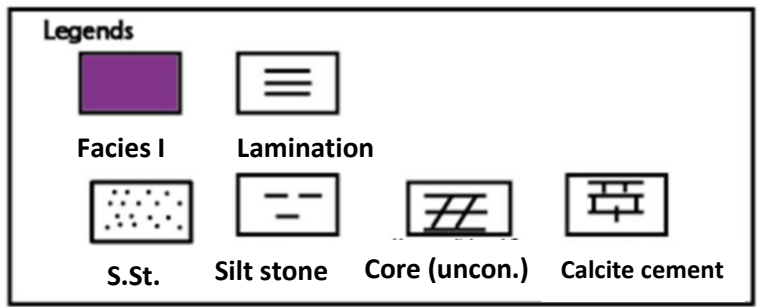
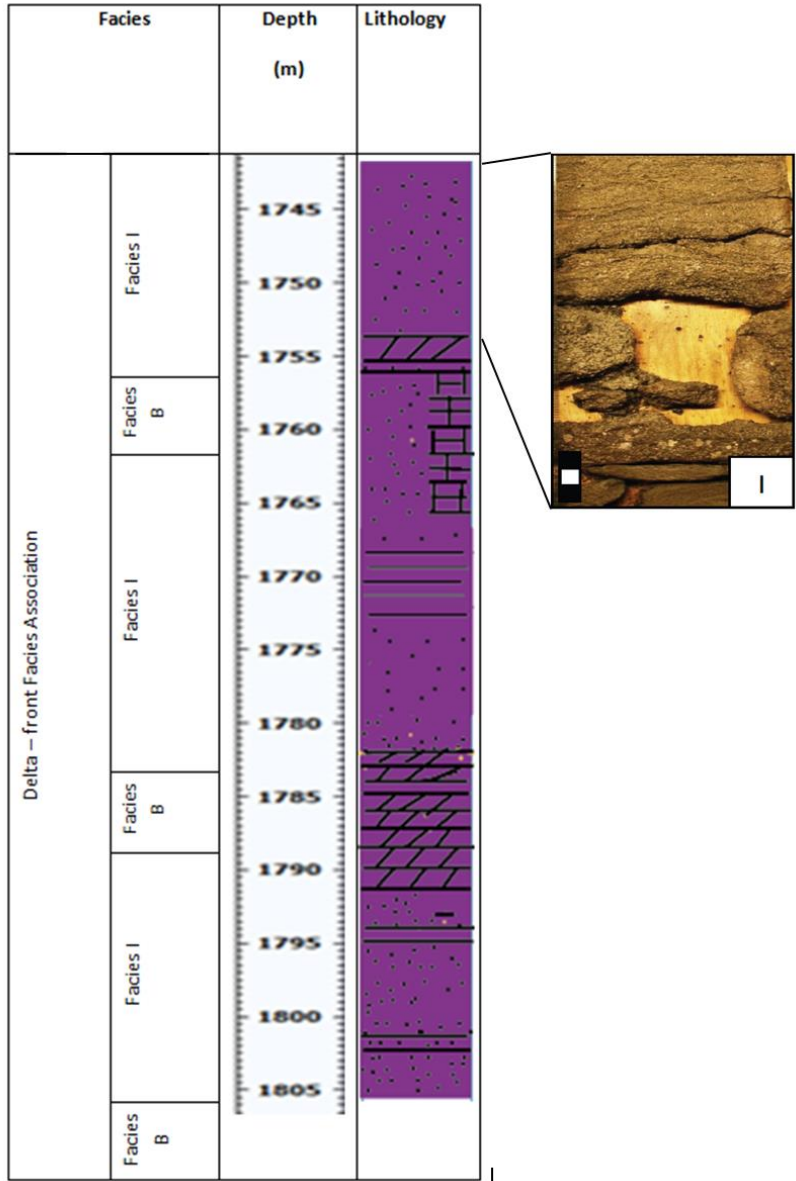
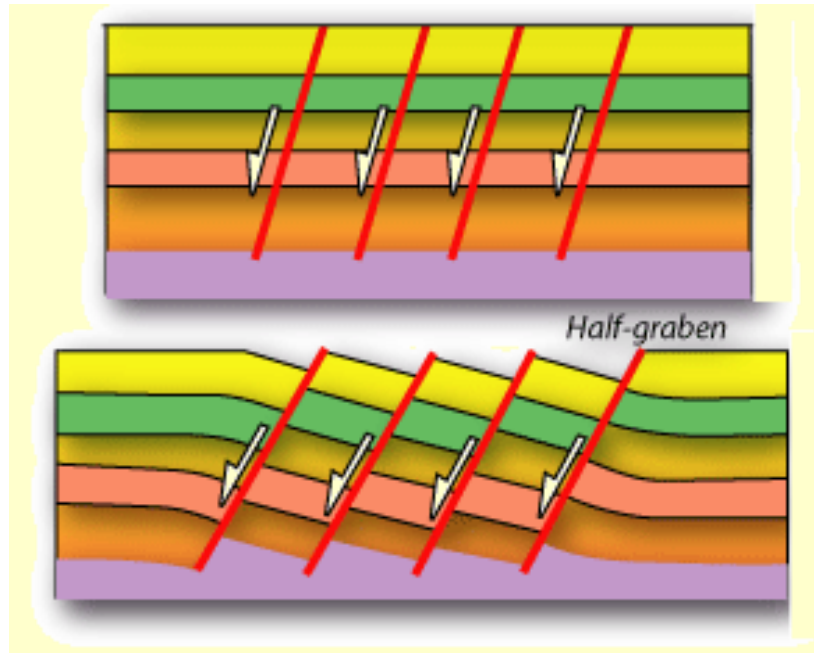


Figure 4.64: Lithological column of the Krossfjord Formation.

## 5 DISCUSSIONS

### 5.1 Fault Trend

Troll west field is separated into the Troll West Gas Province (TWGP) and the Troll East Oil Province (TWOP) by two major north-south trending curved major faults. The faults are normal planar and make prominent domino structure as shown in (Fig. 4.29). In domino structure the faults dip in similar direction and every fault slips down relative to next fault as shown in Fig. 5.1



**Figure 5.1:** Showing the development of half graben from series of normal faults dipping in similar direction ([www.geosci.usyd.edu.au](http://www.geosci.usyd.edu.au))

The strata along major faults shows roll over dragging as shown in Fig. 4.32. Similar example is shown from Pearl River mouth basin, china offshore in Fig. 5.2

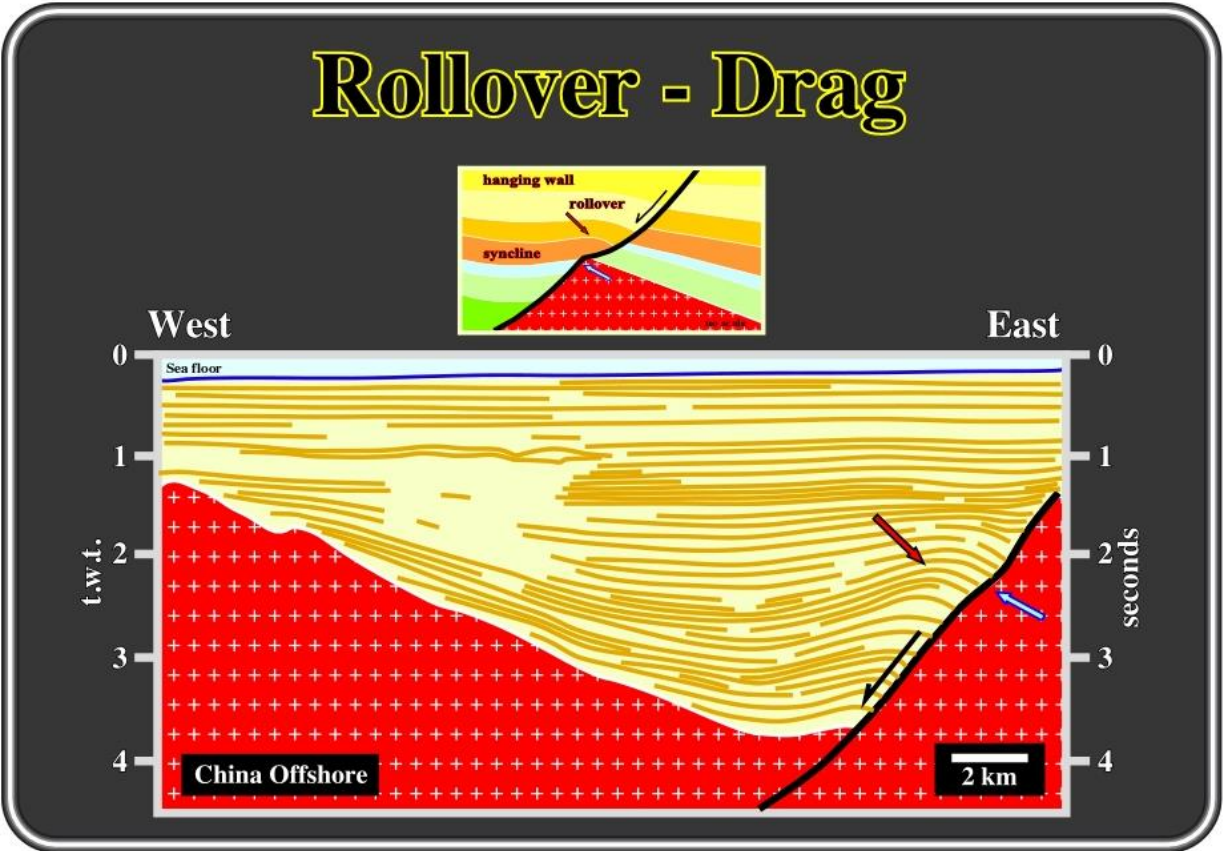
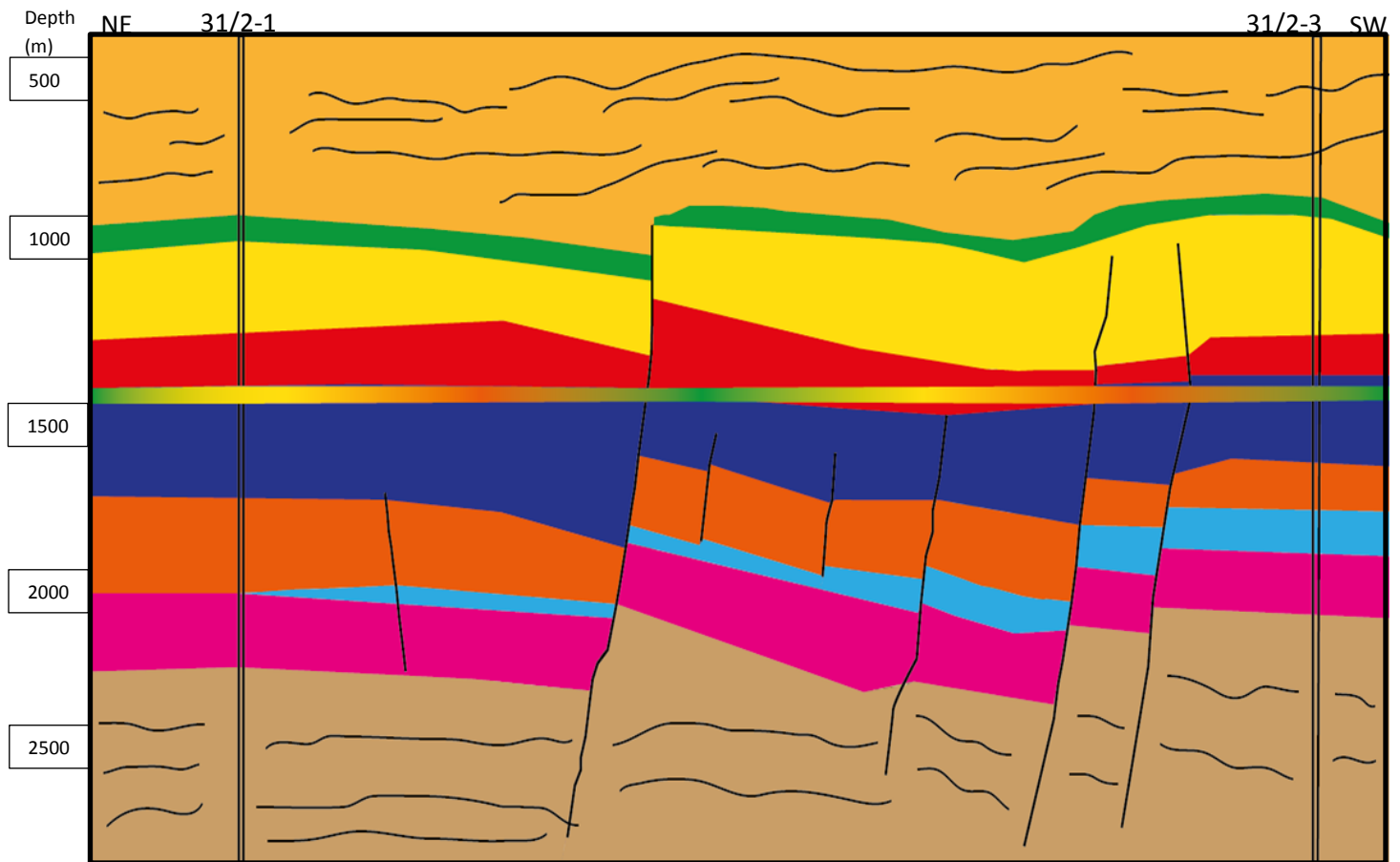


Figure 5.2: Rollover dragging of the strata along normal fault (www.homepage.ufp.pt).

## 5.2 Geological cross section

Geological cross section made from interpreted horizons is shown in Fig. 5.3. The series of north-west-south-east trending normal faults cut the Troll West field into different compartments. The two major curved north-south trending normal faults separate the field into the Troll West Gas province (TWGP) with an oil column with total thickness of 11-13 m and the Troll West Oil Province (TWOP) with an oil column of 22-26 m. The discovery well 31/2-1 is in TWGP. The flat-spot is the main characteristics of seismic data and it is very prominent as shown in cross section. The main reservoir unit Sognefjord is thick in well 31/2-3 and thins towards west. The thinning of Sognefjord is also shown by well correlation fig.5.5. The Heather A unit also thins towards west as shown in cross section due to progradation of strata towards west.



**Legends**

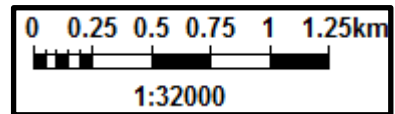
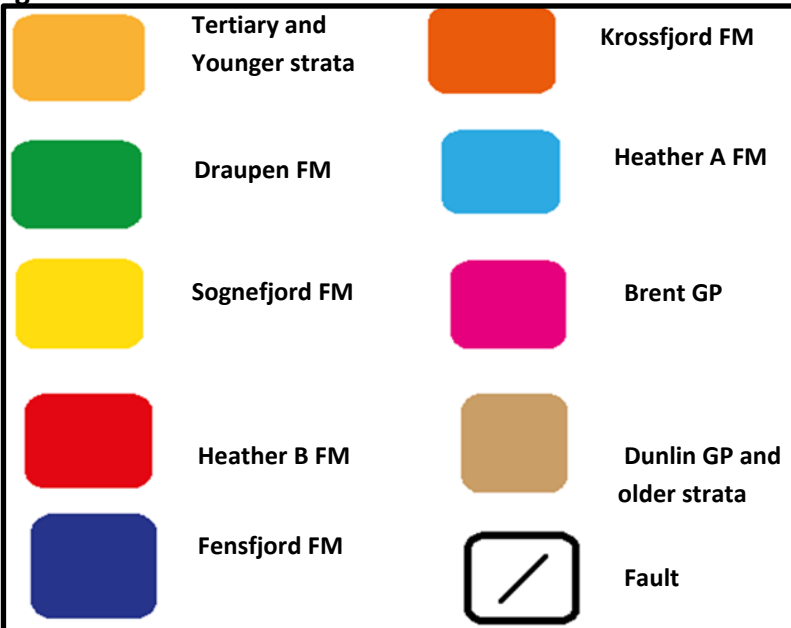


**Figure 5.3:** Geological cross section of the Troll Field made from interpreted horizon.

### **5.3 Depositional model for the Sognefjord Formation**

The facies distribution during Early Oxfordian shows the highest energy sand facies at top of each depositional cycle (Fig. 4.45) along the Troll West area. High energy sand bodies show gradual westward progradation (Fig. 4.46 and 5.4). There is evidence that the position of high energy sands may have been controlled by structural features. The small tilting of the Horda platform during the Late Callovian-Oxfordian resulted in thin or absent Heather "C" unit in the Troll West field. Thus high energy conditions were dominant because this area was above the normal wave base for longer periods. The south-west offlapping (Fig. 4.46) of the Sognefjord sand bodies shows the sediment derivation from north-east direction by longshore or tidal currents (Fig. 5.7). This thinning is also shown by well correlation in Fig. 5.5. The shoreface may have separated in spit-like projection from the coast and separated a low energy marine embayment in the Troll east from the open sea (Stewart et al., 1995).

The local mouth-bar environments formed where the distributaries entered into the sea. The progradation of spit resulted in clinoform succession consisting of sands of offshore transition origin. These sands are overlain by lower shoreface sands that pass upward into clean and coarse grained upper shoreface foreshore origin (Fig. 4.45), (Dreyer et al., 2005).



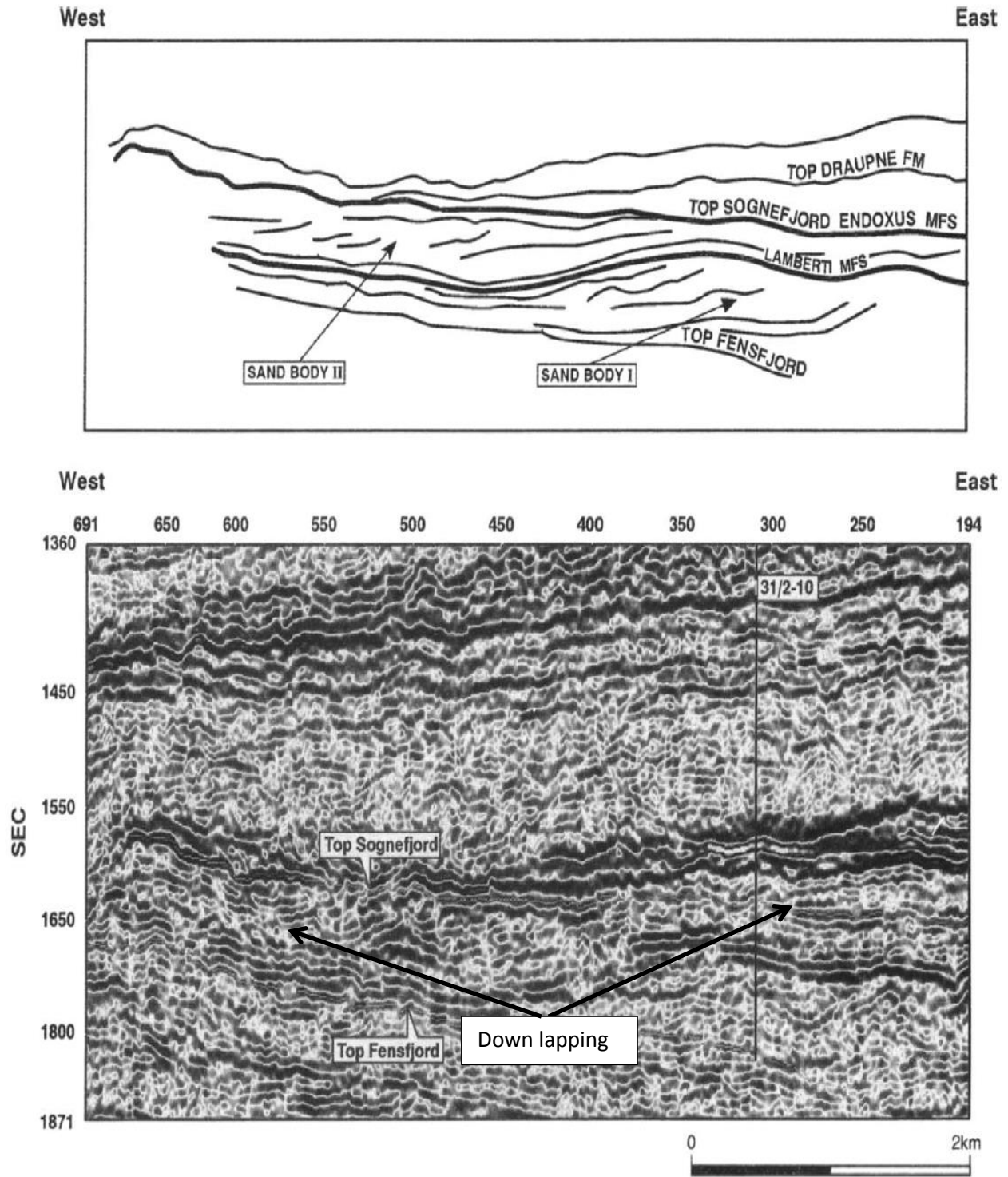


**Figure 5.4:** 3D seismic section from Troll West Field showing down lapping of seismic reflectors towards west (Stewart et al., 1995)

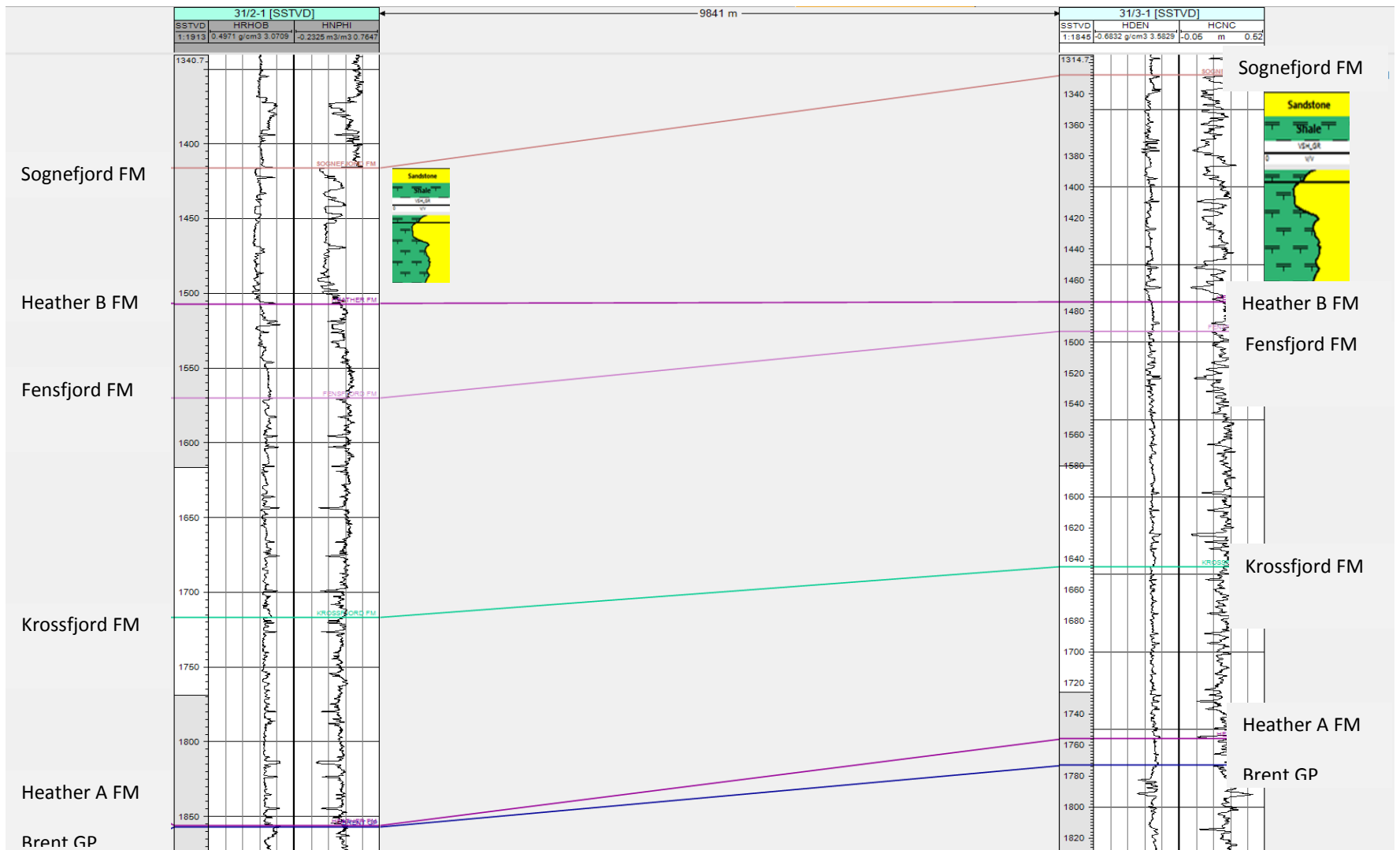


**Figure 5.5:** The NE-SW Correlation between well 31/3-1 and 31/2-1 shows thinning of the Sognefjord Formation towards west. For location of wells see Fig. 3.1

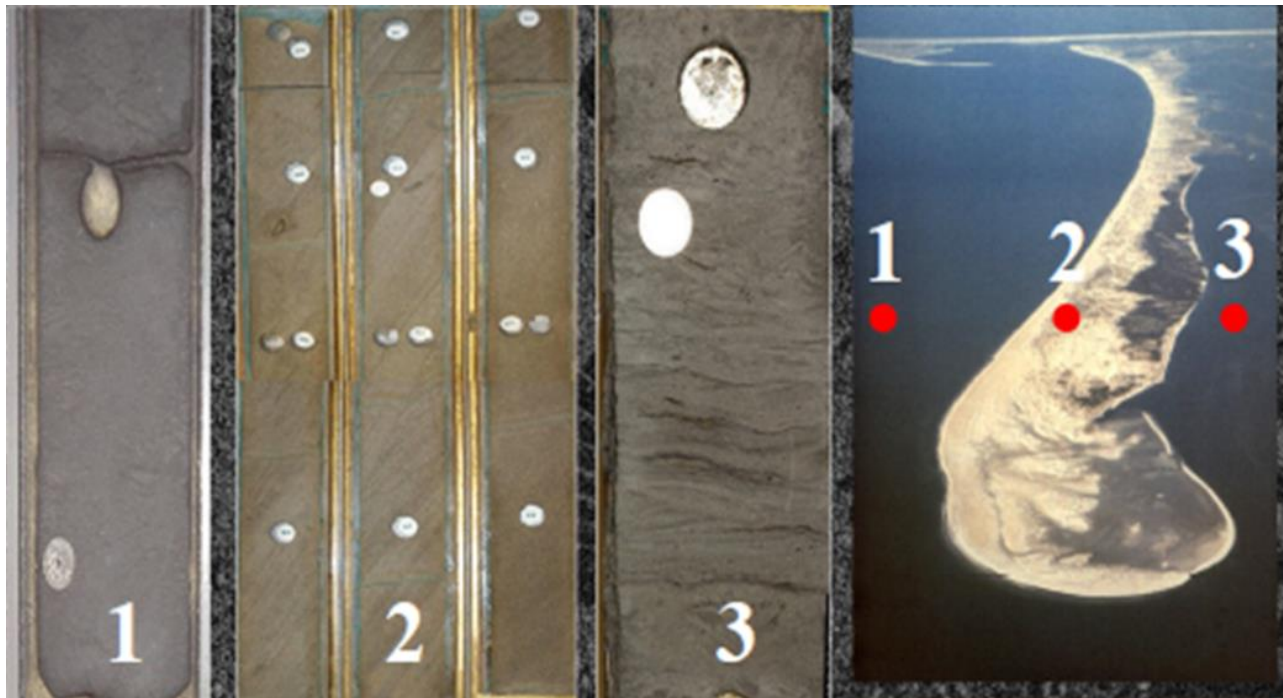
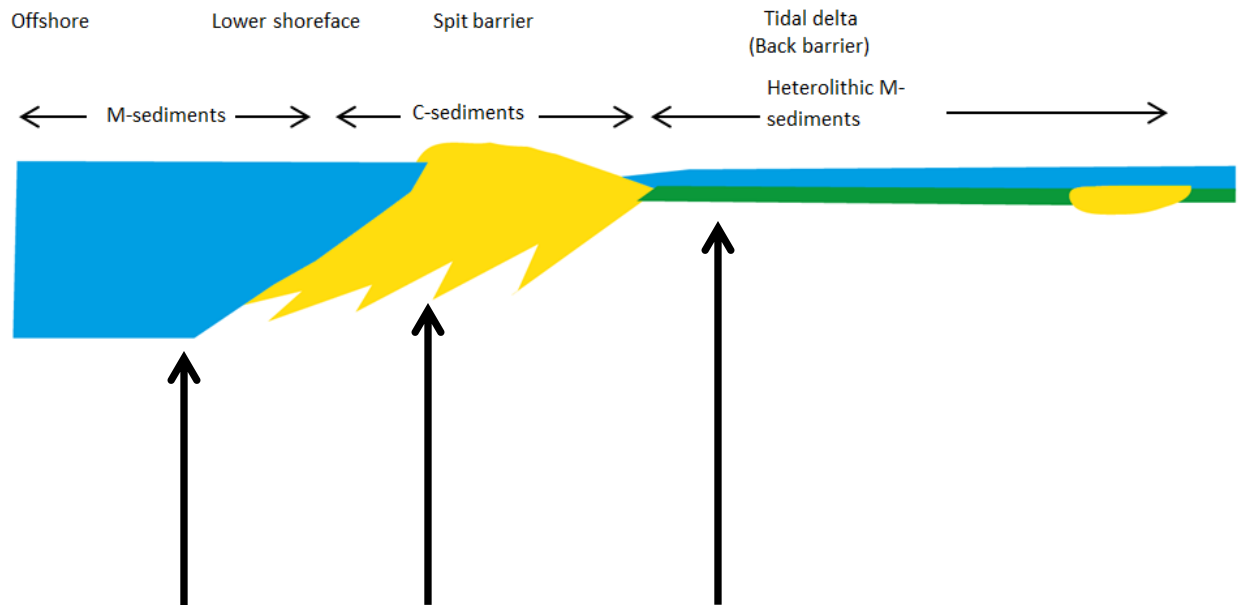


**Figure 5.6:** Generalized depositional model of Upper and lower Sognefjord FM showing tide influenced delta, spit barrier and lower shoreface (modified from Dreyer et al., 2005).

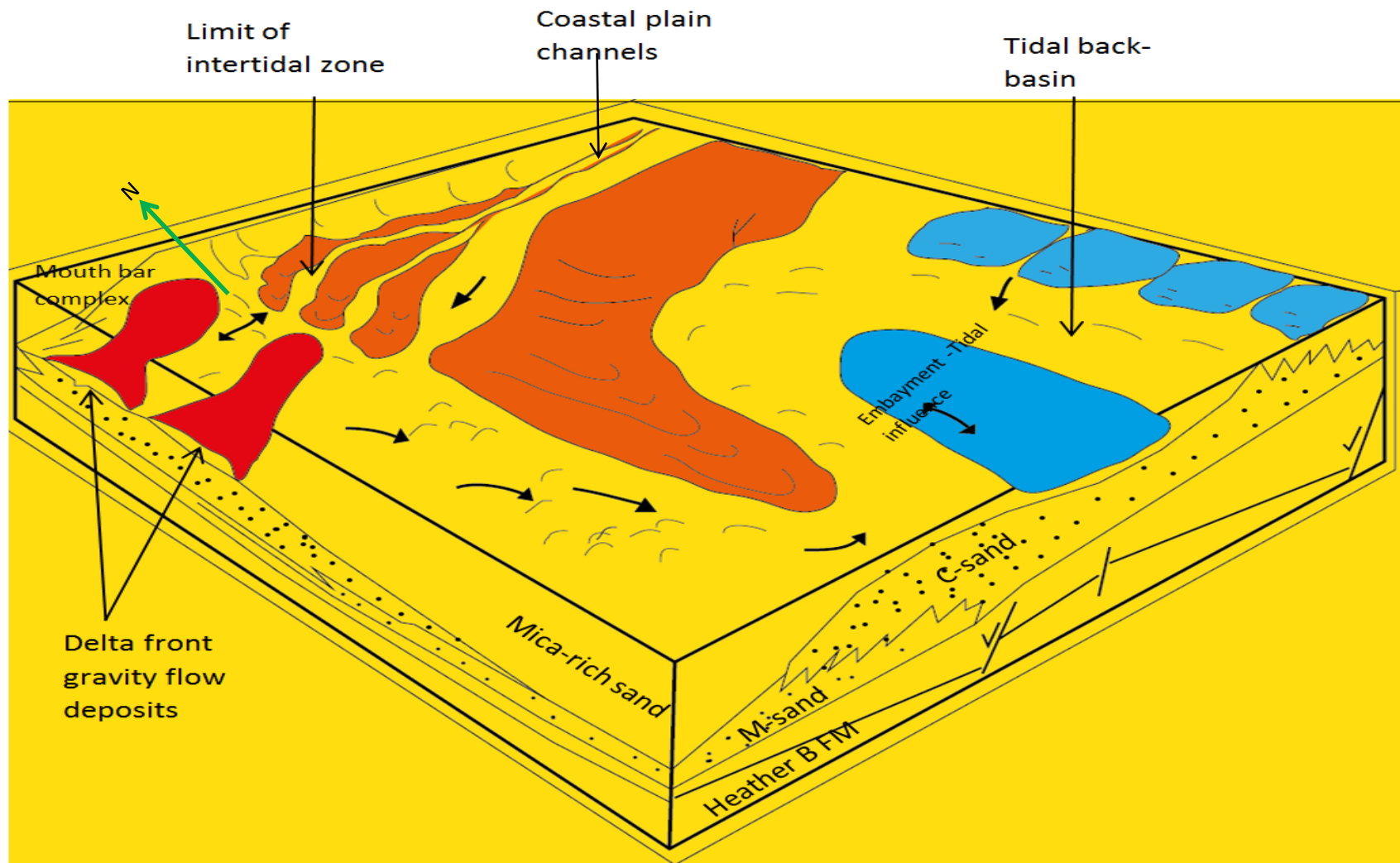


**Figure 5.7:** Block diagram for depositional model of the Sognefjord Formation showing coastal plain channels, tidal back basin and tide influenced embayment (modified from Dreyer et al., 2005).

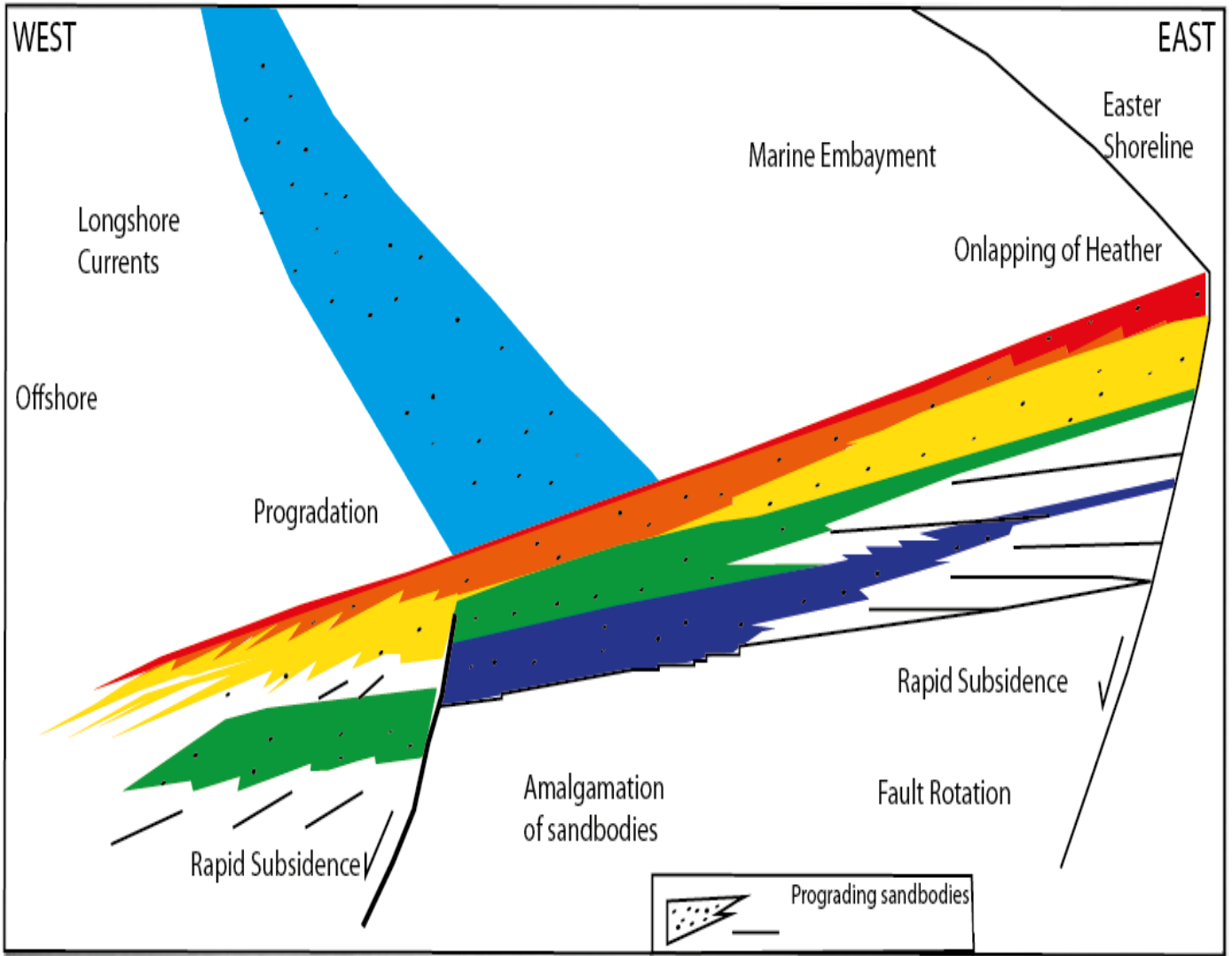


**Figure 5.8:** The model shows gentle Troll fault block tilted eastwards. Less accommodation space and erosion took place over Troll West resulted in high energy conditions due to the elevation of the area above wave base for a longer period (modified from Stewart et al., 1995).

**5.4 Depositional model for the Krossfjord and Fensfjord Formations**

The well log studies of the Krossfjord and Fensfjord Formations (Fig. 4.56 and 4.62-63) and Fig.5.10) show that there is complex distribution of facies-association belts within the Troll Field, in broad similar range of shallow marine environments. The facies associations in the Krossfjord and Fensfjord formations are similar to facies association of the Sognefjord Formation (Dreyer et al., 2005), suggesting that the same depositional model (s) may be applied to all three formations in the Viking Group. The sedimentological and stratigraphical key aspects of the Krossfjord and Fensfjord Formation are discussed in the following three subsections: (1) the east to west change in depositional environments in the Troll Field; (2)

vertical increase in abundance from wave dominated- lower shore face to wave dominated-upper shoreface facies association (Fig. 5.10) ; (3) the absence of coastal plain deposits (Holgate et al., 2013).

#### **5.4.1 East to west change in depositional environments in the Troll Field**

In the Troll West Field, the upper part of the Fensfjord Formation is characterized by wave dominated-upper shoreface deposits and lower part is mainly dominated by wave dominated lower shoreface deposits (Fig. 5.10). In the Troll east this formation is characterized by a mix wave-and-tide dominated environment (Holgate et al., 2013).

This change is caused by spatial variation (Fig. 5.10a), temporal variation (Fig. 5.10b) or combination of these two variations (Fig.5.10c) in the depositional process regime. In each model, the source of sediment input is considered to have been situated to the north of the Troll Field (Holgate et al., 2013).

##### **5.4.1.1 Depositional model 1**

The first depositional model (Fig. 5.10a) shows the spatial variation in depositional environment. Sediments were supplied by a fluvio-deltaic source in the north. Then sediments were redistributed by wave-generated longshore currents in order to form a spit in the Troll West Field. These longshore currents were south-directed. The seawards face of spit is characterized by a wave-dominated shoreface. The landward areas were protected from wave energy by spit, therefore these areas are characterized by tide-dominated embayment and back-basin setting in Troll East (Holgate et al., 2013).

##### **5.4.1.2 Depositional model 2**

The second depositional model shows the temporal variation in environments with early progradation of tide-dominated, embayed shoreline and later progradation of mix wave-tide dominated shoreface and finally progradation of wave-dominated shoreface. The width of the shelfal platform is decreased and wave process has become dominant due to the continued progradation (Holgate et al., 2013). The driving source for the gradual change in the depositional process was progradation of the shallow marine depositional system, which shows the interplay between sediment supply, accommodation space and basin physiography (Ainsworth et al., 2008).

#### **5.4.2 Vertical Increase in abundance of tide dominated deposits**

Lithological columns of the Krossfjord and Fensfjord Formations (Figs. 4.57 and 4.64) show that there is vertical increase in abundance of tide dominated deposits. The Krossfjord Formation dominated by tide-dominated deltaic facies association. The upward increasing tidal influence reflects the progressive progradation (Holgate et al., 2013).

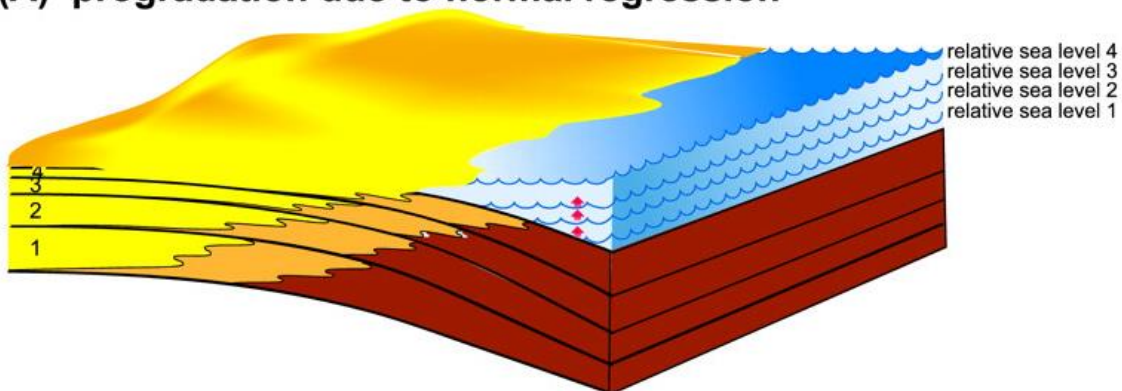
### 5.4.3 Absence of coastal plain deposits

Coastal plain deposits are not present in the Krossfjord and Fensfjord Formation because either: (1) Palaeosols were removed by transgressive erosion; (2) Due to forced regression, the palaeosols were not developed; (3) Due to broad, shallow, subaqueous platform, the palaeosols were not developed (Holgate et al., 2013).

Transgressive surfaces are identified in both formations (Fig. 5.10a). Transgressive erosion can erode up to 20 m of substrate (Demarest and Kraft 1987). Forced regression may also be reason of complete absence of coastal plain deposits (Fig. 5.9). Posamentier and Morris (2000) used three criteria to recognize forced regression in the Krossfjord and Fensfjord formations:

- (1) Increased average grain size in regressive deposits;
- (2) Thin character of the para sequences due to decreased accommodation space;
- (3) The absence of coastal plain deposits over regressive successions (Holgate et al., 2013).

#### (A) progradation due to normal regression



#### (B) progradation due to forced regression

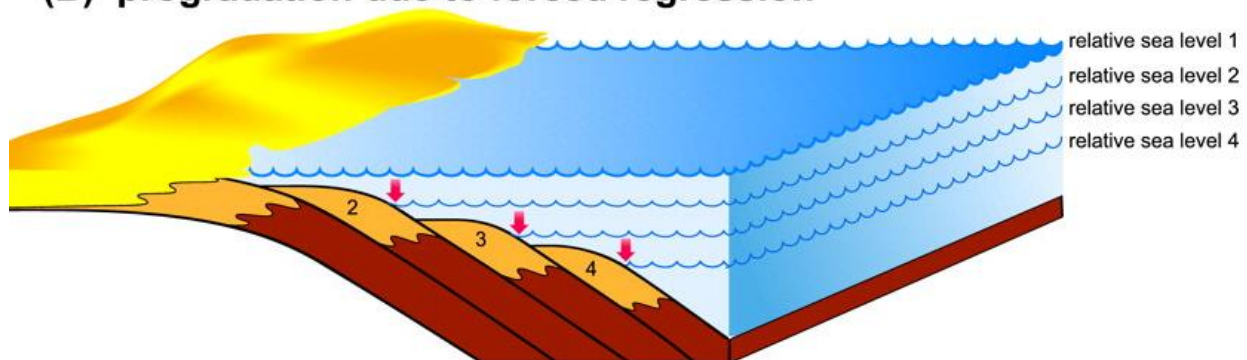
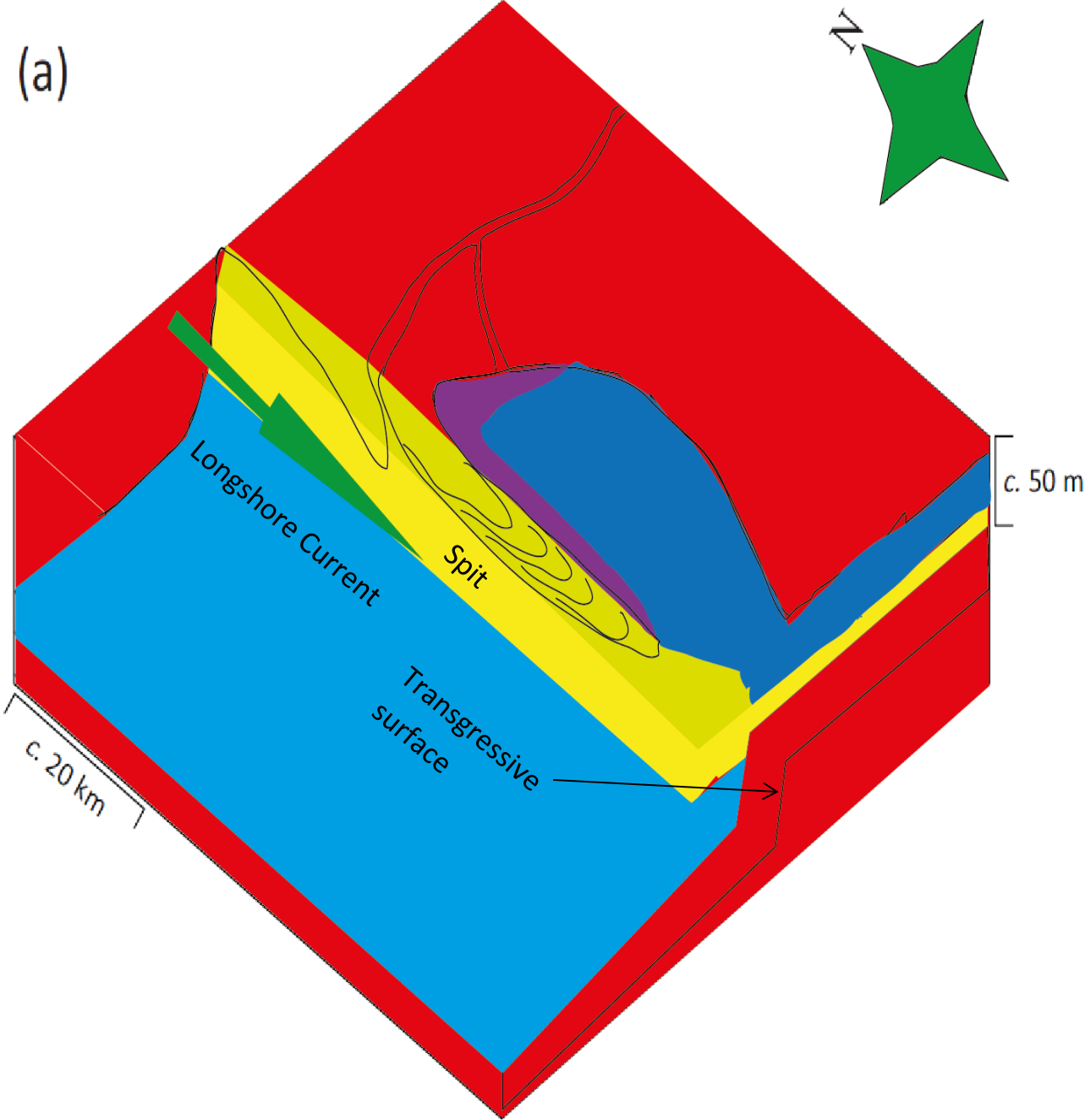


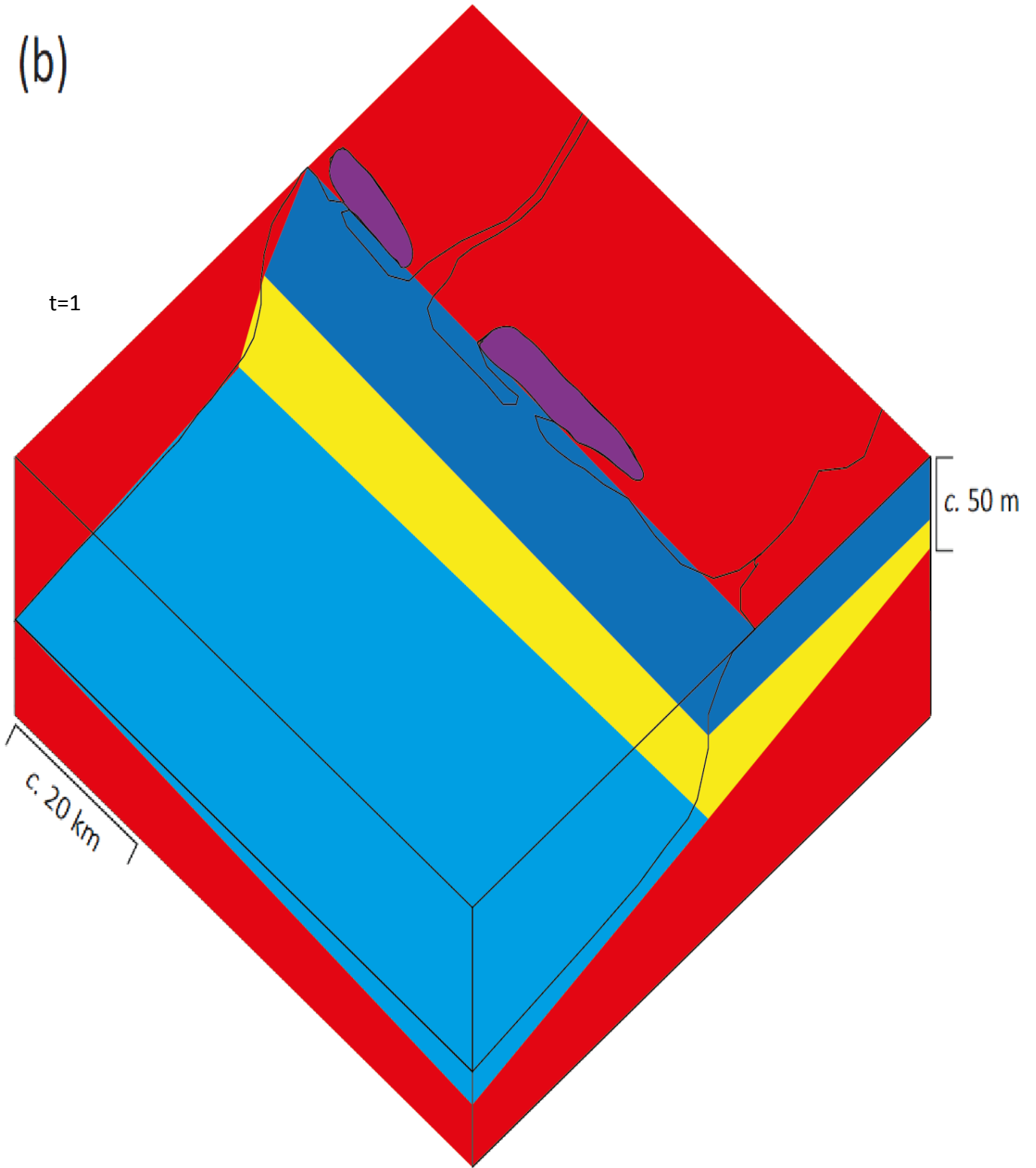
**Figure 5.9:** Forced regression cause more erosion as compared to normal regression ([www.aapg.org](http://www.aapg.org)).

An alternative interpretation for the absence of coastal plain deposits is that the area of the Troll Field was subaqueous and this platform was repeatedly constructed during each progradation episode (Holgate et al., 2013).

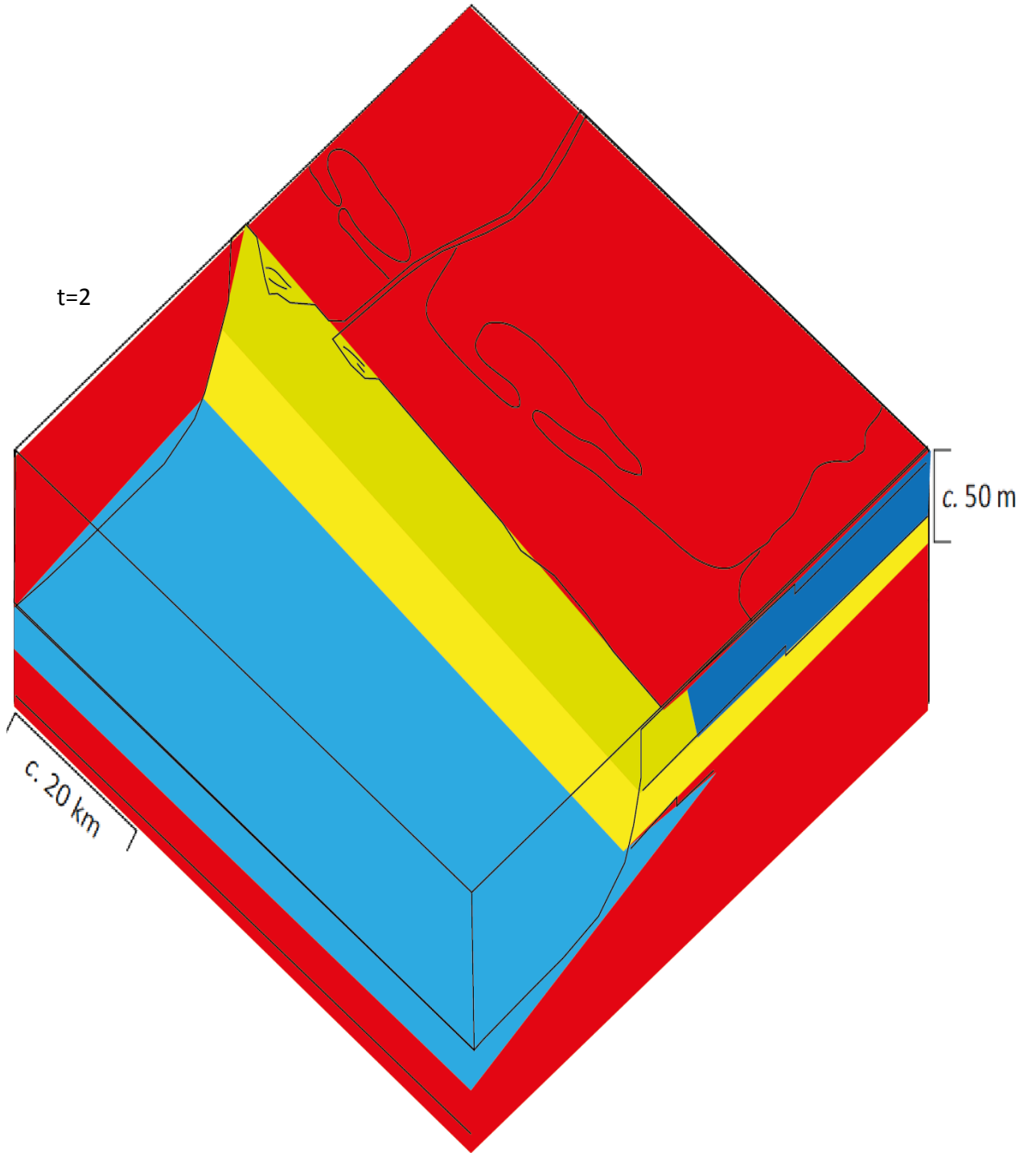




(b)



(c)



## Key

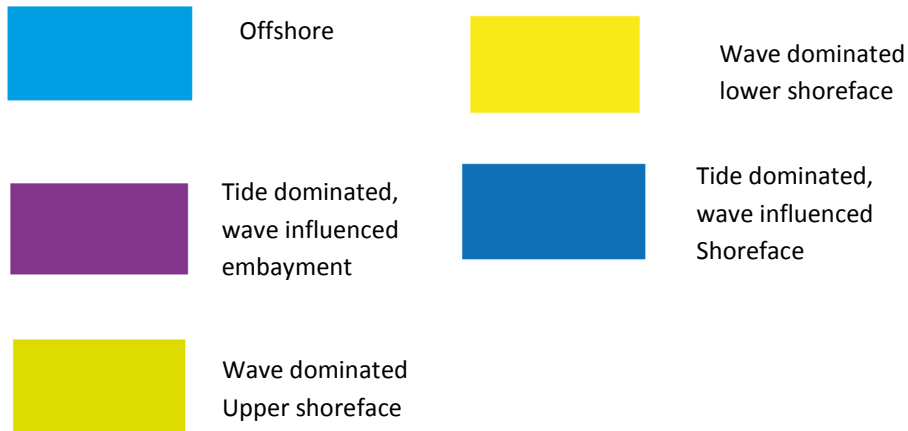


**Figure 5.10:** Block diagram showing depositional models. Two models are shown: (a) spatial variation in depositional environments with a wave-dominated spit system ; and (b) temporal variation in depositional environments with tide dominated, wave influenced embayment and development of shoreface on inner-middle shelf (t=1), Evolving into wave-dominated shoreface due to progradation to the outer shelf (t=2), (c) combination of spatial and temporal variation. (Modified from Holgate et al., 2013).

## 6 CONCLUSIONS

The main conclusions of this study are:

1) The Sognefjord Formation in the Troll West Field deposited in shallow marine environments:

Lower Sognefjord Formation: spit-shoreface system (wave dominated)

Upper Sognefjord Formation: Tide dominated delta

This formation is seismically characterized by low angle clinoforms. The overall geometry of the Sognefjord Formation is controlled by local tectonics elements. The faulting was mainly NE-SW. Sediments were transported along axis of these depressions i.e. north-east to south-west as indicated by south-west prograding clinoforms on seismic data.

2) The Krossfjord and Fensfjord Formations were deposited in shallow marine environments. The deposits are wave-dominated shoreface and trending north-south. The east to west change in depositional environments from tide dominated to wave dominated is caused either by spatial variation in depositional process regime within an asymmetrical delta fronted by a spit, or temporal variation because the system prograded from inner-shelf location in the east to an outer-shelf location in the west.

3) Coastal plain deposits are not present in the Krossfjord and Fensfjord Formation because either Palaeosols were removed by transgressive erosion, or by forced regression, or due to the development of broad, shallow, subaqueous platform during repeated regressions.

## 7 FURTHER RESEARCH

Although there is gap of 25 years between first seismic discovery of the Troll field in the early 1970s and first gas production in 1996 and the Troll Field is now a mature field, but inspite of that, the further research in seismic interpretation of the the Troll Field may play important role in the front-end technology, for example multiphase pipelines, deep water platforms and horizontal drilling.

Broad band seismic can also play important role. The recording of the full range of frequencies ( low as well as high) is very important for high resolution imaging. This kind of data provides deeper penetration for clear imaging of deep targets.

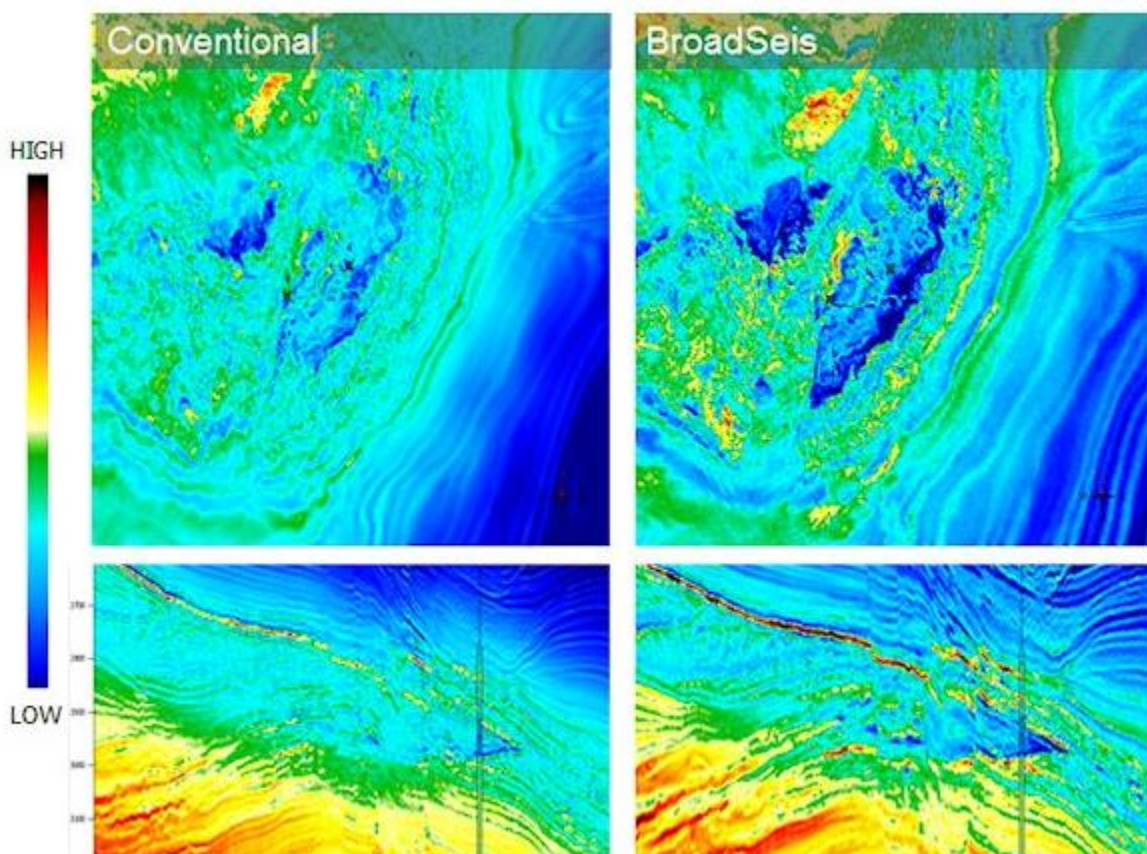


Figure 7.1: The Broadseis data is showing more detail and dynamic range than the conventional data ([www.cggveritas.com](http://www.cggveritas.com))

## REFERENCES

- Ainsworth, R. B., Hasiotis, S.T. et al. (2012). "Tidal signatures in an intracratonic playa lake. *Geology*, ." **40**: 607–610.
- Bolle, L.1992. TrollField: Norway's giant offshore gas field,In: M.T. Halbouty (Editor), *Giant Oil and Gas Fields of the Decade, 1978-1988*.Proceeding of Conference, Stavanger Norway, September 8-12, 1990. *Am.Assoc.Pet.Geol.,Mem.,*54:447-458.
- Bourgeois, J. "A transgressive shelf sequence exhibiting hummocky stratification; the Cape Sebastian Sandstone (Upper Cretaceous), southwestern Oregon. ." *Journal of Sedimentary Research*, **50**: 681–702.
- Brown, A. R., 2005, pitfalls in 3D seismic interpretation: keynote presentation at the 11<sup>th</sup> Annual 3-D seismic symposium, Denver: *The Leading Edge*, v. 24, no. 7, p. 716-717.
- Christiansson, P., Faleide, I. J. & Berge, A. M. (2000), "Crustal structure in the northern North Sea: an integrated geophysical study." *Geological society, London, special publication*, January 1,2000. **v.167**: p.15-40.
- Coward, M. P., Dewey, J. F., Hemton, M. & Holroyd, J. (2003), Tectonic evolution. p. 17-33 in *The Millennium Atlas: petroleum geology of the central and northern North Sea*. Evan, D., Graham, C., Armour, A., & Bathurst, P. (editors and coordinators). (London: The Geological Society of London).
- D.J. Stewart, M. S. a. L. B. (1995). "Jurassic depositional systems of the Horda Platform, Norwegian North Sea: practical consequences of applying sequence stratigraphic models." *Sequence Stratigraphy on the Northwest European Margin\_(NPF Special Publication)*: 291-323,.
- Demarest, J.M. & Kraft, J.C. 1987. Stratigraphic record of Quaternary sea levels: Implications for more ancient strata. *In: Nummedal, D., Pilkey, O.H. & Howard, J.D. (eds) Sea Level Fluctuation and Coastal Evolution*. SEPM, Special Publications, **41**, 223–239.
- Dore, R. H. G. a. A. G. (1995.). "History of tectonic models on the Norwegian continental shelf." *Petroleum Exploration and Exploitation in Norway\_(Norwegian Petroleum Society)*: 333-368,.
- Dott, R. H. Bourgeois, J. (1982). "Hummocky stratification: Significance of its variable bedding sequences." *Geological society of America Buletin*, **93**, **663**.
- Dreyer, T., et al. "From spit system to tide-dominated delta: integrated reservoir model of the Upper Jurassic Sognefjord Formation on the Troll West Field."*Geological Society, London, Petroleum Geology Conference series*. Vol. 6. Geological Society of London, 2005.
- Duke, W.L. 1985. Hummocky cross-stratification, tropical hurricanes, and intense winter storms. *Sedimentology*, **32**, 167–194.

Faleide, J. I., Bjørlykke, K. and Gabrielsen, R. H., (2010). "Geology of the Norwegian continental shelf. In: Bjørlykke K. (ed.), Petroleum Geoscience: From Sedimentary Environments to rock Physics.":p. 467 – 499.

Gabrielsen, R., Færseth, RB, Steel, RJ, Kløvjan, OS (1990). Architectural styles of basin fill in the northern Viking Graben. *Tectonic Structure of the North Sea Rifts*: 158-179.

Gabrielsen, R. H., Doré, Anthony G. (1991). "History of tectonic models on the Norwegian continental shelf." *Petroleum Exploration and Exploitation in Norway Proceedings of the Norwegian Petroleum Society Conference*,: 333-368.

Hart, B.S. & Plint, A.G. 1995. Gravelly shoreface and beach deposits. *In: Plint, A.G. (ed.) Sedimentary Facies Analysis: A Tribute to the Research and Teaching of Harold G. Reading.* International Association of Sedimentologists, Special Publications, **22**, 75–90.

Holgate, N. E., C. A. L. Jackson, G. J. Hampson and T. Dreyer (2013). "Sedimentology and sequence stratigraphy of the middle-Upper Jurassic Krossfjord and Fensfjord formations, Troll Field, northern North Sea." *Petroleum Geoscience* **19**(3): 237-258.

Hellem, T, Kjemperud, A. and Ovrebo, O.K., 1986. The Troll Field: a geological/geophysical model established by the PL085 Group. *In: A.M. Spencer et al. (Editors), Habitat of Hydrocarbons on the Norwegian Continental shelf.* Norwegian Petroleum Society, Graham and Trotman, London, pp 217-238.

Johnsen Jan R., R. H., Nilsen Dag Erik (1995). "Jurassic reservoirs; field examples from the Oseberg and Troll fields: Horda Platform area." *Petroleum Exploration and Exploitation in Norway Proceedings of the Norwegian Petroleum Society Conference*, 9-11 December 1991, Stavanger, Norway **4**: 199-234.

John S. Sneider, Phillippe de Clarens and Peter R. Vail P. d. (1995.). Sequence stratigraphy of the Middle to Upper Jurassic,. *Sequence Stratigraphy on the Northwest European Margin*, pp. 167-197,.

Mulder, T., Syvitski, J.P.M., Migeon, S., Faugères, J.-C. & Savoye, B. 2003. Marine hyperpycnal flows: Initiation, behavior and related deposits. A review. *Marine and Petroleum Geology*, **20**, 861–882.

Michael E. Badley, T. E. a. O. N. (1984). "Development of rift basins illustrated by the structural evolution of the Oseberg feature, Block 30/6, offshore Norway." *Journal of the Geological Society*: 639-649.

Olariu, C., Steel, R.J. & Petter, A.L. (2010). "Delta-front hyperpycnal bed geometry and implications for reservoir modeling: Cretaceous Panther Tongue delta, Book Cliffs, Utah." American Association of Petroleum Geologists Bulletin, **94**: 819–845.

Osborne, P. a. E., S., (1987). "The Troll Field: reservoir geology and field development planning." North Sea Oil and Gas Reservoirs, Norwegian Institute of technology (Graham and Trotman): 39-60.

Posamentier, H. W. M., W.R. (2000). "Aspects of the stratal architecture of forced regressive deposits. In: Hunt, D. & Gawthorpe, R.L. (eds) Sedimentary Responses to Forced Regressions." **172**: 19–46.

Ravnas, R. a. k. B. (1997). "Architecture and controls on Bathonian-Kimmeridgian shallow-marine synrift wedges of the Oseberg-Brag area, northern North Sea. " Basin Research." 197-226.

Whitacker, M.F., 1984. The usage of palynostratigraphy and palynofacies in definition of Troll Field Geology. Offshore Northern Seas-Reduction of uncertainties by innovative reservoir geomodelling, Norsk Petroleumsforening, Conf. Pap., Art. G6, Stavanger 21-24<sup>th</sup> August, 27.

(u.d.). Hentet fra [www.homepage.ufp.pt](http://www.homepage.ufp.pt):

<http://homepage.ufp.pt/biblioteca/WEBVolumeProblems/Pages/Page11.htm>

(u.d.). Hentet fra [www.geosci.usyd.edu.au](http://www.geosci.usyd.edu.au):

[http://www.geosci.usyd.edu.au/users/prey/ACSGT/EReports/eR.2003/GroupD/Report2/web%20pages/Types\\_of\\_Structures.html](http://www.geosci.usyd.edu.au/users/prey/ACSGT/EReports/eR.2003/GroupD/Report2/web%20pages/Types_of_Structures.html)

(u.d.). Hentet fra [www.nhm2.uio.no](http://www.nhm2.uio.no): [http://nhm2.uio.no/norlex/NORLEX\\_pub\\_2010.pdf](http://nhm2.uio.no/norlex/NORLEX_pub_2010.pdf)

(u.d.). Hentet fra [www.npd.no](http://www.npd.no): <http://factpages.npd.no/factpages/Default.aspx?culture=en>

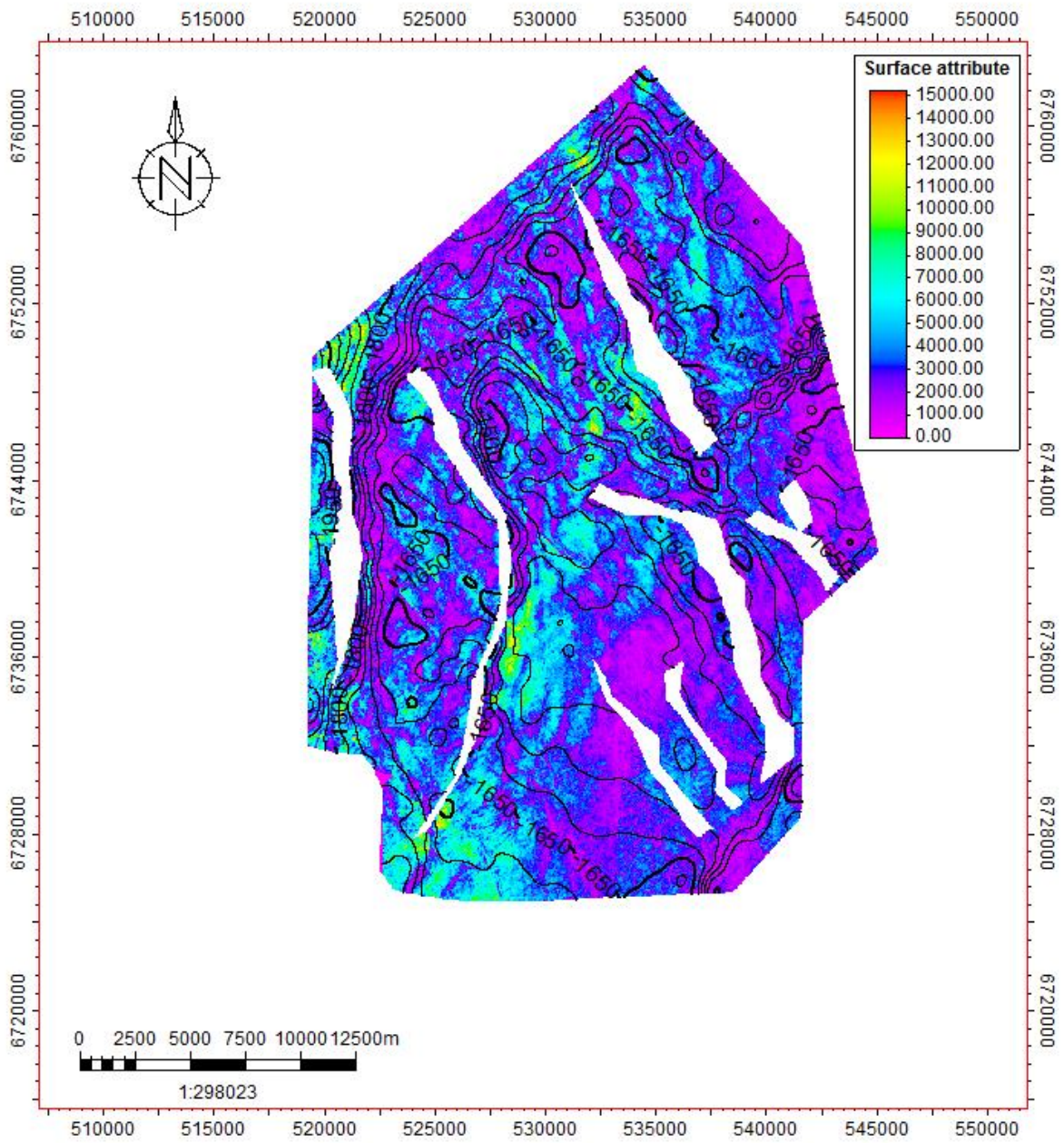
(u.d.). Hentet fra [www.aapgbull.geoscienceworld.org](http://www.aapgbull.geoscienceworld.org):

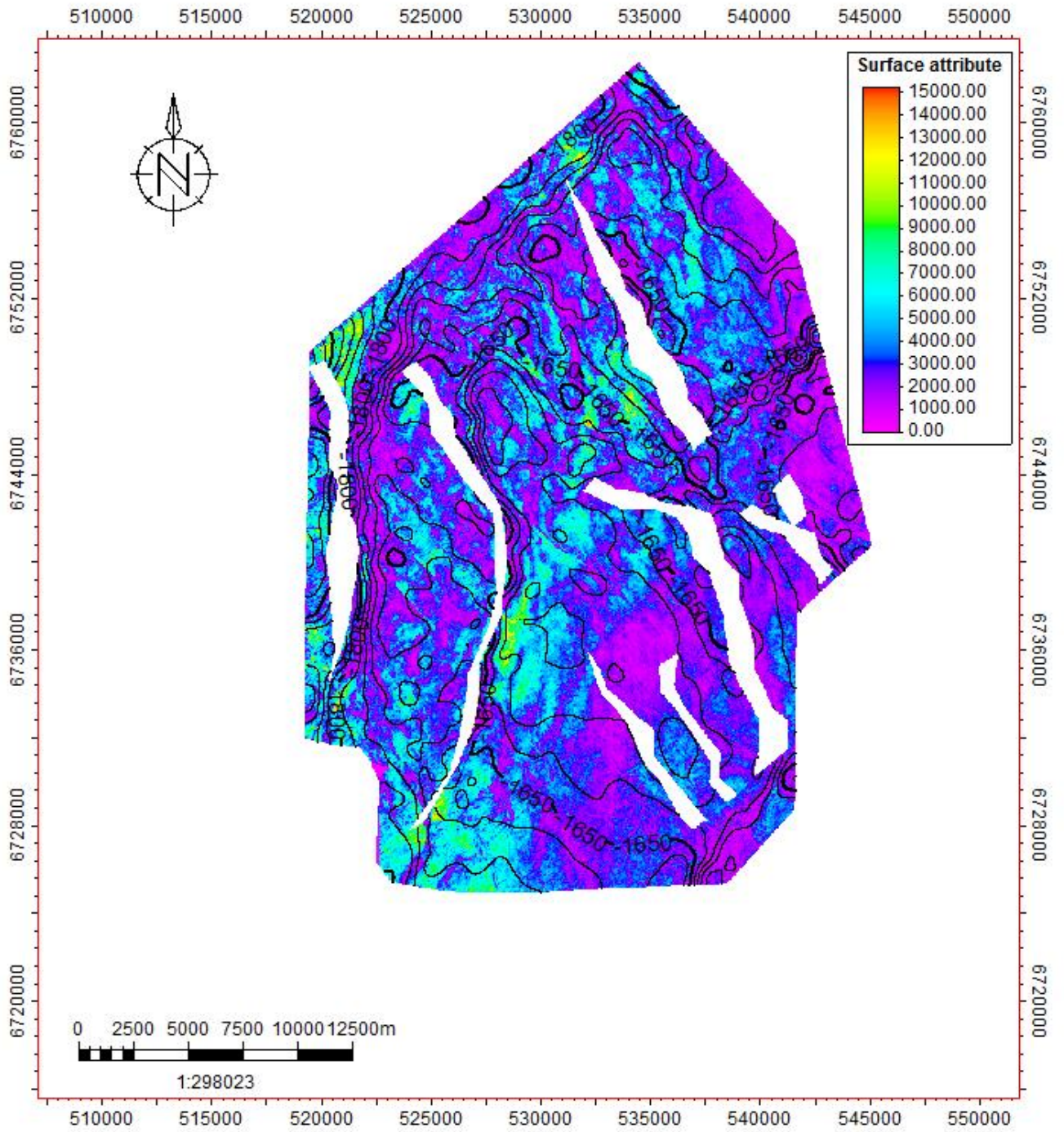
<http://aapgbull.geoscienceworld.org/content/94/8/1267/F11.large.jpg>

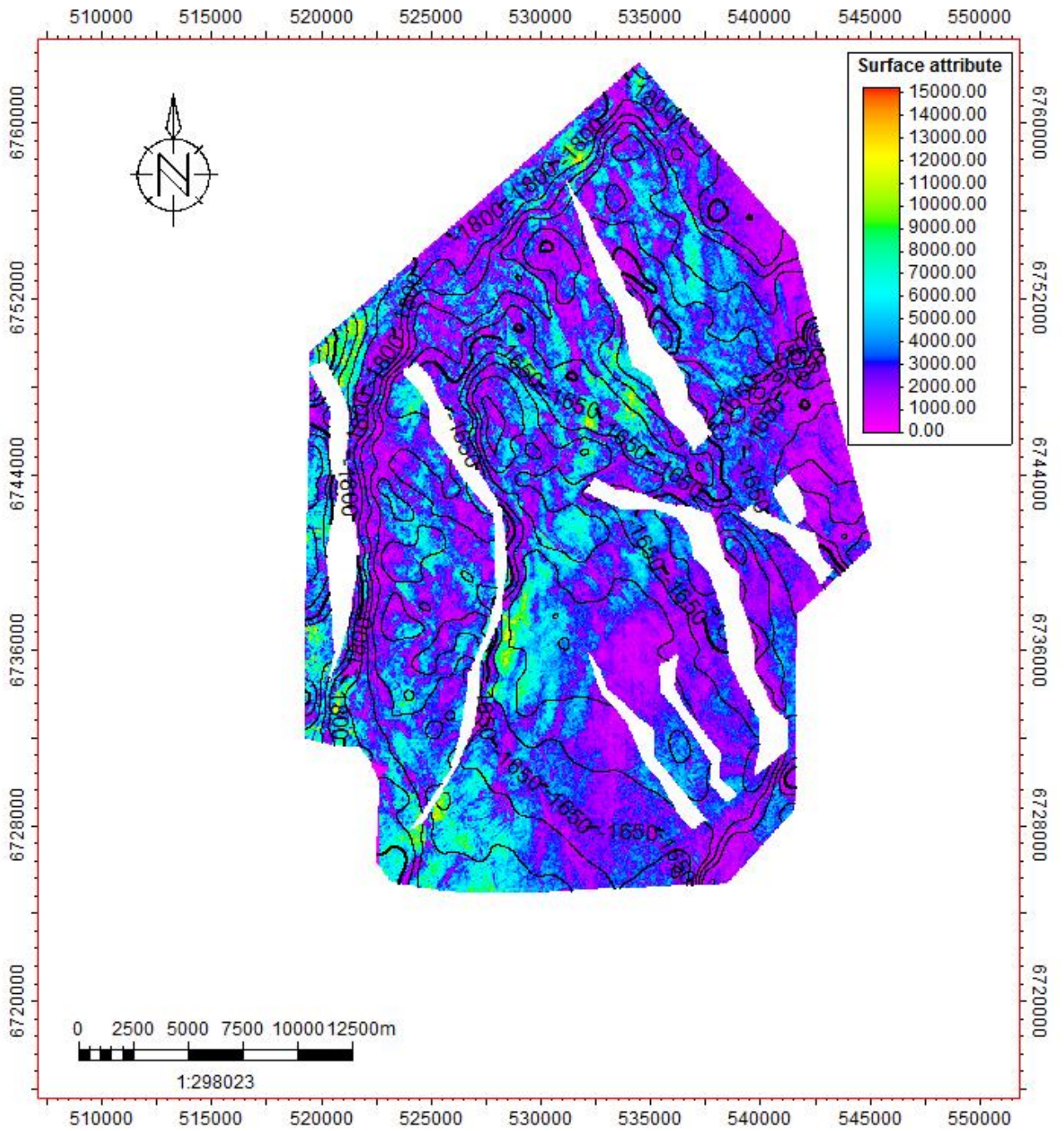
(u.d.). Hentet fra <http://www.cggveritas.com>: <http://www.cggveritas.com/default.aspx?cid=3802>

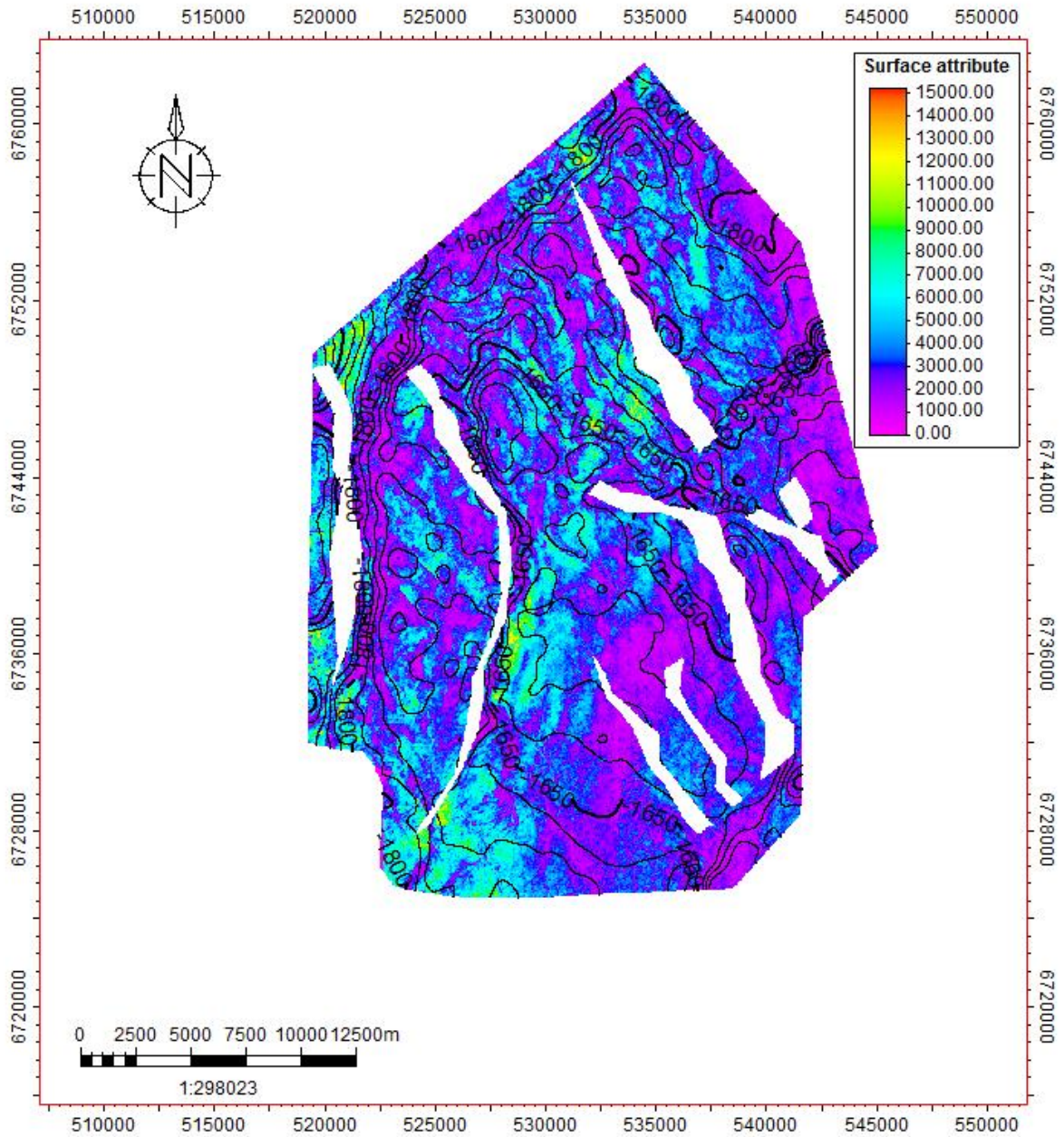


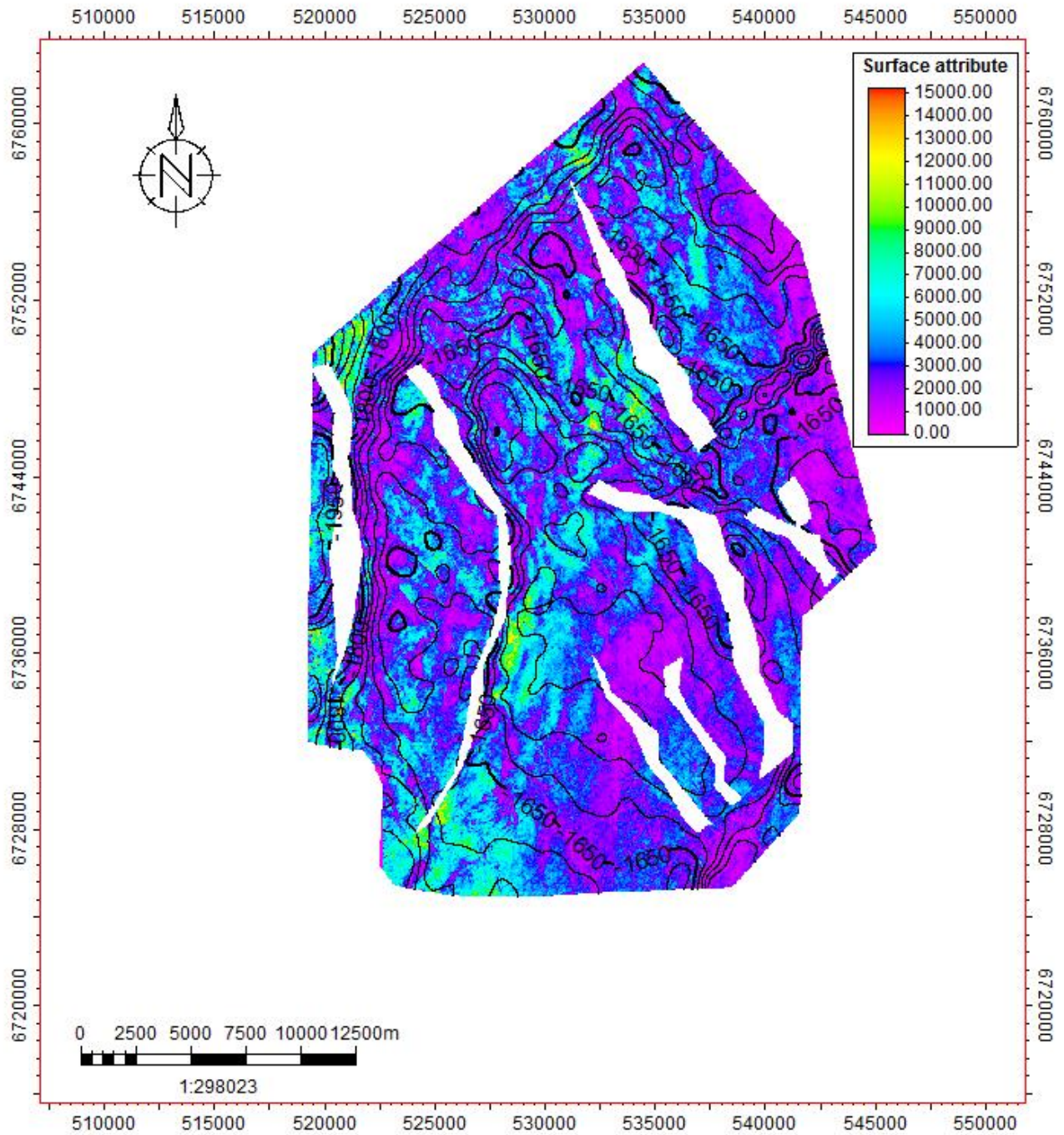
# APPENDIX











**Appendix A:** RMS maps of the Sognefjord Formation at equal intervals of 20 ms to observe the changes in Flat Spot.

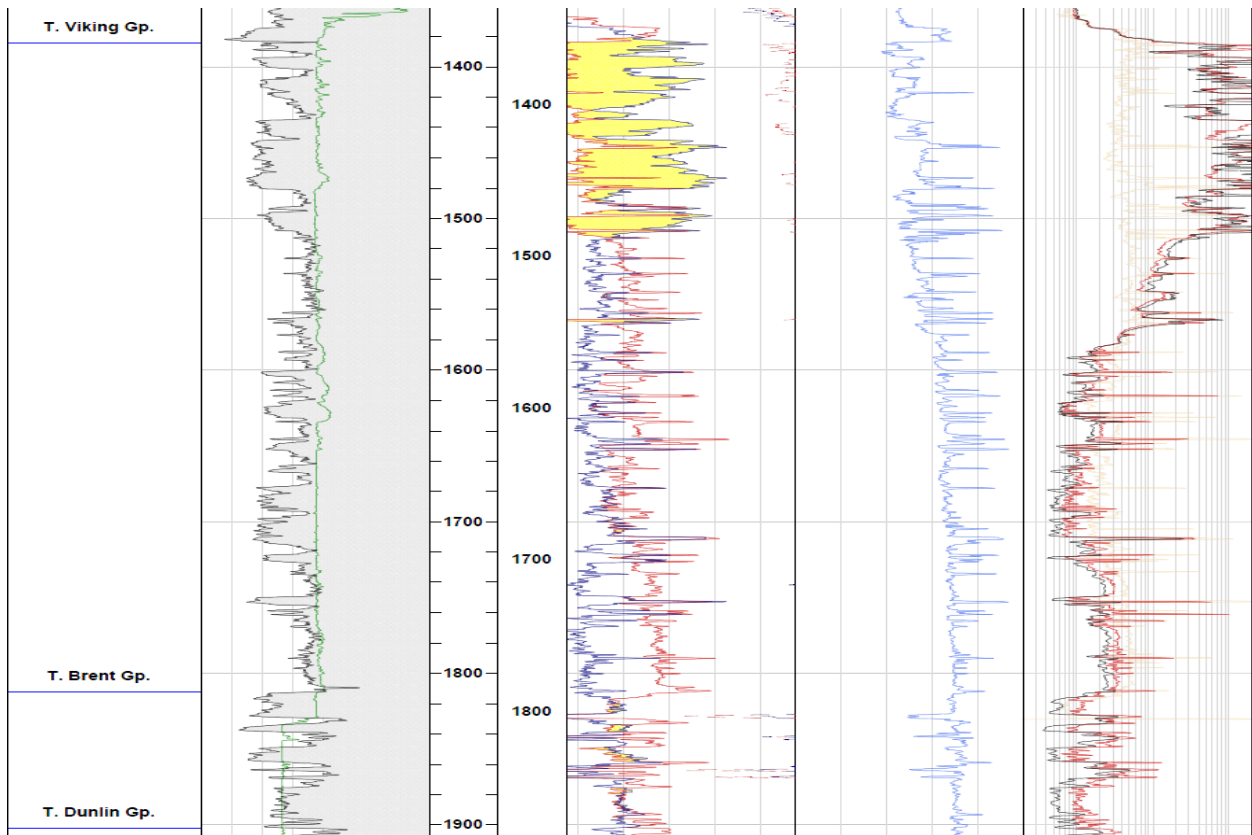
# Wellbore 31/2-3



RKB 25 m

For more information see the NPD factpages at [www.npd.no](http://www.npd.no).

GR-II		cross-over					
CALIFER		BULK DENSITY				SHALLOW RESISTIVITY	
0	(in)	24	1.95	(g/cm <sup>3</sup> )	2.95	0.2	(ohm.m)
GAMMA RAY		NEUTRON POROSITY				MEDIUM RESISTIVITY	
0	(gAPI)	150	0.45	(m <sup>3</sup> /m <sup>3</sup> )	-0.15	0.2	(ohm.m)
GAMMA RAY		BULK DENSITY				DEEP RESISTIVITY	
150	(gAPI)	300	0.95	(g/cm <sup>3</sup> )	1.95	0.2	(ohm.m)
MD	TVDSS	NEUTRON POROSITY		SONIC / ACOUSTIC			
1 : 2000	m	1.05	(m <sup>3</sup> /m <sup>3</sup> )	0.45	240	(us/ft)	40



Appendix B1: Composite well log through well 31/2-3 (npd.no)

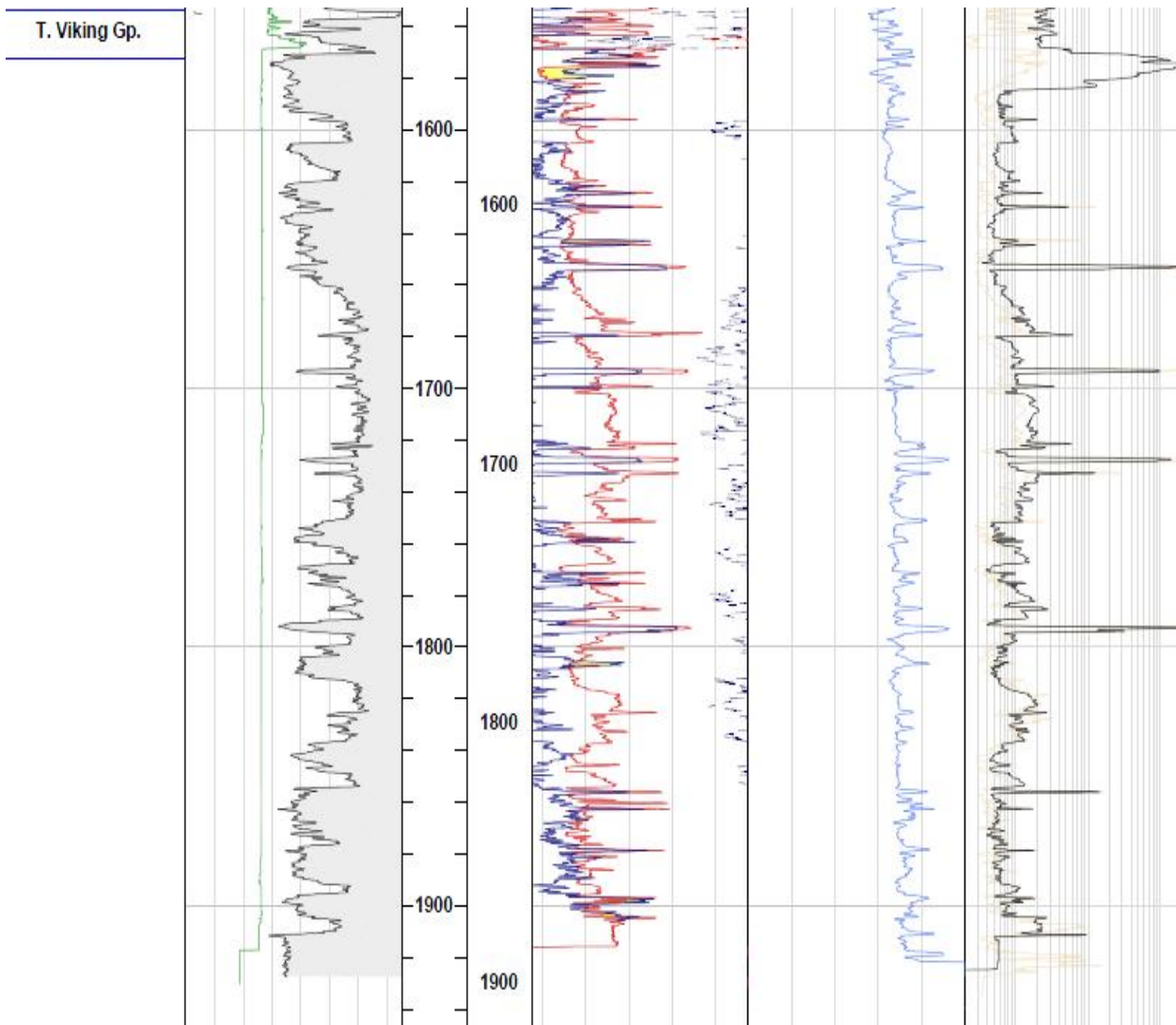
# Wellbore 31/5-5



RKB 29 m

For more information see the NPD factpages at [www.npd.no](http://www.npd.no).

GR-fill		cross-over		BULK DENSITY		SHALLOW RESISTIVITY			
CALIPER		BULK DENSITY		NEUTRON POROSITY		DEEP RESISTIVITY			
0	(in)	24	1.95	(g/cm <sup>3</sup> )	2.95	0.2	(ohm.m)	200	
GAMMA RAY		BULK DENSITY		NEUTRON POROSITY		SONIC / ACOUSTIC			
0	(gAPI)	150	0.45	(m <sup>3</sup> /m <sup>3</sup> )	-0.15	240	(us/ft)	40	
GAMMA RAY		BULK DENSITY		NEUTRON POROSITY		SHALLOW RESISTIVITY			
150	(gAPI)	300	0.95	(g/cm <sup>3</sup> )	1.95	0.2	(ohm.m)	200	
GAMMA RAY		NEUTRON POROSITY		SONIC / ACOUSTIC		DEEP RESISTIVITY			
150	(gAPI)	300	1.05	(m <sup>3</sup> /m <sup>3</sup> )	0.45	240	(us/ft)	40	
MD		TVSS		SONIC / ACOUSTIC		SHALLOW RESISTIVITY			
1 : 2000		m		240		(us/ft)		40	
						SHALLOW RESISTIVITY			
						0.2		(ohm.m)	200
						DEEP RESISTIVITY			
						0.2		(ohm.m)	200



Appendix B: Composite well log through well 31/5-5 (npd.no)